ENZYME-REPLACEMENT THERAPY IN LYSOSOMAL STORAGE DISEASES

Julie Bielicki BSc

Thesis submitted for the degree of

Doctor of Philosophy

in

The University of Adelaide

(Faculty of Medicine)

Lysosomal Diseases Research Unit
Department of Chemical Pathology
Women's and Children's Hospital
South Australia

and

Department of Paediatrics
Faculty of Medicine
University of Adelaide
South Australia

2003

TABLE OF CONTENTS

Chapter 2: Materials and methods

Chapter 3: Mucopolysaccharidosis type VI

ABBREVIATIONS

α-MEM	α-minimal essential medium
4MUF	4-methylumbelliferyl fucopyranoside
4MUS	4-methylumbelliferyl sulphate
4S	N-acetylgalactosamine-4-sulphatase
AAV	adeno-associated virus
ALP	alkaline phosphatase
BBB	blood-brain barrier
BFR/BS	bone formation rate
BM	basement membrane
BME	basal medium Eagle's
BMT	bone marrow transplantation
BS/TV	bone surface density
BSA	bovine serum albumin
BV/TV	bone mineral volume
C4S	chondroitin-4-sulphate
CAM	cell adhesion molecule(s)
CD-M6PR	cation dependent-mannose-6-phosphate receptor(s)
cFUC	canine α-L-fucosidase
CHO	Chinese hamster ovary
CHO/rcFUC	recombinant canine α-L-fucosidase expressed in Chinese hamster ovary cells
CI-M6PR	cation independent-mannose-6-phosphate receptor(s)
CNS	central nervous system
CPC	cetylpyridium chloride

CS	chondroitin sulphate
CSF	cerebrospinal fluid
CSPG	chondroitin sulphate proteoglycan(s)
CVO	circumventricular organ(s)
DMEM	Dulbecco's modified Eagle's medium
DMG	dimethylglutaric acid
DOTAP	N-[1-(2,3-dioleolyloxy)propyl]-N,N,N-trimethylammonium-methyl sulphate
DS	dermatan sulphate
DTE	dithioerythritol
DTNB	dithio-bis-(2-nitrobenzoic acid)
EDC	ethyldimethylaminopropyl carbodiimide
EDTA	ethylenediaminetetraacetic acid
Elisa	enzyme-linked immunosorbent assay
ER	endoplasmic reticulum
ERT	enzyme-replacement therapy
FACS	fluorescence-activated cell sorting
FCS	foetal calf serum
FITC	fluorescein isothiocyanate
FUC	α-L-fucosidase
GAG	glycosaminoglycan(s)
GalNAc	N-acetylgalactosamine
GalNAc4S	N-acetylgalactosamine-4-sulphate
GGT	γ-glutamyl transpeptidase
GlcNAc	N-acetylglucosamine
HA	hyaluronic acid

HeBS	HEPES-buffered saline
HEPES	N-[2-hydroxyethyl]-1-piperazine-N'-[2-ethanesulfonic acid]
HIV	human immunodeficiency virus
HPLC	high pressure liquid chromatography
HRE	high-resolution electrophoresis
HRP	horseradish peroxidase
HS	heparan sulphate
HSC	haematopoietic stem cell(s)
HSPG	heparan sulphate proteoglycan(s)
ID	injected dose
IEF	iso-electric focussing
Ig	immunoglobulin
IGFII	insulin-like growth factor II
IgG	class G immunoglobulin
KS	keratan sulphate
L	length of L5 vertebra
L5	fifth lumbar vertebra
LAMP	lysosome-associated membrane protein
LSD	lysosomal storage disease(s)
M6P	mannose-6-phosphate
M6PR	mannose-6-phosphate receptor(s)
MAR	mineral apposition rate
MDCK	Madin-Darby canine kidney
MDCK/rcFUC	recombinant canine α-L-fucosidase expressed in Madin-Darby canine kidney cells
MPS	mucoploysaccharidosis(es)

MS/MS	tandem mass spectrometry
m/z	mass/charge
NAD	nicotine adenine dinucleotide
NGF	nerve growth factor
NHS	N-hydroxy succinimide
OX26	mouse anti-rat transferrin receptor monoclonal antibody
PBS	phosphate-buffered saline
PCR	polymerase chain reaction
PDPH	3-(2-pyridyldithio)propionyl hydrazide
PG	proteoglycan(s)
pH_{opt}	optimum pH
pI	isoelectric point
PS	penicillin and streptomycin sulphate
rcFUC	recombinant canine α-L-fucosidase
rf4S	recombinant feline N-acetylgalactosamine-4-sulphatase
rh4S	recombinant human N-acetylgalactosamine-4-sulphatase
RSA	rat serum albumin
SAM	sheep anti-mouse antibody
SAM-FITC	fluorescein isothiocyanate-labelled sheep anti-mouse antibody
SAM-HRP	sheep anti-mouse antibody conjugated to horseradish peroxidase
SAR	sheep-anti rabbit antibody
SAR-FITC	fluorescein isothiocyanate-labelled sheep anti-rabbit antibody
SAR-HPR	sheep anti-rabbit antibody conjugated to horseradish peroxidase
SATA	N-succinimidyl S-acetylthioacetate
SDS-PAGE	sodium dodecyl sulphate-polyacrylamide gel electrophoresis
SF	skin fibroblast(s)

SOD	superoxide dismutase
SPDP	sulfosuccinimidyl 6-[3'-(2-pyridyldithio)proprionamido]hexanoate
TbN	trabecular number
TbS	trabecular separation
TbTh	trabecular thickness
Tf	transferrin
TGN	trans golgi network
TLC	thin layer chromatography
TNB	thionitrobenzoic acid
VEGF	vascular endothelial growth factor
W	width of L5 vertebra
WBC	white blood cell(s)

THESIS ABSTRACT

The lysosomal storage diseases (LSD) encompass a number of genetically inherited disorders, which include the mucopolysaccharidoses (MPS) and the oligosaccharidoses as well as others. Each disorder results from a primary deficiency in one specific gene product that in most diseases is a unique enzyme activity. These enzymes are predominantly involved in the degradation of glycosaminoglycans, oligosaccharides and glycolipids. Failure to degrade these macromolecules leads to their accumulation in lysosomes of most cell types which in turn results in progressive organ dysfunction and clinical symptoms.

In all LSD there is soft tissue involvement, however, the two main sites of pathology are the skeleton and the central nervous system. In some LSD both sites may be affected while in others one predominates. For example, MPS VI, which is caused by a deficiency of N-acetylgalactosamine-4-sulphatase (4S), is a disorder with mainly skeletal pathology while fucosidosis, which results from a deficiency of α-L-fucosidase (FUC), is a largely neurological disease. Two animal models of these disorders, the MPS VI cat and the fucosidosis dog, have proven invaluable in studies of skeletal and neurological pathology and their treatment. Pathology in these animal models closely parallels that observed in the human condition.

Enzyme-replacement therapy (ERT) in the MPS VI cat using recombinant human 4S from birth has been demonstrated to be effective in improving most soft tissue and bone pathology. Improvement in bone pathology was dependent on dose and age at commencement of therapy. Reactions typical of anaphylaxis were observed in all cats treated with human enzyme. One of the aims of this thesis was to evaluate the efficacy of using species-specific enzyme, namely recombinant feline 4S, in the treatment of MPS VI cats. Towards this end, enzyme was purified and characterised and therapy was instigated from birth in two cats for six months. Results indicated that there was an advantage in using species-specific enzyme in that the effect was as good as a five times higher dose of human 4S. The implications of this result in terms of correct dosage for treating human patients, in what is an expensive and lifetime therapy, are significant.

In LSD with neurological symptoms, penetration of proteins from the circulation into brain is a major limitation to effective ERT. The morphological and physiological characteristics of the

cerebrovascular endothelium form the basis of the blood-brain barrier (BBB). Non-invasive methods for delivering proteins, which are normally unable to cross the BBB, include the use of vector systems and chemical alteration of the protein charge. The main aims of this section were (i), to express, purify and characterise recombinant canine α-L-fucosidase (rcFUC) which is deficient in canine fucosidosis; (ii), to modify rcFUC by cationization, and to synthesise chimeric proteins of rcFUC with a transport vector which is known to be transported into brain (such as insulin), and then to test these modifications for transcytosis into brain in a normal rat prior to evaluation in the dog model and (iii), to evaluate the efficacy of ERT in a fucosidosis dog using unmodified rcFUC.

rcFUC was expressed in Chinese hamster ovary and Madin-Darby canine kidney cells and both forms were found to be similar, apart from some differences in glycosylation. ERT was commenced at 2 months of age in a single fucosidosis dog and continued for up to one year of age. This animal appeared to show a later onset of neurological symptoms compared to untreated affected dogs.

Attempts to modify enzyme to enhance transport into brain revealed various problems. In cationization studies, maintenance of enzymatic activity had to be balanced against increased cationization. In addition, compared to native enzyme, cationized rcFUC tested in a rat showed no evidence of improved targeting to brain. A vector system involving covalent linkage to a tryptic fragment of insulin was ultimately considered technically too difficult and unlikely to provide a conjugate with the required properties. The production of conjugates using rcFUC and the mouse antibody to the rat transferrin receptor, OX26, was found to be more practicable although some problems were encountered including the ability to control the reaction to achieve a favourable stoichiometry of vector to passenger molecules and the maintenance of the critical binding regions of both molecules as well as FUC activity. The conjugates produced were not tested in a rat, as it became increasingly obvious that the need for a more sensitive detection system to assess accurately enzyme transported into brain tissue was required. Initial results suggested that Europium labelling may provide this.

In terms of therapeutic strategies, the results described in this thesis indicate that use of same-species enzyme is superior to non-same-species enzyme and although only one fucosidosis dog was treated, ERT with unmodified rcFUC appeared to delay onset of neurological symptoms.

Although technically difficult to produce, chimeric proteins may provide a means of treatment for neurological symptoms in LSD.

DECLARATION

This thesis contains no material which has been accepted for the award of any other degree or diploma in any university or other tertiary institution and, to the best of my knowledge and belief, contains no material previously published or written by another person, except where due reference is made in the text.

I give consent to this copy of my thesis being available for photocopying and loan if accepted for the award of the degree.

SIGNED: DATE: 20/6/03.

ACKNOWLEDGEMENTS

I would like to thank the following people for their contribution to the work described in this thesis:

Firstly, my supervisors, Dr. Don Anson and Professor John Hopwood, for helpful discussions and in addition Dr. Don Anson for technical assistance with the capillary depletion experiments.

Professor Peter Gray and Jodie Varnai from the Biotechnology Department, University of NSW, for large-scale production of rf4S medium.

Dr. Allison Crawley for her veterinary assistance and expertise with the MPS VI cats, and animal care attendants at the IMVS Gilles Plains facility for daily care of the cats.

Leanne Hein for instruction in bone histomorphometric techniques and Viv Muller for isolation of fucosidosis dog brain products.

Callum Gillespie from the Child Health and Research Institute, WCH, for instruction in jugular catheterization.

Dr. Rosanne Taylor and Sarah Pomroy (Honours student) from the Department of Veterinary Sciences, University of Sydney, for veterinary assistance with the fucosidosis dogs.

Finally, all members of the Department of Chemical Pathology who helped over the course of this thesis.

Chapter 1: Introduction and review

1.1 Preface

The lysosomal storage diseases (LSD) comprise a group of debilitating and life-threatening inherited diseases, each of which results from the deficiency of a unique enzyme activity. The multitissue involvement of these disorders presents a particularly difficult challenge to any single treatment regime. Enzyme-replacement therapy (ERT) is a treatment strategy that involves the systemic infusion of normal enzyme to replace deficient or non-functioning enzyme. The development and evaluation of the efficacy of ERT has been expedited by the discovery of a number of naturally occurring, and the generation of additional artificially created, animal models of LSD and by the availability of recombinant enzyme.

Two animal models that have been intensively used to evaluate ERT in LSD are the mucopolysaccharidosis type VI (MPS VI) cat and the MPS VII mouse. MPS VI cats exhibit the bone pathology characteristic of many of the LSD, but have no central nervous system (CNS) involvement. ERT from birth in MPS VI cats, using human N-acetylgalactosamine-4-sulphatase (4S), proved largely successful in correcting somatic pathology and bone disease. However, the use of human 4S in cats leads to immune reactions. In addition, human 4S may be of reduced efficacy in its non-native environment.

In contrast to the MPS VI cat, the MPS VII mouse has both CNS and bone pathology. Commencement of ERT from birth with mouse β-glucuronidase demonstrated successful correction of CNS, as well as most somatic pathology, including that of bone. However, neurological improvement was fortuitous as the blood-brain barrier (BBB), which in most animal species is impenetrable to proteins, is 'leaky' or immature for up to 10-14 days post birth in mice (Laterra *et al.*, 1992; Vogler *et al.*, 1993; Sands *et al.*, 1994). In the human condition, for instance, endothelial tight junctions are laid down by the first trimester of foetal life (Mollgoard and Saunders, 1975). Therefore, mouse models of the LSD are not always ideal for the evaluation of treatments for CNS pathology and results from such studies must be interpreted with caution. Larger animal models, such as the fucosidosis dog, provide a more accurate reflection of the human situation where the BBB is closed at birth. Additionally, if ERT for CNS pathology is to be successful, different strategies must be considered to circumvent the BBB. For example, conjugation of enzyme to vectors known to cross the BBB,

and chemical modification by cationization, are two potential methods to enhance transcytosis of enzyme into brain.

The main aims of the work presented in this thesis were firstly, to evaluate the efficacy of ERT in MPS VI cats using feline, rather than human, 4S, and secondly, to develop strategies for the delivery of replacement enzyme to the CNS *via* intravenous injection.

In the remainder of this chapter an overview of lysosomes, their biogenesis and function and the substrates they degrade will be presented. This will be followed by a discussion of LSD, with particular reference to MPS and oligosaccharidoses, their clinical description, diagnosis and pathogenesis. Finally, a review of therapies, past, present and future, for LSD in patients and animal models of disease will be presented. MPS VI and fucosidosis, the main subjects of study in this thesis, will be reviewed in more detail. The specific aims of this thesis will be outlined at the conclusion of this chapter.

1.2 Lysosomes

Historically, lysosomes were defined as cytoplasmic organelles that contained acid hydrolases (De Duve *et al.*, 1955). We now ascribe the term lysosome to an organelle bounded by a single membrane that contains a set of highly glycosylated integral membrane proteins and encloses an acidic intracellular compartment rich in mature hydrolases. In particular it can be distinguished from earlier compartments in the endocytic pathway in that it forms the terminal high-density organelle in the endosomal system and is devoid of mannose-6-phosphate receptors (M6PR) (Storrie, 1988; Hopwood and Brooks, 1997). Most of the properties of lysosomes are shared with a group of cell type-specific compartments referred to as 'lysosome-related organelles' that include, amongst others, melanosomes, lytic granules, MHC class II compartments and basophilic granules (Dell'Angelica *et al.*, 2000). As well as lysosomal proteins, these organelles contain cell type-specific components that are responsible for their specialised functions. However, this discussion will be restricted to classical lysosomes only.

The main function of the lysosome is the catabolism of intra- and extracellularly derived macromolecules such as glycosaminoglycans (GAG), glycoproteins and glycolipids, which enter the lysosome *via* endocytosis or autophagy. These macromolecules are degraded by

lysosomal hydrolases into their constituents for reuse within, or transport out of the cell following their exit from the lysosome. In the next sections lysosomal biogenesis and the synthesis, transport and targeting of lysosomal enzymes will be discussed.

1.3 Lysosomal biogenesis

The elements of the vacuolar network, of which lysosomes and endosomes are major components, are shown in Figure 1.1 and have been reviewed in Hopwood and Brooks (1997). Lysosomal biogenesis is believed to start with the budding of vesicles from the trans-Golgi network (TGN). Specific adaptor proteins (e.g., HA-1 adaptor), the binding of an adaptin complex and phosphorylation of the M6PR are required for the formation of clathrin-coated vesicles and their subsequent transport from the TGN. These vesicles fuse with early endosomes and mature into late endosomes/prelysosomes and finally into lysosomes through a process of progressive acidification. Proteins destined for early endosomes/lysosomes, to the cell surface or for secretion, are sorted in the TGN on the basis of specific signals present on these proteins. Most soluble proteins transported to endosomes/lysosomes carry a mannose-6-phosphate (M6P) signal (sections 1.4 and 1.5). In lysosome-associated membrane proteins (LAMP) the tyrosine residue in the His-Ala-Gly-Tyr motif found in the C-terminal cytoplasmic tail, and its distance from the membrane spanning domain, are critical signals for transport to the lysosomal membrane (Peters *et al.*, 1990a).

Endocytosis at the cell surface also occurs *via* clathrin-coated pit structures, although the adaptor proteins involved in their formation are distinct from those required for vesicles originating from the TGN (Seaman *et al.*, 1993). These structures deliver macromolecules from the cell surface, as well as membrane proteins and receptor-ligand complexes, to the endosome/lysosome network. The constant movement of organelles within the vacuolar network is organised along microtubules. Unlike 'lysosome-related organelles' such as lytic granules, classical lysosomes appear unable to fuse directly with the plasma membrane to exocytose their contents. Undegraded macromolecules found in plasma and excreted in urine are presumably the consequence of cell death.

Figure 1.1 Elements of the vacuolar network.

N, nucleus; ER, endoplasmic reticulum; CGN, cis-Golgi network; TGN, trans-Golgi network; MT, microtubule; SV, secretory vesicle; CS, cell surface; CCP, clathrin-coated pits; EE, early endosome; ECV, endosome carrier vesicle (or multivesicular body); LE, late endosome (or prelysosomal compartment); L, lysosome (Hopwood and Brooks, 1997).

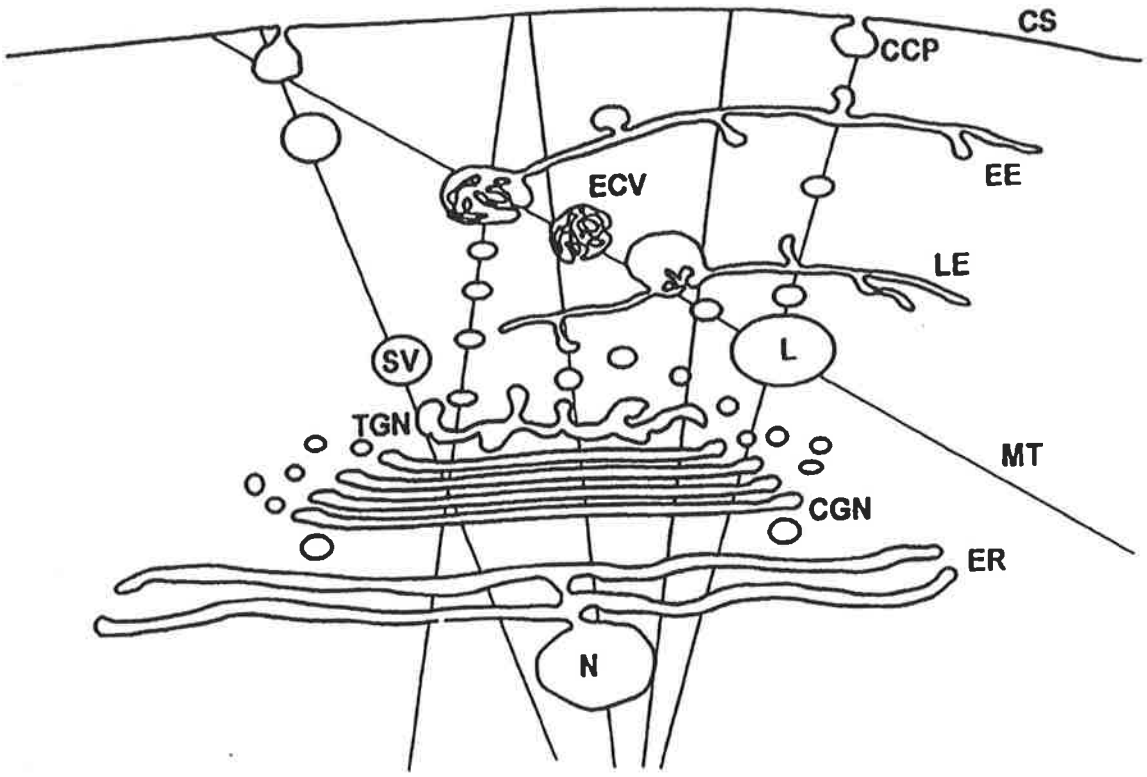
CS
CCP
EE
ECV
LE
SV
L
TGN
MT
CGN
ER
N

1.4 Lysosomal enzymes

More than 50 acid-dependent enzymes (glycosidases, sulphatases, nucleases, lipases and phospholipases, proteases and phosphatases) are found within the lumen of the lysosome. Lysosomal enzymes are glycoproteins and their synthesis and processing (Hasilik and von Figura, 1984; Kornfeld and Mellman, 1989; Hasilik, 1992) as well as trafficking (von Figura and Hasilik, 1986; Kornfeld, 1987; Pfeffer, 1988; Kornfeld and Mellman, 1989; Hopwood and Brooks, 1997) have been reviewed.

Lysosomal enzymes are initially translated in the rough endoplasmic reticulum (ER). After removal of the signal peptide and during translocation through the ER, preassembled glycan chains composed of nine mannose, two N-acetylglucosamine (GlcNAc) and three glucose residues attached to dolicholdiphosphate, are transferred *en bloc* by glycosyltransferase to an appropriate asparagine residue, which conforms to the sequence motif asparagine-x-serine/threonine (N-X-S/T) (Gavel and von Heijne, 1990; Mellquist *et al.*, 1998). Competition between glycosylation and chaperonin-assisted folding of nascent protein chains, which occurs concurrently, at least partly explains the lack of utilisation of all potential N-glycosylation sites, which may be rapidly rendered inaccessible to glycosyltransferases (Holst *et al.*, 1996). On transport to the Golgi apparatus further carbohydrate processing occurs which involves the addition of galactose, fucose and N-acetylgalactosamine (GalNAc) by other glycosyltransferases, to produce one of three common subtypes of N-glycans; high-mannose, complex and hybrid-type chains. The crucial step in complex-type glycan biosynthesis is the attachment of GlcNAc at the α-(1→3)-linked D-mannose residue before the α-(1→6)-linked arm has been completely processed. Further introduction of GlcNAc residues results in the generation of multiantennary structures. The arrangement of glycosyltransferases and the level of substrates are critical and adjustable factors that control the glycosylation potential of the Golgi apparatus (Colley, 1997; Varki, 1998). Sialylation, the final modification in complex-type chains, occurs *via* the action of the corresponding sialyltransferase in the TGN (Lennarz, 1987).

Sorting of N-glycosylated proteins/enzymes to the lysosome is achieved by preferential phosphorylation of terminal α-(1→2)-linked mannose units in a two-step reaction. The first step involves the transfer of GlcNAc-1-phosphate to the C6-hydroxyl group of these mannose

residues by UDP-GlcNAc-phosphotransferase to produce GlcNAc-1-phospho-6-mannose. In the second step, N-acetylglucuronyl-phosphodiesterase catalyses the removal of GlcNAc from GlcNAc-1-phospho-6-mannose units leaving a M6P moiety. Mannose-6-phosphorylation of glycoproteins enables binding to M6PR present in the TGN with subsequent targeting to lysosomes *via* a pre-lysosomal/endosomal compartment.

1.5 M6PR-mediated transport of lysosomal enzymes

Mammalian cells possess two distinct M6PR that mediate transport of newly synthesised soluble lysosomal enzymes from the TGN to a pre-lysosomal compartment in the endocytic pathway (Pfeffer, 1988; Kornfeld, 1992). The cation-independent M6PR (CI-M6PR) and the cation-dependent M6PR (CD-M6PR) are transmembrane glycoproteins that have an apparent Mr of 300 kDa and 46 kDa, respectively. The two receptors share a homologous extracytoplasmic domain, which in the CI-M6PR comprises fifteen repeating units as opposed to one in the CD-M6PR. The CI-M6PR is bifunctional and also controls extracellular levels of insulin-like growth factor II (IGFII) by mediating its rate of internalisation.

What determines which receptor is used for lysosomal trafficking from the TGN is unclear. Studies with CI-M6PR-deficient cells showed that between 30-50% of newly synthesised cathepsin was retained intracellularly. This level was increased to approximately 90% when the CI-M6PR was over-expressed (Lobel *et al.*, 1989; Johnson and Kornfeld, 1992). In CD-M6PR-deficient cells expressing wild type levels of CI-M6PR, over-expression of CD-M6PR resulted in secretion of up to 50% of newly synthesised lysosomal enzymes (Chao *et al.*, 1990). This implies that CD-M6PR can bind all newly synthesised lysosomal enzymes in the TGN but releases its ligands at a site where they can access the extracellular medium. It has been suggested that dissociation may apply preferentially to low-affinity ligands.

Analysis of M6PR-deficient cell lines from mice with targeted disruption of both M6PR genes has shown that in the absence of both receptors 85-95% of total activity of a variety of lysosomal enzymes is recovered in medium. However, over-expression of CD-M6PR only partially compensates for loss of CI-M6PR (Watanabe *et al.*, 1990). In contrast, overexpression of the CI-M6PR completely corrects the missorting of lysosomal enzymes in the absence of the CD-M6PR. However, 25% of the lysosomal enzymes were transported along a secretion-

recapture pathway that is sensitive to M6P. This pathway is not observed in normal cells. In conclusion, it appears that over-expression of either receptor is not sufficient for intracellular targeting of lysosomal proteins. Both receptors obviously contribute to the targeting of newly synthesised lysosomal enzymes but there appears to be some overlap between the complements of lysosomal enzymes transported by each receptor (Kasper *et al.*, 1996).

Constitutive cycling of the two receptors occurs between the TGN and the endosomal compartment. Additionally, both receptors cycle between the cell surface and the endosomal network. However, only the CI-M6PR has the capability to bind ligands at the cell surface and internalise them. The basis of the concept of ERT in LSD relies fundamentally on this principle, that is, that an external source of purified mannose-6-phosphorylated enzyme can be sequestered into cells *via* the CI-M6PR thus replacing the defective enzyme. The function of cell surface CD-M6PR is unknown. Its inability to function efficiently in endocytosis is believed to reflect poor binding of ligand at the cell surface rather than its failure to recycle to the plasma membrane (Stein *et al.*, 1987).

In the increasingly acidic environment of the late endosomal compartment, the receptor dissociates from the lysosomal enzyme and is recycled back to the TGN. Once in the endosomal/prelysosomal compartment further proteolytic and glycosidic processing of the lysosomal enzyme can occur as well as removal of the M6P signal by dephosphorylation *via* the action of purple acid phosphatase (Bresciani and Von Figura, 1996). There is also evidence that lysosomal enzymes are continually recycled from end-stage lysosomes to the endosomal compartment and hence back into lysosomes (Bright *et al.*, 1997).

The process of receptor recycling can be interrupted by addition of lysosomotropic amines that raise the pH of the endosome thus preventing the dissociation of receptor and ligand (Chang *et al.*, 1988). The consequent unavailability of free M6PR prevents further trafficking to lysosomes. Under these conditions newly synthesised lysosomal enzymes are secreted from the cell *via* secretory vesicles. This mechanism has been exploited in enzyme expression systems *in vitro* to increase the levels of recombinant mannose-6-phosphorylated enzyme in culture medium.

1.6 M6PR-independent transport of lysosomal enzymes

Not all lysosomal enzymes are transported to lysosomes *via* M6PR. In M6PR-deficient cells, normal intracellular levels of acid phosphatase were observed and none was found secreted in medium (Kasper *et al.*, 1996) implying another mechanism for transport to the lysosome. Over-expression of α-L-iduronidase in MPS I fibroblasts using retroviral vectors (Anson *et al.*, 1992a) resulted in the induction of a phenotype analogous to mild I-cell disease. The α-L-iduronidase over-corrected cells had decreased levels of several lysosomal enzymes but again acid phosphatase levels were normal due to an alternative M6P-independent lysosomal targeting signal (Lemansky *et al.*, 1985). Trafficking of newly synthesised lysosomal acid phosphatase occurs *via* the cell surface. The enzyme is then re-internalised after recognition of either a Tyr or Phe signal in the cytoplasmic tail sequence by the adaptor complex required for cell surface internalisation (Waheed *et al.*, 1988). On the cell surface of different cell types, in addition to the M6PR, other carbohydrate specific receptors are present in various amounts including fucose, mannose and galactose receptors and these may provide alternative targeting mechanisms to lysosomes (Hasilik, 1992).

1.7 Glycosaminoglycans and proteoglycans

The function of lysosomal enzymes is to degrade macromolecules such as GAG, oligosaccharides and glycolipids. The structure and role of GAG and oligosaccharides, their synthesis and degradation will be discussed in the following sections. This thesis is concerned with two disorders in which the degradation of such macromolecules is impaired. These are MPS VI and fucosidosis, which involve GAG and oligosaccharide degradation, respectively.

1.7.1 Structure and function

A detailed review of GAG structure, synthesis and degradation can be found in Roden (1980), Fransson (1987), Hopwood and Morris (1990) and Kjellen and Lindahl (1991), accordingly only a brief description will follow.

GAG form a distinct group of complex carbohydrates that are generally defined as unbranched acidic polysaccharides produced from repeating disaccharide units. The composition of this disaccharide unit gives rise to five main types of GAG (Figure 1.2). Chondroitin sulphate (CS), which is the most abundant mammalian GAG, and dermatan sulphate (DS), comprise

alternating hexuronic acid and GalNAc residues. In CS the hexuronic acid is glucuronic while in DS both glucuronic and its C5 epimer, iduronic acid, are present. Keratan sulphate (KS) is devoid of hexuronic acid residues and instead has a repeating disaccharide containing galactose and GlcNAc. Heparan sulphate (HS) differs from DS in that GalNAc is substituted by GlcNAc. Hyaluronan (HA) is made up of alternating glucuronic acid and GlcNAc residues. In addition, monosaccharides in the GAG chain can be variously modified. The glucosamine residues in HS can be N-acetylated, N-sulphated or O-sulphated at the C3 and C6 positions while the hexuronic acids (glucuronic or iduronic) can be C2 O-sulphated. These modifications, together with variable configuration of the glycosidic linkages and length of each polysaccharide chain, confer an enormous potential for heterogeneity within this class of macromolecules. Heparin, for example, is highly substituted and is distinguished from HS by the presence of a high proportion (>80%) of N-sulphation of glucosamine residues (Roden, 1980). HA, on the other hand, displays the lowest degree of modification, is totally unsulphated and in addition is the only GAG not found covalently linked to protein (Laurent and Fraser, 1992).

Proteins with covalently bound GAG chain(s) are referred to as proteoglycans (PG) (Yanagishita, 1993). PG are structurally diverse having core proteins which can vary from 10-400 kDa and can contain a single GAG chain (e.g., decorin), or over a hundred (e.g., aggrecan). The GAG chains have unique biophysical properties, such as elasticity and ability to hold water, and thus contribute to the bulk effects of PG. They also contain a variety of binding sites for various extracellular cytokines, growth factors, enzymes and inhibitors (Turnbull *et al.*, 1992). PG are ubiquitously distributed throughout animal tissues and are the major components of cartilage, cornea and connective tissues. Aggrecan, the major PG of cartilage, is associated with collagen, and when complexed with HA, it forms a structure that is particularly resilient to compressional forces. Decorin and biglycan are two of the smallest PG having one and two DS chains, respectively. Both have been associated with growth plate and newly deposited osteoid although their precise function in bone growth and development is unknown (Poole *et al.*, 1986; Bianco *et al.*, 1990).

Figure 1.2: The five main classes of GAG.

Basic structure of the main classes of GAG. The repeating disaccharide units which make up the five classes of GAG and their possible modifications are shown.

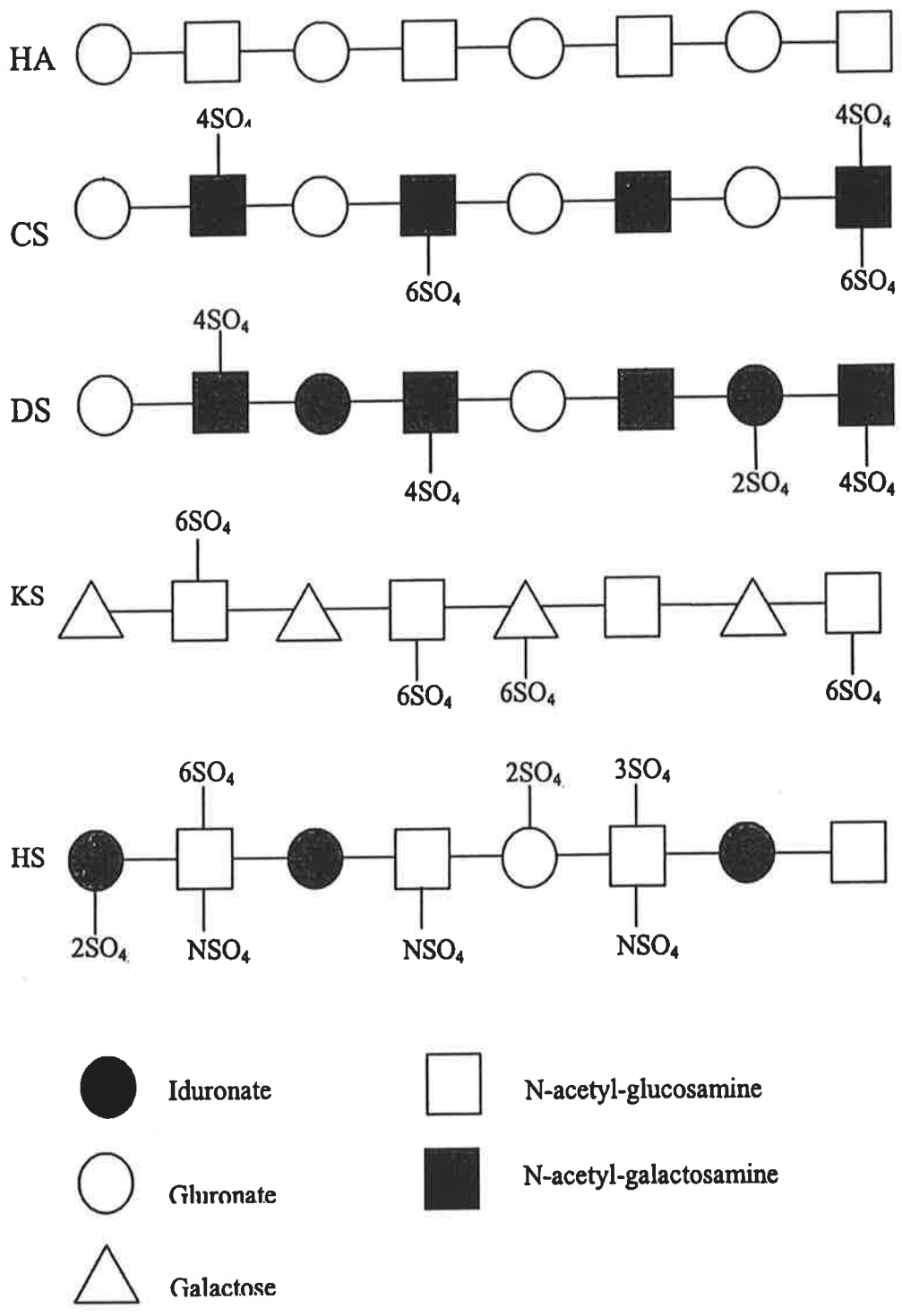
HA
CS
4SO4
4SO4
6SO4
6SO4
DS
4SO4
4SO4
2SO4
4SO4
KS
6SO4
6SO4
6SO4
6SO4
HS
6SO4
2SO4
3SO4
2SO4
NSO4
NSO4
NSO4
Iduronate
Gluronate
Galactose
N-acetyl-glucosamine
N-acetyl-galactosamine

The role of PG in neural tissue has been reviewed extensively (Margolis and Margolis, 1993; Oohira *et al.*, 1994a). Two major species of PG, chondroitin sulphate PG (CSPG) and heparan sulphate PG (HSPG) are found in the CNS. Keratan sulphate PG are also present but in smaller amounts. These neural PG play pivotal roles both in cell-cell and cell-substratum interactions during various stages of brain development and function. Neurocan, a developmentally regulated CSPG has been localised in the early post-natal rat brain and is also involved in the pathway for early axonal extension (Oohira *et al.*, 1994b). Expression of a 200 kDa HSPG, designated H5-PG, is spatially and temporally regulated in the CNS. H5-PG is associated with the axonal surface and is involved in axonal outgrowth and/or synaptogenesis in the rat brain (Watanabe *et al.*, 1996). High levels of HS and CS are synthesised by astrocytes, members of the class of non-neuronal cells called neuroglial cells that comprise approximately 50% of the mass of the CNS (Margolis and Margolis, 1989). In conclusion, PG are widely distributed in organs and tissues and play pivotal structural (e.g., cartilage and connective tissue) and developmental (e.g., neuronal development) roles, some of which are only now being understood (Rapraeger, 2000; Esko and Lindahl, 2001; Yamaguchi, 2001).

1.7.2 Biosynthesis

PG synthesis occurs *via* a well-defined series of reactions (Roden, 1980). Following core protein synthesis in the ER, the transfer of xylose from UDP-xylose, by xylosyltransferase, onto hydroxyl groups of specific serine residues within the polypeptide chain occurs during its translocation to the Golgi apparatus. The subsequent sequential addition of two galactose residues in the TGN is catalysed by two separate β-galactosyltransferases whose substrates are xylose-serine and galactose-xylose-serine. Finally, attachment of glucuronic acid by glucuronysyltransferase completes the tetrasaccharide GAG-protein linkage region, which is identical for all four classes of GAG discussed above, and serves as a primer for further elongation of the GAG chain. The subsequent alternating stepwise addition of an N-acetylhexosamine or uronic acid residue requires another two enzyme activities, namely, GlcNAc (or GalNAc) transferase and glucuronyl (galactosyl) transferase. The mechanism or signal required for chain termination of GAG synthesis is as yet unknown. Epimerisation of glucuronic acid to iduronic acid is the result of the action of uronosyl epimerase. Further modification of monosaccharides by sulphotransferases is then carried out at selected N and O positions before the PG is secreted for later incorporation into extracellular matrices at the cell surface, in pericellular matrices, and for other functions.

1.7.3 Degradation

The reactions involved in the degradation of PG are also well established (Fransson, 1987; Hopwood, 1989; Neufeld and Muenzer, 2001). Degradation of the protein moiety and the polysaccharide chains occurs independently of each other. Hydrolysis of some peptide bonds may take place extracellularly or in the cytoplasm, but the carbohydrate portion is degraded only within the endosome/lysosome. Extracellular and membrane-associated GAG reach these cell organelles *via* adsorptive pinocytosis and fusion of endocytic vesicles with lysosomes. Intracellular GAG enter the degradative pathway *via* autophagy. The GAG chains released by protease digestion are degraded to oligosaccharides ranging from 4-10 kDa by the action of endoglycosidases in a pre-lysosomal/endosomal compartment. Fusion of endosomes with, or maturation of endosomes to, lysosomes exposes these oligosaccharides to various glycosidases and sulphatases culminating in their catabolism to monosaccharides and free inorganic sulphate. The stepwise degradation commences at the non-reducing terminal end of the GAG chain fragment and proceeds in a sequential manner relying on a series of exquisitely specific substrate-enzyme interactions, whereby the product of one enzymatic reaction becomes the substrate for the next enzyme in the sequence.

As an example of these processes, the sequence of reactions involved in the degradation of DS is shown in Figure 1.3. In this particular schema, iduronate-2-sulphatase hydrolyses the C-2 sulphate ester from the terminal iduronic acid residue. The resultant product becomes the substrate for the next enzyme in the pathway, α-L-iduronidase, which hydrolyses the α-(1→3) glycosidic bond between iduronic acid and N-acetylgalactosamine-4-sulphate (GalNAc4S) thus releasing iduronic acid. Prior to liberating GalNAc, desulphation of the C-4 sulphate by 4S must occur. β-Hexosaminidase, which comprises A and S isomers, then releases the N-acetygalactosamine residue. The last enzyme in the DS degradation pathway is β-glucuronidase which releases glucuronic acid.

As HS also comprises glucuronic acid, its 5'epimer iduronic acid and their C2-sulphated variant, β-glucuronidase, α-L-iduronidase, iduronate-2-sulphatase and glucuronate-2-sulphatase are also necessary for the degradation of HS. In addition to these enzyme activities degradation of HS requires five other enzymes. These are sulphamidase, α-N-acetylglucosaminidase, glucosamine-N-acetyltransferase, glucosamine-6-sulphatase and

Figure 1.3: The sequential degradation of DS.

A diagrammatic representation of the degradative pathway of DS oligosaccharides in the lysosome (from Hopwood and Morris, 1990). The five exoenzymes involved and the MPS disorders resulting from the deficiency of each enzyme are shown. An alternate pathway of DS degradation *via* the action of β-hexosaminidase, which was proposed by Hopwood and Elliott (1985) and has since been confirmed by Ramsay *et al.* (2003), is also shown.

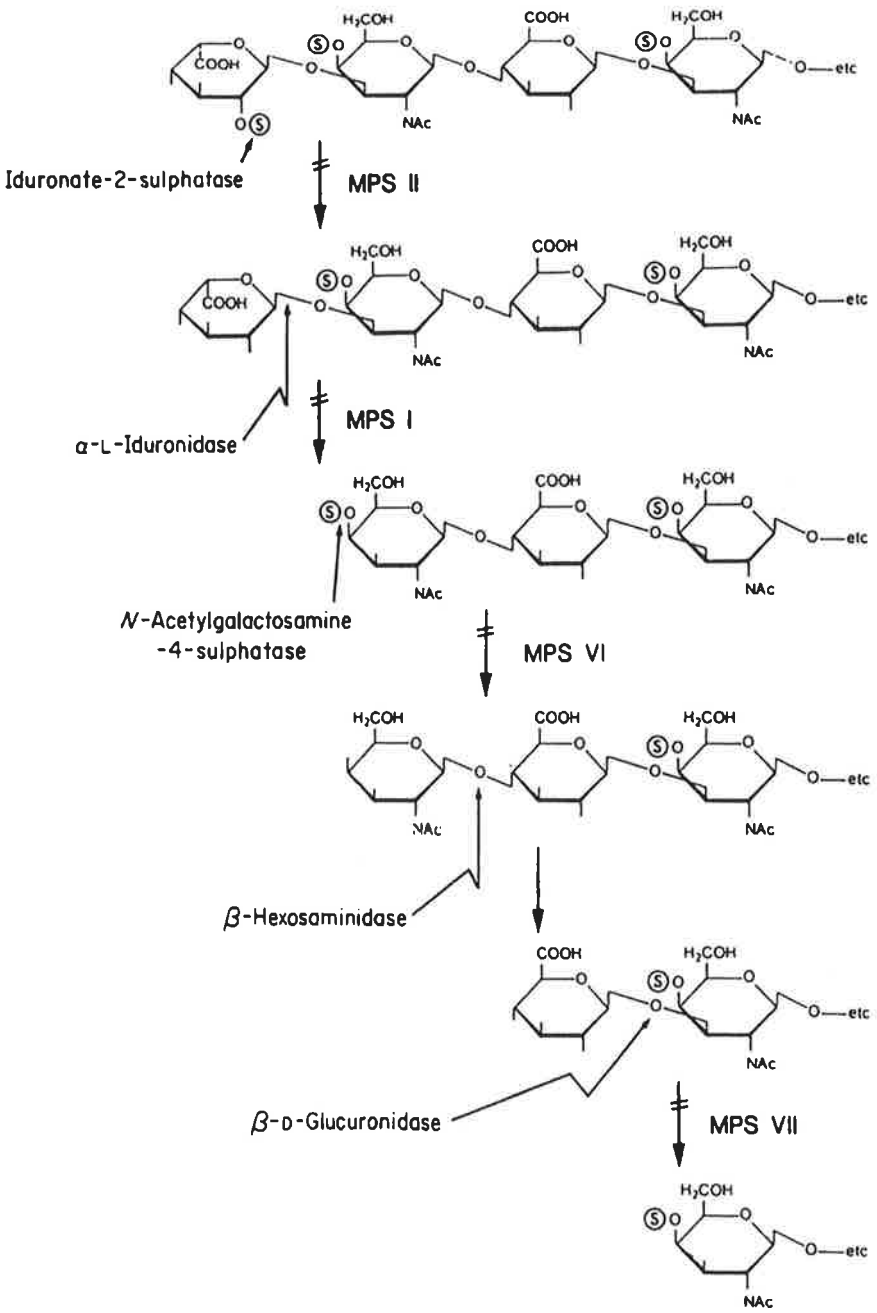

Alternate pathway

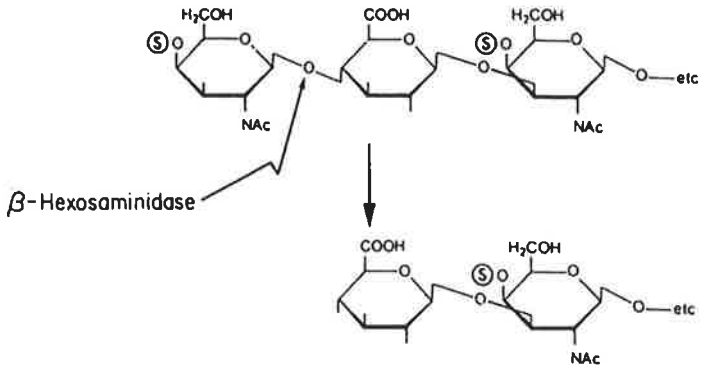

glucosamine-3-sulphatase (Hopwood, 1989). HS is exceptional in its metabolism in that liberation of sulphate from N-sulphated glucosamine by sulphamidase results in the formation of a glucosaminyl residue. This residue has an unsubstituted amino group that cannot be hydrolysed enzymatically in mammalian cells unless it is first biosynthetically acetylated with the membrane-associated glucosamine-N-acetyltransferase that uses cytoplasmic Acetyl-CoA as the acetyl donor.

The vital relevance of PG is illustrated by various disease states that result from impairment in their synthesis, assembly or degradation. For example, mouse matrix deficiency is caused by a 7 bp deletion in the aggrecan gene (Watanabe *et al.*, 1994). There is also a correlation between decorin deficiency and the development of a progeroid syndrome due to reduced activity of an abnormally thermolabile galactosyl transferase I, the enzyme that transfers galactose to xylose in the initial step of GAG synthesis (Kresse *et al.*, 1987; Quentin *et al.*, 1990). The MPS, a well-characterised class of diseases in which the stepwise degradation of GAG chains is defective, will be discussed later (section 1.10).

1.8 Glycoproteins

1.8.1 Structure and function

The lysosome is also the site of glycoprotein degradation. Glycoproteins are proteins that have been post-translationally modified by the addition of glycan chains (Kornfeld and Kornfeld, 1976; Kornfeld and Kornfeld, 1985). They may be glycosylated either by N-linked or O-linked saccharides or a combination of both.

The presence of glycan chains on proteins adds a further level of complexity to protein structure and can thus enlarge their capacity to encode information. Compared to amino acids and nucleotides, saccharides have a potentially enormous capacity for encoding function. However, this is an area not fully understood at present. Glycoproteins, like PG, occur widely in cells and in various organelles as well as on the cell surface. The glycan moiety on proteins may be necessary for targeting, protein stability, signal transduction and various other biological functions. For example, complete deglycosylation of β-glucosidase causes a total loss of activity (Grace and Grabowski, 1990) and lysosomal enzymes, if not glycosylated, lose the targeting signal necessary for their delivery to the lysosome (Kornfeld, 1986). Furthermore,

when deglycosylated, human β-chorionic gonadotrophin will still bind to its receptor with similar affinity to fully glycosylated enzyme, but fails to transmit a signal *via* stimulation of adenylate cyclase (Chen *et al.*, 1982). Failure of lysosomal degradation of glycoproteins results in a group of storage disorders known as oligosaccharidoses (section 1.11).

1.8.2 Biosynthesis

The biosynthesis of N-linked glycoproteins is identical to that of lysosomal enzymes as discussed in section 1.4. After glycosylation, depending on the particular signal motifs present on the glycoproteins, they are sorted to either secretory vesicles for transport out of the cell, to the cellular membrane or to endosomes/lysosomes. Only glycoproteins with N-linked oligosaccharide chains that have been mannose-6-phosphorylated, such as most lysosomal enzymes, are trafficked to the endosomal network. The M6PR-mediated transport of these proteins is not 100% efficient as lysosomal enzymes are also found extracellularly. This arises from differences in affinity between the M6PR and the various glycoproteins as well as in the availability of free M6PR. A certain percentage of mannose-6-phosphorylated proteins that are secreted extracellularly can be recaptured by M6PR present on the cell surface (section 1.5), which, as mentioned previously, is the mechanistic basis for systemic ERT.

1.8.3 Degradation

As glycoproteins are ubiquitous intra- and extracellular proteins, they are continuously being degraded in lysosomes during normal cellular function and turnover. Glycoproteins destined for degradation in the lysosome are either endocytosed from the extracellular medium in endosomes that fuse with the vacuolar network, or undergo autophagy from within the cytoplasm. Prior to degradation of the oligosaccharide chains, the bulk of the protein core is proteolytically removed by cathepsin, resulting in the release of glycopeptides. These glycopeptides are then degraded in the lysosome. The complexity of the degradation of N-linked oligosaccharide chains is commensurate with the complexity of the oligosaccharide present which, as previously mentioned, can be high-mannose, complex or hybrid-type. The oligosaccharide chains can also be bi, tri, tetra or multi-antennary. The step-wise degradation is regulated by the type of sugars present and proceeds in an orderly fashion from the non-reducing terminus after proteolytic digestion, which leaves the glycan moiety linked to an asparagine residue. Up to eight separate enzyme activities may be involved depending on the composition of the oligosaccharide chain (Aronson and Kuranda, 1989; Thomas, 2001).

Figure 1.4 illustrates the steps involved in the degradation of a complex-type oligosaccharide structure. These structures are capped with sialic acid and, in addition, have galactose, GlcNAc, mannose and fucose residues linked to asparagine. The sequence of reactions is as follows. Hydrolysis occurs from the non-reducing end of the oligosaccharide chain and is carried out by a number of exoglycosidases catalysing the sequential removal of single sugar moieties from the oligosaccharide branches. The lysosomal enzymes involved include firstly, neuraminidase that removes terminal sialic acid residues. This is followed by β-galactosidase, which cleaves the bond between galactose residues and N-acetylglucosamine. The next residue, a β-linked GlcNAc, is cleaved by the action of β-hexosaminidase A or B. Mannose residues linked α-(1→4) or α-(1→6) to the core mannoside are removed by the action of α-mannosidase while β-mannosidase is required to hydrolyse the core β-mannoside from the GlcNAc of the chitobiose core, which in turn, is cleaved by β-Hexosaminidase A or B. Aspartylglucosaminidase cleaves the bond between the asparagine residue and the adjoining GlcNAc. However, if the GlcNAc residue is fucosylated, the α-linked fucose moiety must first be removed by α-L-fucosidase (FUC). Fucoside residues have also been found linked to galactose or GlcNAc residues distinct from the chitobiose core, as in certain blood group substances such as Le^a, Le^b and H (Watkins, 1980) and these too must be removed before the rest of the chain can be degraded. Enzymatic digestion of the chitobiose core by endo-β-N-acetylglucosaminidase can therefore result in fucose-containing storage products which are not asparagine-linked. If any of the enzymes involved in the catabolism of the glycan moieties of glycoproteins are defective or missing, a specific inherited metabolic disorder will result (section 1.11).

Figure 1.4: Degradation of a complex oligosaccharide chain.

The stepwise lysosomal degradation of a complex oligosaccharide chain present on glycoproteins. Shown are the exoenzyme activities involved. Deficiencies of neuraminidase, α-mannosidase, β-mannosidase, α-L-fucosidase and aspartylglucosaminidase result in the oligosaccharidoses sialidosis, α-mannosidosis, β-mannosidosis, fucosidosis and aspartylglucosaminuria, respectively. (Thomas, 2001).

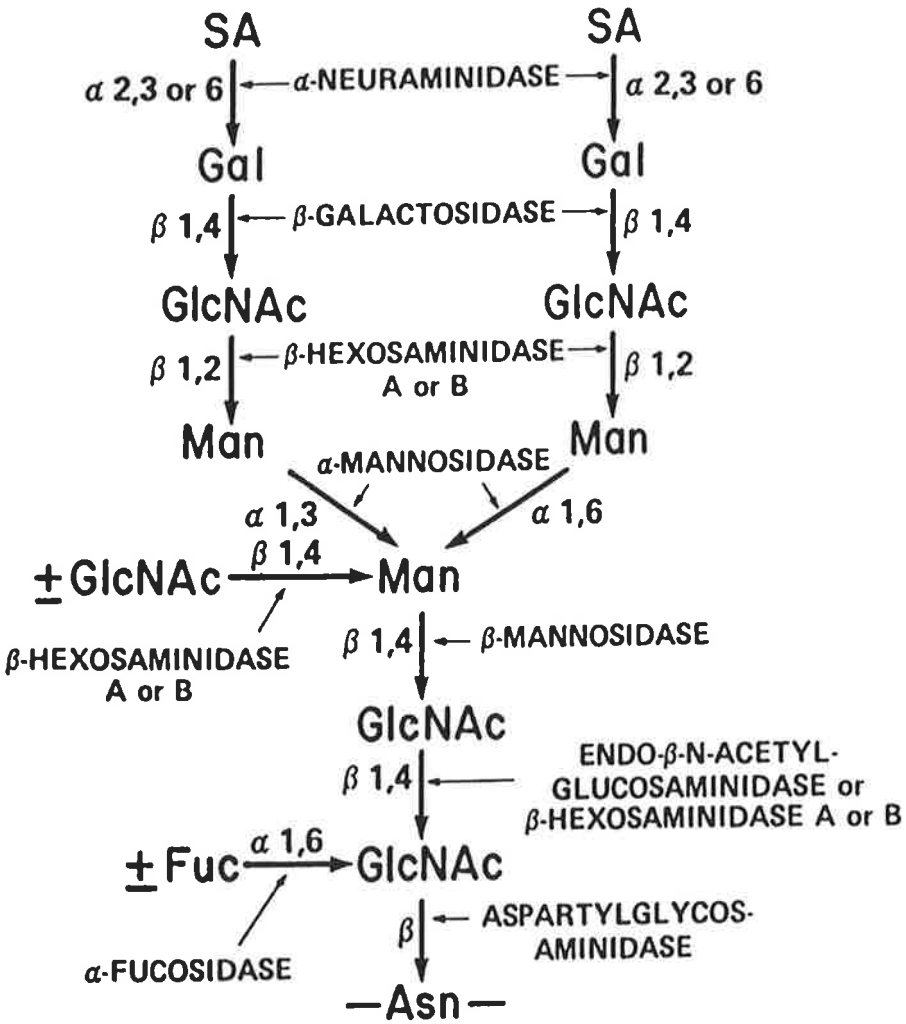
SA
SA
α 2,3 or 6
α-NEURAMINIDASE
α 2,3 or 6
Gal
Gal
β 1,4
β-GALACTOSIDASE
β 1,4
GlcNAc
GlcNAc
β 1,2
β-HEXOSAMINIDASE
A or B
β 1,2
Man
Man
α-MANNOSIDASE
α 1,3
α 1,6
β 1,4
±GlcNAc
Man
β-HEXOSAMINIDASE
A or B
β 1,4
β-MANNOSIDASE
GlcNAc
β 1,4
ENDO-β-N-ACETYL-
GLUCOSAMINIDASE or
β-HEXOSAMINIDASE A or B
α 1,6
±Fuc
GlcNAc
β
ASPARTYLGLYCOS-
AMINIDASE
α-FUCOSIDASE
—Asn—

1.9 Lysosomal storage diseases

LSD are monogenic inherited metabolic disorders, the majority of which result from a deficiency of a specific lysosomal enzyme involved in the degradation of macromolecules. This deficiency leads to the storage and accumulation in lysosomes of substrate(s) upon which the enzyme normally acts. In a few cases the substances accumulating in the lysosome are not undegraded macromolecules but are the products of hydrolytic degradation that are meant to leave the lysosomal compartment for metabolic recycling (Mancini *et al.*, 2000).

Two such LSD are cystinosis and Salla disease where a specific membrane-bound transport molecule for cystine and sialic acid monomers from the lysosome, respectively, is missing or malfunctioning (Gahl *et al.*, 1989). In three LSD a deficiency of from two to several lysosomal enzyme activities may occur as a result of a mutation in a single regulatory protein. In multiple sulphatase deficiency the activity of many known sulphatases are markedly reduced due to a mutation in the enzyme that converts the active site cysteine residue to α-formylglycine (Schmidt *et al.*, 1995; Dierks *et al.*, 1997; Dierks *et al.*, 1998). The gene encoding the C_{α}-formylglycine generating enzyme has recently been cloned (Cosma *et al.*, 2003; Dierks *et al.*, 2003). In I-cell disease lysosomal enzymes are not trafficked to the lysosome because of the absence of the phosphotransferase activity that is responsible for introducing the M6P signal to these enzymes (Nolan and Sly, 1989). Galactosialidosis is due to a deficiency of both β-galactosidase and neuraminidase, which is secondary to a defect in another lysosomal protein, the protective protein/cathepsin A (Galjart *et al.*, 1988).

In total at least 44 known separate LSD have been described. These can be classified according to the affected pathway and the nature of the accumulated substrate, for example, the mucopolysaccharidoses, oligosaccharidoses and sphingolipidoses. Within each disease group, almost all the LSD show clinical variability particularly with respect to age at onset and progression of symptoms. Clinically three different forms are usually distinguished: severe (infantile onset), intermediate (juvenile onset) and mild (adult onset) although this is generally an arbitrary separation of what is in fact a continuum of severity. Apart from Hunter, Fabry and Danon disease, which are X-linked, LSD are transmitted in an autosomal recessive manner. All LSD that have been subjected to molecular genetic analysis show a variety of different mutations. Clinical severity can be explained by the nature of the mutations present, the

corresponding level of residual enzyme activity and the amount of substrate synthesised from individual to individual. Genetic background also appears to have an influence on the expression of the disease. The incidence of all LSD in Australia is 1 in 7,500 live births (Meikle *et al.*, 1999a).

1.10 The mucopolysaccharidoses

The MPS have been extensively reviewed (Dorfman and Matalon, 1976; Neufeld and Muenzer, 2001). They result from defects of GAG (or mucopolysaccharide) degradation with the resulting accumulation of oligosaccharides in lysosomes and their excretion in urine. The discovery of mucopolysaccharidiuria as a diagnostic tool (Dorfman and Lorincz, 1957) was a milestone in the elucidation of the defect in MPS. To date there are eleven known enzyme deficiencies that result in seven distinct MPS types. These disorders, together with the corresponding enzyme deficiency, are shown in Table 1.1. The relationship between the storage product and the enzyme deficiency is illustrated in Figure 1.3 showing the degradation of DS. A deficiency of α-L-iduronidase causes MPS I (Hurler and Scheie syndromes) and storage products derived from DS and HS have α-linked iduronic acid residues at their non-reducing termini. MPS II or Hunter syndrome results from a deficiency of iduronate-2-sulphatase and both DS and HS fragments having non-reducing end iduronate-2-sulphate residues accumulate in lysosomes of most cell types. MPS III (Sanfilippo syndrome), which was originally classified as a single disorder based on clinical and urinary analysis, comprises four distinct subtypes (A, B, C and D) that result from different enzyme deficiencies, namely, sulphamidase, α-N-acetylglucosaminidase, glucosamine-N-acetyltransferase and glucosamine-6-sulphatase, respectively. The primary storage product in MPS III is HS. MPS VI (Maroteaux-Lamy syndrome) is the result of 4S deficiency and will be discussed in more detail in section 1.12. MPS VII (Sly syndrome) is caused by a deficiency of β-glucuronidase and both HS and DS accumulate in tissues and are excreted in urine. Disorders of KS degradation, namely, MPS IV A and IV B, are due to two distinct enzyme deficiencies, N-acetylgalactosamine-6-sulphatase and β-galactosidase, respectively. Both diseases share a similar clinical presentation, Morquio syndrome, with spinal and corneal problems being particularly damaging. MPS IX has been added to the list of known MPS after the recent report of the only patient with hyaluronidase deficiency (Natowicz *et al.*, 1996; Triggs-Raine *et al.*, 1999). This patient displayed a mild phenotype that included periarticular soft tissue masses, mild short

stature and an absence of neurological and visceral involvement. Although no patients to date have been diagnosed with deficiencies of glucuronate-2-sulphatase or glucosamine-3-sulphatase (enzymes required for HS degradation), it is expected that a MPS condition, with symptomatology similar to the Sanfilippo phenotype, would result from such a deficiency.

Table 1.1: Classification of the mucopolysaccharidoses

MPS disease	Syndrome	Enzyme deficiency	Stored substrates*
I	Hurler/Scheie	α-L-iduronidase	DS, HS
II	Hunter	Iduronate-2-sulphatase	DS, HS
IIIA	Sanfilippo	Sulphamidase	HS
IIIB	Sanfilippo	α-N-acetylglucosaminidase	HS
IIIC	Sanfilippo	AcetylCoA:α-glucosaminide N-acetyltransferase	HS
IIID	Sanfilippo	Glucosamine-6-sulphatase	HS
IVA	Morquio	Galactose-6-sulphatase	KS, CS
IVB	Morquio	β-D-galactosidase	KS
VI	Maroteaux-Lamy	N-acetylgalactosamine-4-sulphatase	DS, CS
VII	Sly	β-D-glucuronidase	DS, HS, CS
IX		Hyaluronidase	HA

*Stored substrates are DS, dermatan sulphate; HS, heparan sulphate; KS, keratan sulphate; CS, chondroitin sulphate; HA, hyaluronic acid.

The MPS share clinical features though in variable degrees. These include organomegaly, dysostosis multiplex, abnormal facies and in addition impaired vision, hearing, joint mobility and cardiopulmonary function. Mental retardation is present in all MPS except MPS IV and VI, which in turn manifest skeletal problems that are also found in all MPS with the exception of the subtypes of MPS III. As a group the incidence of MPS in Australia is 1 in 22,500 live births (Meikle *et al.*, 1999a).

1.11 The oligosaccharidoses

The oligosaccharidoses (Thomas, 2001) comprise a group of 5 disorders and are extremely rare (Table 1.2). In most of these disorders the number of cases documented worldwide is less than 100. The normal function of enzymes involved in this group of disorders is the sequential catabolism of asparagine-linked oligosaccharides on glycoproteins, as well as those derived from glycolipids, KS and blood group substances. Impaired function of one of these enzymes results in storage of these oligosaccharides in tissues and their urinary excretion. In fucosidosis (FUC deficiency) fucoglycoconjugates, including glycopeptides and glycolipids, constitute the main storage products. Sialidosis results from a deficiency of neuraminidase and storage products are terminated in sialic acid residues. In α-mannosidosis up to 17 different storage products, with increasing numbers of mannose residues linked to GlcNAc, have been detected in patient urine. β-Mannosidosis has only recently been described and only 13 patients have been documented. A deficiency of β-mannosidase is associated with storage and excretion of mannoside-β-(1→4)-GlcNAc. N-Acetylglucosaminyl-asparagine is the major storage product found in aspartylglucosaminuria patients who are predominantly of Finnish origin. The enzyme deficiency is aspartylglucosaminidase. Clinical features similar to those of the MPS, such as coarse facies, mental and motor deterioration, dysostosis multiplex, organomegaly and haematological abnormalities, are generally observed. Patients with oligosaccharidoses are biochemically distinguished from MPS patients by the lack of mucopolysaccharidoses. Instead they have a characteristic urinary oligosaccharide excretion pattern (Humbel and Collart, 1975; Sewell, 1979).

Table 1.2: The Oligosaccharidoses

Disease	Enzyme deficiency	Stored substrates
α-Mannosidosis	α-Mannosidase	α-mannoside
β-Mannosidosis	β-Mannosidase	β-mannoside
Sialidosis	Neuraminidase	sialyloligosaccharides
Fucosidosis	α-L-fucosidase	fucoglycoconjugates
Aspartylglucosaminuria	Aspartylglucosaminidase	aspartylglucosaminide

1.12 Human MPS VI

1.12.1 Historical

MPS VI (Maroteaux-Lamy syndrome) was first described as a separate and distinct MPS by Maroteaux and colleagues in 1963 (Maroteaux *et al.*, 1963). Excessive urinary excretion of DS (HS not elevated) and absence of mental retardation were the key factors in distinguishing it from other MPS types, particularly as a Hurler syndrome variant. A 'corrective factor' for MPS VI was first reported as a semi-purified fraction from urine when it was shown to be able to correct GAG storage in cultured MPS VI fibroblasts. Later this was identified as 4S (Barton and Neufeld, 1972).

1.12.2 Genetics

MPS VI is inherited as an autosomal recessive disorder with an incidence of 1 in 250,000 live births in Australia (Meikle *et al.*, 1999a). The gene for human 4S has been cloned (Peters *et al.*, 1990b; Schuchman *et al.*, 1990) and localised to chromosome 5p11-5q13 (Litjens *et al.*, 1989). The broad continuum of clinical phenotypes from mild to severe is a reflection of the many different mutations in the 4S gene. At least 45 individual mutations (31 missense and 7 nonsense mutations, 7 small deletions and/or insertions) have been identified (Litjens and

Hopwood, 2001). As most patients are compound heterozygotes prediction of disease severity is generally complicated by the presence of two different mutations. However, severity is normally a reflection of the level of residual enzyme activity and the corresponding level of storage.

1.12.3 Clinical

The clinical features of MPS VI patients (reviewed in Neufeld and Muenzer, 2001) vary from mild to severe. Severely affected MPS VI patients occasionally present at birth with an enlarged or irregularly shaped head and deformed chest. Most often, however, the disease manifests as a failure to achieve normal growth between 2-3 years of age. Typically growth arrest occurs by 6-8 years of age with patients reaching a maximum height of between 110-140 cm. Skeletal abnormalities, termed dysostosis multiplex, are a major feature of MPS VI. They include abnormally shaped long bones, ribs and vertebrae with epiphyseal dysplasia, flared iliac wings of the pelvis and acetabular hypoplasia. Spinal kyphosis and an enlarged skull as well as hypoplastic odontoid processes are often observed. These changes are chronic and progressive and are the result of impaired bone formation (Neufeld and Muenzer, 2001).

Because there is no CNS involvement in MPS VI, normal intelligence is observed. Mental retardation has been reported although its cause has been attributed to other factors (Vestermark *et al.*, 1987). The major neurological problems are caused by bone abnormalities. Spinal cord compression in the upper cervical and/or thoracicolumbar regions can result in paresis/paralysis and is directly related to dural thickening (Wald and Schmidek, 1984). Carpal tunnel syndrome due to nerve entrapment is also common (Haddad *et al.*, 1997).

Progressive degeneration of all joints is prominent and leads to restricted movement culminating in an inability to walk. MPS VI patients also suffer from corneal clouding, which may progress to total blindness (this is not present in MPS II or III), hearing loss, thickened skin, facial dysmorphia and hepatosplenomegaly although the latter is not as severe as in MPS I. Heart valve and tracheal thickening lead to cardiac insufficiency and narrowing of the air passages, respectively. The latter, in conjunction with a shortened neck, contributes significantly to complications during anaesthesia. Severely affected patients generally die from cardiac and respiratory failure in the second decade of life. In less severe cases of MPS VI,

symptoms are attenuated and disease progression is slower with some patients attaining normal height and surviving to at least 60 years of age.

1.12.4 Biochemistry

1.12.4.1 Storage and pathology

As previously mentioned, storage of fragments of DS occurs in tissues and these fragments are excreted in urine. The heterogeneity of the storage products is due to the variable species of DS found in different tissues and to cleavage by endoglycosidases. 4S is involved in the degradation of both DS and CS. However, CS is not stored to any great degree in MPS VI. This is attributed to the action of hyaluronidase, a lysosomal endoglycosidase which has broad specificity in hydrolysing internal glycosidic bonds within CS oligosaccharides. Although elevated levels of sulphated mono, di, tri, tetrasaccharides and higher oligosaccharides are found in MPS VI patient urine only tetrasaccharides and higher can be detected using gradient-PAGE (Byers *et al.*, 1998). However, mono and disaccharides that have been fluorescently labelled can be detected on gradient-polyacrylamide gels after electrophoresis (E. Ranieri, Department of Chemical Pathology, WCH, unpublished observations). Alternatively, these small saccharide species can be detected by tandem mass spectrometry (MS/MS) (Ramsay *et al.*, 2003). A distinction between CS and DS tetrasaccharides cannot be made without further *in vitro* enzymatic digestion and analysis. Interestingly, GalNAc4S monosaccharides are also found in the urine and tissues of MPS VI patients (Hopwood and Elliott, 1985). Apart from the degradation pathway for DS described in section 1.7.3, an alternate pathway has been proposed (Figure 1.3). It is known that β-hexosaminidase A or S can hydrolyse the glycosidic bond between GalNAc4S and the adjacent uronic acid thus releasing free GalNAc4S. In normal individuals, desulphation of the GalNAc4S by 4S would then follow. However, at present it is not known to what extent this alternative pathway contributes to DS degradation in normal and MPS VI affected individuals.

Examination of tissue storage by light microscopy gives distinctive metachromatic inclusions while electron microscopy reveals clear vacuoles, which result from extraction of storage material during fixation, in most cells particularly those of mesenchymal origin such as fibroblasts of skin, aorta and heart valve, as well as in Kupffer cells, hepatocytes, corneal keratocytes and cartilage chondrocytes. Distinctive storage in white blood cells (WBC) is also observed.

1.12.4.2 Enzymology

4S deficiency is consistent with the type of storage product observed in MPS VI. This enzyme has been purified from human liver and its properties studied (McGovern *et al.*, 1982; Gibson *et al.*, 1987). It is synthesised as a 66 kDa precursor polypeptide which is processed to a mature form of 58 kDa which comprises three disulphide-linked subunits of 43, 7 and 8 kDa (Kobayashi *et al.*, 1992). Recombinant human 4S (rh4S), produced at high levels in Chinese hamster ovary (CHO) cells, has similar properties (Anson *et al.*, 1992b). 4S shares nucleotide and amino acid sequence homology with other known aryl and non-aryl sulphatases (Robertson *et al.*, 1988). A CTPSR motif is conserved amongst all the sulphatases and forms part of the active site (Bond *et al.*, 1997). A post-translational modification of the cysteine residue is essential for enzyme activity (Schmidt *et al.*, 1995; Dierks *et al.*, 1997; Cosma *et al.*, 2003; Dierks *et al.*, 2003)

The production of monoclonal antibodies to human 4S has enabled the development of immunochemical techniques to determine the level of residual 4S protein and activity and hence catalytic capacity of mutant enzyme (Brooks *et al.*, 1991). Some mutations in the 4S gene have been engineered into the normal 4S gene and expressed in CHO cells to determine the effect of individual mutations on enzyme activity, processing and targeting. In addition, the 3-D crystallographic structure of rh4S (Bond *et al.*, 1997) has been a valuable tool in determining the effect of mutations on enzyme structure and function (Litjens and Hopwood, 2001). While it is possible to demonstrate some correlation between MPS VI genotype and clinical phenotype a strict correlation is not found, presumably due to the influence of genetic background.

1.12.5 Diagnosis

A definitive diagnosis of MPS VI based solely on clinical or radiological assessment is not possible due to similarity in presentation with other MPS types. For the same reasons histological examination of blood smears for the presence of metachromatic inclusions in peripheral leucocytes is also non-informative in this regard. Diagnosis of MPS VI, as with other MPS, relies on a two-step approach. The first step involves urine analysis for elevation of GAG. This is followed by the identification of the enzyme deficiency in cultured skin fibroblasts or peripheral leucocytes using specific enzyme assays.

1.12.5.1 Urine analysis

Cetylpyridium chloride (CPC) precipitation of urinary GAG followed by quantification using the Alcian Blue method (Di Ferrante *et al.*, 1972) is usually the first step in the diagnosis of MPS. An elevated total GAG level, taking into account age-related reference ranges for both urinary GAG and creatinine, is generally indicative of a MPS disorder. The main disadvantage of this method is the inability to detect GAG of <3000 Da which are not precipitated by CPC (Hopwood and Harrison, 1982). The other disadvantage of this method is that in some MPS types, for example, MPS III and IV, and mild cases of MPS, total urine GAG is within normal limits, even though one particular GAG type may be elevated.

Determination of the type of GAG stored simplifies diagnosis. This can be achieved by high-resolution electrophoresis (HRE) where GAG classes are separated on the basis of charge and solubility in barium-ethanol (Hopwood and Harrison, 1982) and detected by Alcian Blue staining. A characteristic pattern is observed for the four main types of MPS (MPS I, II and VII have a similar storage pattern), each type showing an elevation in the particular stored substrate(s), for example, DS in MPS VI. Densitometric analysis then allows for the quantification of each GAG type. However, as this method does not give an unambiguous diagnosis for all the MPS, confirmation of a provisional diagnosis by enzyme analysis is required. Recently Ramsay *et al.* (2003) have used MS/MS to confirm the finding reported by (Hopwood and Elliott, 1985), by showing that elevated GalNAc4S and GalNAc4,6S support the diagnosis of MPS VI.

1.12.5.2 4S activity

An enzymatic diagnosis of MPS VI is indicated by reduced levels (<10% of normal control values) (Hopwood *et al.*, 1986, Litjens *et al.*, 1996) of 4S activity in cultured skin fibroblasts or peripheral leucocytes. To eliminate the possibility of multiple sulphatase deficiency, normal levels of other sulphatases must be demonstrated.

Assays to determine 4S activity have used both p-nitrophenol sulphate and the fluorophore, 4-methylumbelliferyl sulphate (4MUS). However, these synthetic substrates have poor specificity and are turned over equally well by other arylsulphatases (i.e., arylsulphatases A, C, D, E and F, although not arylsulphatase G (Ferrante *et al.*, 2002), and to a lesser extent by non-arylsulphatases (Bielicki *et al.*, 1998), thus potentially confusing diagnosis. In contrast, a

radiolabelled trisaccharide substrate derived from chondroitin-4-sulphate (C4S), closely resembles the natural substrate and is both highly specific for 4S and more sensitive than 4MUS (Hopwood *et al.*, 1986). The detection of carriers of MPS VI by 4S assay is not reliable as there is a large degree of overlap in the range of values for normal and carrier populations. However, molecular genetic analysis where one family member is affected allows for subsequent carrier detection and prenatal diagnosis.

For population studies or mass newborn screening the above methods are prohibitively time consuming. Alternative methods under development for rapid and direct analysis of GAG for newborn screening of MPS are the use of dimethylene blue, a cationic dye which binds to GAG (Whitley *et al.*, 2002), and MS/MS (Meikle *et al.*, 1997; Meikle *et al.*, 1999b). The latter method, which strives to encompass most of the LSD and not just the MPS, involves the detection of elevated levels of markers of LSD, such as LAMP-1 and saposin C, in dried blood spots followed by a second-tier MS/MS screen to determine the particular metabolite stored (e.g., GalNAc4S for MPS VI).

1.13 Bone synthesis and growth

In MPS VI and other LSD, skeletal dysplasia, characterised by shortened and disfigured bones, is a prominent feature. In order to understand the pathogenesis of this condition, a brief description of bone synthesis and growth follows.

1.13.1 Synthesis

Synthesis of bone during appositional bone formation occurs during developmental modelling, and at skeletal maturity, remodelling (Recker, 1992; Robey *et al.*, 1992). This is a complex process involving the coordinate activity of two major cell types, osteoblasts and osteoclasts, which are each regulated by the action of growth factors, hormones and cytokines. Osteoblasts are bone synthesising cells, which produce an extracellular matrix consisting predominantly of collagens and to a lesser extent PG. These structural components of the extracellular matrix are then modified to allow mineralisation to occur. Osteoclasts are bone-resorbing cells that require specific attachment to a bone surface in order to function. They dissolve bone mineral by increasing the acidity of the surrounding microenvironment through the action of osteoclast bound proton pumps. Acid proteases released from the osteoclast degrade protein in the

extracellular matrix creating pits into which osteoblasts can then bind. Bone formation takes place only where bone resorption has previously occurred.

1.13.2 Elongation/growth

Bone elongation also entails a complex sequence of events. During vertebrate development the fundamental mechanism for longitudinal bone growth is known as endochondral bone formation. This involves a highly regulated sequence of cell and extracellular matrix changes during which cartilage, an avascular tissue, is replaced by bone in a process called endochondral ossification. During this process the epiphyseal growth plate undergoes morphogenesis (reviewed in Howell and Dean, 1992). A region of resting chondrocytes at the distal end of the growth plate differentiates into a zone of proliferating chondrocytes that arrange into vertical columns. The extracellular matrix of the septae, which separate the columns of cells, is comprised predominantly of collagen and PG. In the hypertrophic zone, which is at the lower end of the growth plate, chondrocytes become enlarged and extracellular matrix modification occurs resulting in calcification of the septae *via* hydroxyapatite deposition. This is followed by vascular invasion from the metaphysis to remove apoptotic chondrocytes leaving behind mineralised cartilage septae which function as a scaffold for the attachment of bone producing cells (i.e., the osteoblasts and osteoclasts). The net result is lengthening of the bone while the thickness of the growth plates remains relatively constant. The growth plate is a transitory tissue responsible for longitudinal bone growth during childhood. At skeletal maturity the growth plate is resorbed and metaphyseal and epiphyseal bone become continuous.

In some of the MPS the process of bone synthesis and elongation is impaired and bone changes are severe and progressive. The deposition of DS in cartilage chondrocytes of the growth plate inhibits endochondral ossification resulting in short stature. In addition, a decrease in bone matrix mineralisation causes osteopaenia. This may be due not only to a reduction in the number and function of osteoblasts and osteoclasts in bone tissue but also to an incomplete maturation of these cells. The cause of skeletal pathology in the oligosaccharidoses has not been elucidated but presumably storage of oligosaccharides in cells associated with bone formation may affect the processes involved in a similar way as in the MPS. In Gaucher disease, which is one of the disorders of glycosphingolipid catabolism, bone pathology is a direct consequence of storage in macrophages, the cell lineage from which osteoblasts are

derived. In MPS IV, where the defect is in KS catabolism, the pattern of skeletal dysplasia is distinctive. One of the most common findings is odontoid hypoplasia, which together with ligamentous laxity can result in atlantoaxial subluxation that is life-threatening.

Bone formation and remodelling are complex processes and are likely to be affected in MPS VI at several levels. However, the end result is shortened stature and dysostosis multiplex, particularly of the pelvis, vertebrae and long bones.

1.14 Human fucosidosis

1.14.1 Historical

In the 1960s several cases were published as pseudo-Hurler disease on the basis of bone lesions similar to those found in Hurler disease and related conditions. Although severe CNS involvement was observed in all these cases, a distinct aetiology was proposed as no abnormal mucoploysaccharidurıa was detected. In 1966, Durand and colleagues (Durand *et al.*, 1966) reported two Italian siblings with progressive psychomotor degeneration, accumulation of lipid and glycans in vacuolated liver and skin cells and death before 5 years of age. The enzyme deficiency in this disorder was retrospectively found to be FUC after the subsequent identification of this enzyme (van Hoof and Hers, 1968) in a Belgian patient of Italian descent. The disease was originally called MPS F because of its resemblance to the MPS, but it is now referred to as fucosidosis as suggested by (Durand *et al.*, 1969). At about the same time, α-mannosidosis, sialidosis and aspartylglucosaminuria were also described and together with fucosidosis, were recognised as a new group of disorders, the oligosaccharidoses, resulting from defects in lysosomal enzymes that are responsible for glycoprotein catabolism.

1.14.2 Genetics

The incidence of fucosidosis is extremely low with approximately 100 patients reported worldwide. The majority of patients are from Reggio Calabria in Italy and the Mexican-Italian population of the USA. Because of the identification of many different mutations in these ethnic populations, a founder effect is probably not the explanation for this ethnic association. A high incidence of consanguineous matings (40%) would appear to be a contributing factor. Since the isolation of the human FUC gene (O'Brien *et al.*, 1987; Occhiodoro *et al.*, 1989), 22 mutations, which are spread throughout the gene, have been identified (Willems *et al.*, 1999).

These include 4 missense mutations and 18 nonsense mutations consisting of 7 stop codon mutations, 6 small deletions, 2 large deletions, one duplication, one small insertion and one splice mutation. All but two mutations are found in homozygous form, confirming the high rate of consanguinity in fucosidosis families. All the mutations result in almost the complete absence of FUC activity and protein.

1.14.3 Clinical

A clinical review of 77 patients, from 54 sibships, affected with fucosidosis has been published (Willems *et al.*, 1991). Since that time only a few additional patients have been reported. Briefly, the major clinical feature of fucosidosis is neuronal degeneration with progressive mental and motor deterioration. The most common clinical symptom at presentation is psychomotor delay between the ages of 0-5 years. Neurological involvement manifests as progressive muscle hypertonicity or spasticity. Most severely affected patients are unable to learn to talk, walk, sit or stand. Seizures are common and mental deterioration generally progresses to dementia. Radiological examination shows signs of dysostosis multiplex with enlarged skull, dorso-lumbar kyphosis and scoliosis and oval shaped vertebral bodies that show anterior beaking. Long tubular bones have a thin cortex and wide diaphyses and bones are usually osteoporotic. In addition patients may have a large coarse face with prominent forehead, a broad and flattened nose, thick lips and enlarged tongue. The skin is unusually thick, with profuse sweating and raised NaCl levels. Angiokeratoma corporis diffusum are also present, however, since they tend to develop at an older age this clinical sign is not usually observed in very severe patients who die at an early age. Cardiomegaly and hepatosplenomegaly are usually evident. Ocular abnormalities are not a major problem in fucosidosis, in contrast to the MPS where blindness may result from corneal clouding and glaucoma. Recurrent infections are common. Muscle wasting leads to cachexia, and death by 5 years of age is usually due to pneumonia. In less severe forms of fucosidosis, disease progression is not as rapid and patients may live to adulthood.

1.14.4 Pathology

Neuropathologic findings include prominent neuronal loss in the thalamus, hypothalamus and cerebral cortex, Purkinje cells and dentate nucleus (Durand *et al.*, 1969). Nerve cell bodies are distended and appear empty or filled with a slightly basophilic material. Although the cells usually appear vacuolated, unusual lamellated fibrilogranular intracellular inclusion bodies can

also be seen possibly because of accumulation of glycolipids. Severe damage to myelin sheaths and depletion of oligodendroglia have also been observed. Pathological abnormalities include varying degrees of vacuolation in all cell types from almost all tissues. Those cells with extensive vacuolation have a foamy cell appearance. These vacuoles appear clear on electron micrographs after fixation, as the storage products are water-soluble. However, in neural cells, dark inclusions with dense granular material and so-called zebra bodies are observed. These result from the storage of fucoglycolipids that are not water-soluble and hence remain after fixation. At postmortem several tissues are enlarged such as the liver, heart, brain, spleen and pancreas. This correlates with the ultrastructural studies that demonstrate high levels of storage in these tissues (Willems *et al.*, 1991).

1.14.5 Diagnosis

The deficiency of FUC activity results in elevated levels of fucoglycoconjugates in patient urine. Fucosidosis can be distinguished from other oligosaccharidoses by the distinctive chromatographic pattern of the orcinol/resorcinol-stained material upon thin layer chromatography of urine (Humbel and Collart, 1975; Sewell, 1979). Following this initial analysis, a definitive diagnosis based on residual FUC activity in either peripheral leucocytes, or cultured skin fibroblasts, using the fluorogenic substrate 4-methylumbelliferyl fucopyranoside (4MUF), is possible. Enzymatic levels below 10% are generally indicative of a fucosidosis phenotype.

1.15 Pathogenesis of LSD

The underlying cause of the vast majority of the LSD is the deficiency of a single lysosomal enzyme that results in the accumulation of a variety of endogenous substrates. These substrates have terminal residues that require the hydrolytic action of the deficient enzyme for cleavage. The type of substrate stored is dependent on the tissue or organ involved and the ensuing pathology reflects the location of the major sites of storage where undegraded GAG has impaired normal cell and organ function. Disease severity is dependent on the degree of residual enzyme activity. It is proposed that mild disease presents when enzyme activity is just below 10% of normal activity while <1% enzyme activity leads to a severe disease presentation.

Whatever the defect observed in any one LSD, the result is intracellular accumulation of storage material which eventually leads to cell and organ dysfunction. The precise relationship between lysosomal storage and impaired cellular function is unclear. It has been observed that cells with massive lysosomal storage, such as in neurones and hepatocytes, not only survive for long periods but also retain normal function (Hers, 1973). However, eventually the storage material impacts on cell function and several mechanisms have been proposed to explain this effect. The first of these is physical obstruction of cell function and interruption of metabolic pathways by large, storage-laden, intracytoplasmic vacuoles. An alternate explanation is that substances that accumulate may cause feedback inhibition in intracellular biochemical pathways. Toxic damage to cells caused by the accumulating substrates is another possibility. In Krabbe disease, for example, psychosine, an intermediate product, accumulates. When psychosine is injected into normal brain tissue damage such as nerve demyelination results (Suzuki and Suzuki, 1973). Primary stored substrates may inhibit the lysosomal degradation of other substrates. For example, HS has been shown to inhibit sialidase which is needed for the turnover of gangliosides (Jones *et al.*, 1997). Accumulation of gangliosides has been shown to be neurotoxic (Walkley, 1995; Walkley *et al.*, 1995). However, in general, stored substrates in LSD do not cause cell toxicity and it appears that the act of storage itself results in functional changes in the cell irrespective of the type of storage product (Huxtable and Dorling, 1985). It has also been observed that ultimately storage accumulation results in cell apoptosis. In one study it was shown that apoptotic chondrocytes from animals with DS storage disease released nitric oxide and inflammatory cytokines suggesting that these may be responsible for degenerative joint disease observed in the MPS (Simonaro *et al.*, 2001).

Distension of tissues either by excessive lysosomal storage or deposition of extracellular matrix, or both, as in enlarged and thickened trachea and aorta, also have a mechanistic (biophysical) impact on organ function.

In all LSD pathology in viscera is observed to varying degrees. However, two crucial sites are the skeletal system and the CNS. In those disorders where DS catabolism is affected, such as in MPS I, II, VI and VII, skeletal pathology is paramount, manifesting as dwarfism, dysostosis multiplex, epiphyseal dysplasia and osteopaenia. Normal bone growth in patients with these disorders is disrupted due to accumulation of DS fragments in the lysosomes of growth plate

chondrocytes. DS accumulation in osteoblasts and osteoclasts may also prevent proper bone mineralisation and remodelling resulting in dysostosis multiplex in these disorders.

Compared to bone and joints, the CNS has very little extracellular matrix and therefore very little DS. It is devoid of supporting collagenous tissue which is confined to penetrating blood vessels and meninges which invest the entire surface of the brain. Consequently, neurological symptoms are generally not seen in MPS VI where only DS is stored. In contrast, in those conditions where only HS degradation is affected, such as MPS III, neurological pathology predominates due to the involvement of HS in neural tissue development (Oohira *et al.*, 1994a). Neurological symptoms may also arise as a result of the secondary storage of gangliosides (see comments above) due to inhibition of neuraminidase by HS (Jones *et al.*, 1997). In those LSD where degradation of both HS and DS are impaired, both neurological and skeletal symptoms are observed.

In the oligosaccharidoses fucoglycoconjugate accumulation predominantly affects the CNS although the skeletal system may also be involved. In the sphingolipidoses, for example, Gaucher types 2 and 3, and Krabbe disease, undegraded glycosphingolipids cause severe neurological problems (reviewed by Beutler and Grabowski, 2001; Wenger *et al.*, 2001).

1.16 Therapies for LSD

1.16.1 Medical and surgical

Management of LSD patients has mainly involved surgical and medical intervention for the alleviation of symptoms as and when required (Muenzer, 1986; Neufeld and Muenzer, 2001). For example, corneal transplantation is used to replace cloudy corneas, tracheostomy alleviates obstructive airway disease, artificial heart valves have been used to replace diseased valves and surgery has been used to relieve severe joint contractures due to nerve entrapment, particularly of the carpal tunnel. Orthopaedic surgery is often used for the correction of deformed bones and joints, and hearing aids can restore some of the lost auditory function. Liver and/or spleen reduction or removal is also used to ease the burden of hepatosplenomegaly. However, none of these management strategies is capable of addressing the underlying disease itself.

1.16.2 Organ and tissue transplantation

The principle idea behind organ grafts was to replace a defective organ and at the same time provide a permanent self-renewing source of enzyme which could be taken up by deficient cells to clear the accumulated storage material. Transplantation studies using organs such as liver, kidney and spleen were attempted in the 1970s but without success (Desnick *et al.*, 1973a; Desnick *et al.*, 1973b; Groth *et al.*, 1973; Philippart, 1973). Transplantation of tissues other than solid organs, for example, amnionic cells, foetal and adult fibroblasts and foetal liver cells (Gibbs *et al.*, 1980; Tylki-Szymanska *et al.*, 1985), were considered safer than solid organs as these are simpler to transplant, requiring no invasive surgery, and rejection of the transplant is not life threatening. However, tissue transplants also failed to demonstrate any substantial or sustained benefit to the recipient patients.

1.16.3 Bone marrow transplantation

Based on the results of coculture experiments, which demonstrated that transfer of enzyme from lymphocytes to deficient fibroblasts was possible (Olsen *et al.*, 1981), and coupled with the increased ability to provide effective immunosuppression and so avoid graft rejection, bone marrow transplantation (BMT) became a feasible strategy for providing a permanent supply of replacement enzyme. Because of their predominantly multivisceral involvement, LSD were considered good candidates for BMT (Hobbs *et al.*, 1981).

However, BMT poses significant risks of morbidity and mortality to the patient. One of the main problems is the lack of suitable allogeneic bone marrow donors thus forcing reliance on the use of matched unrelated bone marrow. This results in transplant-related mortality estimated at between 20-50%, compared to 10% if allogeneic donor marrow were used (Hoogerbrugge *et al.*, 1995). The destruction of the patient's bone marrow by cytotoxic drugs and radiation, and immunosuppression to reduce graft versus host disease, also have significant side effects.

Despite these complications, BMT was until recently the only therapy available to treat most LSD. Limited numbers of MPS VI and MPS I patients have been treated with BMT and the main effects observed after successful engraftment have been on somatic pathology with subsequent improvement in quality of life and survival (Hobbs *et al.*, 1981; Krivit *et al.*, 1984; Hopwood *et al.*, 1993; Hoogerbrugge *et al.*, 1995). Joint mobility and cardiopulmonary

function are significantly improved, hepatomegaly is reduced, and as the levels of enzyme increase, there is a concomitant decrease in urinary GAG excretion and storage in liver and other tissues. Corneal clouding and some skeletal pathology are not improved although their progression is somewhat retarded. An accurate assessment of the efficacy of BMT is difficult as the LSD are clinically heterogeneous. Additionally, the age at which the transplants are performed is variable. It was apparent, however, that the crucial factor in effective BMT was treatment before the establishment of irreversible pathology. For example, MPS I patients transplanted early in life showed a slower than expected rate of mental decline (Hopwood *et al.*, 1993; Whitley *et al.*, 1993). A comprehensive follow-up of 54 MPS I patients reinforced the finding that children transplanted before two years of age showed a significantly better developmental trajectory compared with children transplanted after two years of age. Thus the older the child was at BMT the higher the likelihood of poor neuropsychological outcome (Peters *et al.*, 1998). In a number of MPS II patients receiving BMT, the procedure had no apparent effect on CNS pathology (Peters and Krivit, 2000). BMT in MPS VI patients has a similar outcome to that observed in MPS I patients with resolution of soft tissue such as reduction in hepatomegaly and spleen size as well as improvement in cardiopulmonary function and joint mobility. However, skeletal pathology and corneal opacity remained unaltered (McGovern *et al.*, 1986). Interestingly, BMT in a MPS III A patient showed no advantage in altering the clinical course of the disease despite being transplanted before the onset of CNS-related clinical symptoms (Sivakumur and Wraith, 1999).

Following the relative success of BMT in the fucosidosis dog model (section 1.21) this treatment was performed on an 8 month old presymptomatic fucosidosis patient whose early diagnosis, based on low FUC levels in plasma and peripheral leucocytes, was facilitated by having an older sibling diagnosed with the same condition (Vellodi *et al.*, 1995). Eighteen months after the transplant there was evidence of mild neurodevelopmental delay, which was far greater in his brother at the same age. Although this effect may be attributed to BMT, the possibility of intrafamilial variation cannot be excluded. A four year follow up of a female fucosidosis BMT patient also found improved psychomotor development as confirmed by evaluation of evoked sensory potentials and MRI brain scans (Miano *et al.*, 2001).

1.16.4 Enzyme-replacement therapy

The main focus for treatment of the LSD is to provide replacement enzyme to the affected tissues so correcting the metabolic defect. The seminal work that laid the foundations for ERT was carried out by Fratantoni *et al.* (Fratantoni *et al.*, 1968; Fratantoni *et al.*, 1969) who were first to demonstrate the cross-correction of fibroblasts from Hurler and Hunter patients by coculturing, or by using culture supernatant. Correction was subsequently observed using urine, serum and leucocyte extracts as a source of enzyme (Mapes *et al.*, 1970) as well as enzyme purified from tissues. However, initial ERT studies in patients using enzyme infusions were of limited success mainly due to the lack of purity of the infused enzyme, the problems of maintaining sufficient quantities of purified enzyme for treatment and the lack of a source of the mannose-6-phosphorylated form of the enzyme (Neufeld and Ashwell, 1980). With a greater understanding of cell surface receptors and the targeting mechanisms of lysosomal enzymes, and better purification techniques, ERT has resurfaced as a major treatment strategy in the 1990s. Renewed enthusiasm for ERT was brought about by the successful treatment of a Gaucher type I patient with deglycosylated human placental β-glucocerebrosidase (Barton *et al.*, 1991). The N-linked complex carbohydrate chains were treated to produce mannose-terminated oligosaccharides which facilitated specific uptake by macrophages of the reticuloendothelial system, which in type 1 Gaucher disease, is the main site of pathology. Treatment resulted in a reversal of splenomegaly thus eliminating the need for splenectomy, an increase in blood platelet numbers and haemoglobin concentration as well as an improvement in bone pathology. With the isolation of the gene for human β-glucocerebrosidase and the development of recombinant DNA technology, patients are now treated with recombinant enzyme which has also been manipulated to have mannose-terminated N-linked oligosaccharide chains. To date over 3000 patients with non-neuronopathic Gaucher disease, one of the more common LSD, have been treated. No difference between the efficacy of native placental β-glucocerebrosidase (Ceredase) and recombinant enzyme (Cerezyme) has been noted (Friedman *et al.*, 1999). Immunological responses to replacement enzyme have been minimal and only two patients have had therapy discontinued due to the generation of neutralising antibodies to β-glucocerebrosidase (Ponce *et al.*, 1997). A number of patients have generated an antibody titre to replacement enzyme. However, this has had no effect on the efficacy of therapy. Allergic reactions are treatable with anti-histamine premedication or slower rates of infusion (Pastores *et al.*, 1993; Richards *et al.*, 1993).

In 2001 the results of a one year trial in which ten MPS I patients ranging in age from 5 to 22 years, who were given weekly intravenous infusions of recombinant human α-L-iduronidase (0.5 mg/kg body weight), were published (Kakkis *et al.*, 2001b). In the six prepubertal patients the rate of growth, in terms of both height and weight, increased significantly. Hepatomegaly was reduced and in eight patients liver size was normalised by 26 weeks of therapy. Urinary GAG excretion was also reduced after 3-4 weeks of treatment with a mean reduction to 63% of baseline values. There was also a significant improvement in joint flexibility, particularly of the shoulder and elbow, and the number of episodes of apnea and hypopnoea during sleep was decreased by 61%. Serum antibodies to infused enzyme were detected in 4 patients but these did not impact on therapy (Kakavanos *et al.*, 2003). Trials of ERT in MPS VI, MPS II, Pompe and Fabry patients are in progress.

However, ERT has not benefited patients with the neuronopathic forms of Gaucher disease (Bove, 1995; Altarescu, 2001). In Gaucher type 2 disease, the acute neuronopathic form, the onset of neurological symptoms occurs between 3-6 months of age and progressive cerebral dysfunction leads to death before 1 year of age. Intravenous infusion of β-glucocerebrosidase in one patient with type 2 Gaucher disease, treated from 7 months of age, had no effect on disease progress, the patient dying at age 9 months. A sibling who was treated presymptomatically at 4 days of age had infusions continued until death at age 15.2 months. It appeared that therapy had prevented soft tissue pathology in this patient but had only delayed CNS dysfunction by a few months, using the older sibling for comparison of neurological disease progression. This study showed that ERT may have a minor effect in slowing CNS disease progression but it does not prevent the development of lethal CNS pathology even when initiated presymptomatically. Results of ERT in patients with type 3 Gaucher disease (the chronic neuronopathic form) are inconsistent (Schiffmann *et al.*, 1997).

1.16.5 Somatic cell gene therapy

The rationale behind gene therapy is the introduction of a functional copy of a defective gene into a patient's cells. Because LSD are monogenic disorders, and since many of the genes encoding lysosomal enzymes have been cloned, somatic-cell gene therapy for these disorders has become feasible. This can be achieved either by direct transfer of the gene into a specific tissue (*in vivo* gene therapy), or by introduction of the gene into a specific cell type isolated from a patient and then grafting these cells to an appropriate site in the patient (*ex vivo* gene

therapy). Theoretically either approach can provide a permanent and renewable source of enzyme, not only to the transduced cells but also to other cells which may recapture secreted enzyme *via* receptor-mediated uptake (M6PR).

Gene transfer can theoretically be accomplished either by transfection of plasmid DNA or transduction using viral vectors. However, in practice viral vectors are generally preferred and retroviral, adenoviral and adeno-associated viral (AAV) vectors have all been used. Of these, retroviral and AAV vectors are favoured as both are capable of chromosomal integration and therefore stable expression. Recently retroviral vectors have been designed based on lentiviruses, rather than Moloney murine leukemia virus, as lentiviruses, being able to transduce non-dividing cells, provide greater flexibility in approach (Verma and Somia, 1997). Lentivirus-mediated gene transfer has been used to correct airway cystic fibrosis transmembrane conductance regulator function in mice with cystic fibrosis (Limberis *et al.*, 2002)

There are two main approaches to somatic cell gene therapy. With the exception of haematopoietic stem cells (HSC), *ex vivo* gene therapy using other cell types (e.g., fibroblasts and myoblasts) has been generally abandoned due to problems in obtaining stable engraftment and expression. HSC-mediated gene therapy in murine systems has demonstrated the power of this approach but achieving efficient gene delivery to human HSC has proven difficult. *In vivo* gene delivery has now been widely explored and intravenous and intracranial delivery of vectors has been used successfully in a number of animal models. For example, a single stereotactic intracranial injection of rAAV containing a β-glucuronidase cDNA into the adult MPS VII mouse striatum showed that 10% of the injected hemisphere was positive for β-glucuronidase activity at 16 weeks post-injection. A complete reversion of lysosomal storage in this area, as well as in surrounding neurons and in the non-injected hemisphere, was also observed (Bosch *et al.*, 2000a). In a similar study intracerebral injection of the rAAV-β-glucuronidase vector in MPS VII mouse brains resulted in levels of enzyme activity of between 50 and 240% of normal levels and storage reduction was maintained for 3 months (Sferra *et al.*, 2000). Using the same vector Skorupa *et al.* (1999) also demonstrated persistence of β-glucuronidase activity up to 5 months after a single intracranial injection. No evidence for the presence of the vector genome on the contralateral side was found which indicated that retrograde transport of the vector did not occur. However, clearance of storage in areas distant

from transduced cells showed that correction at these sites was mediated by uptake of secreted enzyme that had diffused through the neural extracellular matrix from the transduced cells. The implication arising from this study was that larger areas of the brain could be treated by multiple intracranial injections strategically spaced to achieve overlapping spheres of enzyme diffusion. A study in which multiple injections (three into each hemisphere and one into the cerebellum) of a lentivirus vector containing the β-glucuronidase cDNA, demonstrated that 10 and 20% of the entire brain of adult MPS VII mice had β-glucuronidase staining at 6 and 16 weeks post-injection, respectively (Bosch *et al.*, 2000b). This was accompanied by a reduction in lysosomal storage, which in most areas of the brain was either complete or partial at 16 weeks. In areas where correction was partial, lesions persisted preferentially in glia and perivascular cells, but not in neurons, suggesting that enzyme endocytosed by neural extensions in areas of intense β-glucuronidase secretion undergoes retrograde transport to lysosomes in remote neural bodies.

To date, intravenous infusion of viral vectors has shown no advantage in treating CNS pathology. However, somatic pathology was improved in MPS VII mice receiving the rAAV-β-glucuronidase vector accompanied by induction of hepatocyte replication (Gao *et al.*, 2000). In addition, neonatal MPS VII dogs treated in a similar fashion with a retroviral vector showed a marked improvement in clinical pathology including absence of corneal clouding, a resolution of cardiac disease and a reduction in skeletal pathology which resulted in these dogs being ambulatory to at least 17 months post-treatment in contrast to untreated affected dogs that are unable to walk by 6 months of age (Ponder *et al.*, 2002).

Gene therapy approaches are also associated with the potential risk of cancer as random insertion of retroviral vectors into the host genome can disrupt oncogenes. Two cases of leukemia in patients treated for severe combined immunodeficiency disease with retroviruses have been reported recently (Kaiser, 2003). A long-term study of MPS VII mice treated with gene therapy has also shown the presence of tumours in these mice (Donsante *et al.*, 2001).

1.16.6 Substrate deprivation therapy

The approaches to therapy described previously rely on the direct or indirect provision of the deficient enzyme. Another strategy, which may be generally applicable to those LSD involving

predominantly glycosphingolipid storage, is substrate deprivation therapy. This method involves the use of a specific inhibitor of glycosphingolipid biosynthesis, thus reducing the amounts of these compounds synthesised. The success of this strategy relies on the presence of some residual enzyme activity to balance the reduced rate of glycosphingolipid synthesis. N-Butyldeoxynojirimycin is a potent inhibitor of glucosyltransferase, which is involved in the first step of the synthesis of glucosylceramide glycosphingolipids. This compound has been evaluated in the murine model of Tay-Sachs disease, which results from a deficiency in the β-hexosaminidase A isoenzyme that degrades GM_2 ganglioside. Positive results were seen in this study with an approximately 50% reduction in brain GM_2 gangliosides compared to untreated controls (Platt *et al.*, 1997). Electron microscopic analysis of neurons from the brains of treated mice also revealed a marked reduction in lysosomes containing lipid. A similar reduction in storage was observed with Sandhoff mice (Jeyakumar *et al.*, 1999). These mice also had increased longevity compared to untreated Sandhoff mice, which generally died within 6 weeks.

A recent trial of N-butyldeoxynojirimycin in Gaucher type 1 patients had little effect on the haematological abnormalities although liver and spleen volume were markedly reduced. Some adverse effects such as weight loss, diarrhoea and peripheral neuropathies were also reported (Cox *et al.*, 2000). In Krabbe disease and metachromatic leukodystrophy, where the biosynthesis of galactosylceramide and sulphatide storage material, respectively, are initiated by galactosyltransferase, the same approach is feasible although a different inhibitor would be required. The application of this therapy to human glycosphingolipid LSD such as Gaucher disease type 2 and 3, which do not respond to ERT, as well as Fabry, Tay-Sachs and Sandhoff disease, would appear feasible providing the treatment has few side effects. Similar approaches are now being developed for the MPS using inhibitors of GAG synthesis (Berkin *et al.*, 2000).

1.16.7 Neural and embryonic stem cell therapy

Therapeutic intervention by neural cell transplantation is one means of providing a new supply of neural tissue to replace the cells damaged by disease as well as a source of corrective factors. Transplants of human foetal neural tissue have had encouraging results in Parkinson's disease (Yurek and Sladek, 1990). However, the clinical use of a foetal tissue strategy is not only limited by the availability of quality controlled foetal tissue but also by ethical and societal issues. A possible solution to these problems lies in the recent discovery of embryonic

neural stem cells that are self-renewing and capable of differentiating into both neurons and brain supporting glial cells. As well as replacing cells lost to neurodegenerative disease, neural progenitor cells may also serve as a vector for gene therapy. This approach has been applied in the treatment of MPS VII mice (Snyder *et al.*, 1995). Intraventricular engraftment of neonatal MPS VII mice with neural stem cells transduced with a β-glucuronidase expression construct revealed diffuse migration of these cells throughout the brain and widespread correction of lysosomal storage in neurons and glial cells. The advantage of using neural stem cells over non-neural cell lines such as fibroblasts for the introduction of genes into the brain is the ability of the former cells to migrate within the parenchyma as well as to differentiate and integrate into the existing cellular architecture of the brain. However, research into both neural stem cells and their application is still at an early stage.

Damage to neurons in the CNS is usually permanent, as neural repair and renewal are generally not seen in the postnatal brain. However, the concept of irreversible neural damage has recently been challenged on the basis of results from a study in which injection of a feline immunodeficiency virus-based vector expressing β-glucuronidase into the striatum of MPS VII mice not only corrected cellular pathology but also behavioural function (Brooks *et al.*, 2002).

In conclusion, many therapies are being developed to treat patients with LSD. The most immediately applicable is ERT and the clinical use of ERT is expanding rapidly. Of the others, the approaches that appear more likely to proceed to clinical trials in the short to medium term include substrate deprivation therapy and some of the less contentious gene therapy approaches.

1.17 Animal models of LSD

Although cell culture systems have proved useful for studying the biochemical aspects of cellular pathology and correction of the LSD, they are unable to effectively model the complex biology/pathology of the clinical condition. Therefore, animal models of human disease for preclinical assessment of treatment modalities are superior as they more accurately reflect the disease state in patients. Breeding colonies of various animal models of the LSD have been established and these have been exploited to study the pathogenesis of analogous human disease, and more recently, to evaluate experimental treatment strategies, especially where

these may be difficult to justify in human subjects on ethical grounds. In contrast to human disease states where clinical heterogeneity is common because of a variety of mutations in the same gene, breeding colonies of animal models of disease have a uniform genetic cause thus making interpretation of results more straightforward.

A considerable number of naturally occurring animal models of LSD has been described. These have been detailed in a recent comprehensive review (Jolly and Walkley, 1997). Most are large domestic or farm animals such as the MPS IIID Nubian goat, α-mannosidosis Angus cattle, MPS VI and VII cats and dogs, GM_2 gangliosidosis dog and sheep and fucosidosis dogs. For laboratory experimentation, smaller animals have the advantage of being more easily and inexpensively housed and handled. Some of these naturally occurring small animal models include the MPS VII (Birkenmeier *et al.*, 1989) and MPS IIIA (Bhaumik *et al.*, 1999) mice, the MPS VI rat (Yoshida *et al.*, 1993a; Yoshida *et al.*, 1993b) and the α-mannosidosis guinea pig (Crawley *et al.*, 1999). Recently targeted gene disruption has been used to generate knockout murine models of MPS I (Clarke *et al.*, 1997) and MPS VI (Evers *et al.*, 1996), among others. Mice in particular are useful as animal models as they have short gestation times, large litter sizes and their genome size and number of genes is similar to humans. Generally, these animal models display pathology that parallels the corresponding human disease in all respects. However, differences have been noted, such as in the Tay-Sachs mouse, which escapes disease through partial catabolism of accumulated GM_2 by sialidase, the murine enzyme having a greater affinity for GM_2 than the human enzyme (Sango *et al.*, 1995). Mouse and rat models also differ anatomically and physiologically from humans in ways that may invalidate the conclusions drawn from experimental studies in these animals. For example, BBB development and bone growth plate closure are significantly different in rodents. This means that great care must be taken in extrapolating results from experimentation in mice to the human situation. The shortened time frame of mouse development can also make some treatment strategies difficult to assess.

Animal models of LSD can also be drug-induced. Ingestion of an indolizidine alkaloid, swainsonine, which is found in certain plant species, is a potent inhibitor of α-mannosidase and causes α-mannosidosis in livestock (Dorling *et al.*, 1978). In addition, dicationic amphiphilic drugs such as tilorone (Bispinck *et al.*, 1998) and its analogues (Hein and Lullmann-Rauch,

1989) can induce a LSD by formation of GAG-drug complexes which cannot be degraded by lysosomal enzymes and hence accumulate.

In the study of disease pathogenesis and effective therapies the MPS VII mouse, which has both skeletal and CNS pathology, has been especially important. However, to simplify analysis it may be preferable to study the somatic/skeletal system and the CNS in isolation. This is possible as some of the LSD exhibit predominantly neurological or skeletal symptoms. MPS VI in particular displays almost the full range of somatic pathology, especially joint and bone disease, which are of major importance in the LSD, in the absence of any detectable neurological disease. MPS VI is therefore an ideal choice to study the pathogenesis of somatic and skeletal disease and the effects of therapies in the absence of CNS involvement.

Naturally occurring MPS VI has been described in several animal models including a Siamese cat (Cowell *et al.*, 1976; Jezyk *et al.*, 1977), a miniature pinscher (Neer *et al.*, 1995) and a rat (Yoshida *et al.*, 1993a). A knockout MPS VI mouse has also been created by targeted disruption of the 4S gene (Evers *et al.*, 1996). In all species, lysosomal storage was observed in all somatic tissues and dysostosis multiplex and dwarfism were obvious in all species except the mouse. Cloudy corneas and degenerative joint disease, common in MPS VI patients, were seen only in the dog and cat. Therefore, to study the effects of therapies on these aspects of pathology, particularly skeletal dysplasia and joint disease, the MPS VI cat was considered an ideal animal model and a breeding colony was established in Adelaide from 'Family 3' heterozygotes (Haskins *et al.*, 1979a) obtained from Professor M. Haskins at The School of Veterinary Medicine, University of Pennsylvania, Philadelphia, USA.

Human fucosidosis has considerable neurological and skeletal pathology but the canine model of this disease has essentially neurological pathology only. Canine fucosidosis as a model of CNS pathology will be discussed in detail in section 1.20.

1.18 Feline MPS VI

MPS VI was first documented in a Siamese cat in the USA (Cowell *et al.*, 1976) and subsequently in other Siamese cats in Italy (Di Natale *et al.*, 1992) and various states in the USA (Haskins *et al.*, 1979b; Haskins *et al.*, 1983b). These cats had DSuria, significantly lower

levels of 4S compared to normal cats and metachromatic inclusions in neutrophils on blood smears. Disease severity was similar for all cats regardless of their origin. This implied either a predisposition for the same mutation in this breed of cats, or more likely, common ancestry. Clinical features of feline MPS VI and disease progression were similar to that observed in severe human MPS VI. Development in MPS VI cats is normal until 3-4 months of age at which time facial dysmorphia, corneal clouding and failure to thrive are noticeable. Between 4-7 months of age animals show signs of hindlimb paresis, possibly from bone growth abnormalities of the thoracicolumbar region of the spine resulting in spinal cord compression. Dysostosis multiplex, degenerative joint disease and lysosomal vacuolation in cells of most tissues are also observed. Cats appear to have normal intelligence and in contrast to human MPS VI where there is only slight liver enlargement cats display no obvious hepatomegaly (Haskins *et al.*, 1983a; Haskins *et al.*, 1983b; Haskins *et al.*, 1992).

The gene for feline 4S was isolated in 1992 and localised to feline chromosome A1 (Jackson *et al.*, 1992). The mutation responsible for feline MPS VI was identified in 1996 (Yogalingam *et al.*, 1996). The missense mutation L476P causes an almost complete lack of 4S activity. By analogy to the 3-D structure of rh4S (Bond *et al.*, 1997), which shares 91% homology with rf4S, the mutation is believed to cause disruption of a β-sheet, rendering the protein unstable and resulting in its degradation in the lysosome.

The identification of a second independently inherited missense mutation (D520N), was instrumental in resolving some anomalies observed in the MPS VI cat, particularly with regard to disease phenotype (Crawley *et al.*, 1998; Yogalingam *et al.*, 1998). For example, some cats with very low levels of 4S appeared normal apart from degenerative joint disease and inclusions in peripheral leucocytes and chondrocytes. The two mutations found in MPS VI cats result in three different genotypes, namely, L476P homozygotes, L476P/D520N heterozygotes and D520N homozygotes. The L476P homozygotes have the most severe phenotype (as described above) while the D520N mutation causes a milder phenotype. When homozygous the D520N mutation by itself is relatively harmless; double heterozygous cats may present late with degenerative joint pathology. The disease mutations are interesting in that they cover a spectrum of disease from mild to severe that is not normally observed in an animal model (Crawley *et al.*, 1998). Most mild cases of disease in animals remain undetected, as the animals are generally asymptomatic until old age. The development of a rapid polymerase chain

reaction (PCR)-based screening method has facilitated genotyping of cats at birth to distinguish between the mild and severely affected cats. This in turn has enabled better colony management and breeding outcomes. The P/N mutation was shown to be present in a number of MPS VI cat colonies that have been independently established supporting the hypothesis of a common ancestor (Crawley *et al.*, 2003).

1.19 Therapies for feline MPS VI and other animal models of LSD

1.19.1 Bone marrow transplantation

The effect of BMT in two studies using MPS VI cats has been evaluated. Two MPS VI cats given transplants at 6 months and 2 years of age demonstrated improvement in joint mobility and showed some resolution of facial dysmorphia. In addition, corneal clouding was reduced and 4S activity in liver and white blood cell extracts was normalised, as was urinary GAG excretion (Gasper *et al.*, 1984; Wenger *et al.*, 1986). In a later study five kittens treated at 10 weeks of age also showed improvement in bone density and trabecular bone formation as well as reduced disfigurement of long bones and improved motor skills (Norrdin *et al.*, 1993). In a larger study involving ten MPS VI cats, allogeneic BMT at between 3 to 47 months of age resulted in decreased GAG concentration, specifically DS (Dial *et al.*, 1997).

BMT has also been performed in other animal species. In newborn MPS VI rats BMT was less encouraging for treatment of bone pathology with only one rat out of the 24 engrafted showing clinical and/or radiographic improvement. 4S activity levels were normal in this animal as well as in 20 other animals that showed clinical improvement in several visceral organs such as liver and spleen and particularly in trachea and aorta (Simonaro *et al.*, 1997).

1.19.2 Enzyme-replacement therapy

The cloning of the human 4S gene (Peters *et al.*, 1990b; Schuchman *et al.*, 1990) facilitated the production of large amounts of recombinant enzyme carrying M6P (Anson *et al.*, 1992b) and the evaluation of ERT in the MPS VI cat. A preliminary trial of intravenously infused rh4S in older cats, using a variety of dosing conditions, was encouraging (Crawley *et al.*, 1996). It showed a dose-dependent retardation in disease progression and analysis of bone pathology indicated that an earlier onset of therapy resulted in a better prognosis. A significant antibody

titre was reported in one adult cat and this may have reduced the efficacy of treatment. In a second trial (Crawley *et al.*, 1997) weekly ERT was initiated at birth with 0.2, 1, and 5 mg rh4S/kg body weight. Apart from clearance of storage in liver Kupffer cells, virtually no effect on soft tissue and skeletal pathology was observed with the lowest dose of enzyme. However, with the higher dose rates a reduction in urinary GAG, tissue storage and bone pathology was observed. These were dose-dependent (Byers *et al.*, 1997; Crawley *et al.*, 1997). Cartilage chondrocytes and corneal keratocytes remained unaffected by treatment at all doses. In an attempt to enhance penetration into joints and cornea by decreasing the net negative charge of the enzyme, it was modified with polylysine or 1-ethyl-3-(3-dimethylaminopropyl) carbodiimide (EDC). However, this did not lead to any improvement in these tissues (Byers *et al.*, 2000). Treatment of cats from birth with rh4S appeared to induce tolerance to foreign enzyme as the majority of cats experienced only mild allergic reactions to enzyme infusions that did not compromise therapy. In addition, none of these animals developed antibody titres to h4S.

ERT studies in other animal models of LSD generally had similar effects. ERT in a feline model of MPS I using weekly intravenous doses of 0.1 and 0.5 mg recombinant human α-L-iduronidase/kg body weight over 3-6 months demonstrated enzyme in a wide variety of tissues, with spleen and liver having the highest levels (Kakkis *et al.*, 2001a). These tissues had a marked decrease in GAG storage and one cat in this study showed clearing of pre-existing corneal clouding. Enzyme was also consistently found in various brain samples although no improvement in histological appearance and ganglioside profiles was observed. Antibody titres to replacement enzyme were detected in several cats and these were higher in animals receiving the higher enzyme dose.

Several studies of ERT have been carried out in MPS VII mice. A preliminary trial of a single injection of recombinant human β-glucuronidase into new born mice sacrificed one hour after infusion indicated that enzyme was present to greater than normal levels in all tissues tested including brain (Vogler *et al.*, 1993). Another study compared the effects of treating MPS VII mice with one injection at 6 weeks of age with those receiving six weekly injections from birth (Sands *et al.*, 1994). Mice infused with a single dose of enzyme showed a decrease in lysosomal distension in fixed tissue macrophages but were phenotypically identical to untreated MPS VII mice. However, those treated from birth were difficult to distinguish from

age-matched normal control mice. Their body weights were nearly normal and they had reduced facial dysmorphia and skeletal pathology. Marked clearance of lysosomal storage in liver, spleen and kidney, and to a lesser extent in osteoblasts, was also observed although there was no improvement in chondrocytes, glia and some neurons, and cornea and aortic media had persistent lysosomal storage. In a following study, the impact of therapy from birth for six weeks on disease progression after discontinuation of therapy was assessed (Vogler *et al.*, 1996). Results indicated that although therapy improved survival and growth, storage rapidly reaccumulated to levels seen in untreated MPS VII mice. For example, by the 29th and 85th day after the final infusion storage in bone and fixed tissue macrophages, respectively, was identical to that seen in untreated MPS VII mice. However, the short course of therapy markedly improved bone growth, and morphological evidence of dysplasia was reduced even after one year, illustrating the importance of early intervention of therapy in improving GAG turnover in the period when the skeletal system is undergoing rapid growth.

Most of these initial studies of ERT in animal models were carried out using the human variant of the deficient enzyme as, for example, in feline MPS VI (Crawley *et al.*, 1996; Crawley *et al.*, 1997), canine MPS I (Shull *et al.*, 1994; Kakkis *et al.*, 1996) and murine MPS VII (Sands *et al.*, 1994; Sands *et al.*, 1997), and although clinical benefit was demonstrated, the full potential of ERT may not have been shown as the enzyme used was not native. Therefore, one of the aims of the work in this thesis was to determine the effects of using native enzyme, that is feline 4S, in the MPS VI cat, thus allowing a direct comparison of efficacy with the previous study in which human 4S was used.

1.20 Canine fucosidosis

Fucosidosis was first described in English springer spaniel dogs in Australia (Hartley *et al.*, 1982), and later in England (Littlewood *et al.*, 1983) on the basis of neurological symptoms and pathological abnormalities. A retrospective diagnosis of fucosidosis was assigned when the enzyme defect was identified in two littermates displaying similar signs of progressive neurological disease (Kelly *et al.*, 1983). A breeding colony was established in Australia at the University of Sydney, NSW by Professor Brian Farrow, Dr. Rosanne Taylor and Dr. P. Healy in 1984 to study the natural clinical and pathological course of the disease.

A detailed description of canine fucosidosis can be found in Taylor *et al.* (1987) and Kelly *et al.* (1983) and only a brief description will follow. Fucosidosis pups appear physically and neurologically normal at birth and progressively gain weight and height. However, as they grow they develop a longer, thicker coat and excessive feathering compared to normal dogs. In all cases of canine fucosidosis the main clinical sign is progressive neurological deterioration. One of the earliest signs, noticeable at about 4 months of age, is excessive anxiety, particularly on restraint. As mental dysfunction advances behavioural problems become exacerbated as dogs lose learned behavioural patterns. By 30 months of age they appear unresponsive to their environment and erratic, unpredictable and inappropriate behaviour develops.

Motor deficits are a characteristic feature of the disease and these become apparent at 12 to 15 months of age, although to a trained observer subtle changes are obvious much earlier. Mild hypermetria, a wide-based stance and limb proprioceptive deficits during movement, (particularly on turning) can be detected by 6-8 months of age as can other signs of significant psychomotor degeneration including ataxia, loss of balance and postural reactions such as wheelbarrowing, hopping and jumping. Sight and hearing progressively decline and dysphonia and hyperaesthesia become more pronounced. Signs of peripheral neuropathy are not observed and pain perception is maintained throughout the course of the disease. Most dogs with fucosidosis do not survive beyond 3 years of age when severely ill dogs are generally euthanased.

Although affected male dogs are sexually active until about 15 months of age, when psychomotor problems impede their ability to mount female dogs, they can still mate naturally with assistance up to about 20 months of age. However, affected male dogs are infertile due to low sperm counts. Sperm also show poor motility and morphological abnormalities. Fucosidosis females, despite irregular oestrus cycles, are reproductively normal up to 2 years of age. They bear small litters and generally mismother their pups (Taylor *et al.*, 1987; Taylor *et al.*, 1989b).

The disease in dogs parallels human fucosidosis in many respects although some differences are present. These are summarised in Table 1.3. The absence of bone abnormalities in fucosidosis dogs is presumably due to the onset of motor deficits occurring after bone maturation which occurs at puberty (approximately 9 months of age in these dogs). Compared

to patients, who have significantly shortened stature, fucosidosis dogs grow to a normal height. In human fucosidosis, neurological disease causes spasticity and rigidity resulting in patients being confined to bed from an early age. As disease progresses abnormal bone formation including delayed bone maturation and osteoporosis result due mainly to disuse atrophy. Other notable features of human fucosidosis not observed in the canine disease are facial abnormalities, thickened skin, profuse sweating, angiokeratoma, visceromegaly and recurrent infections.

Gross pathological examination of affected dogs at autopsy reveals massive peripheral nerve enlargement, especially of the cervical vagus and ulnar nerves. The latter is palpable in dogs with advanced disease. However, abnormalities in nerve conduction due to storage are not observed. Demyelination of nerves is also not seen although it has been reported in some fucosidosis patients. Conversely, peripheral nerve enlargement is not a feature of the human form of the disease (Willems *et al.*, 1991).

At the microscopic level, diffuse and generalised vacuolation of neurons and glial cells in the CNS is characteristic of both human and canine fucosidosis. It is progressive from birth and in dogs is widespread by 3 months of age. Enlargement of peripheral nerves is caused by vacuolated phagocytic cells and Schwann cells. Despite extensive vacuolation of soft tissues such as liver, spleen and heart in the dogs, these organs are not enlarged, whereas in human fucosidosis they are. Vacuolated lymphocytes are also present in blood, cerebrospinal fluid (CSF) and bone marrow in both human and canine fucosidosis.

Low FUC activity levels are detected in fucosidosis plasma, peripheral blood leucocytes, bone marrow, CSF and in all tissues tested including brain and nerves. Diagnosis of fucosidosis is made on the basis of low FUC activity levels (<10% of normal control levels) in plasma and peripheral blood leucocytes using the artificial fluorogenic substrate 4MUF. β-Hexosaminidase activity, rather than protein concentration, is generally used as a reference parameter for FUC activity. An empirically chosen discriminant function is used to differentiate between normal, carrier and affected animals. (Healy *et al.*, 1984). Biochemically, the canine disease resembles the most severe form of human disease, as there is almost complete absence of enzyme activity.

Table 1.3: Comparison of the disease features in human and canine fucosidosis.

	Human fucosidosis	Canine fucosidosis
Inheritance	autosomal recessive	autosomal recessive
Mutation	22 different mutations	14 bp deletion
Chromosome location	1p 32-34	chromosome 2
Residual FUC activity	<5-10%	<1%
Age of onset: mild clinical signs	5-24 months	6-15 months
severe clinical signs	1-3 years	1-3 years
Motor and mental deterioration	+	+
Coarse facies	+	-
Organomegaly	+	-
Angiokeratoma	+	-
Urinary oligosaccharides	+	+
Growth retardation	+	-
Dysostosis multiplex	+	-
Weight loss	+	-
Hyperhydrosis	+	-
Dysphagia	+	+/-
Vision loss	+	+
Hearing loss	+	+
Tissue accumulation of substrates	+	+
Peripheral nerve enlargement	-	+
Fertility	-	♀+/♂-

Data compiled from Willems *et al.* 1991 and (Taylor *et al.*, 1987; Taylor *et al.*, 1989b; Taylor *et al.*, 1989d).

Storage is similar in both species with fucoglycoconjugates accumulating in all tissues and excreted in urine. Fast atom bombardment mass spectrometry analysis of isolated storage products from brain show they contain asparagine as well as fucose, galactose, mannose and GlcNAc therefore confirming these are asparagine-linked oligosaccharides. The accumulation of glycoasparagines suggests that the hydrolysis of fucose by FUC is the rate-limiting step in the release of oligosaccharide from the asparagine residue (Barker *et al.*, 1988).

Canine fucosidosis in Australia and England can be traced back to a common English ancestor. The isolation of the gene for canine FUC (cFUC) and the mutation responsible for fucosidosis in dogs has been established (Occhiodoro and Anson, 1996; Skelly *et al.*, 1996). This mutation, a 14 bp deletion, causes a frame-shift and a premature stop codon at the 3' end of exon 1. Consequently FUC activity and protein are almost totally absent in all cells and plasma. Discovery of the mutation in dogs has enabled the development of a PCR-based screening test to detect both carriers and affected dogs.

Having considered the clinical, biochemical, neurological and genetic properties of canine and human fucosidosis it is apparent that canine fucosidosis is a useful animal model of the human disease because of the considerable similarities identified. Clinically, it more closely resembles the intermediate form of human fucosidosis while biochemically a severe phenotype is predicted due to almost negligible residual FUC activity. Other factors enhance the usefulness of canine fucosidosis as an animal model. Heterozygote/heterozygote matings result in large litter sizes (five to eight pups) thus ensuring breeding of adequate numbers of affected and carrier animals, to study disease pathogenesis and treatments, and at the same time to establish a breeding colony to secure the defective gene which is inherited in an autosomal recessive manner (Healy *et al.*, 1984). Furthermore, late onset of disease permits breeding from affected female dogs thereby increasing the chance of affected animals. Rapid and reliable enzymatic analysis of plasma and circulating peripheral leucocytes for FUC/β-hexosaminidase activity enables diagnosis within 24 h of birth. Phenotype can be confirmed later by PCR-based mutation analysis.

Compared to cattle and goats, the dog is a more convenient size to handle, accommodate and evaluate clinically under laboratory conditions. In assessing treatment strategies large animals are preferable in that sequential tissue and blood sampling is not restricted to the same extent as

in rodent models. In addition neurological and clinical observations after treatment can be monitored more easily than in smaller animals. The absence of skeletal pathology in the fucosidosis dog does not confuse interpretation of clinical observations. It is also believed that therapies in larger animals may more accurately reflect what would happen in affected children. In addition, longer-term studies are possible in larger animals compared to rodents and these are more relevant to the human condition. Finally, as disease progression in other LSD follows a similar course, canine fucosidosis may be of more general interest to the study of other neurovisceral LSD, particularly the oligosaccharidoses and the neurological aspects of some MPS.

1.21 Therapies for canine fucosidosis and other animal models of LSD

BMT has been evaluated in fucosidosis dogs aged between 4 and 30 months of age at the time of transplant using total lymphoid irradiation as the sole form of immunosuppression (Taylor *et al.*, 1986). Successful engraftment was monitored by plasma and peripheral leucocyte FUC activity levels. These increased to 30% and 100% of plasma and leucocyte donor levels, respectively, after 3 months of engraftment and stabilised thereafter. FUC activity levels in viscera and peripheral nerves were higher than in CNS, which required engraftment of greater than 6 months to achieve 20% of normal levels. A reduction in the histological storage lesions in these tissues was also observed (Taylor *et al.*, 1989d). However, BMT in fucosidosis dogs with advanced disease had no effect in preventing normal disease progression. In contrast, one dog transplanted at 4 months of age developed only mild clinical symptoms 3 years after BMT, whereas transplantation of slightly older dogs clearly demonstrated a delay in the onset of neurological dysfunction (Taylor *et al.*, 1989a).

Two important observations arose from these studies. Firstly, early intervention before the onset of symptoms is crucial for the successful treatment of neurological symptoms (Taylor *et al.*, 1989a; Ferrara *et al.*, 1992; Taylor *et al.*, 1992). Secondly, correction of CNS pathology by BMT is a slower process, requiring up to 6 months, compared to correction of visceral tissues and peripheral nerves which takes place within 2 months (Taylor *et al.*, 1989c). Under normal circumstances few monocytes or macrophages migrate into the CNS, except when precipitated by immune reactions, and it would appear from the fucosidosis dog studies that at least 6

months is necessary for donor-derived macrophages to achieve significant repopulation of the CNS.

Experimentation with BMT in other animal models of LSD has underscored the importance of instituting BMT as early as possible to achieve optimal therapeutic outcome, especially for CNS disease. For example, BMT in an 8-week-old α-mannosidosis kitten resulted in the greatest clinical improvement compared to kittens transplanted at 10 and 12 weeks of age. α-Mannosidase activity in the brains of these cats reached levels of up to 40% of normal control levels with a corresponding decrease in storage lesions in neurones and glia (Walkley *et al.*, 1994). Similarly, BMT-treated MPS I dogs (Shull *et al.*, 1987; Shull *et al.*, 1988; Shull and Walker, 1988; Haskins *et al.*, 1991) showed a reduction in disease severity and had slower disease progression. Histological examination of brain tissue demonstrated a reduction in storage lesions in neurons and brain supporting cells which was attributed to low levels of α-L-iduronidase activity (1-3% of normal control levels). There was also a noticeable improvement in skeletal pathology, corneal and cardiovascular disease and urinary GAG excretion was reduced. Response to BMT in 'twitcher mice' (a model of Krabbe disease) was also dependent on age at transplant. Ten-day-old mice had improved CNS symptoms and increased lifespan compared to mice transplanted at 21-28 days of age when neurological problems are already obvious. In 'twitcher mice' peripheral nerve demyelination is caused by psychosine toxicity as a result of galactosylceramidase deficiency. However, in response to BMT, remyelination of nerves has been noted (Yeager *et al.*, 1984; Hoogerbrugge *et al.*, 1988; Suzuki *et al.*, 1988; Hoogerbrugge *et al.*, 1989).

Syngeneic BMT in MPS VII mice was effective in prolonging life span by up to three-fold and resulted in essentially complete correction of liver, spleen, cornea and glomerular mesangial cells while only partial correction of meninges, perivascular cells in the brain and renal tubular epithelial cells was noted (Birkenmeier *et al.*, 1991). A comparative study of BMT in adult and new born MPS VII mice (Sands *et al.*, 1993) revealed that lysosomal storage in many tissues, but not skeleton or brain, was decreased in the adult mice. However, newborn bone marrow transplanted mice enjoyed a longer life, had less severe facial dysmorphia and were more mobile with increased levels of β-glucuronidase activity in liver, spleen, kidney and brain and a corresponding reduction of lysosomal storage, although this was minor in brain neurons. In bones, joints and periarticular tissue there was less histological evidence of lysosomal storage

compared with untreated MPS VII mice. Long bone growth retardation and cerebellar and retinal dysplasia, seen in the newborn mice, were associated with the use of radiation ablation therapy and were not seen in adult mice receiving BMT.

Most forms of therapy for LSD in animal models, whether BMT, systemic enzyme replacement or gene therapy, have shown that somatic, and to some extent skeletal pathology, can be prevented, reversed or delayed depending on the age of onset of therapy and the severity of the disease. However, apart from BMT, which relies on the slow migration of macrophages into brain to supply enzyme, CNS pathology has remained refractory to those therapies that require enzyme to penetrate into the brain from the peripheral circulation. The presence of the highly selective BBB prevents most macromolecules, including lysosomal enzymes, from entering the brain from circulation. The properties of the BBB and possible strategies to circumvent it to allow effective ERT for the CNS will be discussed in the following sections.

1.22 The blood-brain barrier

Despite the demonstration of the existence of the BBB by German microbiologist Ehrlich more than 100 years ago, it was not until 1967 that electron microscopy revealed that the BBB is an endothelial barrier present in capillaries that surround the brain (Reese and Karnovsky, 1967). Reviews of the BBB include Pardridge (1991), Pardridge (1993), Rubin and Staddon (1999) and Bickel *et al.* (2001). Briefly, the BBB is a physical, limiting barrier, which separates the brain interstitial fluid from the blood circulation. It serves the dual purpose of ensuring homeostasis within the CNS and of delivering essential nutrients to the brain. The barrier consists of a non-fenestrated, continuous endothelial lining of microvessels. The endothelial cells are held together by tight junctions and form an epithelial-like high resistance barrier. The major components of the BBB are illustrated in Figure 1.5. The lumen of the capillary is thought to be very narrow, approximating the diameter of a red blood cell. The lumenal surface of the endothelial cells is coated with a glycocalyx composed of glycoproteins, which confer a net negative charge to this surface. Endothelial cells have few pinocytic vesicles but abundant mitochondria, as their role in maintaining homeostasis within the brain is a highly energy-dependent process. In addition to, or forming part of, the glycocalyx are receptors, cell adhesion molecules (CAM), integrins and other ligands. The gaps or 'windows' that are present between the cells in most tissues are absent in brain endothelial cells. Instead tight

junctions made up of opposing plasma membranes are found (Brightman and Tao-Cheng, 1993). These tight junctions prevent trans-capillary cell migration and movement of macromolecules. Specific proteins identified in these tight junctions include ZO-1 (zonula occludens-1), ZO-2, occludin and neurolethin (a member of the Ig superfamily of CAM). These proteins have been postulated to have both a structural and a signal transduction function (Staddon and Rubin, 1996; Bolton *et al.*, 1998).

The basement membrane (BM) holds the endothelium together and helps to maintain its overall tubular shape. It is made up of non-fibrillar type IV collagen, laminin, PG (e.g., HSPG) and fibronectin. Embedded in the BM are pericytes. These are contractile cells analogous to the smooth muscle cells of microvessel circulation and are involved in regulating blood flow. Pericytes also have phagocytic activity, are involved in antigen presentation and have a role in the regulation of the immune interface between the blood and brain. This is linked with their role in the control of BBB permeability.

Astrocytes are members of the largest class of brain cell, the glial cells. The astrocyte end feet (*glia limitans*) ensheath the capillaries and contribute to the structural integrity of the BBB, not just physically, but also *via* the production of soluble factors. These factors are involved in the induction of tight junctions. Culturing brain endothelial cells *in vitro* does not result in cells with tight junctions while co-cultivation with astrocytes or astrocyte-conditioned medium induces their formation (Arthur *et al.*, 1987; Janzer and Raff, 1987).

The blood-CSF barrier is another barrier separating the CNS from the periphery (Bickel *et al.*, 2001). It is located at the circumventricular organs (CVO) and has the properties of a secreting epithelium with leaky capillaries lacking endothelial tight junctions. The diffusion barrier within the CVO lies at the level of the ependymal cells, which are connected by tight junctions. The main CVO is the choroid plexus, which lines the ventricles and secretes CSF. Because the surface area of the CVO is an order of magnitude smaller than that of the BBB, delivery of therapeutics by diffusion into CSF, or intraventricular administration *via* intrathecal catheters, is not considered an efficient way of delivering these substances into the brain and will not be considered further in this thesis.

Figure 1.5: The blood-brain barrier.

Diagrammatic representation showing endothelial cells joined by tight junctions, which form the basis of the BBB. The endothelial cells have large numbers of mitochondria and few pinocytic vesicles and the lumenal surface is coated by a glycocalyx which confers a net negative charge to this surface. Structural support is provided by the basement membrane and astrocytes, which ensheath the endothelial cells and synthesise factors important in maintaining tight junctions. Pericytes are involved in regulating blood flow through the brain capillaries.

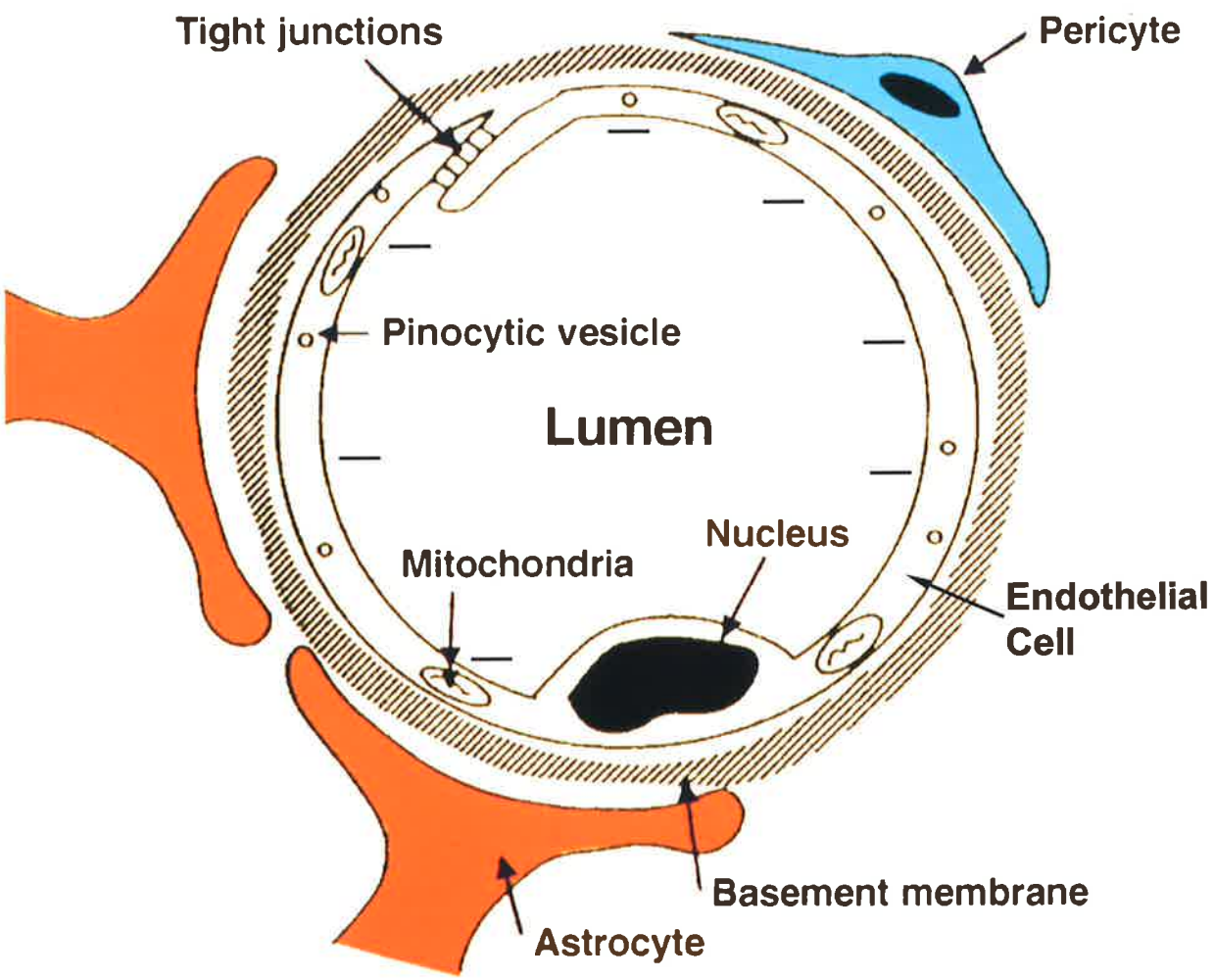
Tight junctions
Pericyte
Pinocytic vesicle
Lumen
Nucleus
Mitochondria
Endothelial Cell
Basement membrane
Astrocyte

1.23 Mechanisms for transport into the brain

Several strategies for brain drug delivery are known (Pardridge, 1991; Bickel *et al.*, 2001). These can be broadly classified as invasive or non-invasive. Invasive strategies involve surgical intervention, for example, by intraventricular infusion *via* an intrathecal catheter. Due to CSF circulation in brain being in a rostral to caudal direction, and because the rate of turnover of CSF is very high (21 ml/hr in an adult human brain), any substance administered *via* CSF is rapidly cleared (Shapiro *et al.*, 1975). Any substance taken up by brain tissue is generally restricted to the periphery and does not penetrate into the deeper tissue layers of the brain.

Apart from intracerebral implants, which are associated with high risk, BBB disruption is another method for drug delivery. BBB disruption is the induction of a temporary and reversible opening of the BBB by hyperosmolar shock which involves intra-carotid injection of a 1.4 M solution of either mannitol, L+arabinose, sucrose or urea (Rapoport, 1996). Electron microscopy studies show that this increases permeability by shrinking endothelial cells, resulting in the rupture of tight junctions (Greenwood *et al.*, 1988). The major drawbacks to the use of hyperosmolar shock include induction of strokes, seizures and brain oedema. Repetitive hyperosmolar opening of the BBB is associated with neuropathological changes in the brain (Salahuddin *et al.*, 1988b; Salahuddin *et al.*, 1988a; Sokrab *et al.*, 1988). Moreover it involves general anaesthesia and would not be practical to treat large numbers of patients on a regular basis.

Non-invasive methods are either pharmacologically based, rely on lipidization strategies for small molecules, or emanate from an understanding of the anatomy and physiology of BBB transport processes (Pardridge, 1991; Poduslo *et al.*, 1994). These will be discussed in more detail below.

Paracellular pathway: All the known mechanisms of transport across the BBB are summarised in Figure 1.6. The paracellular pathway for the diffusion of circulating solutes through the BBB is not applicable to macromolecules because of the existence of tight junctions. Bulk fluid-phase endocytosis or pinocytosis, which involves the internalisation of a

small portion of extracellular fluid environment, is also not applicable as few pinocytic vesicles are present in BBB endothelial cells.

Transcellular pathway: The transcellular pathway is used to move small peptides and proteins against their concentration gradient. It is a non-saturable, temperature and energy-dependent process, which is also dependent on the lipophilicity and molecular weight of the molecule. It is generally applicable to compounds of <600 Da. The large surface area of the BBB (approximately 12 m^2 with a vascular volume of 1.2 ml) (Zlokovic and Apuzzo, 1998) provides a vast lipid surface for this transcellular pathway. This pathway allows certain molecules to gain ready access to the brain because they are lipid soluble, (that is, they have a high octanol-water partition coefficient). For example, diacetylmorphine (heroin) is lipid soluble and therefore passes readily through the BBB. Morphine, however, which is the deacetylated form of heroin, is more polar and is taken up by brain 100 times more slowly (Oldendorf *et al.*, 1972).

Liposomes and nano-particles have limited application in the transport of large proteins across the BBB. Particles larger than about 50 nm are taken up predominantly by the reticuloendothelial system (Gregoriadis, 1989; Gennuso *et al.*, 1993). Specific targeting to the brain has been attempted using small particles and those of a composition which were predicted to favour uptake at the BBB. However, these have not been successful (Umezawa and Eto, 1988; Schroeder *et al.*, 1998).

Carrier-mediated transport: Carrier-mediated transport is used to transport nutrients such as glucose, nucleotides and amino acids across the BBB. This mechanism is saturable, temperature and energy-dependent, stereospecific and occurs *via* a number of highly specific transporter molecules. GLUT-1, for example, is the brain specific glucose transporter. L-dopa is transported *via* the neutral amino acid transporter and the tyrosine transporter will mediate transport of small peptides with tyrosine tails, such as encephalin (Mr 5,000 Da). Although the exact mechanism of the transmembrane movement of these molecules is not known, these transporters are both biochemically and sterically limited to transport of specific molecules (Broadwell, 1989). Therefore glucose or amino acids cannot be used as carriers for the transport of larger molecules such as peptides and proteins.

Receptor-mediated transcytosis: Two types of endocytic mechanisms have also been described for transport of molecules across the BBB (Friden, 1994; Poduslo *et al.*, 1994; Abbott and Romero, 1996; Pardridge, 1997). The first of these is specific or receptor-mediated transcytosis, a process involving binding of macromolecules to specific receptor sites on the endothelial cell surface. It is a saturable, energy and temperature-dependent process shown to operate for insulin (Pardridge *et al.*, 1985), transferrin (Tf) (Jefferies *et al.*, 1984) and IGF (Duffy *et al.*, 1988) *via* receptors found on the endothelial cell surface. The importance of these receptors to CNS function comes from evidence that there is no synthesis of the corresponding ligand within the CNS (that is, as shown by undetectable levels of mRNA), while the ligand itself is found, sometimes at high levels (Baskin *et al.*, 1983).

The mechanism of receptor-mediated uptake involves a number of steps (Broadwell, 1989). Binding of ligand to its specific membrane receptor initiates the process by inducing clathrin-coated pits to invaginate and form endocytic vesicles. Fusion with an acidic pre-lysosomal compartment causes dissociation of the receptor-ligand complex allowing the free receptor to recycle to the plasma membrane. Following dissociation, the ligand is thought to bind to a second intracellular receptor system to enable transport of the ligand to the ablumenal surface for exocytosis.

Adsorptive-mediated transcytosis: The final mechanism for transport of molecules across the BBB is adsorptive-mediated transcytosis (Pardridge, 1991). This process is ten-fold slower compared to receptor-mediated transcytosis but there is a greater capacity to move material by this process (due to the vast surface area of the BBB) than by receptor-mediated transcytosis. Again it is an energy and temperature dependent process, however, it does not involve specific plasma membrane receptors and instead is dependent on the charge interactions between the surface of the endothelial cells (negative) and the charge of the compound. Endocytosis is initiated by electrostatic interaction and then transcytosis proceeds in a similar way to receptor-mediated transcytosis as discussed above.

Figure 1.6: Mechanisms of transport across the BBB.

A diagrammatic representation of the BBB showing routes for transport across the brain endothelium. (a) Tight junctions between endothelial cells permit the diffusion of small water-soluble compounds only (paracellular aqueous pathway). (b) The large surface area of the lipid membranes of the endothelium provides an effective diffusive route for small lipid soluble compounds (transcellular lipophilic pathway). (c) Transport proteins found in the endothelium deliver mainly nutrients such as glucose, amino acids, nucleotides and other substances. This pathway is sometimes referred to as carrier-mediated transport. (d) Certain proteins such as insulin and transferrin are taken up by specific receptor-mediated endocytosis. (e) Most native plasma proteins are poorly transported, however, cationization can increase their uptake by adsorptive endocytosis (Abbott and Romero, 1996).

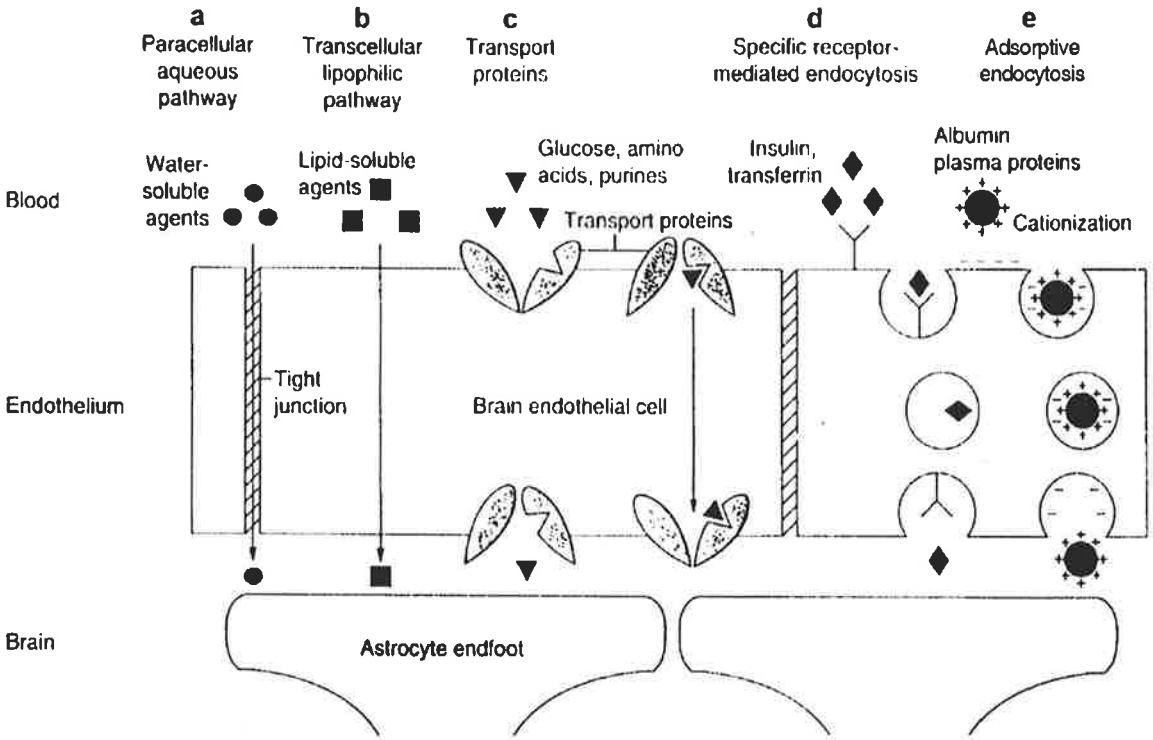
a
Paracellular aqueous pathway
b
Transcellular lipophilic pathway
c
Transport proteins
d
Specific receptor-mediated endocytosis
e
Adsorptive endocytosis
Blood
Endothelium
Brain
Water-soluble agents
Lipid-soluble agents
Glucose, amino acids, purines
Transport proteins
Insulin, transferrin
Albumin plasma proteins
Cationization
Tight junction
Brain endothelial cell
Astrocyte endfoot

1.24 Transport of conjugates and modified proteins into the brain

Of the non-invasive transport mechanisms discussed above the two with greatest potential for transporting proteins and peptides into brain are receptor and adsorptive-mediated transcytosis.

1.24.1 *Via* adsorptive-mediated transcytosis

Adsorptive-mediated transcytosis relies on the attraction between the endothelial cell surface and the compound to be transported. Therefore increasing electrostatic interaction by increasing the positive charge on the protein, a process known as cationization, should enhance uptake through the BBB.

The chemical process of cationization converts the surface carboxyl groups of acidic side chains of amino acids, such as aspartic and glutamic acids, into basic moieties. This is accomplished by coupling of diamino molecules such as hexamethylenediamine, or polyamines such as polylysine, to carboxyl groups that have been activated using EDC. This leads to the formation of an amide bond and to the introduction of one primary amino group for each conjugated polyamine molecule. EDC-activated polyamine cationization of proteins is dependent on the number of surface acidic amino acids and on the temperature and pH of the reaction. The extent of cationization is inversely related to pH and can be experimentally determined by isoelectric focussing.

In vivo experiments in rats with BSA cationized by covalent coupling with hexamethylenediamine (pI >10) demonstrated enhanced uptake into the brain compared with native BSA (pI 4) (Triguero *et al.*, 1990). Approximately 15% of the cationized BSA taken up by brain was transcytosed into the brain parenchyma as determined by capillary depletion. Similarly, cationized rat serum albumin (RSA) accumulated to 0.14% of the injected dose in brain tissue one hour after intravenous injection while native RSA was undetectable (Pardridge *et al.*, 1990b). Importantly, repeated daily injections of cationized RSA over 8 weeks were non-toxic to rats as evident by a gain in body weight which was comparable rate to control rats receiving native RSA (Pardridge *et al.*, 1990b).

As a means of providing antibody therapeutics to brain tissue, IgG molecules have also been cationized with hexamethylenediamine resulting in an increase in pI >10.7 (Triguero *et al.*, 1990; Bickel, 1995). Cationized IgG molecules showed similar kinetics of brain uptake to cationized BSA. Transcytosis of cationized IgG into brain was clearly demonstrated by thaw mount autoradiography of brain slices following internal carotid artery perfusion, as well as from total brain homogenates after capillary depletion to eliminate cationized IgG sequestered in the vasculature. A more detailed study with cationized superoxide dismutase (SOD), using the naturally occurring polyamines putrescine, spermidine and spermine has been reported (Poduslo and Curran, 1996b). Putrescine has two amino groups and hence two positive charges, while spermidine and spermine have three and four, respectively (Figure 4.17). Cationization with these compounds therefore results in the addition of one, two and three positive charges, respectively, for each polyamine moiety linked to an acidic carboxylic acid group on the protein. Experiments with SOD modified at low pH (4.7), although demonstrating a 22-fold increase in permeability into brain compared to unmodified SOD, also resulted in a significant loss of enzyme activity (95%). Interestingly there was an inverse relationship between the degree of valency and transcytosis into the brain suggesting that too great a positive charge was not necessarily beneficial for transcytosis across the BBB. These observations suggested that mechanisms other than simple electrostatic interaction involving charge density play a role in enhancing permeability. In addition, polyamine-modified proteins do not affect permeability directly at the BBB as native SOD transcytosis into brain was not enhanced in the presence of putrescine-modified SOD (Poduslo and Curran, 1996b). Consequently, in order to minimise the reduction in SOD activity, reaction conditions were changed. This was achieved by performing cationization at a higher pH (5.7) resulting in the retention of 50% of activity. However, this caused a ten-fold decrease in permeability (Poduslo and Curran, 1996a). Similar results were obtained with catalase, another antioxidant enzyme (Wengenack *et al.*, 1997b). Polyamine modified SOD with preserved enzyme activity, also significantly reduced hippocampal CA1 neuron loss following global cerebral ischaemia in rats (Wengenack *et al.*, 1997a) directly demonstrating a biological effect of an enzyme delivered by adsorptive-mediated transcytosis.

1.24.2 *Via* receptor-mediated transcytosis

One way of taking advantage of receptor-mediated transcytosis for transport of proteins normally excluded from the brain is to produce chimeric peptides. This involves the formation of a conjugate or chimera between the non-transportable protein and a transport vector, which is known to be actively transported into the brain, such as insulin and Tf, alternatively the transport vector can be an antibody to their receptors on the BBB. A chimeric protein can be made by covalently joining these two protein components using a suitable crosslinking reagent. Such chemical crosslinkers are heterobifunctional reagents consisting of two dissimilar functional groups of different specificities (Figure 1.7). For example, sulfosuccinimidyl 6-[3'-(2-pyridyldithio)-proprionamido] hexanoate (SPDP) is a heterobifunctional crosslinker which has one reactive functional group, N-hydroxysuccinimide (NHS), that is selective for amino groups, and the other, pyridyl disulphide, that is reactive towards a sulphydryl group. At alkaline pH primary amines are unprotonated and will react by nucleophilic attack on the NHS esters resulting in the formation of an amide bond and the release of NHS. The pyridyl disulphide group will react with a free thiol group to form a disulphide bond, releasing pyridine-2-thione as a by-product. In addition, some heterobifunctional crosslinkers have a spacer arm, or bridge, connecting the two reactive ends. This has the advantage in overcoming steric hindrance when linking two complex molecules. Other crosslinkers include N-succinimidyl S-acetylthioacetate (SATA) and 3-(2-pyridyldithio) propionyl hydrazide (PDPH). As these heterobifunctional crosslinkers can be used to link proteins in a step-wise manner, the occurrence of unwanted side-reactions such as homoprotein polymer formation can be controlled.

The principle of chimeric peptide delivery to brain tissue is identical to receptor-mediated transcytosis as previously described (section 1.23). The entire conjugate is transported across the BBB and release of the protein from its transport vector is mediated by disulphide reductases present in brain tissue (Pardridge *et al.*, 1990a; Bickel *et al.*, 1995). The released protein can then bind to its receptor on brain cells to carry out its biological function.

Figure 1.7: Structure of heterobifunctional crosslinkers.

Shown are three heterobifunctional cleavable crosslinkers; SATA, SPDP and PDPH. They each contain two reactive moieties such as N-hydroxysuccinimide and pyridyldisulphide as in SPDP, which react with primary amines and sulphydryls, respectively. In PDPH the hydrazide residue reacts with oxidised carbohydrate groups. A spacer arm or bridge connecting the two reactive moieties (illustrated in SPDP) allows for greater flexibility of the crosslinker especially in overcoming steric hindrance when joining two complex molecules. The reactions involved in generating protein conjugates using these crosslinkers are depicted in Figure 4.12.

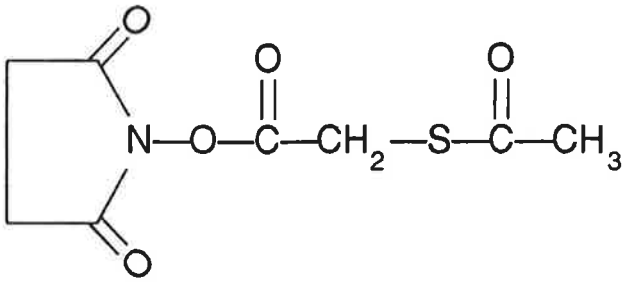

SATA
N-Succinimidyl *S*-Acetylthioacetate
MW 231.22

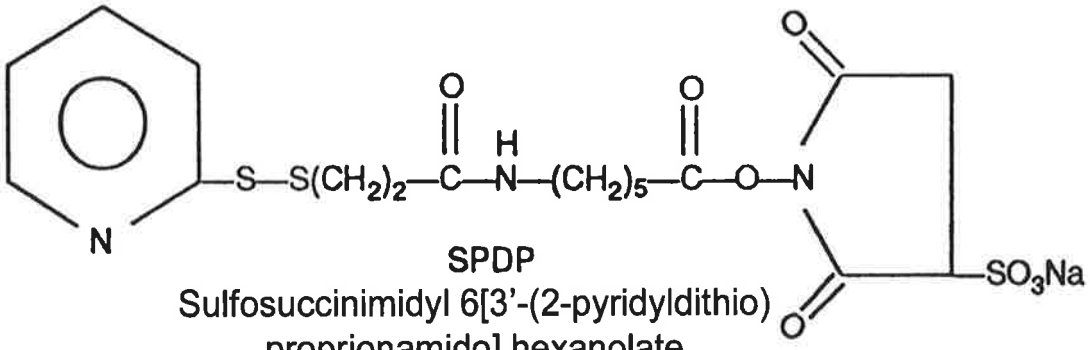

SPDP
Sulfosuccinimidyl 6[3'-(2-pyridyldithio)
proprionamido] hexanolate
MW 527.26

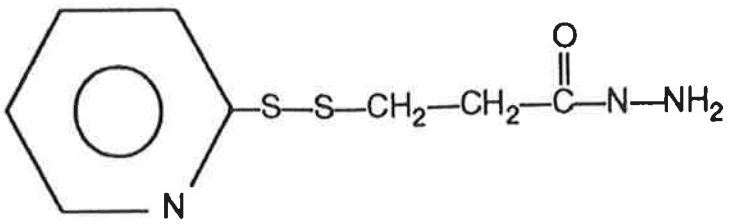

PDPH
3-(2-pyridyldithio)propionyl Hydrazide
MW 229.31

Insulin was one of the first peptides for which binding to cerebral microvessels and transcytosis through the BBB was demonstrated (van Houten and Posner, 1979). Autoradiography of brain slices following infusion of radiolabelled insulin demonstrated the transcytosis of the peptide into brain parenchyma. Saturability of uptake was proved by co-infusion with a high concentration of unlabelled insulin, which completely suppressed transcytosis of labelled insulin. Insulin was therefore considered a good candidate for the production of chimeric peptides. A horseradish peroxidase (HRP) insulin conjugate was detected in the brains of mice at 0.7% of the injected dose (Fukuta *et al.*, 1994). However, a major drawback to the use of insulin was the induction of hypoglycaemia. The same authors also described the isolation of a fragment of insulin which was reported to abrogate the hypoglycaemic effect while still able to bind to the insulin receptor. This fragment (F007) was isolated by tryptic digestion, and when linked to HRP, it retained the ability to bind to cultured bovine brain microendothelial cells, although with 10-fold diminished affinity. Experiments to determine the transcytosis of F007-HRP in mice were not reported.

As shown by immunohistochemistry, abundant Tf receptors are found on rat BBB endothelial cells suggesting that Tf may be another suitable vector for coupling to therapeutic reagents. Radiolabelled Tf was found to accumulate in the brains of rats up to 0.4% of the injected dose after 24 h (Friden *et al.*, 1991). However, due to its high endogenous plasma concentrations Tf itself may be of limited value as a transport vector since Tf receptors are almost completely saturated under physiological conditions. As an alternative approach, anti-receptor antibodies have been evaluated as transport vectors. The mouse anti-rat Tf receptor monoclonal antibody, OX26, appeared promising as it binds to an extracellular domain on the Tf receptor which is distinct from the Tf binding site and therefore does not interfere with Tf binding (Jefferies *et al.*, 1984; Pardridge *et al.*, 1987). An internal carotid artery perfusion/capillary depletion experiment in rats showed that OX26 was taken up by brain *in vivo*. Furthermore, levels of OX26 in the postvascular supernatant, which represents transcytosis through the BBB as opposed to mere binding to the brain capillary endothelial cells, were higher than those of cationized albumin and cationized IgG indicating that, at least for OX26, receptor-mediated transcytosis appeared to be more efficient than adsorptive-mediated transcytosis (Triguero *et al.*, 1990).

OX26 has therefore been conjugated to a number of proteins to determine if it could be used as a delivery vehicle. Nerve growth factor (NGF), a 26 kDa peptide not able to penetrate the BBB in significant amounts, is one such example (Friden *et al.*, 1993; Granholm *et al.*, 1994). When conjugated to OX26 and delivered by intravenous injection, it was taken up by rat brain reaching a maximum level 5 hours after administration. The level in brain after capillary depletion was 0.5% of the injected dose. A physiological effect was demonstrated in a model system utilising intraocular transplants of septal tissue. OX26-NGF conjugates significantly enhanced the growth of these septal transplants compared to infusion of either NGF or OX26 alone. OX26 was also shown to deliver sufficient amounts of vasoactive intestinal peptide across the BBB to induce a biological response (Bickel *et al.*, 1993; Wu and Pardridge, 1996) and OX26-avidin conjugates reached similar levels in the brain as unconjugated OX26 (Yoshikawa and Pardridge, 1992). Observations with CD4, a cell surface glycoprotein, which is a high affinity receptor for the HIV envelope protein gp120, parallel these results (Walus *et al.*, 1996). Intravenous administration of OX26-CD4 conjugates reached levels of approximately 0.6% of the injected dose 4 hours post-injection. Similar levels were obtained in the African green monkey when CD4 was conjugated to anti-human/primate Tf receptor antibodies (Walus *et al.*, 1996).

In conclusion, in terms of delivering effective ERT to the CNS, cationization of lysosomal enzymes and the formation of enzyme-vector conjugates for receptor-mediated transcytosis, are two approaches that would appear as possible candidates for circumventing the BBB. One of the main disadvantages of both treatment strategies is the rapid clearance of the modified proteins by other tissues, particularly liver, kidney and spleen. However, given the non-invasiveness of this strategy and the fact that only very low levels of enzyme activity in brain are required for correction of CNS pathology (Shull *et al.*, 1987; Shull and Walker, 1988), its application to the treatment of neurological disease may have potential benefit to many patients.

1.25 Aims of the project

The overall objectives of this thesis were twofold. Firstly, to evaluate efficacy of ERT in MPS VI cats from birth using same-species enzyme in order to (i), minimise the possibility of an immune response and (ii), simulate more accurately a clinical trial of ERT in MPS VI patients. Secondly, to explore means of modification of enzymes which would enhance transcytosis into the CNS thus allowing effective ERT in the CNS.

In order to achieve these objectives the specific aims were to:

1. purify rf4S and determine its physical, enzymatic and functional properties *in vitro.*

2. undertake a six-month trial of ERT with rf4S in newborn MPS VI cats and compare its efficacy with a previous study in which rh4S was used.

3. develop a mammalian expression system and a purification procedure for rcFUC and to determine its physical, enzymatic and functional characteristics.

4. assess the response to rcFUC replacement therapy in a fucosidosis pup treated for up to one year of age using unmodified enzyme.

5. modify rcFUC by cationization and by conjugation to various transport vectors and assess enzyme and vector functional integrity after modification.

6. analyse the effects of these modifications in enhancement of transcytosis across the BBB, initially in normal rats.

Chapter 2: Materials and methods

2.1 Materials

2.1.1 Tissue culture

Disposable polystyrene tissue culture flasks, plates and pipettes were supplied from Corning Glass Works, Corning, New York, USA. All other materials for tissue culture were obtained from the following suppliers.

Dulbecco's modified Eagle's medium (DMEM)	Gibco-BRL, Grand Island, NY, USA
F-12 nutrient medium (Ham's)	Gibco-BRL, Grand Island, NY, USA
α-Minimal essential medium (α-MEM)	Gibco-BRL, Grand Island, NY, USA
COON'S/DMEM	CSL Ltd., Parkville, Vic., Australia
Foetal calf serum (FCS)	CSL Ltd., Parkville, Vic., Australia
Phosphate-buffered saline (PBS) without Ca^{+2}/Mg^{+2}	CSL Ltd., Parkville, Vic., Australia
Trypsin-versene	CSL Ltd., Parkville, Vic., Australia
L-Glutamine	CSL Ltd., Parkville, Vic., Australia
Basal medium Eagle's (BME)	Biomedicals Inc., Aurora, Ohio, USA
RPMI 1640 medium	Trace Scientific Ltd., Vic., Australia

2.1.2 Antibiotics

Penicillin/Streptomycin (PS)	CSL Ltd., Parkville, Vic., Australia
G418 sulphate (Neomycin) Geneticin	Gibco-BRL, Grand Island, NY, USA
Penicillin G	Sigma Chemical Co., St. Louis, MO, USA

2.1.3 Cell lines

Chinese hamster ovary (CHO-K1)	ATCC, CRL 9618
Madin-Darby canine kidney (MDCK)	CSL Ltd., Parkville, Vic., Australia
OX26 hybridoma	ECCC No. 84112014
Ag82P3653 myeloma	Dr. D Brooks, WCH, SA, Australia
H4IIE rat hepatoma	Dr. H. Brereton, FMC, SA, Australia

2.1.4 Gel chromatography media

Sephadex G10	Pharmacia Fine Chemicals, Uppsala, Sweden
PD-10	Amersham Biotech AB, Uppsala, Sweden
Affi-Gel 10	Bio-Rad Laboratories, Hercules, CA, USA
DEAE-Sephacel	Pharmacia LKB Biotech, Uppsala, Sweden
Fucosylamine-linked agarose (C-24)	Sigma Chemical Co., St. Louis, MO, USA
Fucosylamine-linked agarose (C-1)	Sigma Chemical Co., St. Louis, MO, USA
TSK G3000SW Ultrapac	LKB, Bromma, Sweden
Superose 12	Pharmacia Fine Chemicals, Uppsala, Sweden
Hi-Trap Protein G	Bio-Rad Laboratories, Hercules, CA, USA
Dynamax 60AC8	Rainin, Woburn, MA, USA
PBE 94 chromatofocussing medium	Pharmacia Fine Chemicals, Uppsala, Sweden
AG-501-X8(D) mixed bed resin	Bio-Rad Laboratories, Hercules, CA, USA

2.1.5 Heterobifunctional crosslinkers

Sulfosuccinimidyl 6-[3'-(2-pyridyldithio)-proprionamido]hexanoate (SPDP)	Pierce, Rockford, ILL, USA
3-(2-pyridyldithio)propionyl hydrazide (PDPH)	Pierce, Rockford, ILL, USA
N-succinimidyl S-acetylthioacetate (SATA)	Pierce, Rockford, ILL, USA

2.1.6 Enzymes

TPCK-Trypsin	Cooper Biomedical
PNGase F	New England Biolabs, Beverley, MA, USA
Fucose dehydrogenase	Sigma Chemical Co., St. Louis, MO, USA

2.1.7 Antibodies

Antibodies from Silenus Labs Pty. Ltd., Melbourne, Australia included:

Sheep anti-mouse (SAM) Ig

SAM Ig-horse radish peroxidase conjugate (SAM-HRP)

SAM Ig-fluorescein isothiocyanate conjugate (SAM-FITC)

Sheep anti-rabbit (SAR) Ig

SAR Ig-HRP conjugate (SAR-HRP)

SAR Ig-FITC conjugate (SAR-FITC)

Serotec Ltd., Oxford, UK supplied the following antibodies:
Sheep anti-dog Ig-HRP conjugate
Mouse anti-human insulin IgG-HRP conjugate

Goat anti-cat Ig was from the Jackson ImmunoResearch Laboratories Inc., West Grove, PA, USA.
F58.3 monoclonal antibody was donated by CSL Ltd., Parkville, Vic., Australia.

2.1.8 Radiochemicals

All radiochemicals were from DuPont NEN Research Products, USA:
$Na_2{}^{35}SO_4$ (543 mCi/mmol, 2 mCi/ml)
^{3}H-leucine (150 Ci/mmol, 1 mCi/ml)
^{3}H-fucose (84 Ci/mmol)
^{14}C-inulin (2.85 mCi/g)

2.1.9 Substrates for enzyme reactions

4-methylumbelliferyl sulphate (4MUS)	Sigma Chemical Co., St. Louis, MO, USA
4-methylumbelliferyl fucopyranoside (4MUF)	Sigma Chemical Co., St. Louis, MO, USA
4-methylumbelliferyl-2-acetamido-2-deoxy-β-D-glycopyranoside	Melford Laboratories Ltd., England
Radiolabelled 4S trisaccharide substrate (GalNAc4S-GlcA-GalitolNAc4S)	V. Muller, Dept. Chemical Pathology, WCH

2.1.10 Electrophoresis reagents

Acrylamide	Bio-Rad Laboratories, Hercules, CA, USA
N,N'-Methylene-bis-acrylamide	Gradipore, Pyrmont, NSW, Australia
Ammonium persulphate	Bio-Rad Laboratories, Hercules, CA, USA
Temed (N,N,N',N'-Tetramethylenediamine)	Bio-Rad Laboratories, Hercules, CA, USA
BioLyte® 3/10 ampholytes	Bio-Rad Laboratories, Hercules, CA, USA

Bromophenol blue	BDH Chemicals Ltd., Poole, England
Coomassie brilliant blue R250	Sigma Chemical Co., St. Louis, MO, USA
Sodium dodecyl sulphate (SDS)	Sigma Chemical Co., St. Louis, MO, USA
Phenol red	Merck, Darmstadt, Germany
Tricine	Sigma Chemical Co., St. Louis, MO, USA

2.1.11 Animal colonies

The MPS VI cat colony in Adelaide was established from 'Family 3' heterozygotes obtained from Professor M. Haskins at The School of Veterinary Science, University of Pennsylvania, Philadelphia, USA.

The fucosidosis dogs used for studies described in this thesis were from a colony originally established from purebred English springer spaniels in 1984 by Professor B. Farrow, Dr. R. Taylor and Dr. P. Healy at the University of Sydney. The dog colony is now located at the Vivarium, Westmead Hospital, NSW, Australia and is under the supervision of Dr. R. Taylor.

Ethics approval for studies in MPS VI cats and normal rats was granted by the Animal Ethics Committees of the Women's and Children's Hospital, the Adelaide University and the Institute of Medical and Veterinary Science, and for studies in fucosidosis dogs by the University of Sydney and Westmead Hospital Animal Ethics Committees. All procedures carried out in these animals were in accordance with the guidelines set out by these committees.

2.1.12 Buffers and solutions

Glycine buffer	200 mM glycine, 157 mM Na_2CO_3, 125 mM NaOH, pH 10.6
PBS	137 mM NaCl, 2.7 mM KCl, 4.3 mM KH_2PO_4, pH 7.2
2x Fairbank's sample loading buffer	10% (w/v) sucrose, 0.2% (w/v) SDS, 1.88 mM EDTA, 0.1 mg bromophenol blue/10 ml 2 mM Tris-HCl buffer, pH 6.8

SDS-PAGE electrophoresis buffer	25 mM Tris-HCl, 192 mM glycine, 0.1% (w/v) SDS, pH 8.3
Capillary depletion buffer	10 mM HEPES, 141 mM NaCl, 4 mM KCl, 2.8 mM $CaCl_2$, 1 mM $MgSO_4$, 1 mM NaH_2PO_4 and 10 mM D-glucose, pH 7.4
Enhancement solution	0.1% (w/v) Triton X100, 6.8 mM potassium hydrogen phthalate, 100 mM acetic acid, 50 µM tri-n-octyl phosphine oxide, 15 µM 2-naphthoyltrifluoroacetone
Isoelectric focussing (IEF) solutions	Monomer Concentrate: 24.25% (w/v) acrylamide, 0.75% (w/v) N,N'-methylene-bis-acrylamide Glycerol Solution: 25% (v/v) glycerol
IEF 5% (w/v) acrylamide gel	For one gel: 2.2 ml Monomer Concentrate, 2.2 ml Glycerol Solution, 0.55 ml BioLyte ampholytes 3/10 in a total volume of 10 ml with water. Degas 5 min and then add 10 µl Temed and 50 µl of 10% (w/v) ammonium persulphate
Transfer buffer	25 mM Tris-HCl, 192 mM glycine in 20% (v/v) methanol
1 x HAT	0.1 mM hypoxanthine, 0.4 µM aminopterin, 16 µM thymidine

2.1.13 Chemicals

1-ethyl-3-(3-dimethylaminopropyl) carbodiimide (EDC)	Sigma Chemical Co., St. Louis, MO, USA
3-Phenylphenol (hydroxydiphenyl)	Aldrich Chemical Co., Milwaukee, USA

4-Chloro-1-naphthol	Sigma Chemical Co., St. Louis, MO, USA
Acetonitrile	Asia Pacific Specialty (APS) Chemicals Ltd., NSW, Australia
Alcian Blue 8GX	Koch-Light Laboratories, Berks, England
Aminopterin	Sigma Chemical Co., St. Louis, MO, USA
Ammonium chloride	Ajax Chemicals, Auburn, Australia
Ammonium formate	BDH Chemicals Ltd., Poole, England, UK
Barium acetate	BDH Chemicals Ltd., Poole, England, UK
Bovine pancreatic insulin	Sigma Chemical Co., St. Louis, MO, USA
Bovine serum albumin (BSA) Fraction V	Sigma Chemical Co., St. Louis, MO, USA
Butyric acid	Sigma Chemical Co., St. Louis, MO, USA
Calcein	Sigma Chemical Co., St. Louis, MO, USA
Cetylpyridium chloride (CPC)	Sigma Chemical Co., St. Louis, MO, USA
Chondroitin 4-sulphate (C4S) type A	Sigma Chemical Co., St. Louis, MO, USA
Citric acid	APS Chemicals Ltd., NSW, Australia
Copper sulphate	Ajax Chemicals, Auburn, Australia
Dextran Grade B	BDH Chemicals Ltd., Poole, England, UK
D-glucuronic acid lactone (glucuronolactone)	Sigma Chemical Co., St. Louis, MO, USA
Digitonin	Sigma Chemical Co., St. Louis, MO, USA
Dimethylformamide	Merck, Darmstadt, Germany
Dimethylglutaric acid (DMG)	Sigma Chemical Co., St. Louis, MO, USA
Diploma skim milk powder	Bonlac Foods, Melbourne, Vic, Australia
Disodium hydrogen orthophosphate, anhydrous	APS Chemicals Ltd., NSW, Australia
Dithio-bis-(2-nitrobenzoic acid) (DTNB)	Pierce, Rockford, ILL, USA
Dithioerythritol (DTE)	Sigma Chemical Co., St. Louis, MO, USA
Ethylendiaminetetraacetic acid, disodium salt (EDTA)	Ajax Chemicals, Auburn, Australia
Ethylene glycol	Merck, Darmstadt, Germany
Folin-Ciocalteu reagent	Merck, Darmstadt, Germany
Formic acid	Ajax Chemicals, Auburn, Australia
Freund's complete adjuvant	Gibco® Laboratories, Life Technology Inc., Grand Island, NY, USA.

Freund's incomplete adjuvant	Sigma Chemical Co., St. Louis, MO, USA
Gelatine	Ajax Chemicals, Auburn, Australia
Glycine	BDH Chemicals Ltd., Poole, England, UK
Heparin (porcine mucous)	David Bill Laboratories, Vic, Australia
HRP substrate kit (ABTS)	Bio-Rad Laboratories, Hercules, CA, USA
Hydrogen peroxide (30% (v/v))	Ajax Chemicals, Auburn, Australia
Hydroxylamine hydrochloride	Pierce, Rockford, ILL, USA
Hypoxanthine	Sigma Chemical Co., St. Louis, MO, USA
L(-)Fucose	Sigma Chemical Co., St. Louis, MO, USA
Lithium chloride	BDH Chemicals Ltd., Poole, England, UK
Mannose-6-phosphate (M6P)	Sigma Chemical Co., St. Louis, MO, USA
N-[1-(2,3-dioleolyloxy)propyl]-N,N,N-trimethylammonium methyl sulphate (DOTAP)	Boehringer Mannheim, Germany
N-[2-hydroxyethyl]-1-piperazine-N'-[2-ethanesulfonic acid] (HEPES)	Sigma Chemical Co., St. Louis, MO, USA
N^1-(p-isothiocyanatobenzyl)-diethylene triamine-N^1,N^2,N^3-tetraacetic acid (Europium chelate)	Wallac, Sollentuna, Sweden
NCS-II Tissue solubilizer	Amersham Canada Ltd., Oakville, ONT, Canada
Neocuproine	Sigma Chemical Co., St. Louis, MO, USA
N-hydroxy succinimide (NHS)	Pierce, Rockford, ILL, USA
Nicotinamide adenine dinucleotide (NAD)	Boehringer-Mannheim, Germany
OptiPhase 'HiSafe' 3 scintillant	Fisher Chemicals, Leicester, England
Orcinol	Sigma Chemical Co., St. Louis, MO, USA
Ovalbumin	Sigma Chemical Co., St. Louis, MO, USA
Oxytetracycline	Pfizer Pty. Ltd., West Ryde, NSW, Australia
Phosphate buffered saline (PBS) tablets	Sigma Chemical Co., St. Louis, MO, USA
Polybuffer 74	Pharmacia Fine Chemicals, Uppsala, Sweden
Polyethylene glycol	BDH Chemicals Ltd. Poole, England, UK
Potassium sodium tartrate	BDH Chemicals Ltd., Poole, England, UK
Propidium iodide	Sigma Chemical Co., St. Louis, MO, USA
Putrescine dihydrochloride	Sigma Chemical Co., St. Louis, MO, USA

Resorcinol	Merck, Darmstadt, Germany
Sodium 5,5-diethylbarbitone	Ajax Chemicals, Auburn, Australia
Sodium acetate	BDH Chemicals Ltd., Poole, England, UK
Sodium azide	Sigma Chemical Co., St. Louis, MO, USA
Sodium carbonate	BDH Chemicals Ltd., Poole, England, UK
Sodium chloride	Merck Pty. Ltd., Victoria
Sodium deoxycholate	BDH Chemicals Ltd., Poole, England, UK
Sodium dihydrogen orthophosphate, monohydrate	BDH Chemicals Ltd., Poole, England, UK
Sodium formate	BDH Chemicals Ltd., Poole, England, UK
Sodium hydroxide	Ajax Chemicals, Auburn, Australia
Sodium periodate	Ajax Chemicals, Auburn, Australia
Sodium tetraborate	Ajax Chemicals, Auburn, Australia
Sodium bicarbonate	Ajax Chemicals, Auburn, Australia
Sulphosalycylic acid	Ajax Chemicals, Auburn, Australia
Thymidine	Sigma Chemical Co., St. Louis, MO, USA
Trichloroacetic acid	Sigma Chemical Co., St. Louis, MO, USA
Trifluoroacetic acid	Pierce, Rockford, ILL, USA
Tris base	Boehringer Mannheim, Germany
Tri-sodium citrate	BDH Merck Pty. Ltd.
Triton X100	Sigma Chemical Co., St. Louis, MO, USA
Tween 20	BDH Chemicals Ltd. Poole, England, UK
Urea	Ajax Chemicals, Auburn, Australia

2.1.14 Miscellaneous materials

BRL Cell Porator	BRL Life Technologies, MD, USA
Cytodex 2 microcarrier beads	Pharmacia Fine Chemicals, Uppsala, Sweden
DC2 Hollow fibre concentrator	Amicon, Danvers, MA, USA
Diaflo® YM10 ultrafiltration membrane	Amicon, Danvers, MA, USA
Dialysis tubing for Diacult culture	Cellu SepT3, Membrane Filtration Products Inc., Seguin, Texas, USA
Immulon 1 and 1R Removawell strips	Dynex Technologies Inc., Chantilly, VA, USA
IsoStrips	Boehringer Mannheim, Germany

Nitrocellulose membrane (0.45 μm)	Bio-Rad Laboratories, Hercules, CA, USA
Polyvinyl microtitre plates	Costar, Cambridge, MA, USA
Tapered tissue grinder	Wheaton, Millville, NJ, USA
Titan III cellulose acetate plates	Helena Laboratories, Beaumont, Texas
TLC acid resistant silica gel plates	Schleicher and Schull, Dassel, Germany
Ultra T25-Turrax Homogeniser	Janke & Kunkel, IKAR Labortechnik, Staufen, Germany
Ultrafiltration stirred cell	Amicon, Danvers, MA, USA

2.2 Methods

2.2.1 Tissue culture

All cells were cultured at 37 °C in a 5% CO_2 humidified atmosphere.

2.2.1.1 CHO-K1 cells

CHO-K1 cells and CHO-K1 cells expressing rf4S (CHOf4S-2, see section 2.2.2) or rcFUC (CHO/rcFUC) (CHOcFUC40-A2-4, see section 2.2.22) were routinely grown in COON'S/DMEM, 10% (v/v) FCS and PS except where indicated otherwise. Cells were subcultured 1:10 to 1:30 with a 10% (v/v) solution of trypsin-versene (stock solution is 0.1% (w/v) trypsin, 0.02% (w/v) versene) in PBS.

2.2.1.2 MDCK cells

MDCK cells or MDCK cells expressing rcFUC (MDCK/rcFUC) (MDCKcFUC8-6 see section 2.2.22) were grown in DMEM, 10% (v/v) FCS and PS and were subcultured 1:2 to 1:10 using 0.1% (w/v) trypsin-0.02% (w/v) versene at 37 °C for 20 to 30 min depending on the degree of confluency. Prolonged exposure to trypsin-versene was required to dissociate MDCK cells from the culture substratum.

2.2.1.3 Human skin fibroblasts

Human diploid fibroblasts were established from skin biopsies submitted to this hospital for diagnosis (Hopwood *et al.*, 1982). Cell lines were maintained at 37 °C in 5% CO_2 in BME, 10% (v/v) FCS and PS. Fucosidosis skin fibroblasts (SF2184) were diagnosed as representing the severe form of the disease based on the almost total lack of residual FUC activity.

Fibroblasts were subcultured no more than 1:2 as required using 0.1% (w/v) trypsin-0.02% (w/v) versene.

2.2.1.4 Feline skin fibroblasts

Normal and MPS VI feline skin fibroblasts (genotype status confirmed as P/N homozygotes by PCR, section 2.2.8) were obtained from tail tip biopsies of newborn kittens as previously described (Yogalingam *et al.*, 1996). These were maintained in DMEM, 10% (v/v) FCS and PS. Cells were subcultured as described above for human skin fibroblasts (section 2.2.1.3).

2.2.1.5 H4IIE rat hepatoma cells

H4IIE cells (a generous gift of Dr. Helen Brereton, Flinders Medical Centre, Bedford Park, South Australia) were grown in DMEM, 10% (v/v) FCS and PS and subcultured 1:10 to 1:50 with a 1/10 dilution of 0.1% (w/v) trypsin-0.02% (w/v) versene in PBS. However, when harvesting for subsequent fluorescence-activated cell-sorting (FACS) analysis (section 2.2.43) the cells were dissociated from the substratum with PBS, 2 mM EDTA for 10 min at 37 ^{o}C. With this method cells tended to be more clumped and required gentle pipetting to produce a single cell suspension.

2.2.2 Large-scale production of rf4S for clinical trial

Cell culture and concentration of media were performed by Jodie Varnai (Department of Biotechnology, University of NSW).

CHOf4S-2 cells were grown to confluence on Cytodex 2 microcarrier beads at 3 g/l in 12 l of DMEM/COON'S F12 medium, 10% (v/v) FCS in a Bioreactor. Once confluency was attained, the culture medium was changed by rapid perfusion to serum-free DMEM/COON'S F12 medium supplemented with 0.5 mM butyric acid and 5 mM NH_4Cl. The production phase of this fermentation was run as a 12 l stirred continuous culture with perfusion carried out at approximately 0.2 volumes/10^6 cells/ml/day. The culture dissolved oxygen concentration (measured *in situ* with an Ingold oxygen probe) was monitored and controlled with FC4 software (Real Time Engineering, Sydney, Australia) and maintained at approximately 40% saturation with sparged oxygen. Culture pH, maintained at pH 7.4 with sparged CO_2, was also measured *in situ* using an Applikon pH probe (Enztech Pty. Ltd., Sydney, Australia) and monitored with the same software. Collected culture supernatant was concentrated using a

Sartocon II cross-flow filtration system with a 30,000 Mr polysulphone ultrafiltration cartridge and stored at 4 °C, after the addition of 0.1% (w/v) sodium azide, until processing.

2.2.3 Purification of rf4S by immunoaffinity chromatography

The anti-human 4S monoclonal antibody F58.3 (Brooks *et al.*, 1994) was coupled to Affi-Gel 10 (section 2.2.4) and used for immunopurification of rf4S. The salt concentration of the medium from CHOrf4S-2 was adjusted to 250 mM before applying to a 100 ml Affi-Gel-F58.3 column (20 cm x 2.5 cm) equilibrated in 20 mM Tris-HCl, 250 mM NaCl buffer, pH 7 at 4 °C. After loading, the medium was washed in with 5 column-volumes of the above buffer followed by elution with 20 mM tri-sodium citrate, 4 M NaCl buffer, pH 4 (4 column-volumes). The eluted enzyme was concentrated in an Amicon stirred-cell with Diaflo® YM 10 ultrafiltration membrane and the buffer exchanged with PBS. The purified enzyme was then characterised by physical and kinetic analysis. Enzyme to be used in the animal studies was sterile filtered (0.2 μm Gradipore filter) and dispensed aseptically into sterile siliconised glass vials and stored at 4 °C until use.

2.2.4 Coupling of F58.3 monoclonal antibody to Affi-Gel 10

The anti-human 4S monoclonal antibody F58.3 (Brooks *et al.*, 1994) (donated by CSL Ltd., Parkville, Victoria, Australia) was stored frozen in 50 mM $NaPO_4$ buffer, pH 7 with 0.02% (w/v) sodium azide at a concentration of 6.45 mg/ml. The antibody was thawed and a 100 ml volume equivalent to 64.5 mg was dialysed against 100 mM $NaHCO_3$ buffer, pH 8.5, overnight at 4 °C. The dialysed antibody was then added to an equal volume of Affi-Gel 10 that had been washed in ice cold H_2O. This mixture was incubated at 4 °C for 16 h with continuous rotation. The Affi-Gel was recovered by centrifugation at 690 ***g*** for 10 min at 4 °C, and washed three times with 20 mM Tris-HCl, 250 mM NaCl buffer, pH 7 (each wash 1 h at 4 °C) to block any remaining reactive groups. The coupled resin was poured into a column (20 cm x 2.5 cm) and equilibrated in 20 mM Tris-HCl, 250 mM NaCl buffer, pH 7. The protein concentration of the unbound antibody was determined using the Lowry method (Lowry, 1951) to allow the calculation of the percentage antibody bound to the column.

2.2.5 Enzyme assays

2.2.5.1 Assay of 4S using 4MUS substrate

4S was routinely assayed using the fluorogenic substrate 4MUS. A 5 µl aliquot of enzyme diluted in 0.05% (v/v) Tween 20, 50 mM sodium acetate buffer, pH 5.6 was added to 95 µl of 5 mM 4MUS, 50 mM sodium acetate buffer, pH 5.6, 0.05 mg/ml BSA and incubated at 37 °C for 20 min. The reaction was stopped by the addition of 1.5 ml glycine buffer (200 mM glycine, 157 mM sodium carbonate, 125 mM NaOH, pH 10.6). Fluorescence was measured on a Perkin-Elmer spectrofluorometer at excitation and emission wavelengths of 366 and 446 nm, respectively, and with 142 µM 4-methylumbelliferyl as the standard.

2.2.5.2 Assay of 4S using trisaccharide substrate

4S activity was determined using a specific radiolabelled trisaccharide substrate *O*-(β-*N*-acetylgalactosamine 4-sulphate)-(1→4)-*O*-**D**-(β-glucuronic acid)-(1→3)-*O*-**D**-*N*-acetyl-[1-^{3}H]galactosaminitol 4-sulphate (GalNAc4S-GlcA-GalitolNAc4S) prepared from rat chondrosarcoma C4S (Hopwood *et al.*, 1986). Unlike the 4MUS assay, which detects other arylsulphatases, this assay is specific for 4S activity. The total assay volume was 12 µl and included 633 pmoles of radiolabelled substrate, 50 mM sodium formate buffer, pH 3.5, 10 nmol β-hexosaminidase inhibitor (2-acetamido-2-deoxy-D-1-gluconolactone), 1 mg/ml BSA and enzyme dialysed and/or diluted in 50 mM sodium formate buffer, pH 3.5. Reactions were incubated at 37 °C for 60 min to 24 h and terminated by snap-freezing in dry ice/ethanol. Thawed samples were transferred to Whatman 3MM chromatography paper and subjected to high-voltage electrophoresis in 0.75 M formic acid, pH 1.7 at 3,000 V for 45 min on a Shandon Southern model L-24 system (Shandon Southern Products, Runcorn, Cheshire, UK), to separate substrate and product. The chromatograph paper was air-dried and then scanned on a Packard model 7201 radiochromatogram (Packard, Chicago, ILL, USA). The percentage conversion of substrate to product was determined by counting the areas of radioactivity of each substrate and product fraction using a liquid scintillation counter (Wallac 1409) and the activity was expressed as pmol/min/ml by computation with reference to the original substrate concentration.

2.2.5.3 Assay of FUC using 4MUF

FUC activity was determined using the fluorogenic substrate 4MUF. Reaction conditions were 0.5 mM 4MUF in 100 mM Na_2HPO_4, 50 mM citric acid, 30 mM NaCl buffer, pH 7. The assay was in a total volume of 100 µl which included 5 µl of enzyme diluted in 0.9% (w/v) NaCl. The reaction mixture was incubated at 37 °C for 20 min and the reaction stopped by the addition of 1.5 ml glycine buffer (section 2.2.5.1). Fluorescence was determined as described in section 2.2.5.1.

2.2.5.4 Assay of β-hexosaminidase

Skin fibroblast and white blood cell lysates were assayed for β-hexosaminidase using the fluorogenic substrate 4-methylumbelliferyl-2-acetamido-2-deoxy-β-D-glycopyranoside according to the method of (Leaback and Walker, 1961). Substrate concentrations were 0.62 mM and 0.66 mM, and the pH of the reaction 4.8 and 4.6, for skin fibroblast and white blood cell extracts, respectively.

2.2.6 Enzyme characterisation

2.2.6.1 Determination of native molecular mass

Native molecular mass was estimated by gel filtration chromatography using both a TSK G3000SW Ultrapac (30 cm x 0.8 cm) and a Superose 12 column (28 cm x 1.25 cm) equilibrated in 15 mM dimethylglutaric acid, 0.5 M NaCl buffer, pH 6, 0.02% (w/v) sodium azide at a flow rate of 0.5 ml/min and pressure of 150 kPa. CHO/rcFUC was also chromatographed in 15 mM dimethylglutaric acid buffer, 150 mM NaCl at pH 3, 4, 5 or 7. Molecular mass protein standards used for column calibration were thyroglobulin (660 kDa), aldolase (158 kDa), BSA (67 kDa), ovalbumin (43 kDa), carbonic anhydrase (30 kDa), chymotrypsinogen (25 kDa) and RNAse (14.4 kDa). The elution volume (V_e) of each standard and test sample was determined from measurement of the distance from the start of fractionation to its peak elution height when graphed. This distance is representative of the volume passing through the column from the application of sample to the peak elution fraction. The elution volume of thyroglobulin was taken as the column void volume (V_o) and that of ^{14}C-glucose as the total bed volume (V_t). K_{av} (an approximate partition coefficient) of all standards and samples was calculated from the formula: $K_{av}=(V_t-V_e)/(V_t-V_o)$ which was subsequently plotted against $\log_{10}$ of molecular mass.

2.2.6.2 Determination of subunit molecular mass

Subunit molecular mass and the molecular mass of unreduced proteins were determined by discontinuous SDS-PAGE according to the method of (Laemmli, 1970). Polyacrylamide gels were generally 10 or 12% (w/v) acrylamide. For visualisation of larger proteins or aggregates of >150 kDa Mr, 5% (w/v) acrylamide gels were used. Samples for electrophoresis were dissolved in an equal volume of 2x Fairbank's buffer (10% (w/v) sucrose, 0.2% (w/v) SDS, 1.88 mM EDTA and 0.01 mg bromophenol blue, 2 mM Tris-HCl buffer, pH 6.8) and denatured by incubation at 100 °C for 2 min in the presence or absence of 30 mM DTE. Gels were stained with 0.05% (w/v) Coomassie Brilliant Blue dissolved in 40% (v/v) methanol, 10% (v/v) acetic acid, for 30-60 min at room temperature, with gentle agitation. Background staining was removed by washing in repeated changes of 40% (v/v) methanol, 10% (v/v) acetic acid. Gels were stored in 5% (v/v) acetic acid or dried between sheets of cellophane using the BioRad Gel Air Drying Frame Assembly (BioRad). Unless otherwise specified, Pharmacia molecular mass protein standards were used for gel calibration and included phosphorylase b (94 kDa), BSA (67 kDa), ovalbumin (43 kDa), carbonic anhydrase (30 kDa), soybean trypsin inhibitor (20.1 kDa) and α-lactalbumin (14.4 kDa).

2.2.6.3 Determination of degree of glycosylation

Ten μg of recombinant enzyme were digested with PNGase F using reagents supplied by the manufacturer and according to the manufacturer's instructions. Briefly, to 10 μg of enzyme in 10 μl PBS was added 1 μl of denaturing buffer (5% (w/v) SDS, 10% (v/v) β-mercaptoethanol) and this was incubated at 100 °C for 10 min. After cooling to room temperature, 1 μl of G7 buffer (500 mM sodium phosphate, pH 7.5), 1 μl of 10% NP-40 and 1 μl of PNGase F (specific activity 1.8 x 10^6 U/mg) were added and the reaction was incubated at 37 °C for 6.5 h. Digestion products were analysed by SDS-PAGE (12% (w/v) acrylamide).

2.2.6.4 Determination of kinetic parameters

a) 4S with 4MUS substrate

The optimum pH (pH_{opt}) for 4S was determined by varying the pH of the reaction described in section 2.2.5.1 from pH 3.0 to 8.73 using 15 mM dimethylglutaric acid buffers. In addition 50 mM sodium acetate buffers covering the range from pH 3.6 to 5.4 were also used. Kinetic data (K_m and V_{max}) were obtained by determining enzyme activity at pH_{opt} with substrate concentrations ranging from 0.5 to 5 mM. K_m and V_{max} values were estimated by extrapolation

of the resultant line-of-best-fit from Lineweaver-Burk plots, in which the reciprocal of the substrate concentration is plotted against the reciprocal of the rate of the reaction at that particular substrate concentration. The intercept on the ordinate gives $1/V_{max}$ and the negative intercept on the abscissa is the reciprocal of K_m, which is the substrate concentration at which the reaction rate is at $\frac{1}{2}V_{max}$.

b) 4S with trisaccharide substrate

Kinetic data of 4S using the radiolabelled trisaccharide substrate were obtained by first ascertaining pH_{opt} using formate buffers with pH ranging from 2.76 to 4.61 and then determining enzyme activity as described in section 2.2.5.2 with concentrations of trisaccharide substrate (10 to 54 μM) at the determined pH_{opt}. K_m and V_{max} were calculated as described above for 4MUS.

c) FUC with 4MUF substrate

The pH_{opt} for FUC was established using the same assay system as detailed in section 2.2.5.3 except pH of citrate/phosphate buffers ranged from 4.29 to 7.39. pH_{opt} was also determined in the following buffers: 15 mM dimethylglutaric acid, pH 2.51 to 7.87, 25 mM sodium acetate, pH 2.5 to 7.8, 25 mM glycine, pH 2.1 to 3.4 and 50 mM sodium barbitone, pH 6.8 to 9.6. Kinetic analysis was performed using concentrations of 4MUF from 0.02 to 0.5 mM at pH_{opt} in citrate/phosphate buffer. K_m and V_{max}, were calculated from Lineweaver-Burk plots as discussed above.

2.2.6.5 pI determination

a) Chromatofocussing chromatography

Purified CHO/rcFUC was dialysed overnight against 20 mM Tris-HCl buffer, pH 7.0 at 4 °C and then applied to a PBE 94 column (5.5 cm x 1.0 cm) equilibrated in the above buffer at a flow rate of 1 ml/min. After loading, the column was washed with 4 column-volumes of the same buffer and bound FUC was then eluted with 100 ml Polybuffer 74 diluted 1 to 18 in water and adjusted to pH 4 with HCl. The column was maintained at 4 °C. All fractions were assessed for FUC activity (section 2.2.5.3) and pH.

b) Isoelectricfocussing (IEF)

Isoelectric point (pI) was determined on 5% (w/v) acrylamide gels (section 2.1.12) with 2% (v/v) ampholytes (BioLyte® 3/10 ampholytes) using a Bio-Phoresis Horizontal Electrophoresis Cell (BioRad) according to the manufacturer's instructions. Gels were pre-focussed at 800 V for 15 min before applying samples (maximum volume 10 µl) and electrophoresed at 1,300 V for 4 h. BioRad isoelectric focussing standards covering the range from pH 4.45 to 9.6 were used. Gels were fixed in 12% (w/v) trichloroacetic acid, 4% (w/v) sulfosalicylic acid and 30% (v/v) methanol for 30 min and then stained with 0.04% (w/v) Coomassie Brilliant Blue R250 dissolved in 27% (v/v) ethanol and 10% (v/v) acetic acid with 0.5% (w/v) $CuSO_4$ (dissolved in H_2O before adding to the dye solution) for 60 min. The gel was subsequently destained with 40% (v/v) methanol and 10% (v/v) acetic acid.

To test for the presence of sialic acid residues on enzyme samples, approximately 20 µg of each enzyme sample was treated with 80 mU of neuraminidase for 60 min at 37 °C. These samples were then subjected to IEF as described above along with the appropriate control, that is, enzyme not digested with neuraminidase.

2.2.7 Correction of storage in feline MPS VI skin fibroblasts with rf4S

Skin fibroblasts from normal (cat 242) and affected MPS VI (cat 236) kittens (section 2.2.1.4) were grown to confluence in DMEM, 10% (v/v) FCS and PS in 25 cm^2 flasks. When confluent, the medium was replaced with fresh DMEM, 10% (v/v) FCS and penicillin only, for 4 h to deplete intracellular sulphate pools. Cells were labelled for 48 h with 10 µCi /ml $Na_2{}^{35}SO_4$ (543 mCi/mmol) in fresh medium at 3 ml/flask. Labelled cells were rinsed with PBS and then exposed to 2.6 nmol/min/ml, or 26 nmol/min/ml, rf4S in the presence or absence of 5 mM M6P, in growth medium for 48 h. Cells were then harvested by trypsin-versene treatment, washed three times with PBS by centrifugation (895 ***g***; 3 min; 25 °C), resuspended in 100 µl of 20 mM Tris-HCl, 250 mM NaCl buffer, pH 7, and then lysed by six cycles of freeze/thaw. Cell lysates were clarified by centrifugation (13,000 ***g***; 5 min; 4 °C) and then assayed for 4S activity, using the radiolabelled substrate (section 2.2.5.2), β-hexosaminidase activity (section 2.2.5.4), radioactivity and total protein (Lowry, 1951).

2.2.8 Experimental animals for feline MPS VI ERT trial

Diagnosis of MPS VI kittens was performed by Allison Crawley (Department of Chemical Pathology, WCH).

Two male MPS VI kittens born one week apart, the result of heterozygote matings from a naturally occurring feline model of MPS VI (Haskins *et al.*, 1979a) were designated cat 249 and cat 250. Diagnosis of the MPS VI phenotype at birth was by the lack of stained eosinophil inclusions in blood films (Crawley *et al.*, 1997). Cat genotype status was later confirmed by PCR-based mutation analysis from blood spots (Yogalingam *et al.*, 1996). Briefly, three mm diameter punched discs of cat venous blood that had been blotted directly onto Guthrie cards and dried at room temperature, were soaked in PCR buffer (Biotech International Ltd., Perth, Australia) with 2.5 mM $MgCl_2$ (30-60 min; 4 °C) and then denatured at 99 °C for 2 h under mineral oil. After denaturation, 330 ng each of f4S7 and f4S9 primers (Yogalingam *et al.*, 1996), 400 μM dNTP and 1.5 units of *Taq* DNA polymerase were added in a final reaction volume of 100 μl. The PCR conditions were 40 cycles of denaturation at 94 °C/30 sec, annealing at 58 °C/30 sec and extension at 72 °C/45 sec. Restriction enzyme digestion of the resultant 296 bp PCR product with HaeIII gave three fragments of 163, 75 and 51 bp on a 5% (w/v) Hi-Res agarose gel in TAE (40 mM Tris-acetate, 1 mM EDTA, pH 8) buffer and these were diagnostic for MPS VI (digestion products of 245 and 51 bp being indicative of a normal phenotype).

2.2.9 ERT protocol for MPS VI cats

All veterinary procedures were carried out by Allison Crawley (Department of Chemical Pathology, WCH).

The protocol followed in this study was essentially as documented previously (Crawley *et al.*, 1997). Briefly, therapy was commenced within 24 h of birth by intravenous infusion of 1 mg rf4S/kg body weight in non-fasting kittens using insulin syringes, on a weekly basis for approximately 6 months. Throughout the course of therapy, the volume of enzyme injected ranged from 0.06 ml to 1.9 ml, and this was generally administered over 5-10 min. To maintain consistency between studies, oral antihistamine premedication was administered from six weeks of age (1 mg cyproheptadine and 1 mg chlorpheniramine at least 30 min prior to

injection). When body weight exceeded 2 kg, the premedication dose was increased to 2 mg of each of the above antihistamines. Cats were monitored on a daily basis for general well-being by animal care attendants and observed on a weekly basis at the time of injection for development of overt MPS VI clinical symptoms. At 90, 150 and 170 days of age, cats were subjected to a rigorous clinical assessment, which included physical, neurological and radiological examination.

Physical features noted included appearance, activity and general demeanour, facial shape, ear size, neck and body length, corneal clarity and spinal curvature, all of which were compared to normal litter-mates.

The neurological examination included an assessment of gait and ability to correct gait after pushing the hindquarters off balance. Also tested were the ability to wheelbarrow and hop, proprioceptive positioning and extensor postural thrust. Animals were graded according to the degree of hindlimb neurological deficits observed. These were classified as being, a) normal when they could rapidly correct overbalancing of hindquarters, b) having mild deficits when they were more clumsy in correcting overbalancing of hindquarters or displayed other gait changes such as a heavy tread or occasional stumbling, c) mild to moderate paresis when hindquarters were easily overbalanced and animals had a tendency to fall over and d) paralysis when hindlimbs were dragged and muscle wasting was apparent. Flexibility was also examined by visually estimating the degree to which animals could move their head laterally (180^{o} being when the nose touched the flank either side of the midline) and to extend their hindlimbs laterally (180^{o} coxofemoral joint movement being when the hindlimbs were parallel to the body).

A radiological examination under anaesthesia involved taking standard radiographic views: lateral cervical spine, lateral lumbar spine, lateral left and right hindlimb and ventrodorsal pelvis. These were used to visualise bone growth and remodelling. To enable quantification of these changes, measurements of the fifth lumbar vertebra (L5) were taken from radiographs of the lateral lumbar spine. Vertebral width (W) was measured with vernier callipers at the narrowest point of the vertebra. At the midway point of this measurement and perpendicular to it, the distance between the epiphyses was designated the vertebral length (L). Ratios of L:W were calculated from these values.

While under anaesthesia for radiological examination, blood samples were taken to test for antibody response to rf4S in plasma and urine samples collected by bladder compression for analysis of urinary GAG. Urine samples taken on days 23 and 49 were collected by reflex urination in response to perineal massage.

2.2.10 Determination of antibody titre in MPS VI cats undergoing ERT using Elisa

The wells of a 96-well polyvinyl microtitre plate (Costar, Cambridge, MA, USA) were coated with 100 µl of a solution containing 2 µg/ml rf4S in 100 mM $NaHCO_3$ buffer, pH 8.5 (37 °C for 2 h and then overnight at 4 °C). Unbound enzyme in the wells was removed by aspiration, the plate was washed with 20 mM Tris-HCl, 250 mM NaCl buffer, pH 7 using a microtitration plate washer (ADIL Instruments, Strasbourg, France) and any unreactive sites were blocked by the addition of 200 µl/well of 1% (w/v) BSA in 20 mM Tris-HCl, 250 mM NaCl buffer, pH 7 (blocking buffer) (2 h at room temperature). Samples of cat plasma obtained by centrifugation of heparinised blood (390 ***g***; 3 min; 10 °C) were serially diluted in blocking buffer, added to wells at 100 µl/well and incubated for 4 h at room temperature. The plate was washed as described above and then HRP-labelled goat anti-cat Ig, diluted 1/1,000 in blocking buffer, was added at 100 µl/well followed by incubation for 1 h at room temperature. After washing the plate as above, the assay was developed using HRP substrate solution (ABTS) and the colour reaction was quantified by measuring absorbance at 414 nm in an automated microtitre plate reader (Ceres 900 Hdi, Bio-Tek Instruments Inc., Winooski, VT, USA). As a control measure, all cat plasma was analysed for non-specific reactivity to wells coated with blocking buffer only. To test antibody titre of rh4S-treated cats, rh4S was substituted in the assay. Control wells with no enzyme and/or no plasma were included for each plate. Antibody titre was determined as being the lowest dilution at which the absorbance at 414 nm is above two standard deviations of the mean background.

2.2.11 Western blot analysis of plasma from rf4S-treated MPS VI cats

rf4S (100 µg) applied to a single 6 cm wide well, and pre-stained molecular mass protein standards (phosphorylase b (105 kDa), BSA (82 kDa), ovalbumin (49 kDa), carbonic anhydrase (33 kDa), soybean trypsin inhibitor (28.6 kDa) and lysozyme (19.4 kDa), BioRad), were electrophoresed on a mini SDS 12% (w/v) acrylamide gel (Laemmli, 1970) and then

electroblotted onto nitrocellulose membrane (0.45 μm, BioRad) at 150 V for 90 min in 25 mM Tris-HCl, 192 mM glycine, 20% (v/v) methanol (transfer buffer). Nonspecific protein binding sites on the nitrocellulose membrane were blocked by incubating in 1% (w/v) skim milk powder, 20 mM Tris-HCl, 250 mM NaCl buffer, pH 7 (blocking buffer) for 2 h at room temperature. After washing the membrane with 20 mM Tris-HCl, 250 mM NaCl buffer, pH 7 (wash buffer) (3 x 5 min) it was then assembled in a BioRad Mini-PROTEAN® II Multiscreen apparatus and individual channels filled with sample. Samples tested included blocking buffer (negative control), rabbit anti-rf4S polyclonal (diluted 1/2,000 in blocking buffer) (positive control) or plasma from various treated and untreated cats (600 μl each). All the cat plasma samples were diluted 1/2 in blocking buffer. After making sure that no air bubbles were present in any of the channels the membrane was incubated overnight at room temperature on a rocking platform. The contents of each channel were then removed by vacuum aspiration and the membrane washed with wash buffer (3 x 5 min). The membrane was then cut to separate the tracks containing the pre-stained standards and rf4S, which had been exposed to blocking buffer and rabbit anti-rf4S polyclonal, respectively, from the remainder of the blot. This section was probed with SAR-HRP diluted 1/1000 in blocking buffer. The remainder of the blot was probed with HRP-labelled goat anti-cat IgG antibody diluted 1/100 in blocking buffer, for 1 h at room temperature. After washing both membranes (3 x 5 min), peroxidase substrate (12 mg 4-chloro-1-naphthol dissolved in 20 ml of 20% (v/v) methanol, 20 mM Tris-HCl buffer, pH 7 with 12 μl 30% (v/v) H_2O_2) was added and the reaction continued until bands were visible. The reaction was stopped by removing the substrate solution and rinsing the membrane in water.

2.2.12 Immunobinding assay for 4S

A 96-well polyvinyl microtitre plate was coated with 100 μl/well of sheep anti-mouse (SAM) IgG antibody diluted 1/100 in 100 mM $NaHCO_3$ buffer, pH 8.5 and incubated at 37 °C for 1 h and then overnight at 4 °C. It was then washed, blocked and washed again as described in section 2.2.10. Monoclonal antibody (100 μl/well) was added and the plate incubated for 4 h at room temperature. Monoclonal antibody F58.3 (Diacult culture medium) was diluted 1/50 in blocking buffer, F22.1 and F66 (hybridoma conditioned medium) were used without dilution. The wash was repeated, rf4S or rh4S at 100 ng/well was then added and the plate incubated at 4 °C for 16 h. After incubation the plate was washed again. The assay was developed by addition of 100 μl 4MUS assay mix (as described in section 2.2.5.1), to each well and

incubating at 37 °C for 20 min. The reaction was stopped by transferring the contents of each well into 1.5 ml glycine buffer, pH 10.6. Fluorescence was determined at 336/446 nm as described in section 2.2.5.1. Control wells with either no monoclonal antibody and/or no enzyme were included.

2.2.13 Sandwich Elisa of monoclonal antibody binding to 4S

A 96 well polyvinyl microtitre plate was coated with rabbit anti-human 4S, or rabbit anti-cat 4S polyclonal antibody at 1 μg/ml, washed and non-reactive sites blocked as described in section 2.2.10. 100 ng rf4S or rh4S was added to the wells coated with antibody to rf4S and rh4S, respectively, the plate was then incubated at room temperature for 4 h and washed before adding the sample (monoclonal antibody) at 100 μl/well. Hybridoma medium was used undiluted, alternatively medium from a Diacult culture was diluted 1/50. The plate was incubated at 4 °C overnight, washed and then SAM-HRP conjugate, diluted 1/1,000 in blocking buffer, was added at 100 μl/well and left at room temperature for 1 h. The plate was washed again before finally adding the HRP substrate solution (ABTS) at 100 μl/well and then reading the absorbance at 414 nm on an automated plate reader. Antibody titre was calculated as described in section 2.2.10.

2.2.14 Urinary GAG analysis

Urine samples were collected at specified times (see section 2.2.9) and stored at -20 °C without preservative until analysed for GAG and uronic acid concentration by the following methods.

2.2.14.1 Alcian Blue spectrophotometric detection of total GAG

Total urinary GAG was measured using the Alcian Blue spectrophotometric method of (Whiteman, 1973) as modified by (Gold, 1979). Briefly, urine samples were thawed, mixed thoroughly and then centrifuged (1560 ***g***; 10 min; 10 °C). The resultant supernatant was then diluted 1/8 in 50 mM sodium acetate buffer, pH 5.8. To one of a duplicate sample of diluted urine (250 μl each) 625 μl of 50 mM sodium acetate buffer, pH 5.8 was added (blank sample) and to the second (test sample) an identical volume of Alcian Blue 8GX (2 mg/ml solution in 50 mM sodium acetate buffer, pH 5.8). Samples were vortexed and allowed to stand at room temperature for 30 min. The samples were then re-vortexed and absorbance at 480 nm measured against the blank sample. Concentration of GAG was calculated from a standard

curve generated using C4S standards ranging from 0-400 mg/ml. Urinary creatinine levels were measured using an autoanalyser method (Synchron CXR System, Beckman Instruments, Inc., Fullerton, CA, USA). Urinary GAG concentration was normalised to creatinine levels and expressed as mg/mmol creatinine.

2.2.14.2 High-resolution electrophoresis of GAG

To the volume of urine equivalent to 300 mg of GAG (as determined by the Alcian Blue method, section 2.2.14.1), an equal volume of 0.1% (w/v) CPC in 54 mM sodium citrate buffer, pH 4.8 was added, mixed and incubated at 37 °C for 30 min. Samples were then centrifuged at 1,500 ***g*** for 10 min at 15 °C, the supernatant removed and the pellets resuspended in 150 µl of 2 M LiCl. After the addition of 800 µl of absolute ethanol, the samples were re-centrifuged and the resultant pellets were allowed to dry overnight at room temperature. The pellets were then dissolved in 10-20 µl of 0.5 mg/ml phenol red and approximately 3 µl loaded on Titan III cellulose acetate plates (6 cm x 9.4 cm) for HRE according to the method of (Hopwood and Harrison, 1982). Briefly, GAG species were separated according to their differential solubilities in ethanol and electrophoretic mobilities in barium acetate buffer at 250 V in a Shandon Model U77 electrophoresis apparatus. The plates were stained in 0.25% (w/v) Alcian Blue for 15 min then destained in 1% (v/v) acetic acid. After drying at room temperature the plates were scanned using a Molecular Dynamics Personal Densitometer Scanner with Molecular Dynamics ImageQuant software, Version 1 (Molecular Dynamics Inc.). Densitometric estimations of the approximate relative proportions of two DS species (DS1 and DS2) were made and these were expressed as a percentage of the total area (i.e., total GAG) under the peaks.

2.2.14.3 Uronic acid quantification of GAG

To quantify GAG as total uronic acid, urine was buffered to pH 5 with 50 mM sodium acetate buffer, pH 5 and chromatographed over a 1 ml DEAE-Sephacel anion exchange column equilibrated in 50 mM sodium acetate buffer, pH 5. Under these conditions, sulphated (i.e., charged) GAG bound to the matrix and were subsequently eluted with 2 M NaCl in 50 mM sodium acetate buffer, pH 5 (3 x 2 ml washes). The concentration of uronic acid in the samples was estimated using the meta-hydroxydiphenyl method (Blumenkrantz and Asboe-Hansen, 1973). Samples were made to 200 µl with H_2O and cooled on ice before the addition of 1.25 ml of 125 mM sodium tetraborate/concentrated sulphuric acid. Tubes were mixed thoroughly,

incubated at 100 °C for 5 min and cooled on ice. A 20 µl aliquot of 0.5 mg/ml meta-hydroxydiphenyl dissolved in 120 mM NaOH was added and samples were mixed by vortexing. Two hundred µl aliquots were then transferred to Immunlon 1R Removawell strips, and absorbance at 550 nm was read in an automated Elisa plate reader. The concentration of uronic acid was determined from a standard curve generated using concentrations of D-glucuronic acid lactone (0 to 10 µg/assay).

2.2.14.4 Gradient-PAGE analysis of GAG

Sulphated GAG eluted from DEAE-Sephacel (section 2.2.14.3) was desalted on Sephadex G10 (25 cm x 0.9 cm) equilibrated in 100 mM ammonium formate buffer, pH 6. Fractions positive for uronic acid (as determined in section 2.2.14.3) but containing no NaCl were pooled, lyophilised and redissolved in 100 mM ammonium formate buffer, pH 6. Uronic acid concentration was re-determined as above and samples containing ~1 µg uronic acid were made 10% (v/v) with glycerol, containing trace amounts of phenol red and bromophenol blue, and then analysed by gradient-PAGE (30-40% (w/v) acrylamide (Turnbull *et al.*, 1997). Electrophoresis was performed at 350 V for 16 h or until the phenol red dye was approximately 1 cm from the bottom of the gel. Standards comprising tetra-, hexa- and octa-saccharides prepared from bovine lung heparin were a generous gift of Dr. J. Turnbull (University of Birmingham, UK). The gel was stained with Alcian blue/silver nitrate according to the method of (Merril *et al.*, 1981), and bands of interest were subjected to densitometric analysis (section 2.2.14.2). A duplicate aliquot of each sample was treated with 10 µmol/min of rf4S for 16 h at 37 °C and analysed in the same manner.

2.2.15 Post mortem examination of MPS VI cats on ERT

The post-mortem examination and assessment of lysosomal storage were performed by Allison Crawley (Department of Chemical Pathology, WCH). Tissue processing and sectioning were done by Richard Davey (Department of Chemical Pathology, WCH).

Following a clinical examination as detailed above (section 2.2.9), cats were euthanased with an overdose of intravenous barbiturate 4 days after the final injection of rf4S. On autopsy, gross examination of tissues and joints was conducted. The spinal cord was exposed and examined for compression by the removal of dorsal vertebral arches between the fourth

cervical and fourth lumbar vertebrae. Samples of tissues for electron microscopy were fixed in 2% (v/v) glutaraldehyde, 2% (v/v) formaldehyde in 100 mM cacodylate, 5 mM calcium chloride buffer, pH 7.4 overnight at 4 °C, and then postfixed in 1% (v/v) osmium tetroxide, 100 mM cacodylate buffer, 5 mM calcium chloride buffer, pH 7.4 for 30-60 min at room temperature. They were then dehydrated through 70%, 90% and 100% (v/v) ethanol and embedded in Spurr's resin. One micron thick sections were stained with 1% (w/v) Toluidine Blue in 1% (w/v) borax and then ultrathin sections cut and stained with 2% (w/v) uranyl acetate, 1% (w/v) lead citrate and examined with a Hitachi H-7000 electron microscope. For light microscopy, tissues were fixed in 10% (v/v) formalin and were embedded in paraffin, sectioned and stained with haematoxylin and eosin. To determine the degree of vacuolation in the cells of tissues, 1 μm sections stained with Toluidine Blue were assessed by light microscopy at 100-400-x magnification and graded subjectively as follows: 3+, severe degree of lysosomal storage; 2+, moderate; 1+, mild; +/-, very mild; 0, no vacuolation.

2.2.16 Bone histomorphometric analysis of MPS VI cats on ERT

To label newly mineralised bone animals were injected subcutaneously with the fluorochrome dye calcein at a dose of 15 mg/kg on days 12 and 13 prior to euthanasia and with oxytetracycline on days 2 and 3 before euthanasia. At autopsy, the fifth lumbar vertebra (L5) was removed, wrapped in gauze soaked in 0.9% (w/v) NaCl and stored at -80 °C until analysis. After thawing, the L5 vertebra was fixed in 19% (v/v) buffered formalin and dehydrated in increasing concentrations of acetone (70-100%) before embedding in methylmethacrylate resin. Undecalcified sections (0.5 μm) were cut and stained with von Kossa stain to visualise mineralised bone. An automated image analysis system was used to quantify trabecular bone in the primary centre of ossification. Static parameters of bone formation including bone mineral volume (BV/TV), bone surface density (BS/TV), trabecular thickness (TbTh), trabecular separation (TbSp) and trabecular number (TbN) were calculated using standard morphometric formulae (Parfitt *et al.*, 1987). Dynamic parameters of bone formation including mineral apposition rate (MAR) and bone formation rate (BFR/BS) were determined from unstained L5 vertebral sections by measuring the distance between the fluorochrome dyes calcein (green) and oxytetracycline (orange) under fluorescent light (420 nm) using a routine manual point counting technique. Standard formulae were then applied to calculate MAR and BFR/BS (Recker, 1983).

2.2.17 Residual 4S activity in MPS VI cat liver

Liver samples were frozen at -20 °C until processing. Samples of liver, (approximately 1-2 g wet weight) were thawed, minced and then homogenised at maximum speed for approximately 1-2 min at 0 °C in twice their volume of 20 mM Tris-HCl, 250 mM NaCl buffer, pH 7, using an Ultra T25-Turrax Homogeniser. The homogenate was freeze/thawed six times and clarified by centrifugation (13,000 ***g***; 10 min; 4 °C) and the resulting supernatant was dialysed overnight at 4 °C against 50 mM sodium formate buffer, pH 3.5, before being assayed for 4S activity using the radiolabelled trisaccharide substrate (section 2.2.5.2). Randomly selected treated and untreated cat livers were processed in the same manner. Results of assays were normalised to total cell protein as estimated by the Lowry method (1951).

2.2.18 Assessment of hepatomegaly in treated MPS VI cats

To assess cats for hepatomegaly, wet weights of liver expressed as a percentage of total body weight at autopsy were compared with those of normal, untreated MPS VI and MPS VI rh4S-treated age and sex-matched animals (two male MPS VI cats treated with 5 mg rh4S/kg and euthanased at 5 months were included in this group). Statistical analysis was carried out using a two-tailed *t* test assuming equal variance and accepting a P value of 0.05 as being statistically significant.

2.2.19 Distribution of ^{3}H-rf4S in kittens

Purified radiolabelled rf4S was prepared as described in section 2.2.26. Four normal 8-day old kittens were injected *via* the cephalic vein with 1 mg rf4S/kg body weight (total cpm/kitten varied between 3.6 x 10^6 and 5 x 10^6). Radiolabelled rf4S was supplemented with unlabelled rf4S to give a final concentration of 1 mg/kg. The volume injected was approximately 600 µl over 20 sec. Immediately after injection a 500 µl heparinised blood sample was collected from the jugular vein of two kittens only and similar samples were collected at time intervals up to 4 h. Blood samples were centrifuged at 1560 ***g*** for 5 min at 10 °C, the plasma collected and a 10 µl aliquot added to 3 ml scintillant and counted in a Wallac 1409 liquid scintillation counter. After four hours the kittens were euthanased with an overdose of intravenous barbiturate. Tissues were collected, weighed and a 1 g portion of tissue, or the entire organ if this was less than 1g, was finely minced with a scalpel before adding 5 ml of 1 N NaOH per sample. The samples were solubilised by rotation at room temperature overnight and then centrifuged at 390

g for 10 min at 15 °C to pellet any insoluble material. A 200 µl aliquot of each supernatant was placed into 20 ml glass scintillation vials to which was added 500 µl of NCS-II Tissue solubilizer:iso-propanol (1:2). Samples were mixed and left at room temperature for 60 min and then 8 drops of 30% (v/v) H_2O_2 were added and mixed. After a further 60 min, 15 ml scintillant was added and the samples counted in a Wallac 1409 liquid scintillation counter. The total number of cpm in each organ was calculated and expressed as a percentage of the total cpm injected.

2.2.20 Construction of cFUC expression vector

This work was carried out by Maria Fuller (Department of Chemical Pathology, WCH).

The isolation of the rcFUC cDNA (Occhiodoro and Anson, 1996) and the expression vector pEFNeo (Bielicki *et al.*, 1993) have been described previously. In order to construct the rcFUC expression vector a *Not*I/*Nhe*I fragment encompassing bases 142 to 1577 of the cFUC cDNA was isolated from the cFUC cDNA clone 3.1 (Occhiodoro and Anson, 1996) and cloned into the *Not*I/*Nhe*I restricted pBluescriptIISK (Stratagene) to give pBlcFUCNotINheI. To complete the reading frame a 169-bp fragment was synthesised as seven complimentary overlapping oligonucleotides encompassing a 5'*Not*I sticky end (bold) and *Eco*RI and *Eco*RV restriction sites (italics and bold italics, respectively), followed by a Kozac consensus sequence (underlined) and the coding sequence for cFUC cDNA beginning at the initiation codon (**GGCC**GC*GAATTC**GATATC***GCCGCCACCATG---) and ending with the 3'*Not*I sticky end corresponding to the *Not*I restriction site at base 158. This fragment was then cloned into the *Not*I site of the pBlcFUCNotINheI and a clone containing the sequence in the proper orientation was identified by DNA sequence analysis and designated pBlcFuc. The complete cFUC coding sequence was then excised as an *Eco*RI fragment and cloned into the expression vector pEFNeo, placing it under the transcriptional control of the human elongation factor-1α gene promoter, to give pEFNeocFUC.

2.2.21 Transfection of cells with pEFNeocFUC

2.2.21.1 Electroporation

CHO-K1 cells in Ham's F12, 10% (v/v) FCS and PS, and MDCK cells in DMEM, 10% (v/v) FCS and PS, were grown to confluency, harvested by trypsin-versene treatment, washed with PBS and finally resuspended in PBS at 1 x 10^7 cells/ml. Cells in 1 ml aliquots were placed into disposable electroporation chambers kept at 0 °C. After addition of 10 μg of pEFNeocFUC (section 2.2.20) the cells were electroporated at 275 V and 330 μF or 800 μF using a Cell Porator. After transfection the cells were grown in non-selective medium for 48 h and then subcultured 1:5 and 1:20 into medium containing 1 or 0.5 mg/ml total G418. Approximately 12 days later clones were visible and these were individually picked using cloning rings. Each clone was maintained and expanded in medium containing 0.5 mg/ml total G418. One-day or three-day conditioned medium from confluent cultures of each selected clone was assayed for FUC activity. Clones expressing the highest level of activity were recloned by limiting dilution and retested for enzyme expression levels.

2.2.21.2 DOTAP

MDCK cells were also transfected using N-[1-(2,3-dioleolyloxy)propyl]-N,N,N-trimethylammonium methyl sulphate (DOTAP) as follows. Sterile solutions of DOTAP (45 μl) in 95 μl HeBS (HEPES-buffered saline), and 6.8 μl (7.8 μg) pEFNeocFUC in 69.5 μl PBS, were combined, mixed gently and left at room temperature for 15 min. This mixture was then added dropwise onto MDCK cells at 50% confluency in fresh DMEM, 10% (v/v) FCS and PS. After 48 h the cells were subcultured into G418-selective medium and clones selected as described for electroporated cells (section 2.2.21.1).

2.2.22 Large-scale production of rcFUC

For large-scale production of rcFUC, CHOcFUC40-A2-4 or MDCKcFUC8-6 cell lines (section 4.1.1) were expanded to 15 confluent 75 cm^2 flasks and were each seeded into a cell factory (Nunc 1200 cm^2). CHOcFUC40-A2-4 cells were grown and seeded in COON's/DMEM, 10% (v/v) FCS and PS and MDCKcFUC8-6 cells in DMEM, 10% (v/v) FCS and PS. FCS concentration was reduced to 2% (v/v) once confluency was achieved in the cell factories. Conditioned medium was collected every 3-4 days. When enzyme production levels started to decrease because of cell death, cell growth was revived by the addition of FCS to 5%

or 10% (v/v) for 3-4 days. This cycling of high/low FCS was continued for the duration of the culture. Conditioned medium from cell factories was clarified by centrifugation (550 ***g***; 10 min; 4 °C).

Cell culture and collection of medium from the Bioreactor were done by Dr. Peter Clements and Chris Boulter (Department of Chemical Pathology, WCH).

CHO/rcFUC for pharmacokinetic and ERT studies in fucosidosis dogs was also produced on a larger scale in a Biostat® B Bioreactor (B. Braun Biotech International, Federal Republic of Germany) which was monitored and controlled for O_2, pH, glucose and lactate. Conditioned medium was collected either continuously at 200 ml/h or in bulk twice daily. The medium collected from the Bioreactor was filtered using Whatman 3MM filter paper.

2.2.23 Purification of rcFUC by affinity chromatography

Medium was made 0.02% (w/v) sodium azide and stored at 4 °C and prior to enzyme purification was concentrated approximately 10 to 20-fold in a DC-2 hollow fibre concentrator using a 10 kDa hollow fibre cartridge. To purify rcFUC, the concentrated conditioned medium was first dialysed against 50 mM sodium acetate buffer, pH 5 (Buffer A) at 4 °C overnight and then centrifuged (3,500 ***g***; 10 min; 4 °C) to remove the precipitate that developed during dialysis. The clarified supernatant was applied to a column of fucosylamine insolubilised on cross-linked 4% beaded agarose *via* a 24-carbon-atom spacer (Sigma F3902) equilibrated in Buffer A. Unbound proteins were removed by washing the column with 5 to 10 column-volumes of Buffer A. The rcFUC was then eluted with 5 column-volumes of 1% (w/v) L-fucose dissolved in Buffer A. Fractions were assayed for FUC activity (section 2.2.5.3) and those fractions containing FUC activity pooled, concentrated and the buffer changed to PBS in an ultra filtration stirred-cell. Protein concentration was determined by the Lowry method (1951) and purity assessed by SDS-PAGE (Laemmli, 1970).

2.2.24 Purification of rat liver FUC

To purify rat liver FUC, the liver of a rat was removed, homogenised and a clarified freeze/thaw extract prepared as described in section 2.2.17. The resultant supernatant was dialysed against 50 mM sodium acetate buffer, pH 5 before chromatography on fucosylamine-agarose as described above.

2.2.25 Correction of storage in human fucosidosis cells with rcFUC

Skin fibroblasts from two unaffected individuals (SF4634, SF4686) and from a clinically severe fucosidosis patient (SF2184) were grown to confluency in 25 cm^2 flasks in DMEM, 10% (v/v) FCS and PS and then labelled with L-[^{3}H]-fucose (84 Ci/mmol) at 10 μCi/ml for 48 h. After labelling, the medium was removed, each flask rinsed with 3 ml PBS and the cells refed with growth medium supplemented with either CHO/rcFUC, or MDCK/rcFUC, at 1.6 or 16 nmol/min/ml in the presence or absence of 5 mM M6P. After 48 h cells were harvested and cell lysates prepared as described above (section 2.2.7). Cell lysates were dialysed against 50 mM sodium acetate buffer, pH 5 (16 h; 4 °C) before assaying for FUC (section 2.2.5.3) and β-hexosaminidase activity (section 2.2.5.4), radioactivity and total protein (Lowry, 1951).

Correction of storage in human fucosidosis cells with 16 nmol/min/ml cationized CHO/rcFUC (section 2.2.45), was done in an identical manner.

2.2.26 Radiolabelling of recombinant enzymes

CHO/rcFUC, MDCK/rcFUC and rf4S were radiolabelled with ^{3}H-leucine as follows. Routinely, 25 flasks (75 cm^2) of cells expressing the relevant enzyme were grown to confluency as described in sections 2.2.1.1 and 2.2.1.2. The cell monolayer was then rinsed with PBS and refed with 5 ml/flask of leucine-free α-MEM containing 10% (v/v) dialysed FCS, 5 mM NH_4Cl, 20 μCi/ml ^{3}H-leucine and PS. After 48 h conditioned medium was collected, centrifuged to remove cell debris (390 ***g***; 5 min; 4 °C) and the clarified supernatant stored at 4 °C with 0.02% (w/v) sodium azide until processing (for methods see sections 2.2.3 and 2.2.23).

To obtain intracellular CHO/^{3}H-rcFUC, which is predominantly of the mature form, the CHO/rcFUC cells remaining after removal of the ^{3}H-labelled medium (25 x 75 cm^2 flasks) were rinsed with PBS, harvested with trypsin-versene and pooled. Cell lysates were prepared essentially as described above (section 2.2.7) except the cell pellet was resuspended in 25 ml lysis buffer. The cell lysate was dialysed against 50 mM sodium acetate buffer, pH 5 before purification on fucosylamine-agarose (section 2.2.23).

Activity was determined using the appropriate assay described above (sections 2.2.5.1 and 2.2.5.3) and purity determined by analysis of SDS-PAGE (Laemmli, 1970).

2.2.27 Growth of OX26 hybridoma cells

OX26 hybridoma cells were purchased from the European Collection of Cell Cultures (ECCC No. 84112014). One vial of frozen cells was thawed, resuspended in 10 ml RPMI 1640 medium containing 10% (v/v) FCS, PS and 2 mM glutamine (RPMI complete medium) and 500 µl aliquots were added to the wells of a 24-well plate in which spleen feeder cells (section 2.2.29) had been seeded in 1 ml RPMI complete medium the previous day. As the OX26 hybridoma cells grew they were expanded to 75 cm^2 flasks and were cultured until they reached a cell density of 1 x 10^7 cells/ml, sufficient to establish a Diacult culture. The Diacult comprised 20 ml of a cell suspension in a sterile dialysis tubing bag placed inside a 175 cm^2 flask (Nunclon^{TM}) containing 100 ml RPMI complete medium. Flasks were rotated on a Diacult 4 (Intermed) rotator in an incubator maintained at 37 °C and 5% CO_2. Medium was changed every 2-3 days for up to 3 weeks. After this time the cell suspension containing the OX26 antibody was removed from the dialysis tubing and clarified by centrifugation (690 ***g***; 10 min; 10 °C). The OX26 antibody isotype was confirmed using Iso-strips according to the manufacturer's instructions. The OX26 was then purified as described in section 2.2.28.

2.2.28 Purification of OX26

OX26 was purified using a 1 ml HiTrap Protein G column equilibrated in PBS. The clarified hybridoma medium was applied to the column at 1 ml/min using an Econo System (BioRad). After loading the medium, the column was washed with 50 ml PBS before eluting with 5 ml 100 mM $NaPO_4$ buffer, pH 2.5. The binding capacity of the column was approximately 7 mg. The eluted OX26 was pooled and dialysed against PBS. Purity was assessed by SDS-PAGE (Laemmli, 1970) and protein concentration determined using the Lowry method (1951).

2.2.29 Production of spleen feeder cells

A Balb/c mouse was sacrificed by CO_2-asphyxiation and the spleen, removed under sterile conditions, was placed in 10 ml pre-warmed RPMI complete medium in a petri dish and the spleen cells teased from the tissue using sterile fine-tipped forceps. Spleen cells were then separated from tissue debris by allowing the latter to settle under gravity in a Falcon tube

(Becton Dickson Labware, Franklin Lake, NJ, USA). Spleen cells were transferred to a clean tube and centrifuged (390 ***g***; 10 min; 15 °C). The supernatant was aspirated and the cell pellet gently resuspended in 10 ml RPMI complete medium. This cell suspension was added to 40 ml RPMI complete medium, mixed by inversion and the cells dispensed in 1 ml aliquots into the wells of two 24-well plates and incubated for up to 5 days before use.

2.2.30 Production of monoclonal antibodies to rcFUC

A standard method for monoclonal antibody production was used (Harlow and Lane, 1988). Briefly, a female Balb/c mouse was injected subcutaneously with 50-100 μg CHO/rcFUC emulsified in an equal volume of Freund's complete adjuvant. At two-weekly intervals two more injections were given in Freund's incomplete adjuvant. Blood was sampled during immunisation and was tested for titre to CHO/rcFUC using a standard direct Elisa protocol as described in section 2.2.10 except that CHO/rcFUC was used to coat the plate and SAM-HRP, diluted 1/1,000 in blocking buffer, was used as the secondary antibody. When a titre >1,000 had developed, a final injection of enzyme in PBS was administered three days prior to sacrifice.

Fusion of spleen cells from the immunised mouse and Ag82P3653 myeloma cells was carried out as follows. The myeloma cells were grown in RPMI complete medium in 75 cm^2 flasks to a density of 2 x 10^7 viable cells/ml. The immunised mouse was killed by CO_2 asphyxiation and spleen cells were extracted as described in section 2.2.29, except that PBS was used instead of RPMI complete medium and the spleen cells were passed over glass wool to remove all traces of tissue. The glass wool was washed with extra PBS to enhance recovery of spleen cells. Spleen lymphocytes were pelleted at 390 ***g*** for 10 min at 15 °C then resuspended in 10 ml RPMI complete medium without FCS (RPMI incomplete medium) and cell viability determined. Myeloma cells were harvested by centrifugation (390 ***g***; 10 min; 15 °C) and the cell pellet resuspended in 20 ml RPMI incomplete medium. Myeloma cells were then added to lymphocytes in a ratio of 1:9. The cell mixture was centrifuged at 390 ***g*** for 10 min at 15 °C, the supernatant discarded and the cells were gently mixed to resuspend the cell pellet. 1 ml of pre-warmed polyethylene glycol (42% (w/v) in 75 mM HEPES buffer, pH 8) was added dropwise over 20-30 sec with shaking. RPMI incomplete medium (10 ml) was then added dropwise with shaking and finally another 40 ml RPMI incomplete medium was added. Cells were pelleted by centrifugation at 390 ***g*** for 10 min at 15 °C, the supernatant discarded and the

cells resuspended in 10 ml 0.1 mM hypoxanthine, 0.4 μM aminopterin, 16 μM thymidine (1 x HAT) in RPMI complete medium which had been supplemented with spleen feeder cells (see section 2.2.29). This cell resuspension was added to approximately 200 ml 1 x HAT in RPMI complete medium, which was also supplemented with spleen feeder cells, mixed and plated out into 24-well plates at 1 ml/well.

After 10-14 day's incubation plates were screened for hybridomas. Direct Elisa, as described at the beginning of this section, was used to test the medium of those wells in which hybridomas were present, for antibody reactivity against CHO/rcFUC. Hybridomas showing positive reactivity were expanded, recloned by limiting dilution and retested. Those hybridomas still positive after retesting were isotyped using IsoStrips according to the manufacturer's instructions. An immunobinding assay was used to determine which hybridomas reacted with native CHO/rcFUC. This assay was essentially the same as described in section 2.2.12 except that CHO/rcFUC instead of rf4S was added to each well after the addition of hybridoma medium, and the appropriate assay mixture (4MUF; section 2.2.5.3) was used. Medium of those hybridomas designated as positive by Elisa was also tested for immunohistochemical detection of cFUC as describe in section 2.2.32. Cross-reactivity with rat liver FUC was also determined using a direct Elisa as described above in this section. Western blot analysis was carried out as in section 2.2.11 except CHO/rcFUC was electroblotted onto nitrocellulose and this was probed with hybridoma medium from Elisa-positive clones and the secondary antibody was SAM-HRP. As a test for positive reactivity, part of the membrane was treated with rabbit anti-rcFUC antibody (section 2.2.31) followed by SAR-HRP antibody.

2.2.31 Production of rabbit anti-rcFUC antibody

Rabbit polyclonal antiserum to rcFUC was produced by the IMVS (Adelaide, South Australia) by immunisation with three injections (300 μg each) of sterile CHO/rcFUC at three-weekly intervals. The titre of the polyclonal antibody was determined using a direct Elisa method (section 2.2.10). Briefly, a 96 well plate was coated with 500 ng/well of rcFUC, the polyclonal serially diluted in blocking buffer and detected with SAR-HRP/ABTS substrate. Titre was determined as described in section 2.2.10.

2.2.32 Immunohistochemical analysis of cFUC expression

CHOcFUC40-A2-4 cells were grown and harvested as described in section 2.2.1.1. A drop of the harvested cells was placed into 1 ml of COON's/DMEM, 10% (v/v) FCS and PS in each well of an eight-well Lab Tek chamber slide (Nalge Nunc International, Naperville, IL, USA) and cultured until confluent. The cells were washed twice with PBS and then fixed with 1% (v/v) formaldehyde in PBS for 30 min at 4 °C, followed by two washes with methanol. The wells were rinsed with PBS and then blocked with three 15-min cycles of 10% (v/v) FCS in PBS (blocking buffer). Anti-CHO/rcFUC hybridoma supernatant was then diluted 1:1 with 1.5 μg/ml digitonin in PBS and an amount of this mixture sufficient to cover the cell layer (approximately 250-500 μl) was placed in each well. After incubation for 3 h at room temperature the antibody was removed and the wells were washed with blocking buffer (three cycles of 5 min each). FITC-conjugated SAM antibody diluted 1/15 in blocking buffer, and pre-absorbed against ovalbumin/BSA-Affi-Gel, was then added to each well for 1 h in the dark at 4 °C. After aspirating the antibody the wells were then washed with PBS (3 x 5 min), the chambers and dividers removed, and a drop of PBS:glycerol (1:1) was added to the cells before applying a cover slip. Cells were examined using a fluorescence microscope.

2.2.33 Preparation of insulin peptide fragment, F007

Essentially, a scaled-down version of the method as described in Fukuta *et al.* (1994) was used. Bovine pancreatic insulin (10 mg) was dissolved in 1 ml 10 mM HCl and then 5 ml 100 mM $NaPO_4$ buffer, pH 7.4 was added followed by the addition of 1.5 mg TPCK-trypsin. The mixture was incubated at 37 °C for 20 h and the reaction stopped by addition of 0.5 ml 1 N acetic acid. The solution was lyophilised, resuspended in 4 ml 1 N HCl and then filtered through a Millipore 0.2 μm filter. The insulin fragments resulting from tryptic digestion were separated on reversed-phase HPLC (Dynamax-60AC8 column) using a 0-100% (v/v) acetonitrile gradient in 0.1% (v/v) trifluoroacetic acid. A sample from each peak fraction was analysed on Tricine-SDS polyacrylamide gels (Schagger and von Jagow, 1987) and the structure of each of the tryptic peptides isolated was confirmed by MS/MS. Before applying to MS/MS a sample from each peak fraction was lyophilised, resuspended in 100 μl of ammonium acetate and boiled for 1 h in the presence of 30 mM DTE. Analysis of mass/charge (m/z) peaks together with fragmentation data and bovine insulin tryptic digest data from the Swiss Prot databank allowed the structure of each fragment to be unambiguously determined.

2.2.34 Pyridyldithiopropionate modification of insulin and rcFUC

Pyridyldithiopropionate modification of insulin and rcFUC was done according to a procedure modified from Fukuta *et al.* (1994). Bovine pancreatic insulin was dissolved in 100 mM $NaPO_4$ buffer, 5 mM EDTA, pH 7.4 (Buffer B) at 1 mg/ml and an 8-fold molar excess of the water-soluble heterobifunctional crosslinker, sulfosuccinimidyl 6-[3'-(2-pyridyldithio)-proprionamido]hexanoate (SPDP) was added. After incubation for 15 min at room temperature, the reaction was stopped by the addition of 10 mM Tris-HCl buffer, pH 7. To remove free SPDP, the reaction mixture was initially chromatographed on a PD-10 column (3 cm x 1 cm) equilibrated in Buffer B but in later experiments was dialysed extensively against Buffer B instead. After dialysis the protein concentration was determined by the Lowry method (1951).

CHO/rcFUC was modified in a similar manner. To a 1 mg/ml solution of purified rcFUC in Buffer B, L-fucose was added to 20 mM and incubated for 15 min at room temperature. This was followed by the addition of 0.07 mg SPDP for 5 min at room temperature. The reaction was quenched and the reaction mixture was dialysed as described above for insulin. FUC activity was monitored at each step of the procedure.

2.2.35 Quantification of pyridyldithiopropionate modification of insulin and rcFUC

To determine the degree of pyridyldithiopropionate modification of insulin and rcFUC an aliquot of the dialysed SPDP-derivatized protein was reduced with 25 mM DTE for 60 min at room temperature (Walus *et al.*, 1996). Release of pyridine-2-thione was measured spectrophotometrically by determination of absorbance at 343 nm. A control blank of underivatized protein in Buffer B with 25 mM DTE was included. Using the molar extinction coefficient of pyridine-2-thione at 343 nm (8.08×10^3 M^{-1} cm^{-1}), and the protein concentration of derivatized protein after correction for background, the number of moles of pyridyldithiopropionate bound per mole of insulin or rcFUC was calculated.

2.2.36 Conjugation of insulin to rcFUC

SPDP-derivatized rcFUC was first treated with 25 mM DTE for 1 h at room temperature and then dialysed against Buffer B at 4 °C as described above (section 2.2.34). After dialysis, SPDP-derivatized insulin was added in a molar ratio of 1:10 (rcFUC:insulin) and allowed to react at room temperature for 16 h with rotation. An aliquot of the reaction mixture was analysed for conjugate formation by SDS-PAGE under non-reducing conditions (Laemmli, 1970).

2.2.37 Thiolation of rcFUC with SATA

Thiolation of rcFUC with SATA was carried out according to a modified procedure of Walus *et al.* (1996). To a 6 mg/ml solution of rcFUC in Buffer B (section 2.2.34) was added a volume equivalent to a 5-fold molar excess of N-succinimidyl S-acetylthioacetate (SATA) dissolved in anhydrous dimethylformamide. The reaction was incubated at room temperature for 30 min and quenched by the addition of 10 mM Tris-HCl buffer, pH 7.4. Free SATA was removed by dialysis against Buffer B as previously described (section 2.2.34) and FUC activity (section 2.2.5.3) and protein concentration (Lowry, 1951) determined.

2.2.38 Quantification of modification of rcFUC with SATA

The extent of modification of rcFUC with SATA was determined using Ellman's reagent (5,5'-Dithio-bis-(2-nitrobenzoic acid), DTNB), a water-soluble compound that can be used for quantitating free sulphydryl groups in solution (Ellman, 1959). It has high specificity for sulphydryl groups at neutral pH values resulting in the release of a yellow product, thionitrobenzoic acid (TNB), which can be quantified by spectrophotometry at 412 nm (molar extinction coefficient of 14.15×10^3 M^{-1} cm^{-1}).

The method involved deacetylation of an aliquot of dialysed SATA-derivatized rcFUC by the addition of 500 mM hydroxylamine, 50 mM $NaPO_4$ buffer, pH 7.5, 25 mM EDTA to give a final concentration of 50 mM hydroxylamine. After incubation at room temperature for 60 min the reaction mixture was adjusted to a final volume of 250 µl with 50 mM $NaPO_4$ buffer, 1 mM EDTA, pH 7.5 and then added to 2.5 ml of 100 mM $NaPO_4$ buffer, pH 8. Next, 50 µl of 10 mM DTNB in 100 mM $NaPO_4$ buffer, pH 8 was added and the reaction allowed to proceed for 15 min at room temperature before measuring absorbance at 412 nm. Control blank samples

included unmodified rcFUC in Buffer B plus 50 mM hydroxylamine. The number of moles of free sulphydryl groups per mole of rcFUC was calculated using the molar extinction coefficient of TNB and the protein concentration of rcFUC (Lowry, 1951).

2.2.39 Conjugation of SATA-derivatized rcFUC with SPDP-derivatized insulin

Conjugation of derivatized rcFUC and insulin were carried out according to a modified method of Walus *et al.* (1996). SATA-derivatized rcFUC was deacetylated with 50 mM hydroxylamine and the SPDP-derivatized insulin at a 10-fold molar concentration greater than that of rcFUC was then added immediately and the mixture incubated overnight at room temperature. Western blot analysis of the resulting reaction products was carried out as described in section 2.2.11 except CHO/rcFUC, insulin and insulin-FUC conjugates were electrophoresed on a 12% (w/v) mini polyacrylamide gel. After transfer, the nitrocellulose membrane was probed with a mouse monoclonal antibody to human insulin, which also cross-reacts with bovine insulin, and reactivity detected using SAM-HRP as the secondary antibody.

2.2.40 Pyridyldithiopropionate modification of OX26 through amine groups

OX26 was prepared and purified as described in sections 2.2.27 and 2.2.28. A 7 mg/ml solution of OX26 in Buffer B (section 2.2.34) was treated with a 5-fold molar excess of SPDP at room temperature for 15 min according to a procedure modified from Walus *et al.* (1996). The reaction was stopped by the addition of 10 mM Tris-HCl buffer, pH 7.4 and then dialysed against Buffer B to remove free SPDP. Quantification of pyridyldithiopropionate modification of OX26 was determined as described in section 2.2.35 except control blanks included OX26 instead of insulin.

2.2.41 Pyridyldithiopropionate modification of OX26 through carbohydrate groups

OX26 (7 mg/ml) in 100 mM sodium acetate buffer, 150 mM NaCl, pH 5 (Buffer C) was oxidised by addition of 1 mM sodium meta-periodate (procedure modified from Walus *et al.*, 1996). The reaction was incubated at 0 °C for 60 min in the dark before quenching with 15 mM ethylene glycol. After dialysis against Buffer B (section 2.2.34) overnight at 4 °C, 100 mM 3-(2-pyridyldithio)propionyl hydrazide (PDPH) in anhydrous dimethylformamide was added to a

15-fold molar excess relative to the (oxidised) OX26. This reaction was allowed to proceed for 60 min at room temperature and was then dialysed against Buffer B at 4 °C overnight. The degree of modification of OX26 with PDPH was determined spectrophotometrically as described in section 2.2.35.

2.2.42 Conjugation of rcFUC to OX26

OX26 modified with pyridyldithiopropionate either *via* amine or carbohydrate groups as described above in sections 2.2.40 and 2.2.41, respectively, was conjugated to an equimolar concentration of SATA-derivatized rcFUC (section 2.2.37) in the presence of 50 mM hydroxylamine overnight at room temperature with constant mixing (method modified from Walus *et al.* (1996)). Conjugates were dialysed against 50 mM sodium acetate buffer, pH 5 before chromatography over fucosylamine-agarose (section 2.2.23) to remove unconjugated OX26.

FUC activity (section 2.2.5.3) was monitored at all stages of the procedure and conjugates were analysed by SDS-PAGE (5% (w/v) acrylamide) under non-reducing conditions before and after chromatography on fucosylamine-agarose.

2.2.43 FACS analysis

Rat hepatoma cells (H4IIE) were grown and harvested as described in section 2.2.1.5. After dispersing cell clumps, 0.5 ml aliquots (approximately 10^5 cells) were dispensed into tubes containing 2 ml of DMEM, 10% (v/v) FCS and PS. The cells were centrifuged at 170 ***g*** for 3 min at 15 °C, the supernatant aspirated and the cells resuspended in 100 µl of fresh medium/tube. The cells were then kept at 4 °C for the duration of the experiment. OX26 (7 µg), rcFUC (9 µg) or OX26-FUC conjugates (8 µg), in the presence or absence of 5 mM M6P, were then added and incubated for 20 min. After this time 5 ml of cold PBS was added to each tube, the samples centrifuged as above, the supernatant removed and the cells resuspended in 100 µl of medium. To assess binding *via* detection of OX26, 1 µl of SAM-FITC (that is, a 1/100 dilution) was added to cells exposed to OX26 and OX26-FUC conjugates for 20 min before washing as above by dilution and centrifugation. Alternatively, for cells exposed to FUC or OX26-FUC conjugates the FUC moiety was detected using rabbit anti-rcFUC polyclonal (titre 1 in 2 x 10^6, diluted 1/100 as above) and the SAR-FITC (final dilution of 1/100 in medium)

reagent with incubation of, and washing between, each antibody as described above. After a final wash step, the cells were resuspended in 200 µl PBS containing 50 µg/ml propidium iodide. Appropriate control samples were included and processed as described above. Cells were analysed for fluorescence intensity using a non-cell-sorting flow cytometer (FACScan, Becton Dickinson) and the results were analysed using Cellquest software version 3.01f (Becton Dickinson). The counting of FITC-positive cells was limited to the live cell population as defined by low propidium iodide fluorescence and by forward/side scatter plots.

2.2.44 Binding specificity of OX26 and OX26-FUC conjugates to Tf receptors on H4IIE cells

H4IIE cells (aliquots of approximately 10^5 cells/100 µl of medium) were prepared as described above (section 2.2.43) and kept at 4 °C throughout the experiment. Cells were exposed to 10-fold incremental concentrations of OX26 (0, 0.7, 7, 70 and 700 µg) for 20 min in the presence or absence of 5 mM M6P. After washing with cold PBS, cells were resuspended in 100 µl fresh medium and then each aliquot was treated with 8 µg of OX26-FUC conjugate and detected with rabbit anti-rcFUC polyclonal antibody/SAR-FITC as in section 2.2.43. To determine background levels of fluorescence control samples were treated as above but omitting OX26-FUC.

2.2.45 Cationization of rcFUC with putrescine

In order to protect the active site of CHO/rcFUC during the cationization reaction, L-fucose was added to 20 mM to a 1 mg/ml solution of the enzyme in 100 mM $NaPO_4$ buffer, pH 7.4, 5 mM EDTA, for 15 min at room temperature. Putrescine, (EDC) and N-hydroxysuccinimide (NHS) were then added to a final concentration of 400 mM, 14 mM and 15 mM, respectively. Cationization was allowed to proceed for 20 min at room temperature after which time the reaction was stopped by the addition of 100 mM sodium acetate buffer, pH 6. The reaction mixture was dialysed against four 2 l changes of PBS over 24 h at 4 °C and then assayed for FUC activity (section 2.2.5.3). The degree of change in pI resulting from cationization was ascertained by IEF as described in section 2.2.6.5b.

^{3}H-labelled CHO/rcFUC (section 2.2.26) was also cationized in the above manner and was used to determine circulating plasma half-life and tissue distribution in rats at 1 mg/kg body weight as detailed in section 2.2.46.

Correction of storage in human fucosidosis SF with rcFUC, cationized as described above, was performed as described in section 2.2.25.

2.2.46 *In vivo* distribution studies and plasma half-life of rcFUC in rats

Hooded Wistar rats weighing between 200 and 360 g were used in the following studies to determine plasma clearance and tissue distribution of radiolabelled enzyme. Rats were anaesthetised by mask inhalation of isofluorane in conjunction with NO_2:O_2 at 1:2. The right jugular vein was exposed by blunt dissection through a skin incision medial to the right shoulder. The vein was cleared of connective tissue and then ligated at its cephalad end with a length of 4-0 silk suture which was held in place with a haemostat. Another suture was looped loosely under the caudal exposed end of the vein and this was also held in place with a haemostat. This rendered a degree of tension to the vein and enabled blood flow control when an incision at 45^{o} using fine scissors was made in the vein between the two sutures. The vein was opened and stretched slightly using curved jewellers forceps, and a 10 cm silastic catheter (id 0.064 cm and od 0.119 cm with cuffs of id 0.12 cm and od 0.16 cm placed at positions 2.5 cm and 2.7 cm from the atrial end) filled with 10 U heparin/ml was inserted into the vein using the forceps as a guide. The catheter was then threaded carefully into the right atrium, the distance of which was designated by the position of the first cuff. The catheter was secured in position by suturing between the first two cuffs. Throughout the procedure the catheter, which was occluded with a syringe filled with 10 U heparin/ml, was tested for patency by withdrawing blood into the catheter and flushing with the heparin solution.

Once the catheter was in place, a 100 µl sample of blood was taken prior to injection of radiolabelled enzyme. The volume of enzyme and the time of infusion were between 150 and 250 µl and 20 to 30 secs, respectively. After injection of the radiolabelled enzyme the catheter was flushed with 100 µl heparin solution and immediately a 100 µl sample of blood was withdrawn and this was designated the zero time point. Successive blood samples were withdrawn at specified times and after each withdrawal the catheter was flushed with an equal volume of heparin solution. After the 1 h sample had been taken the catheter was occluded and

was tunnelled below the skin to the back of the neck through an incision made in the skin. Skin incisions were sutured, anaesthesia was withdrawn and the animal was observed until consciousness was regained. Food and water were supplied until the final blood sample was taken under anaesthesia at 4 h and/or 24 h. After the last blood sample was taken, the animal was killed by CO_2 asphyxiation after exsanguination. The skull was opened and the brain removed and treated as described in the following section. Other organs removed included the liver, kidneys, spleen, lungs, heart, pancreas, aorta, trachea, eyes and, if available, urine. All organs, or samples thereof, were weighed (wet weight), minced finely with a scalpel and then solubilised with 1 N NaOH at 5 ml NaOH/gm tissue, overnight on a rotator at room temperature. Brain samples, including unsonicated total homogenate, parenchyma and capillary pellet were obtained as described in section 2.2.47 and solubilised with NaOH as detailed above. The solubilised tissues were then analysed as described in section 2.2.19.

Heparinised blood samples collected at specified times were centrifuged at 13,000 ***g*** for 5 min at 4 °C. The plasma was removed and 20 µl samples (in duplicate) in 3 ml scintillant were counted in a Wallac 1409 liquid scintillation counter. Circulating half-life was determined from a graph of cpm plotted against time.

2.2.47 Capillary depletion

Technical assistance was provided by Dr. Don Anson (Department of Chemical Pathology, WCH).

The method used to separate the brain parenchyma from brain capillaries was essentially that of Triguero *et al.* (1990). After the brain was dissected it was rinsed in PBS to remove extraneous blood and the two hemispheres separated and weighed. Each hemisphere, which included the cerebrum, cerebellum and base brain, was treated separately but identically as follows. Each hemisphere was homogenised in 3.5 ml physiological buffer (10 mM HEPES, 141 mM NaCl, 4 mM KCl, 2.8 mM $CaCl_2$, 1 mM $MgSO_4$, 1 mM NaH_2PO_4 and 10 mM D-glucose, pH 7.4) with a manual tapered glass homogeniser applying 5 strokes in less than 1 min. A 4 ml solution of 26% (w/v) dextran was added and the brain was rehomogenised (3 strokes). A 500 µl sample of homogenate was removed, and the remainder of the homogenate was carefully layered onto a 1 ml 13% (w/v) dextran/physiological buffer cushion in 10 ml V-bottom polycarbonate tube. After centrifugation at 5,400 ***g*** for 10 min at 4 °C the supernatant,

that is, the brain parenchyma, was carefully removed so as not to disturb the capillary pellet. This pellet was then resuspended in 500 µl physiological buffer. Aliquots of the total brain homogenate, brain parenchyma and capillary pellet were sonicated on ice using an Ultrasonics Processor (Ultrasonics Inc.). Samples were pulsed at 35% duty cycle for 3 x 15 sec with 45 sec intervals between sonication. After sonication the samples were centrifuged (13,000 ***g***; 5 min; 4 °C) and the supernatants assayed for alkaline phosphatase (ALP) and γ-Glutamyl transpeptidase (GGT) using an autoanalyser method (Synchron CXR system, Beckman Instruments Inc., Fullerton, CA, USA) and total protein (Lowry, 1951).

In order to test the level of contamination of brain parenchyma by radioactive protein that is present in capillary blood leaking from the vasculature during homogenisation of the brain, a rat was injected with 5 x 10^6 cpm of ^{14}C-inulin, a peptide known not to cross the BBB (Pardridge, 1991). The rat was sacrificed 10 sec later, the brain was processed as above and analysed for ^{14}C cpm. Measured radioactivity was expressed as a percentage of the total injected dose.

2.2.48 Europium-labelling of OX26

200 µg of the Europium^{+3}-chelate of N^1-(p-isothiocyanatobenzyl)-diethylenetriamine-N^1,N^2,N^3-tetraacetic acid was added to 1 mg of OX26 in 200 µl of 100 mM $NaHCO_3$ buffer, pH 8.5 containing 0.9% (w/v) NaCl and the reaction mixture was incubated at room temperature for 16 h. To remove free Eu^{+3}, and any aggregates that may have formed, the reaction mixture was chromatographed over a Superose 12 column (28 cm x 1.5 cm) equilibrated in 50 mM Tris-HCl buffer, pH 7.8, 0.9% (w/v) NaCl at a flow rate of 0.5 ml/min and pressure of 150 kPa. Fractions containing non-aggregated Eu^{+3}-labelled OX26 were pooled and concentrated using a centricon filter (Amicon) and then assayed for protein (Lowry, 1951). The degree of Eu^{+3} labelling of the OX26 was determined by serial dilution of an aliquot of the concentrated sample in Enhancement Solution (0.1% (w/v) Triton X100, 6.8 mM potassium hydrogen phthalate, 100 mM acetic acid, 50 µM Tri-n-octyl phosphine oxide, 15 µM 2 naphthoyltrifluoroacetone), dispensing 200 µl amounts into microtitre strip wells which were then mixed gently for 10 min on a plate shaker before measuring fluorescence with a dissociation-enhanced time-resolved fluorometer (Wallac Delfia® Research Fluorometer). The concentration of Eu^{+3} was estimated by reference to a 1 nM Eu^{+3} standard supplied by the

manufacturer. The number of moles of Eu^{+3}/mole of OX26 was then calculated from the concentration of Eu^{+3} and protein concentration (Lowry, 1951).

2.2.49 Rat tissue distribution of OX26-Eu^{+3}

OX26-Eu^{+3} (1.25 x 10^{10} counts) was injected *via* a catheter into the jugular vein of a Hooded Wistar rat at 1mg/kg body weight as described in section 2.2.46. Blood samples were taken at specified times and after 4 h the rat was killed and tissues removed and processed as described in section 2.2.46. To determine the fluorescence of plasma samples, 2 µl aliquots, in duplicate, were added to 198 µl of Enhancement Solution (section 2.2.48) in microtitre strip wells, the plate was shaken on a plate shaker for 10 min and then counted in a time-resolved fluorometer.

After capillary depletion of the brain and sonication to determine ALP and GGT activities (section 2.2.47) unsonicated samples of total brain homogenate (100 µl), parenchyma (500 µl) and capillaries (100 µl) were extracted with a volume of 1 N NaOH equivalent to five times the volume of the sample, overnight at room temperature on a rotator. Tissue extracts were centrifuged at 390 ***g*** for 10 min at 10 °C, a sample of the supernatant was neutralised with an equal volume of 1 N HCl and then serially diluted from 1/2 to 1/64 in Enhancement Solution. A 200 µl aliquot of each dilution was placed in microtitre strip wells and shaken for 10 min on a plate shaker before reading fluorescence in a time-resolved fluorometer. Other tissues were treated by taking a known weight of each, mincing and extracting with a volume of 1 N NaOH equivalent to five times the weight of the tissue as above. After extraction, the supernatant of each sample was treated in the same way as described for brain in this section. Results for each tissue were expressed as a percentage of the total fluorescent counts injected.

2.2.50 Isolation and enzyme assays of canine blood leucocytes

Five ml (2-3 ml from newborn pups) venous blood collected into EDTA tubes was sent from Westmead Hospital, NSW at 4 °C and then processed at room temperature. Leucocytes were isolated by dextran sedimentation according to the method of (Kampine *et al.*, 1966). Firstly whole blood was centrifuged at 2,100 ***g*** for 5 min at 10 °C. Plasma was removed to within 2-3 mm above the buffy coat and either stored at 4 °C (if to be assayed within 30 min), or at -20 °C. 0.9% (w/v) NaCl was added to the packed cells to a final volume of 8 ml followed by 2 ml of 5% (w/v) dextran in 0.7% (w/v) NaCl. The blood was resuspended by gentle inversion and

allowed to stand until the red cells had settled out to occupy the lowest one-third of the tube (generally 20-60 min). The supernatant was removed and centrifuged at 1,500 ***g*** for 2 min at 10 °C to pellet the leucocytes which were subsequently resuspended in 4 ml of 0.2% (w/v) NaCl for 45 sec to lyse any contaminating red blood cells. Isotonicity was restored by the addition of 3.2 ml 1.8% (w/v) NaCl and leucocytes isolated by centrifugation at 1,500 ***g*** for 2 min at 10 °C. After discarding the supernatant, pellets were either frozen at -20 °C or, if to be assayed immediately, resuspended in 100-500 µl 0.1% (v/v) Triton X100 and freeze/thawed 6 times. Cell extracts were clarified by centrifugation at 1,500 ***g*** for 5 min at 10 °C and the supernatant assayed for FUC (section 2.2.5.3) and β-hexosaminidase activity (method for white blood cells, section 2.2.5.4). Results were normalised to total cell extract protein as determined by the Lowry method (1951). A discriminant function was used to determine normal, carrier and affected dogs (Healy *et al.*, 1984).

2.2.51 Isolation of canine fucosidosis brain storage products

Isolation and measurement of canine fucosidosis brain storage products were carried out by Vivienne Muller (Department of Chemical Pathology, WCH).

Cerebellum and cerebrum from untreated dogs with fucosidosis were obtained from Drs. Rosanne Taylor and Margaret Ferrara (Westmead Hospital, NSW). A total of 200 mg (wet weight) of minced cerebrum was extracted using chloroform:methanol:water (1:1:0.4) with sonication (Folch *et al.*, 1957; Folch-Pi, 1972). The slurry was filtered through Whatman 3 MM paper and the filter rinsed with extraction solvent. The upper (aqueous) phase of the filtrate was kept, and the protein precipitate collected on the filter was sonicated again in 2 ml water and clarified by centrifugation. The aqueous supernatant and the upper phase were combined, dried and then resuspended in 0.5 ml water. Hexose was measured by the resorcinol colorimetric method (Monsigny *et al.*, 1988) and fucose was measured by the fucose dehydrogenase method (Cohenford *et al.*, 1989) without the neocuproine step.

2.2.52 Thin layer chromatography of fucosidosis dog brain products

Brain products isolated as described above from the cerebrum of an affected untreated fucosidosis dog were digested with CHO/rcFUC and MDCK/rcFUC at pH values ranging from 2 to 7. A volume equivalent to 12 μg hexose was used per assay. This was made up to 22 μl with water and an equal volume of 50 mM buffer, which was either glycine, pH 2; sodium formate, pH 3; sodium acetate, pH 4 and 5; sodium dimethylglutarate, pH 6; or citrate/phosphate, pH 7, was added followed by 1 μl of a 2.5 mg/ml solution of MDCK/rcFuc or CHO/rcFuc, and the reaction incubated at 37 °C for 20 h. Two samples, one at pH 2 and the other at pH 7, were also incubated without the addition of enzyme. After digestion, 50 μl of AG-501-X8(D) mixed-bed resin was added to the reaction mixture, vortexed every 5 min over 15 min, and then centrifuged (13,000 ***g***; 1 min; 25 °C). The supernatant was removed, the resin washed with 100 μl water and after centrifugation as above the supernatant removed and combined with the first supernatant. Samples (pooled supernatant) were lyophilised, resuspended in 3 μl water and applied to an acid-resistant silica gel TLC plate which was chromatographed in butanol:acetic acid:water (2:2:1) for 6 h. A sample of L-fucose (12 μg) was included as a standard. The chromatograph was allowed to dry and was rechromatographed as above. When dry, the chromatograph was sprayed with 0.25% (w/v) orcinol, 0.25% (w/v) resorcinol dissolved in 2 M sulphuric acid in 95% ethanol. The plate was then heated at 110 °C to visualise saccharide containing material.

2.2.53 Tissue distribution of rcFUC in fucosidosis dogs

CHO/rcFUC, purified as described in section 2.2.23, was obtained from pEFNeocFUC40-A4-2 cells grown either in two-tier cell factories or in a Bioreactor (section 2.2.22). Two male fucosidosis dogs diagnosed by having low levels of FUC activity in plasma and peripheral leucocytes (sections 2.2.5.3 and 2.2.51) were from a breeding colony of fucosidosis English springer spaniels housed at Westmead Hospital and under the supervision of Dr. Rosanne Taylor (Department of Veterinary Science, University of Sydney). The two dogs were littermates, were named Bobby and Biggles and at the time of enzyme infusion they were 10 and 16 months of age, and 13 and 18 kg, respectively. The dogs were premedicated with 10 mg acepromazine and 50 mg hydrocortisone 30 min before infusion of CHO/rcFUC at 1 mg/kg *via* the cephalic vein over 10 min. After infusion, heparinised blood samples were collected from the cephalic vein at designated time intervals up to 48 h. Plasma was recovered by

centrifugation at 2,100 ***g*** for 10 min at 10 °C and a 5 µl aliquot of plasma was assayed for FUC activity. After 48 h, the dogs were euthanased with an overdose of intravenous barbiturate. Tissues were collected, weighed and frozen at -20 °C. These tissues were transported on dry ice to the WCH for processing. Typically, a 1 g portion of thawed tissue was finely minced with a scalpel and then homogenised at maximum speed for 1-2 min on ice in twice its volume of 20 mM Tris-HCl, 250 mM NaCl buffer, pH 7 using an Ultra T25-Turrax Homogeniser. The homogenate was freeze/thawed six times and clarified by centrifugation at 13,000 ***g*** for 10 min at 4 °C. The resulting supernatant was assayed for FUC activity (section 2.2.5.3) and for protein using the Lowry method (1951). Thin sections were taken for histological analysis using light and electron microscopy.

2.2.54 Long-term ERT in a fucosidosis dog

All veterinary procedures were performed by Dr. Rosanne Taylor. (University of Sydney, Sydney, NSW, Australia).

A female dog, named Chelsea, was diagnosed within 24 h of birth as being fucosidosis-affected based on having almost undetectable levels of FUC activity in plasma and white blood cells as described above in the previous section. At 2 months of age Chelsea was infused with CHO/rcFUC after premedication as described above for Bobby and Biggles. Hydrocortisone was increased to 25 mg when animal weight exceeded 10 kg. Enzyme was infused on a weekly basis at 1 mg/kg initially and then the dose was decreased to 0.3-0.2 mg/kg as shown in Figure 4.23. The final enzyme infusion at age 12 months was at 1 mg/kg and 48 h before sacrifice. Prior to each infusion, heparinised blood was collected to monitor for immune response to the infused enzyme (section 2.2.55). On several occasions heparinised blood was also collected post-infusion of CHO/rcFUC at specified times to determine circulating plasma half-life (section 2.2.53). Urine was collected throughout the course of therapy and was stored frozen without preservative. Urine was analysed for levels of excreted fucose-containing storage products (section 2.2.56). Chelsea was cared for by animal care attendants at Westmead Hospital on a daily basis and was assessed clinically once a week at the time of enzyme infusion by Dr. Rosanne Taylor. Two weeks prior to euthanasia a rigorous neuroanatomical examination was conducted by Professor Brian Farrow (University of Sydney). This examination included assessment of cranial nerve responses, spinal reflexes, mental status, postural reactions and gait and posture. At the time of euthanasia, a post mortem was

performed and tissues were examined for macroscopic pathology. Designated tissues and nerves were collected, weighed and analysed for residual FUC activity as described in section 2.2.53. Thin sections were also taken for examination of cell vacuolation by light and electron microscopy.

2.2.55 Determination of antibody titre in a fucosidosis dog on long-term ERT

Plasma collected post 16 weeks of therapy was analysed for antibody titre by a modification of the Elisa method as described in section 2.2.10. Immulon 1 flat bottom Removawell strips were coated with CHO/rcFUC at 500 ng/well. Dog plasma was diluted 1/50 and then serially with two-fold dilutions in 0.5% (w/v) gelatine, 0.2% (v/v) Tween 20 in 20 mM Tris-HCl, 250 mM NaCl buffer, pH 7 (gelatine buffer). The secondary antibody was sheep anti-dog IgG antibody-HRP conjugate, diluted 1/10,000 in gelatine buffer.

2.2.56 Urinary analysis of L-fucose

A colorimetric test for free and bound L-fucose was used according to the method of Cohenford (1989). Briefly, the volume of urine used in µl was equivalent to 176 divided by the urine creatinine concentration in mM. This volume was made up to 100 µl with water followed by the addition of 100 µl of 0.2 N HCl. Acid hydrolysis was performed at 100 °C for 60 min in capped glass tubes which were then allowed to cool on ice before centrifugation at 1000 ***g*** for 1 min to collect the condensate. The boiled samples were neutralised with 200 µl of 0.1 N NaOH before adding 1 ml of freshly prepared L-fucose dehydrogenase (0.1 U/ml) and NAD (5.15 µmol) in 15 mM Tris-HCl buffer, pH 8.5. Assay tubes were incubated at room temperature for 50 min and then 1.5 ml of 3 mM $CuSO_4.5H_2O$, 8 mM neocuproine in 200 mM sodium acetate buffer, pH 4.7 was added. The colorimetric reaction was allowed to develop for 15 min before reading absorbance at 455 nm. L-fucose standards (0-75 nmol) were treated in an identical fashion. L-fucose standards were also made up in urine from an affected dog, the amount of which was based on a creatinine equivalent as determined above, and were treated as above except that acid hydrolysis was omitted.

Chapter 3: Mucopolysaccharidosis type VI

3.1 Purification and characterisation of rf4S

3.1 Introduction

The cloning of the human 4S gene (Peters *et al.*, 1990b; Schuchman *et al.*, 1990) and its expression in CHO cells (Anson *et al.*, 1992b), together with the availability of a large animal model, feline MPS VI (Jezyk *et al.*, 1977; Haskins *et al.*, 1979b), have been critical in the development of ERT for this disorder. The significantly larger amounts of 'high uptake' enzyme produced by recombinant DNA technology as compared to the highly labour intensive, low yield of 'low uptake' enzyme obtained by extraction from tissue sources (McGovern *et al.*, 1982; Gibson *et al.*, 1987) has made it possible to undertake realistic pre-clinical trials in MPS VI cats.

In published studies of ERT in MPS VI cats (Crawley *et al.*, 1996; Byers *et al.*, 1997; Crawley *et al.*, 1997) recombinant human enzyme was used. In the first of these studies, in which older cats were treated with rh4S, results indicated that there were variable degrees of clearance of storage from soft tissues and that a reduction in disease progression appeared to be correlated with earlier age of onset of therapy. In the second study, where treatment was commenced at birth, and continued for six months using 1 or 5 mg rh4S/kg body weight, a dose-dependent improvement in somatic and skeletal pathology was observed. However, despite anti-histamine premedication, most animals displayed symptoms typical of hypersensitivity reactions to infused enzyme.

In 1992 the f4S gene was cloned (Jackson *et al.*, 1992) and subsequently expressed in CHO cells (Yogalingam *et al.*, 1996), thus enabling a pre-clinical study to be undertaken using native, that is, feline enzyme in MPS VI cats. Before doing this it was necessary to demonstrate that rf4S had similar properties to rh4S. Therefore, the aims of the experiments described in this section were to purify and characterise rf4S as a preliminary step towards evaluation of species-specific ERT in feline MPS VI.

3.1 Results

3.1.1 Large-scale production of rf4S

The cloning and expression of rf4S are described in Yogalingam *et al.* (1996). To enable production of large amounts of rf4S, various parameters thought likely to affect production and/or subsequent purification of rf4S were assessed in Nunc 1200 cm^2 cell factories. These included the concentration of FCS in, and addition of NH_4Cl to, the culture medium. NH_4Cl, a lysosomotropic amine, prevents the acidification of lysosomes thus enhancing secretion of lysosomal enzymes by preventing the dissociation of the M6PR and its ligand (Chang *et al.*, 1988). CHOf4S-2 cells grown in COON's/DMEM medium with 5% (v/v) FCS produced approximately 8.7 mg rf4S/l of culture medium over 4 days as opposed to 4.2 mg/l when grown in the absence of FCS. Cells grown in medium supplemented with 2% (v/v) FCS expressed intermediary levels of rf4S (5-6 mg/l). Inclusion of 5 mM NH_4Cl only marginally increased production levels (10-15 %) and this was offset by increased cell death. From these results a protocol was developed to facilitate cell growth without overly compromising enzyme expression. This involved growth in COON'S/DMEM medium with 2% (v/v) FCS and no NH_4Cl with media changes every 3-4 days. Exposing the cells to medium supplemented with 10% (v/v) FCS when production levels started to decline enhanced cell regrowth. By cycling conditions in this way cells could be maintained in culture for up to 6 months with media changes every 3-4 days.

Subsequently enzyme was produced on a large-scale in a 12 litre Bioreactor by Jodie Varnai of the Department of Biotechnology at the University of New South Wales. Growth conditions in the Bioreactor were evaluated in DMEM/COON'S F12 serum-free medium with NH_4Cl and butyric acid, known to increase expression of transfected genes (Dorner *et al.*, 1989). Because medium was continuously being exchanged (0.2 vol/10^6 cells/ml/day), and O_2 and pH were constantly monitored and adjusted, cell attrition was less pronounced in the presence of NH_4Cl and butyric acid in the Bioreactor as compared with cell factories. Accordingly, optimal conditions for enzyme production by CHOf4S-2 cells in the Bioreactor system were determined to be DMEM/COON'S F12 serum-free medium with 5 mM NH_4Cl and 0.5 mM butyric acid.

3.1.2 Purification of rf4S

rh4S was purified by a one-step immunopurification procedure. A panel of ten monoclonal antibodies that bind to h4S purified from liver (Brooks *et al.*, 1991; Brooks *et al.*, 1994) was available and these monoclonal antibodies were initially screened against purified human and feline liver 4S to determine cross-reactivity. Of these monoclonal antibodies, F58.3 and F22.1 showed highest reactivity with feline liver 4S in an immunobinding assay, while the other eight reacted poorly or not at all. The monoclonal antibody F66 showed no cross-reactivity and was therefore used as a negative control in subsequent analyses where appropriate. Monoclonal antibodies F58.3, F22.1 and F66 were retested using rf4S and fh4S in a Sandwich Elisa and immunobinding assay. Results indicated that rf4S reacted most strongly with F58.3 in the Sandwich Elisa and this reactivity was four times better than that with F22.1 but was only 61% of the reactivity of F58.3 with rh4S (Table 3.1). In the immunobinding assay, F58.3 captured approximately 21% more rf4S than F22.1, however, this was about 20% less than with rh4S. As expected there was no binding of rf4S with F66 in either the Sandwich Elisa or binding assay (Table 3.1).

Table 3.1: Immunoquantification and enzyme immunobinding assays of purified rf4S and rh4S using the monoclonal antibodies F58.3, F22.1 and F66.

Immunoquantification Assay			
		OD_{414}	
	F58.3	**F22.1**	**F66**
rf4S	1.8	0.48	0
rh4S	3.01	2.5	1.8
Immunobinding Assay			
		FU	
rf4S	56.1	44.5	0
rh4S	69.4	52.5	23.7

Immunoquantification data are in OD_{414} units of Elisa reactivity. Enzyme immunobinding assay results are in arbitrary fluorogenic units (FU).

Because rf4S had a stronger affinity for F58.3 compared to F22.1, a 100 ml column of F58.3 linked to Affi-Gel 10 was prepared for large-scale purification of rf4S. The efficiency of coupling was 85.4% which indicated that 6.5 mg of F58.3 was bound per ml of Affi-Gel. Conditions for binding and elution were identical to those of rh4S (Anson *et al.*, 1992b) and routine yields of between 70-80% of bound enzyme (i.e., approximately 20 mg f4S at column capacity) were obtained. Recoveries from the newly coupled F58.3-Affi-Gel were considerably better than that previously published (Yogalingam *et al.*, 1996) and are attributed to diminished binding of enzyme to the much used and regenerated column matrix used in the original studies.

3.1.3 Characterisation of rf4S

3.1.3.1 Subunit Mr

To determine subunit Mr immunopurified rf4S was electrophoresed under reducing conditions (30 mM DTE) on a SDS polyacrylamide gel. Analysis of the gel showed that rf4S comprised 2 major bands of 66 kDa and 43 kDa, with a minor band at 11 kDa (Figure 3.1). The 66 kDa band is the precursor form of rf4S. The latter two bands constitute the mature form of rf4S, and under non-reducing conditions, these two bands migrate as a 53 kDa polypeptide. It is expected that the smaller subunit of 11 kDa, by analogy to rh4S, is comprised of two disulphide-linked subunits of 7 and 8 kDa which require electrophoresis on Tricine-SDS gels for visualisation (Kobayashi *et al.* (1992) and Bielicki, unpublished data). The relative percentage of precursor to mature was 64:36 as determined by densitometric analysis. The Mr of the precursor form (66 kDa) is slightly smaller than that of the rh4S precursor form (67 kDa) although the relative abundance of this form is greater in the human variant (70-80%) (Figure 3.1). These percentages varied from one preparation to another and were also dependent on the presence or absence of NH_4Cl in the culture medium. In the presence of NH_4Cl the amount of precursor rf4S was increased by approximately 10% (results not shown). Under reducing and non-reducing conditions, the Mr estimates for the mature form of rf4S were also marginally smaller than those recorded for rh4S, that is, 43 kDa and 11 kDa versus 44 kDa and 12 kDa (reduced) and 53 kDa versus 55 kDa (non-reduced) (Figure 3.1). Similar observations were made from western blot analysis (data not shown).

Figure 3.1: SDS-PAGE of purified rf4S.

Lane 1, Mr standards, which include phosphorylase b (94 kDa), BSA (67 kDa), ovalbumin (43 kDa), carbonic anhydrase (30 kDa), soybean trypsin inhibitor (20.1 kDa) and α-lactalbumin (14.4 kDa), are indicated by arrows. Lanes 2 and 3, rf4S and rh4S, respectively, electrophoresed under reducing conditions (30 mM DTE). Lanes 4 and 5, rf4S and rh4S, respectively, electrophoresed under non-reducing conditions.

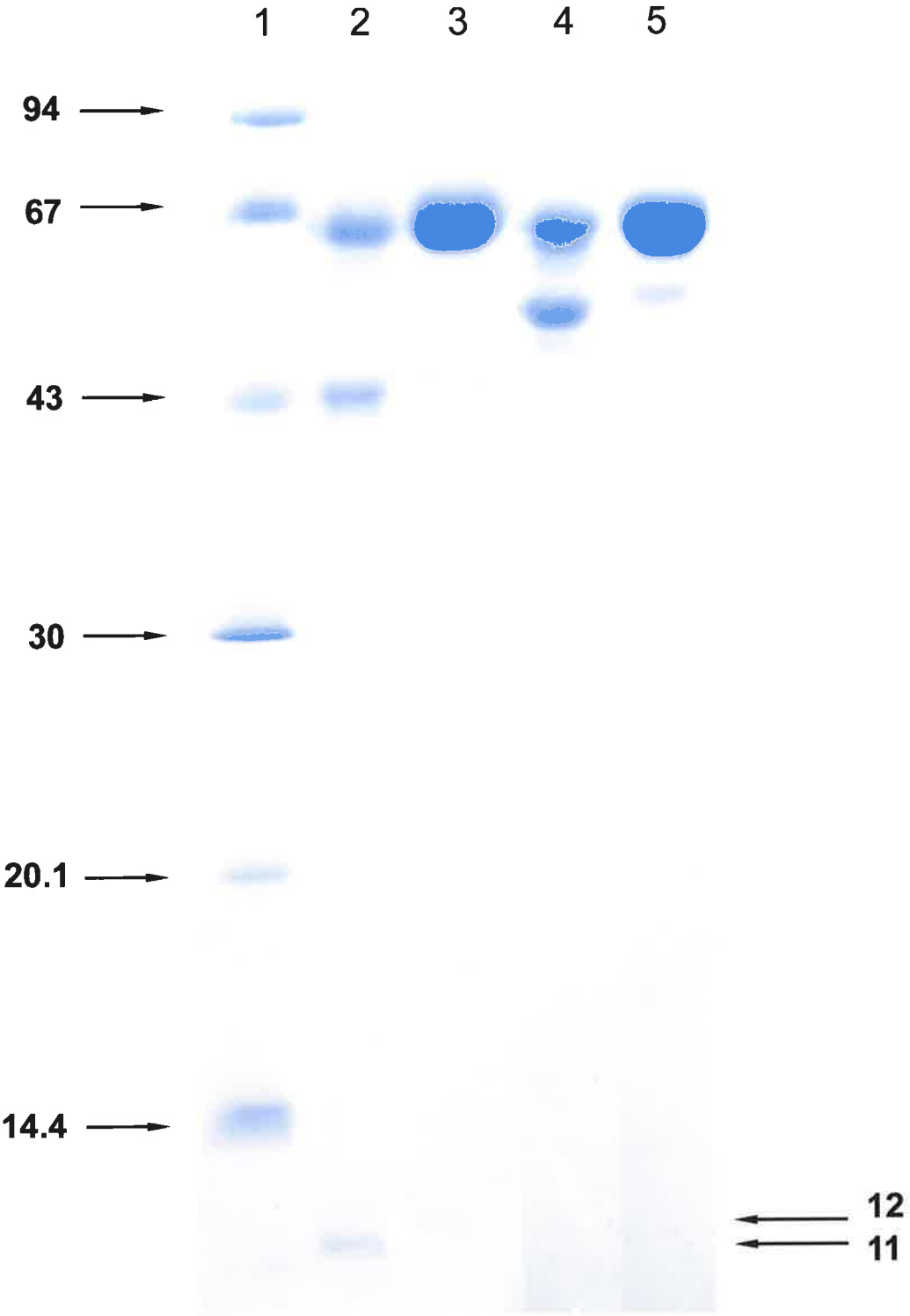
1
2
3
4
5
94
67
43
30
20.1
14.4
12
11

3.1.3.2 Native Mr

The native Mr of either immunopurified rf4S, or rf4S in conditioned medium, was estimated by fast protein liquid chromatography using a TSK G3000SW column. rf4S consistently fractionated at a volume equivalent to the fractionation volume of carbonic anhydrase, which is 30 kDa. In contrast, rh4S fractionated at a volume equivalent to that of BSA, Mr 67 kDa (results not shown). This difference is attributed to interaction of rf4S with the hydrophilic groups of the matrix, and hence retardation during fractionation. IEF data (section 3.1.3.4) support this explanation in that rf4S has a higher pI than rh4S and is therefore more positively charged compared to rh4S. Gel filtration chromatography on Superose 12, which is an inert agarose-based matrix, gave an estimated Mr for rf4S of 62-68 kDa (Figure 3.2) which corresponds to that observed on SDS-PAGE indicating that rf4S does not interact with this matrix. The presence of a 100 kDa homodimer form of rf4S has been suggested (McGovern *et al.*, 1982; Jackson *et al.*, 1992). However, gel fractionation chromatography data showed no activity at a higher Mr and nor was there evidence of a protein band at 100 kDa on SDS-PAGE under non-reducing conditions, with only a very minor band of the expected size present on western blot analysis (Yogalingam *et al.*, 1996).

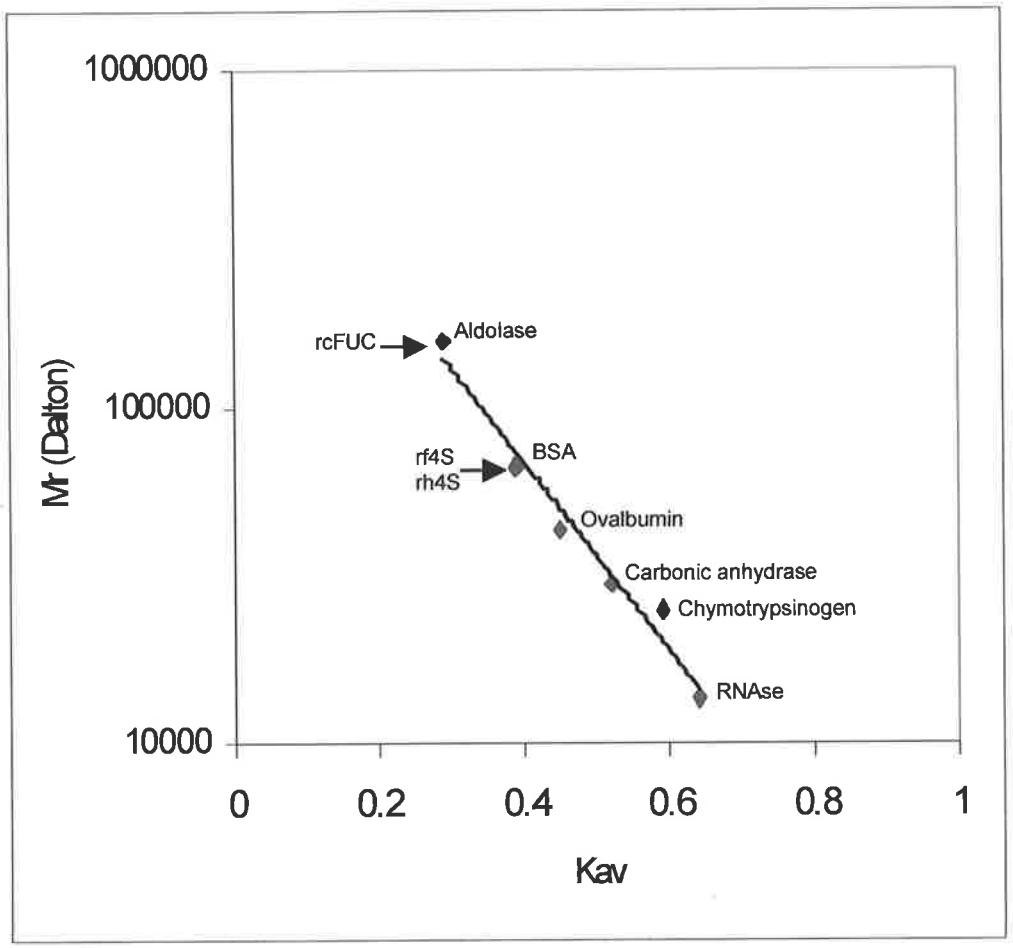

Figure 3.2: Native Mr estimation.

The native molecular weights of rf4S, rh4S and rcFUC were estimated using size exclusion chromatography. A Superose 12 column was calibrated with the following Mr protein standards: thyroglobulin (660 kDa), aldolase (158 kDa), BSA (67 kDa), ovalbumin (43 kDa), carbonic anhydrase (30 kDa), chymotrypsinogen (25 kDa) and RNAse (13.7 kDa). Thyroglobulin was used to determine void volume (V_o) and ^{14}C-glucose to determine total column volume (V_t). K_{av} was determined as described in section 2.2.6.1.

3.1.3.3 Kinetics

Kinetic analysis (Table 3.2) using the fluorogenic substrate 4MUS indicated that rf4S and rh4S have identical pH_{opt} (pH 5.6) and similar K_m (1.57 and 1.18 mM, respectively), V_{max} (35.2 and 48.5 μmol/min/mg, respectively) and specific activity (27.8 and 39.4 μmol/min/mg, respectively) values. At pH_{opt} of 2.85 in 50 mM sodium formate buffer, these catalytic parameters were also similar for both rf4S and rh4S toward the trisaccharide substrate (Table 3.2). At a concentration of 2 mg/ml, f4S had a half-life of approximately 4 years when stored in PBS at 4 °C under sterile conditions.

Table 3.2: Comparison of the catalytic properties of rf4S and rh4S.

	K_m (mM)	V_{max} (μmol/min/mg)	Specific Activity (μmol/min/mg)	pH_{opt}
Fluorogenic substrate				
rf4S	1.57	35.23	27.8	5.6
rh4S	1.18	48.49	39.4	5.6
Trisaccharide substrate				
rf4S	0.024	0.48	0.34	2.85
rh4S	0.022	0.67	0.45	2.85

Recombinant f4S and rh4S were immunoaffinity purified directly from conditioned medium using F58.3-Affi-Gel 10. K_m, V_{max}, specific activity and pH_{opt} were determined using the fluorogenic substrate (4MUS) and the natural trisaccharide substrate (GalNAc4S-GlcA-GalitolNAc4S).

3.1.3.4 Isoelectric focussing

IEF indicated seven major forms of rf4S, and more than ten of rh4S, with pI values ranging from 6.5 to 7.5 for rf4S, and a much broader range of 4.45 to 7.0 for rh4S, indicating that rf4S is more positively charged than rh4S (Figure 3.3). Digestion with neuraminidase resulted in a change in pI towards the cathode of certain isomers of rf4S indicating the presence of sialic acid residues. However, no obvious changes were observed for rh4S. Because several isomers of rf4S were still present after neuraminidase digestion this implies that there are other factors contributing to charge differences apart from sialic acid content.

3.1.3.5 Estimation of degree of glycosylation

To determine the degree of glycosylation on rf4S and rh4S the two enzymes were digested with PNGase F, an amidase that cleaves the bond between the innermost N-acetylglucosamine and asparagine residues of high mannose, hybrid and complex oligosaccharides from N-linked glycoproteins, that is, it removes all N-linked oligosaccharide chains. Digestion of rf4S with PNGase F resulted in a decrease in the molecular mass of both the precursor and mature forms by 14 and 11%, respectively (Figure 3.4). A higher degree of glycosylation was observed for rh4S since the change in molecular mass was greater than for rf4S (22% for the precursor and 20% for the mature form). Both the precursor and mature forms of rf4S and rh4S displayed almost identical molecular masses (56 kDa and 39-40 kDa for the precursor and mature forms, respectively) after treatment with PNGase F indicating that the difference in Mr between the two enzymes is due to differences in glycosylation.

Figure 3.3: IEF of neuraminidase-treated rf4S and rh4S.

Lane 1, IEF standards with their respective pI indicated by arrows; lanes 2 and 4, rf4S and rh4S, respectively; lanes 3 and 5, rf4S and rh4S, respectively, after neuraminidase treatment.

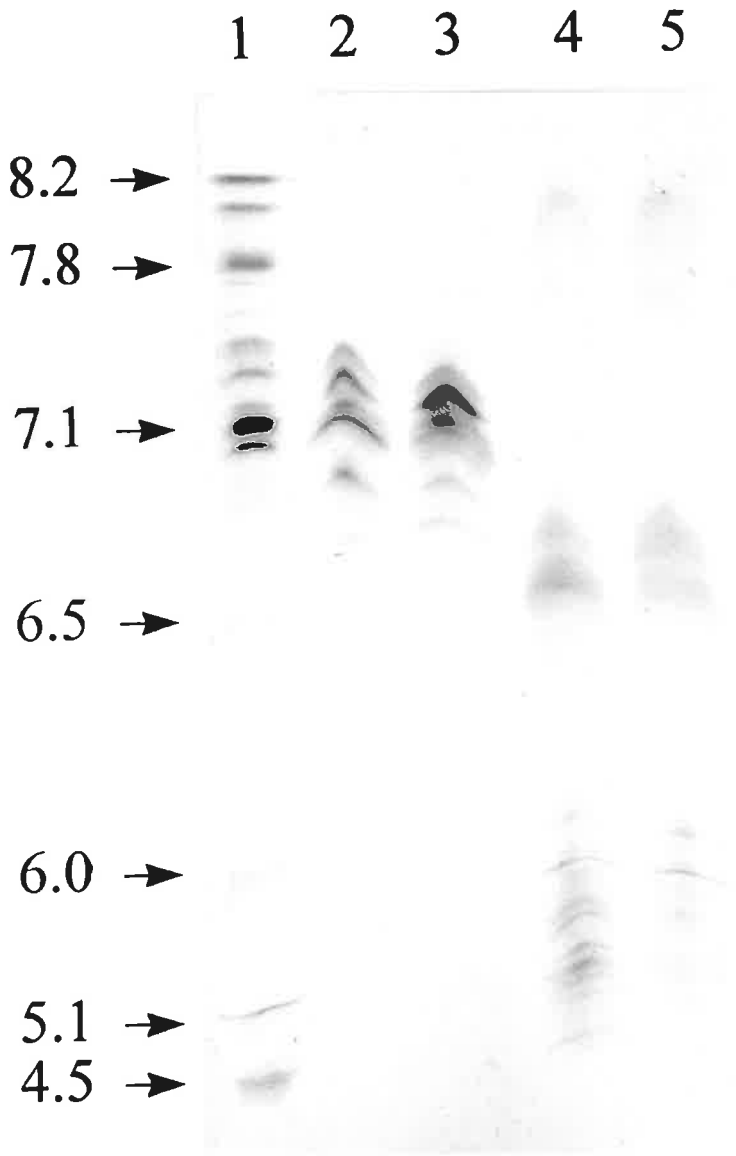
1
2
3
4
5
8.2
7.8
7.1
6.5
6.0
5.1
4.5

Figure 3.4: SDS-PAGE of PNGase F-treated rf4S and rh4S.

Lane 1, Mr standards, which include phosphorylase b (94 kDa), BSA (67 kDa), ovalbumin (43 kDa), carbonic anhydrase (30 kDa), soybean trypsin inhibitor (20.1 kDa) and α-lactalbumin (14.4 kDa), are indicated by arrows. Lanes 2 and 4, untreated rf4S and rh4S, respectively; lanes 3 and 5, rf4S and rh4S, respectively, after PNGase F treatment. The band in lanes 3 and 5 at approximately 36 kDa is PNGase F.

3.1.4 Correction of GAG storage in feline MPS VI fibroblasts with rf4S

Feline MPS VI fibroblasts homozygous for the L476P mutation have less than 1% residual 4S activity, compared with normal feline skin fibroblasts. This deficiency of enzyme activity results in lysosomal storage of predominantly highly-sulphated DS (Fratantoni *et al.*, 1968; Coster *et al.*, 1984). Biosynthetically labelling the accumulated GAG with $Na_2{}^{35}SO_4$ allows quantification of storage. In feline MPS VI fibroblasts there was approximately 15 times more ^{35}S-labelled material compared to normal cat fibroblasts (Table 3.3). Addition of exogenous rf4S at 2.6 nmol/min/ml to the culture medium, as described in section 2.2.7, resulted in normalisation of the levels of both 4S activity and ^{35}S-label. This effect was almost totally reversed in the presence of M6P with 12-fold less enzyme being endocytosed indicating that uptake was *via* the M6PR. With ten times the dose of exogenous rf4S, intracellular levels of 4S were 4.7 times greater than in normal control cells and in the presence of M6P there was still sufficient enzyme endocytosed (10% of levels seen in the absence of M6P) to degrade accumulated storage products to nearly normal levels. β-Hexosaminidase activity levels were elevated in MPS VI cells compared to normal control cells and remained unchanged in the treated MPS VI fibroblasts.

Table 3.3: Correction of GAG storage in feline MPS VI fibroblasts with rf4S.

	rf4S activity (pmol/min/mg)	^{35}S radioactivity (dpm/mg)	β-Hexosaminidase (nmol/min/mg)
SF242	327 ± 28.4	50,851 ± 1,562	79 ± 22
SF236	3.1 ± 0.57	771,939 ± 22,882	119 ± 22
SF236 + rf4s	351.6 ± 50.7	38,578 ± 5,709	120 ± 19
SF236 + rf4S + M6P	26.4 ± 12.2	421,172 ± 62,246	129 ± 10
SF236 + 10 x rf4S	1,227.9 ± 252	35,303 ± 10,086	125 ± 14
SF236 + 10 x rf4S + M6P	119.9 ± 37	65,073 ± 20,454	115 ± 10

Normal (SF242) and MPS VI feline skin fibroblasts (SF236) were metabolically labelled with $Na_2{}^{35}SO_4$ for 48 h and then incubated with 1 x (2.6 nmol/min/ml) or 10 x (26 nmol/min/ml) purified rf4S in the presence or absence of 5 mM M6P for 48 h. Cell lysates were assayed for ^{35}S radioactivity, total protein, β-hexosaminidase activity and 4S activity using the radiolabelled trisaccharide substrate. Results are expressed as the mean (n = 3) ± 1 SD.

3.1 Discussion

rf4S was expressed in milligram amounts using a mammalian expression system (CHO cells) and was readily purified by a one-step immunopurification procedure. When analysed, rf4S was shown to have similar physical and kinetic properties to rh4S. The slightly smaller Mr of the precursor and mature forms of rf4S compared to rh4S were attributed to the latter being more highly glycosylated. This was supported by the lack of molecular size difference after deglycosylation. rf4S has five potential glycosylation sites according to the canonical sequence N-X-S/T while rh4S has 6 (Jackson *et al.*, 1992), the equivalent of the glycosylation site at Asn366 in h4S being missing in f4S. Of the 5 glycosylation sites in rf4S, 3 are on the 43 kDa polypeptide subunit of the mature form of the enzyme (Asn190, Asn281, Asn293) and the other two are on the 7 kDa subunit (Asn 428, Asn460). No glycosylation sites are present on the 8 kDa subunit which constitutes the C-terminus of 4S. The extra glycosylation site in rh4S (Asn366) is on the 44 kDa subunit. Periodic acid Schiff staining of electrophoretically separated mature human 4S has confirmed that oligosaccharide chains are present only on the 43 kDa and 7 kDa subunits (Kobayashi *et al.* (1992) and Bielicki, unpublished data). Multiple isomorphous replacement electron density maps of rh4S show clear evidence for glycosylation at Asn279 and Asn426, with possible carbohydrate at Asn366 and no electron density indicative of glycosylation at the other sites (Bond *et al.*, 1997). However, the absence of electron density cannot be taken as proof of lack of glycosylation at these additional sites.

Complex sialylated carbohydrate chains are present on rf4S as demonstrated by a decrease in number, and a shift towards the cathode, of a number of the isomers seen on IEF after neuraminidase digestion. Oligosaccharide analysis of rf4S has not been undertaken and data from the literature is scant on the composition of N-glycan chains in other variants of 4S. Analysis of human placental 4S indicates that 98% of the oligosaccharide glycans comprised no more than five mannose residues (Laidler and Litynska, 1997). A more detailed analysis of rat liver 4S indicated that complex oligosaccharides predominate with 71% being sialylated (Przybylo and Litynska, 1997). However, the oligosaccharide structures of CHO-derived f4S or h4S cannot be determined by analogy with other 4S variants as glycosylation of any protein is species and cell or tissue type-specific; the pattern of glycosylation being dependent on both the peptide sequence and the cell type in which it is expressed. As both f4S and h4S are produced in CHO cells one would expect the glycosylation patterns may be similar. However,

analysis of oligosaccharide chains of rh4S has indicated that they are not complex or hybrid structures but of the high-mannose type (Dr. P Clements, Department of Chemical Pathology, WCH, personal communication). These oligosaccharides have no sialic acid residues thus corroborating the findings from IEF of rh4S treated with neuraminidase (section 3.1.3.4 and Figure 3.3). The difference in Mr of the h4S polypeptide calculated from amino acid sequence (56 kDa) and that obtained from SDS-PAGE analysis (67 kDa) is almost the same as that determined from SDS-PAGE before and after PNGase F digestion. This difference of between 11 and 14.7 kDa would imply that all N-glycosylation sites in rh4S are glycosylated particularly if the carbohydrate chains are of the high-mannose type (Mr of approx. 2,000 Da/chain). As complex oligosaccharides are generally larger (3,000 Da/chain) than high-mannose types, one would therefore expect fewer sites to be glycosylated in rf4S as the component of Mr contributed by glycosylation (9 kDa) is less than in rh4S (14.7 kDa). It is therefore obvious that glycosylation of rf4S is both qualitatively and quantitatively different from that seen in rh4S. The differences between the two enzymes seen on IEF after neuraminidase treatment, that is, a greater negative charge for rh4S, may be due to increased phosphorylation and/or sulphation of h4S on serine and proline residues, but this has not been determined.

Enzyme uptake into feline MPS VI fibroblasts demonstrated that rf4S was endocytosed by the M6PR-mediated pathway and was then transported to endosomes/lysosomes where it was active in degrading ^{35}S-labelled storage material. This phenomenon has been consistently observed in studies of uptake of a number of lysosomal enzymes (Anson *et al.*, 1992b; Bielicki *et al.*, 1993; Unger *et al.*, 1994; Bielicki *et al.*, 1995; Litjens *et al.*, 1997; Bielicki *et al.*, 1998). One exception is the lysosomal enzyme recombinant human α-N-acetylglucosaminidase (a deficiency of this enzyme results in MPS IIIB) which failed to correct storage in human MPS IIIB fibroblasts to any substantial degree (Zhao and Neufeld, 2000; Weber *et al.*, 2001). It was found that recombinant human α-N-acetylglucosaminidase is poorly mannose-6-phosphorylated but why this should be so compared to other recombinant lysosomal proteins is unclear. The above observation underscores the importance of the M6P recognition signal in proper trafficking of exogenously administered lysosomal enzymes.

Results of uptake studies mentioned above illustrate that only a small percentage of normal enzyme activity is required to eliminate storage from the lysosome. These results support the

observations made in some MPS VI patients who retain measurable amounts of enzyme activity (5-10% of normal levels) and who remain virtually symptom-free until late adulthood (Neufeld and Muenzer, 2001).

3.2 ERT in MPS VI cats using rf4S

3.2 Introduction

In the previous section it was demonstrated that rf4S was similar to rh4S in its physical and kinetic properties and that endocytosis into MPS VI fibroblasts was *via* the M6PR-mediated pathway with subsequent delivery to lysosomes where it was instrumental in hydrolysing stored substrate. These results suggested that rf4S had the necessary properties for use in ERT trials in MPS VI cats. The aim of the experiments described in this section was therefore to evaluate the efficacy of using rf4S in a trial of ERT from birth in MPS VI cats using a protocol identical to that used previously with rh4S (Crawley *et al.*, 1997) thus allowing a direct comparison of the results of both trials.

3.2 Results

3.2.1 Disease assessment in MPS VI cats undergoing ERT

The two male MPS VI cats in this study, designated cat 249 and cat 250, were treated with rf4S as described in section 2.2.9. Cats were regularly examined for physical and clinical signs of MPS VI, and at 90, 150 and 170 days of age, for neurological and radiographic evidence of disease. Blood and urine samples were collected on a regular basis. At autopsy tissues were examined macroscopically and sections of most organs were taken for histological analysis. Results of these analyses were compared with historical data from normal, untreated MPS VI cats and from MPS VI cats treated with rh4S at 1 and 5 mg/kg (Crawley *et al.*, 1997).

3.2.1.1 Physical examination

Injection of enzyme was tolerated well by both cats and neither showed any of the adverse reactions typical of anaphylaxis/hypersensitivity at any stage of therapy. Throughout the course of therapy they progressively gained weight, following the trend observed in normal cats (Figure 3.5). Generally MPS VI cat body weight starts to diverge from normal by approximately 90 days of age such that by 6 months of age their body weight is about 50-60% of normal. Both cats 249 and 250 were in the normal range up to 120 days. Thereafter the weight of cat 250 did not increase as much as that of cat 249. At the end of therapy cat 250 was still heavier than untreated MPS VI cats and his weight was approximately 80% of normal

whereas the weight of cat 249 remained just above the normal range from approximately 90 days onwards.

The two cats appeared well groomed, had shiny coats and were active and playful. Cat 249 had a more outgoing boisterous demeanour than cat 250. Facial shape, ear size, tail thickness and neck and body lengths were normal. Mild corneal clouding, assessed visually rather than by slit lamp examination, was present in both cats from 90 days of age and cat 250 had very mild kyphosis of the thoracicolumbar spine which was apparent from 150 days of age. Both cats were otherwise difficult to distinguish physically from age-matched normal cats (Figure 3.6).

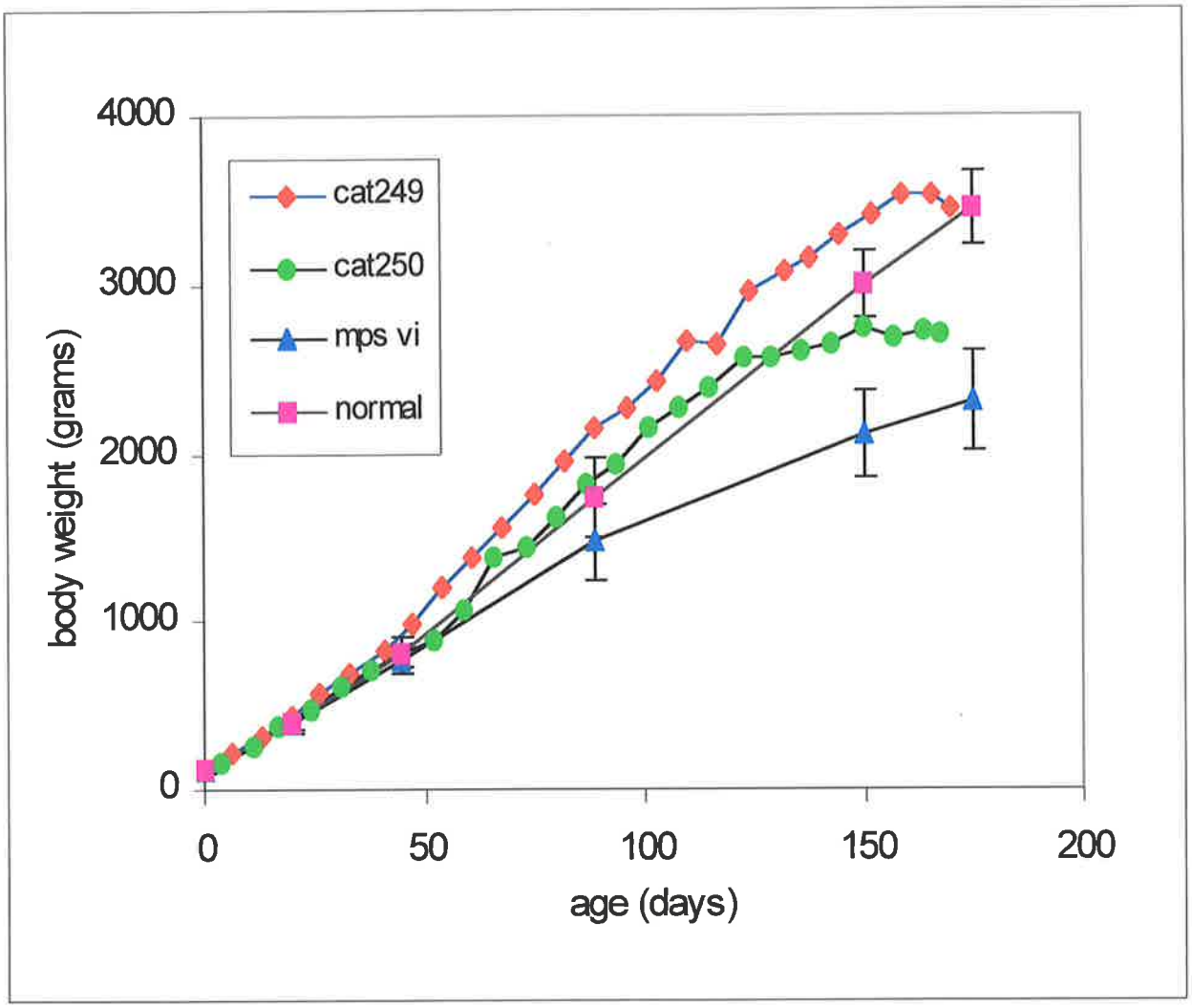

Figure 3.5: Cat body weights from birth to 6 months of age.

Body weights (grams) of cats 249 and 250 compared with normal and MPS VI male cats from birth to 6 months of age. Error bars = ± 1 SD. The number of cats at each time point indicated varied from 3 to 18.

Figure 3.6: Clinical appearance of cats 240 and 250 at 5 months of age.

Cats 249 and 250 were treated with intravenous injections of rf4S at 1 mg/kg body weight weekly from birth. (A) and (B) show the facial appearance of cats 249 and 250, respectively. Compared to a normal cat (E), facial dysmorphia has been resolved but mild corneal clouding is present in both cats although this is not obvious in these photographs. In marked contrast, an age-matched untreated MPS VI cat (F) shows obvious corneal opacity as well as smaller ears and a flattened broad face which are characteristic of MPS VI. In addition, compared to untreated MPS VI controls, cats 249 and 250 have increased body weight, size and length, greater cervical spine flexibility and no hindlimb deficits (C) and (D). The untreated MPS VI cat in (G) has severe hindlimb paresis, spinal kyphosis and is overall smaller.


A
I.M.V.S.


B


C


D


E


F


G

3.2.1.2 Neurological examination

Apart from mild gait changes (shorter, stiffer steps more pronounced in the left hindlimb than in the right) in cat 250 in the last two weeks of therapy, no hindlimb neurological deficits were detected in either cat. Cat 249 corrected its hindlimbs normally and rapidly when pushed off balance and could hop and wheelbarrow proficiently whereas cat 250 appeared to be slightly slower in this regard. Again this defect was only detected in the last two weeks of therapy.

Flexibility (lateral head movement and coxofemoral joint movement) in cat 249 remained unchanged with age and in cat 250 head/neck rotation decreased by 10^{o} on the right side at 150 days of age and a further 10^{o} at 170 days.

3.2.1.3 Radiological examination

Analysis of radiographs at 90, 150 and 170 days of age for dysostosis multiplex demonstrated reduced skeletal pathology in rf4S-treated cats compared with untreated MPS VI controls. Changes included more uniform bone density and smooth subchondral bone surfaces in long bone epiphyses and increased length and improved shape of vertebrae (Figure 3.7). Measurements of L5 vertebrae were made from radiographs taken at 150 days rather than 170 days in order to allow for direct comparison with those cats treated with 5 mg rh4S/kg. Improvements in skeletal appearance in rf4S-treated cats based on L5 vertebral L:W ratios were not substantially different from those observed in rh4S-treated cats. Cats on rf4S therapy showed an improvement in L:W ratio up to 81% of normal, indicating that remodelling of vertebrae had occurred. The shorter, broader and more misshapen vertebrae of MPS VI cats is illustrated by the lower L:W ratio which is only 62% of normal (Table 3.4). However, although the radiological appearance was not very different among all treated groups, the quality of bone did appear to be more improved in the rf4S-treated cats and those given 5 mg rh4S/kg, in comparison to 1 mg rh4S. This was confirmed by bone histomorphometric analysis (section 3.2.4).

Figure 3.7: Lateral radiographs of the lumbar spine in normal, treated and untreated MPS VI cats.

Radiographs of the lateral view of the lumbar spine in 6 month old cats. In normal cats (A) the vertebral bodies are long, narrow and radio-opaque, with smooth, regular epiphyses. In contrast, in an untreated MPS VI cat (B) the vertebrae are shorter, wider and radiolucent. Cats treated with 5 mg rh4S (C) and 1 mg rf4S (D) show a marked improvement in bone density and shape.

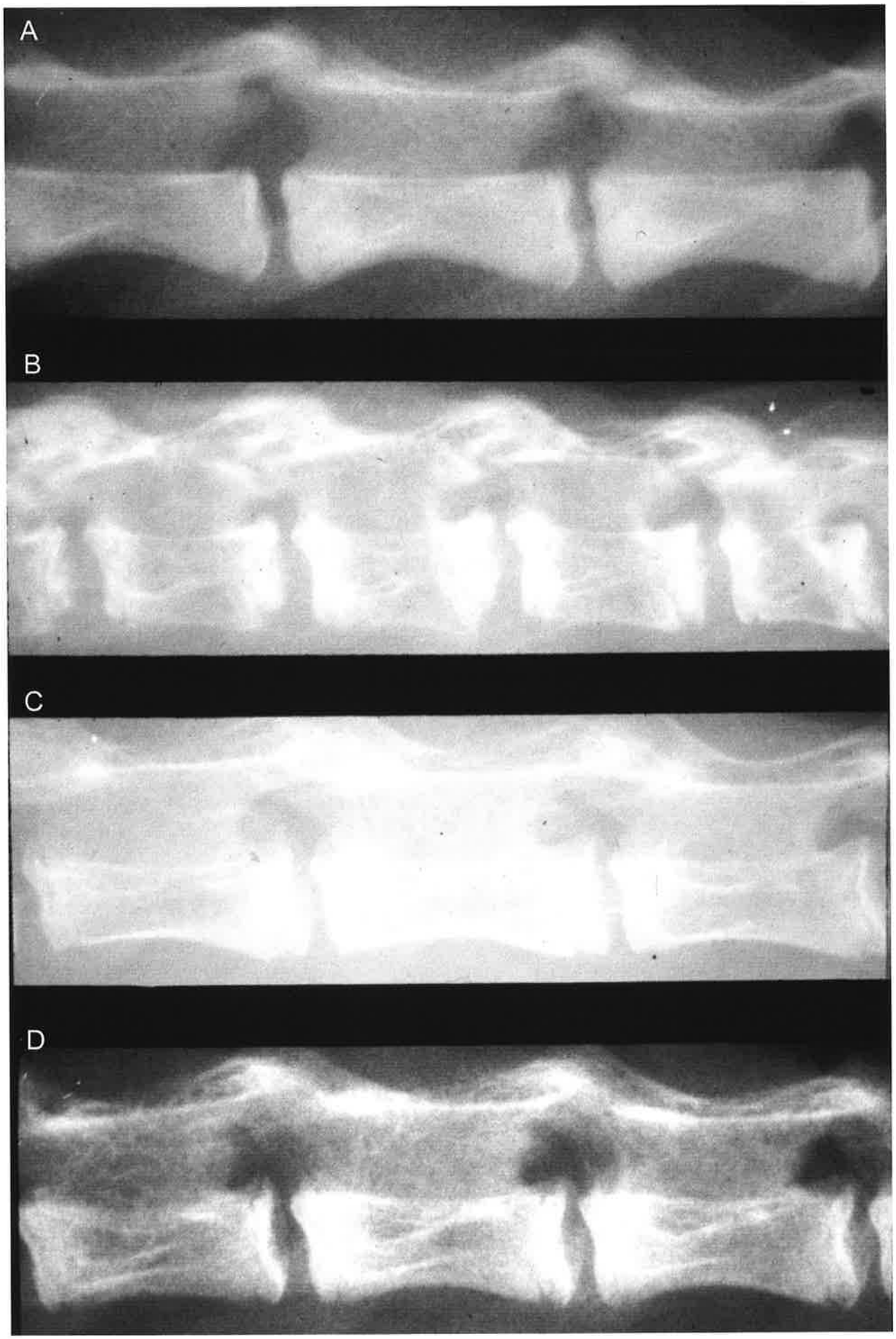
A
B
C
D

Table 3.4: Ratio of L5 vertebral length (L) and width (W) measurements from radiographs of normal male cats and treated and untreated male cats at age 150 days.

	L:W ratio	% normal
Normal (n = 9)	3.576 ± 0.146	100
MPS VI (1 mg rf4S/kg) (n = 2)	2.903	81.3
	(2.848, 2.958)	
MPS VI (1 mg rh4S/kg) (n = 2)	2.867	80.2
	(2.242, 3.492)	
MPS VI (5 mg rh4S/kg) (n = 3)	3.021 ± 0.424	84.6
MPS VI (no ERT) (n = 9)	2.225 ± 0.384	62.3

n is the number of cats in each group. Results are expressed as the mean ± 1 SD. Where n = 2, the mean value is given and individual values are shown in parentheses.

3.2.2 Macroscopic pathology

Gross examination of the soft tissues of cats 249 and 250 at autopsy showed no abnormalities. Cat 249 had considerable abdominal fat deposits compared to cat 250, but the organs themselves were of normal size; for example, liver was 2.7% and 2.89% of body weight for cats 249 and 250, respectively. In age and sex-matched normal male cats this has been calculated as 3.01% ± 0.6%. Throughout the length of the spinal cord no compression was evident in either cat. Examination of joints showed an overall decrease in articular cartilage thickness and improved subchondral bone quality compared to untreated controls. However, significant joint pathology similar to that observed in untreated MPS VI controls was still present (Figure 3.8). Abnormalities included superficial erosion of articular surfaces on both femoral heads (cat 249 only) and fissures in the glenoid surfaces of both scapulae in cat 250. There was no hip subluxation in cat 250 and no obvious bruising on the hindlimbs to explain the change in gait observed in the last two weeks of therapy. However, in both cats the femoral head was slightly smaller and therefore not tightly held in the acetabulum.

Figure 3.8: Joints of MPS VI treated and untreated cats compared with a normal control cat.

Shoulder joints (proximal humerus and glenoid surface of the scapula, cranial aspect) were examined at post mortem at approximately 6 months of age. (A) In a normal control cat the articular cartilage is thin and smooth and the subchondral bone is uniform and pink and clearly visible through the cartilage surface. (B) In an untreated MPS VI cat the cartilage thickness is increased and hence the subchondral bone is not visible. The ball of the proximal humerus may be irregularly shaped and the subchondral bone may be spotty and often focal erosions are present (not shown here) on the cartilage surface. (C) Treatment with 5 mg rh4S/kg results in joints that have thinner cartilage and fewer erosions while treatment with 1 mg rh4S/kg (D) has a lesser effect with joints showing lesions and thicker cartilage although not as thick as in an untreated MPS VI cat. (E) and (F) Cats 250 and 249, respectively, treated with 1 mg rf4S/kg had decreased cartilage thickness (particularly cat 249) compared to an untreated MPS VI cat, although there were some slight irregularities in cartilage thickness over the joint and cartilage was generally thicker around the periphery of the glenoid surface of the scapula. No lesions were present on the articular surface of either cat. In cat 250 a slight fissure was present in the centre of the glenoid cavity of both shoulders.

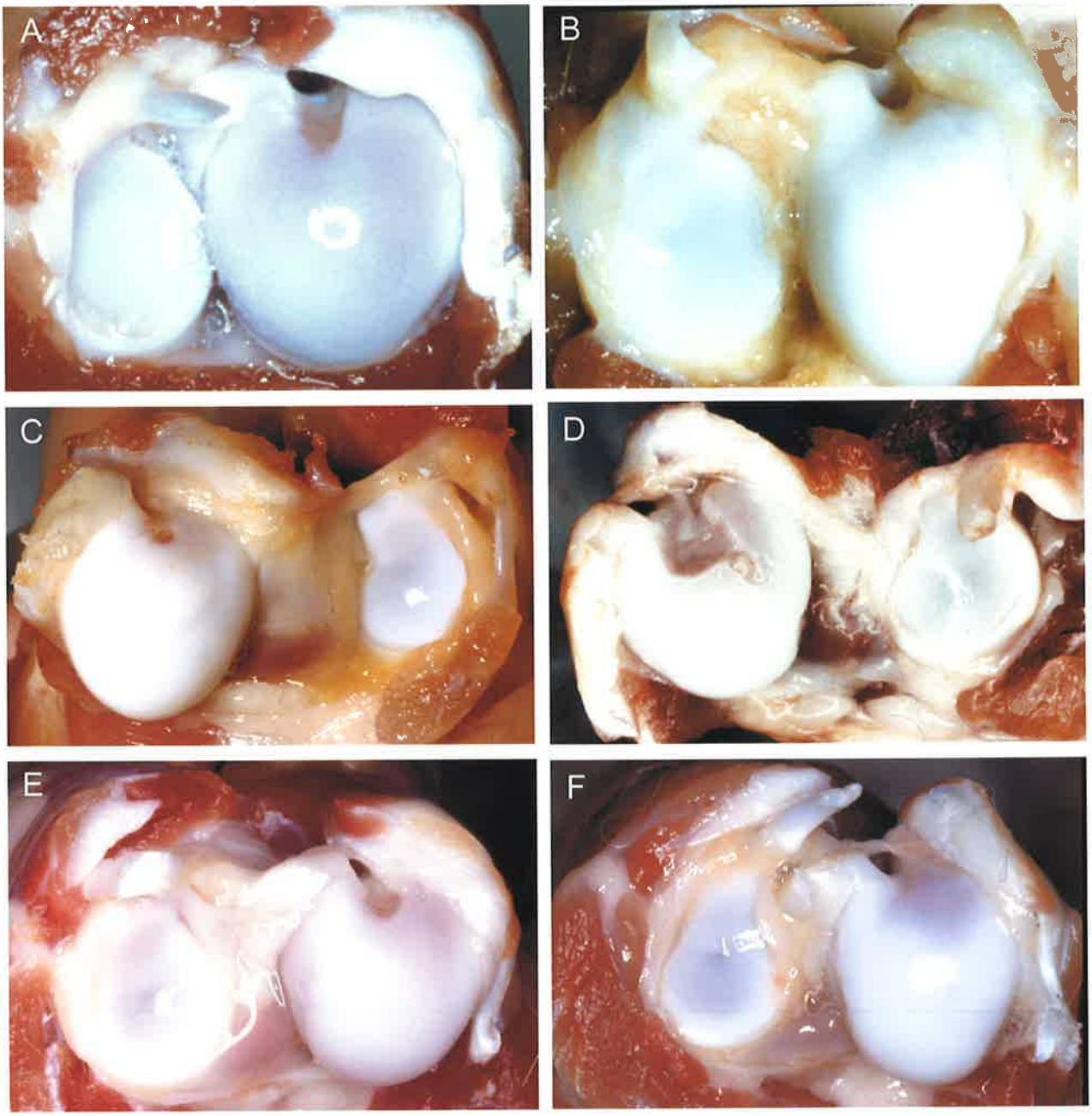
A
B
C
D
E
F

3.2.3 Light and electron microscopy

The results of examination of tissues by light microscopy for the degree of lysosomal vacuolation are shown in Table 3.5. Treatment with rf4S resulted in total elimination of storage from liver Kupffer cells. This was also observed with other treatment strategies. A marked improvement in clearance of lysosomal storage with the feline enzyme was seen in skin fibroblasts, hip joint capsule fibroblasts and dura mater fibroblasts compared with the human enzyme at the same dose. Most striking was the complete elimination of storage in aorta smooth muscle cells across the entire width of the aorta in cat 249 with only very mild storage in cat 250. In comparison with the 5 mg/kg dose of rh4S, storage was still evident from the outer tunica media to the outer wall of the aorta. Figure 3.9; 1A-5A, shows a representative cross-section (x 200 magnification) of the aorta from a normal cat, an untreated MPS VI cat and cats treated with 1 and 5 mg rh4S/kg and 1 mg rf4S/kg (cat 249), respectively, while Figure 3.9; 1B-5B, depicts an identical area of the aorta (indicated by an arrowhead), that is toward the outer tunica media, magnified x 2000 to show detail of lysosomal storage. Compared with normal cats, untreated MPS VI cats have a thickened aorta due to storage across its width. Furthermore, the ordered array of alternating layers of concentric elastin membranes and smooth muscle cells seen in normal cats is severely disrupted in untreated MPS VI cats. Although therapy with rf4S has clearly eliminated storage, reversal of the chaotic array of elastic fibres has not occurred. Electron microscopy of the aorta of a 14 day old MPS VI cat foetus clearly shows considerable storage and a disruption of aortic structures (Figure 3.10). Heart valve fibroblasts showed a similar trend in the reduction of lysosomal vacuolation (Figure 3.11). Electron micrograph of cat 250 showed almost negligible storage. In cat 249 lysosomal storage was moderate but confined to focal regions of the heart as opposed to being spread throughout the tissue (data not shown). In contrast, brain perivascular cells showed a mild to moderate degree of storage with 1 mg rf4S/kg, the same tissue exhibiting only mild to no storage at the equivalent dose of the human enzyme. In addition, compared with untreated MPS VI cats, no reduction in the degree of vacuolation was observed in cartilage chondrocytes or corneal keratocytes with any of the treatment regimens.

Table 3.5: Lysosomal storage in different cell types in untreated and treated MPS VI cats

Tissue-cell type	MPS VI no ERT	MPS VI 1 mg rf4S/kg	MPS VI 1 mg rh4S/kg	MPS VI 5 mg rh4S/kg
Liver-Kupffer cells	3+	0	0	0
Skin-fibroblasts	3+	±	1+ - 2+	0
Dura mater-fibroblasts	3+	0 - 1+	± - 2+	0
Heart valve-fibroblasts	3+	± - 1+	1+ - 2+	0 - ±
Aorta-smooth muscle cells	3+	0 - ±	2+	± - 1+
Hip joint capsule-fibroblasts	3+	0 - 1+	2+ - 3+	± - 1+
Brain-perivascular cells	3+	1+ - 2+	0 - 1+	0
Cornea-keratocytes	3+	3+	3+	3+
Cartilage-chondrocytes	3+	3+	3+	3+
n	3	2	4	2

0, no lysosomal storage; ±, very mild storage; 1+, mild, 2+, moderate, 3+, severe lysosomal vacuolation. No storage was present in normal cats in all tissues examined. n = number of cats in each group.

Figure 3.9: Electron microscopy of aorta in a normal cat and treated and untreated MPS VI cats.

Electron micrographs show the transverse section of aorta from a normal cat (1A), an untreated MPS VI cat (2A), and MPS VI cats treated with 1 mg rh4S/kg (3A), 5 mg rh4S/kg (4A) and 1 mg rf4S/kg (5A), respectively, magnified x 200. Figures 1B-5B depict an identical area of the aorta in the outer tunica media (indicated by an arrow) magnified x 2000. No storage vacuoles are seen in the rf4S-treated cat compared with mild storage in the 5 mg rh4S-treated cat and a moderate degree of storage in the cat treated with 1 mg rh4S. With removal of storage, the width of the aorta is near-normalised. A: Bar = 50 μm. B: Bar = 5 μm.

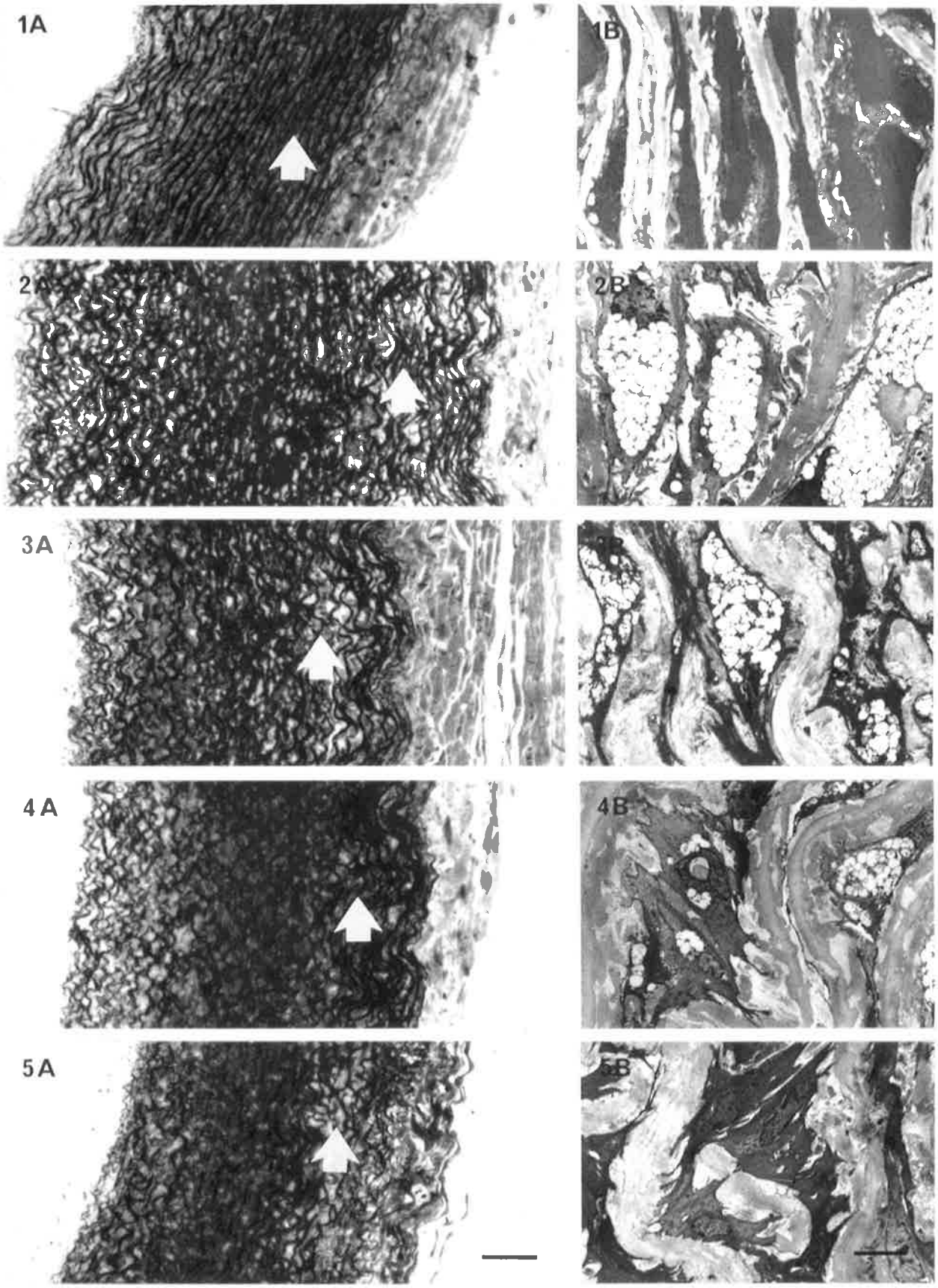
1A
1B
2A
2B
3A
4A
4B
5A

Figure 3.10: Electron micrograph of aorta of a MPS VI affected cat foetus.

The electron micrograph of the aorta of an affected MPS VI cat foetus at 14 days of age displays lysosomal storage and a disordered array of elastin fibres and muscle cells. Magnification x 4,500. Bar = 5 μm.

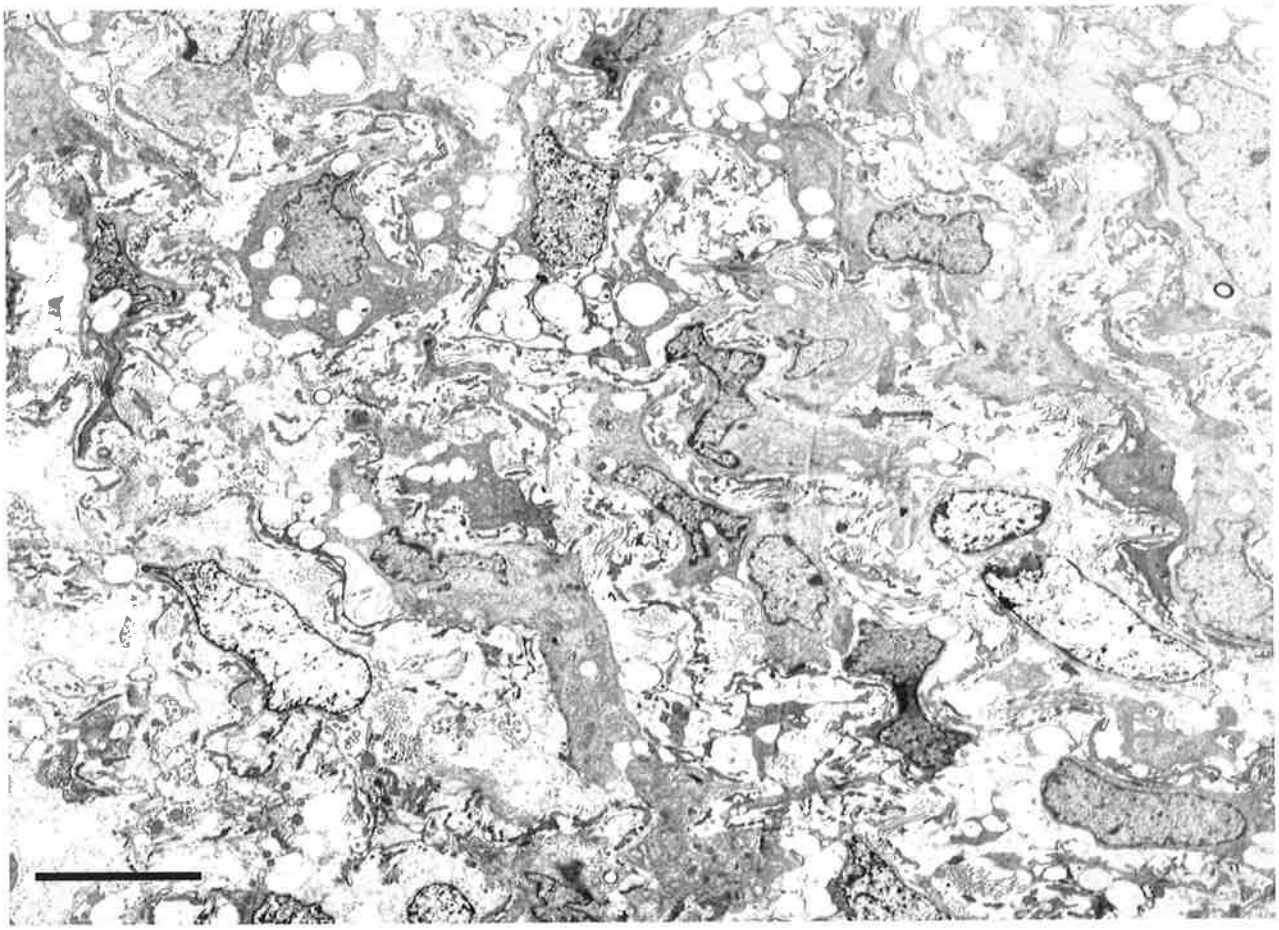

Figure 3.11: Electron microscopy of heart-valve in untreated and MPS VI treated cats. Electron micrographs of heart-valve fibroblasts of an untreated MPS VI cat (A) show cells that are enlarged and distended with storage vacuoles, whereas no storage vacuoles are present in the cells of a MPS VI cat treated with 1 mg rf4S/kg (B) compared to mild and moderate storage in the cells of MPS VI cats treated with 5 mg rh4S/kg (C) and 1 mg rh4S/kg (D), respectively. (E), normal control cat. Bar = 5 μm.

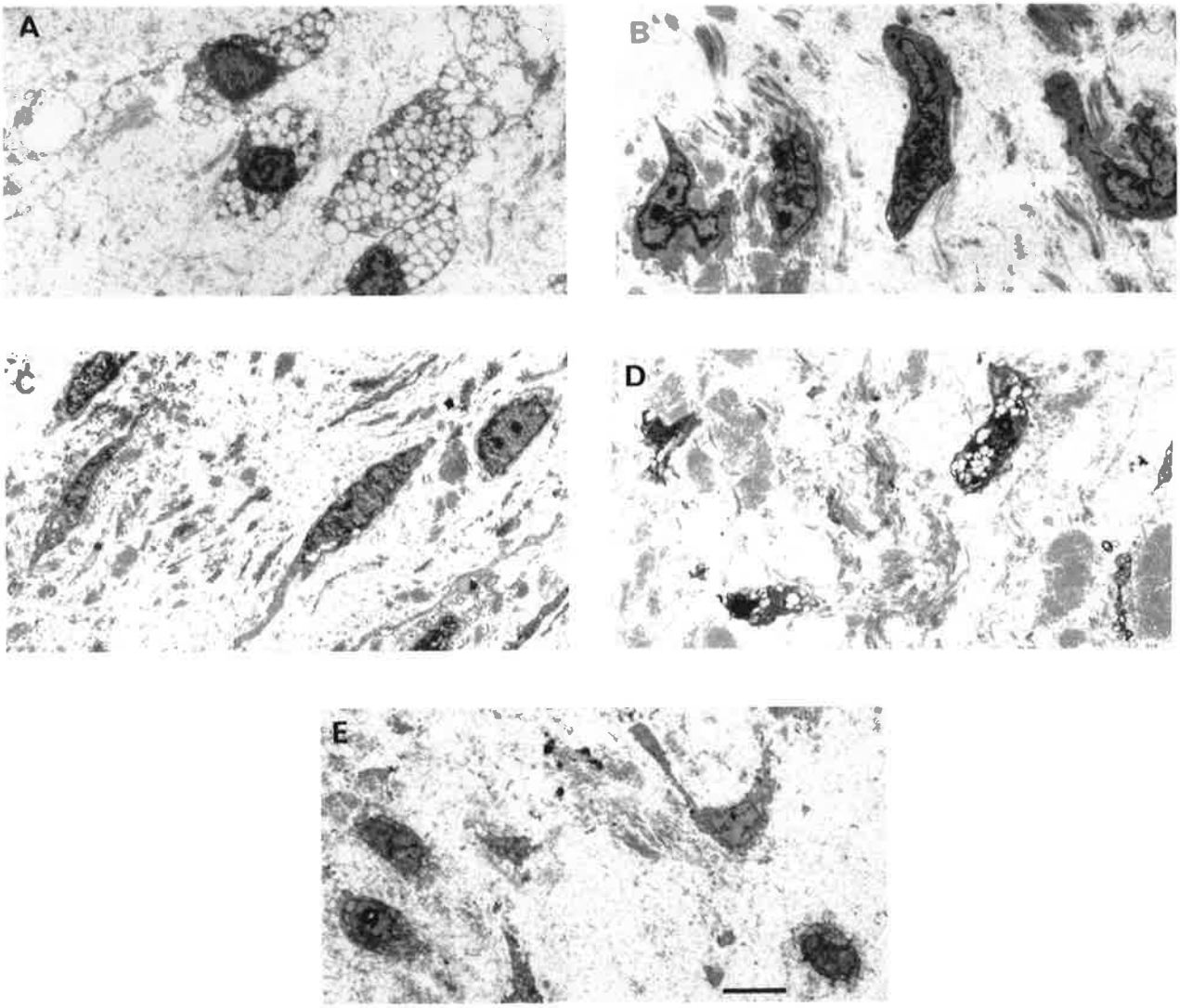
A
B
C
D
E

3.2.4 Bone histomorphometry

The L5 vertebra was used for histomorphometric analysis of trabecular bone. Thin sections stained with haematoxylin and eosin show the degree of bone present (Figure 3.12). In addition to the overall improvement in the size and shape of the L5 vertebrae following ERT, an increase in the number and thickness of the trabecular bone is also evident. From these stained sections it is also obvious that treatment with 1 mg rf4S is more efficacious that the equivalent dose of rh4S.

Static histomorphometric parameters were measured on 5 μm undecalcified sections that had been stained with von Kossa stain as described in section 2.2.16. Results of this analysis are shown in Table 3.6. Treatment with rf4S resulted in an increase of bone mineral volume expressed as a percentage of tissue volume (BV/TV) to 77% of normal. A similar trend was observed for bone surface density (BS/TV, 98% of normal) upon treatment with 1 mg rf4S/kg. TbTh, TbN and TbS, which relate to bone architecture, were also restored to near-normal values. Treatment with the feline enzyme appeared to have a greater effect on reversing these static parameters of pathology compared with the same dose of human enzyme, the latter resulting in a BV/TV of 40% of normal; BS/TV, TbTh and TbN approximately 60% of normal; and the TbSp about twice normal. Indeed, the feline enzyme was more effective than a 5 times higher dose of human enzyme (BV/TV with 5 mg rh4S/kg was 71% of normal; BS/TV, TbTh and TbN were 85% of normal; and TbSp was 22% greater than normal). In contrast, MPS VI cats are severely osteopenic having a bone volume of only 4.4% compared to 20% in age-matched normal control cats. Overall, rf4S-treated MPS VI cats demonstrated a response to species-specific enzyme that was more successful in correcting the measured static parameters of bone architecture than a five-times higher dose of non-native (human) enzyme.

Figure 3.12: L5 vertebral sections of normal and treated and untreated MPS VI cats.
(A) L5 vertebral section from a normal control cat, (B) an untreated MPS VI cat, (C) a MPS VI cat treated with 1 mg rh4S/kg, (D) a MPS VI cat treated with 5 mg rh4S/kg and (E) and (F) cats 249 and 259 respectively, treated with 1 mg rf4S/kg. All cats are approximately 6 months of age. Sections were stained with Haematoxylin and Eosin. Trabecular bone within the L5 vertebrae is stained black.

A

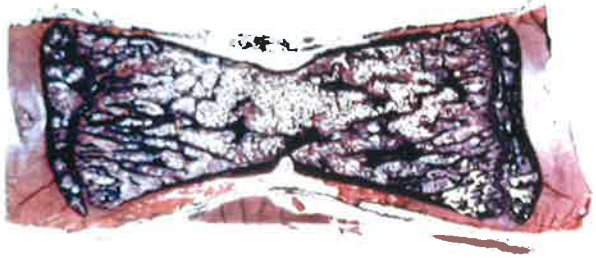

B

C

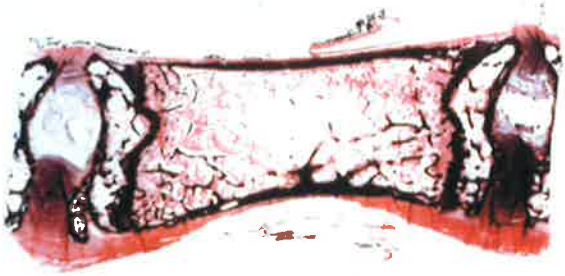

D

E

F

Table 3.6: Histomorphometric measurements of L5 vertebral bone in normal, untreated and treated MPS VI cats.

L5 vertebrae were treated as described in section 2.2.16. The parameters measured included bone mineral volume (BV/TV), bone surface density (BS/TV), trabecular thickness (TbTh), trabecular separation (TbSp), trabecular number (TbN), mineral apposition rate (MAR) and bone formation rate (BFR/BS). Results of histomorphometric measurements of L5 vertebrae of cats 249 and 250 that were treated with rf4S are compared with data obtained for normal, untreated MPS VI cats and 1 and 5 mg rh4S-treated MPS VI cats (Byers *et al.*, 1997). Results are expressed as the mean ± 1 SD. n indicates the number of cats in each experimental group with the exception of ‡ n = 9 and $^{\#}$ n = 10. The individual values for cats 249 and 250 are given in parentheses.

	Normal	MPS VI 1 mg rf4S/kg	MPS VI 1 mg rh4S/kg	MPS VI 5 mg rh4S/kg	MPS VI no ERT
BV/TV (%)	19.67 ± 5.303	15.562 (14.68, 16.45)	8.229 ± 1.792	14.331 ± 0.192	4.104 ± 1.105
BS/TV (mm^2/mm^3)	4.76 ± 0.77	4.678 (4.35, 5.01)	2.952 ± 0.655	4.066 ± 0.596	1.943 ± 0.557
TbTh (mm)	0.081 ± 0.012	0.067 (0.068, 0.066)	0.056 ± 0.008	0.071 ± 0.01	0.043 ± 0.009
TbSp (μm)	0.348 ± 0.076	0.363 (0.392, 0.334)	0.648 ± 0.161	0.426 ± 0.064	1.052 ± 0.254
TbN (per mm)	2.384 ± 0.387	2.399 (2.18, 2.50)	1.476 ±0.327	2.033 ± 0.298	0.971 ± 0.278
MAR (μm/day)	2.20 ± 0.11[‡]	2.19 (2.27, 2.10)	2.16 ± 0.09	2.01	2.09 ± 0.11[#]
BFR/BS (mm^3/mm_2/day)	0.008 ± 0.002[‡]	0.00624 (0.0056, 0.0068)	0.0034 ± 0.001	0.0034	0.0011 ± 0.0005[#]
n	11	2	4	2	15

Dynamic parameters of bone formation, namely BFR/BS and MAR were measured on an unstained section of L5 vertebra as described in section 2.2.16. With regard to BFR/BS a markedly improved response to therapy was observed with rf4S in comparison with human 4S, being corrected to 75% of normal, 1.7 times better than either dose of human enzyme (Table 3.6). BFR/BS in MPS VI cats is severely diminished (14% of normal). MAR does not distinguish between untreated MPS VI and normal cats. Not surprisingly MAR in rf4S-treated cats was not significantly different from either normal or rh4S-treated MPS VI cats. In general bone morphometric data reinforced the view that treatment with feline enzyme resulted in a trend toward normalisation of bone quality that, according to most parameters, was better than a 5 times higher dose of human enzyme.

3.2.5 Urinary GAG analysis

3.2.5.1 Alcian Blue method

The Alcian Blue test for GAG gives a measure of the total GAG in urine. The two cats in this study showed a rapid decrease in total urinary GAG with age (Figure 3.13). This reduction in GAG is a natural phenomenon and is observed in both normal and untreated MPS VI cats. However, the absolute level of urinary GAG in untreated MPS VI cats remains elevated from birth to six months by approximately 4-fold compared with normal cats. Within 25 days of the initiation of treatment with rf4S, the concentration of urinary GAG was approximately halved compared with untreated MPS VI controls, however, this was still double the level found in normal control cats. Between 25 and 45 days of therapy, the concentration of urinary GAG in cats treated with rf4S dropped rapidly to 1.5 times normal, or 28% of MPS VI, levels. From 90 to 170 days of therapy, it stabilised at 41% of MPS VI levels or 1.7 times normal levels. The reduction in total urinary GAG in cats treated with an equivalent dose of the human enzyme was not as great as that seen with the feline enzyme. The reduction was gradual and was maintained at a level of roughly 75% of that in untreated MPS VI controls over the same period. In comparison, the higher dose of human enzyme was slightly better than the 1 mg rf4S/kg dose up to about 100 days of therapy and then a more pronounced effect was observed to 150 days, that is, again better than the 5 mg/kg dose for most of the treatment period.

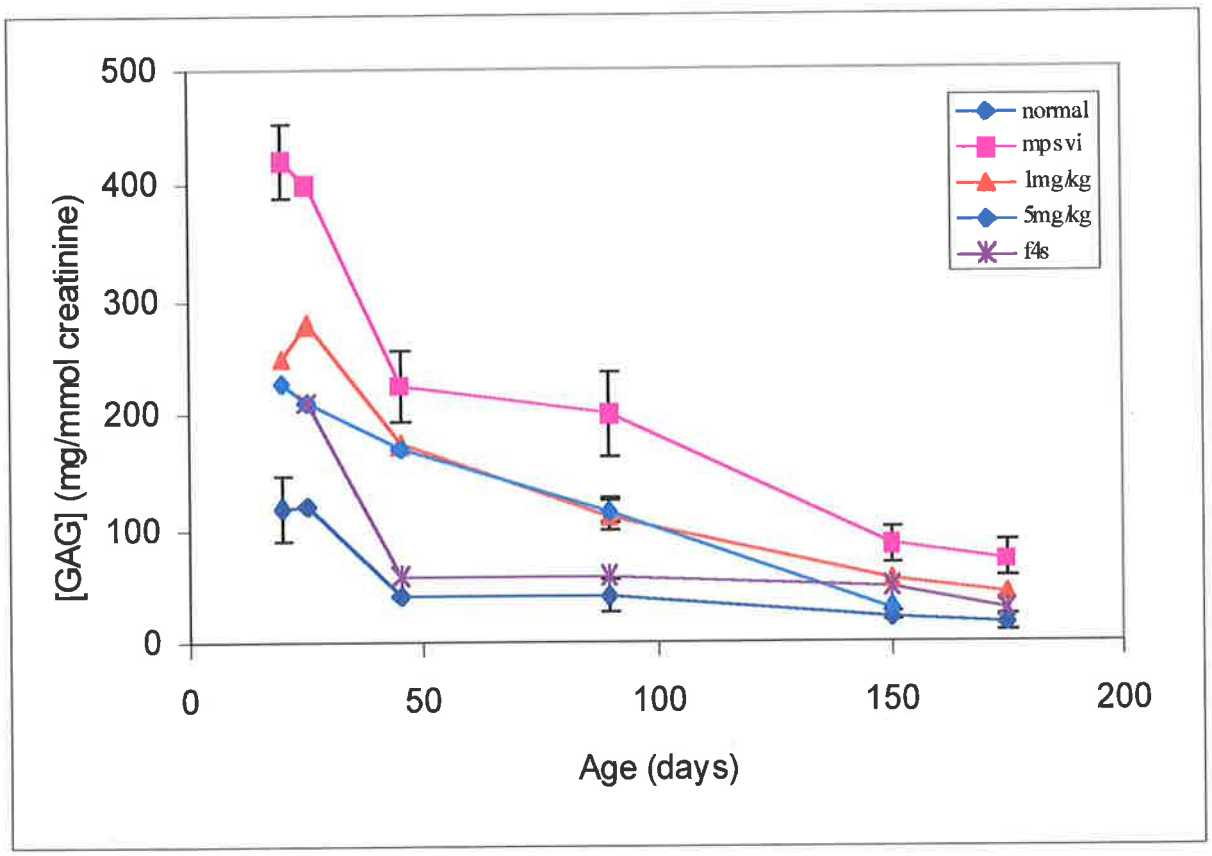

Figure 3.13: Urinary GAG excretion in normal, untreated MPS VI and ERT treated MPS VI cats.

Cat urine was collected from birth to 6 months at the times shown. Total urinary GAG was estimated using the Alcian Blue method (section 2.2.14.1) and was standardised to creatinine (mmol). Error bars, ± 1 SD. Points with no error bars indicate n<3.

3.2.5.2 High-resolution electrophoresis (HRE)

HRE allows a means of visualising the types and patterns of urinary GAG and their quantification by densitometric analysis. Based on the resulting pattern of stained bands, a preliminary diagnosis for a particular MPS can be proposed. In MPS VI, DS is elevated in urine. On HRE, DS migrates as an intensely staining band which remains near the origin (DS1) and as one (or two) diffusely staining bands with have greater mobility that migrate towards the cathode (DS2) (Figure 3.14). Therefore total DS (DS1+DS2) can be expressed as a percentage of total GAG on HRE by densitometric analysis. Apart from the 23 day time point, % DS remained reasonably constant throughout therapy for those cats treated with rf4S, varying from 65% at day 49 to 59% at day 170 (Table 3.7). Compared with untreated MPS VI cats, this indicated a reduction of DS excretion of between 33-41% during therapy. This was better than the equivalent dose of human enzyme, particularly towards the end of therapy (day 170) when the level of DS was the same as in untreated MPS VI cats. The greatest reduction in % DS was observed in cats receiving 5mg rh4S/kg. In these cats % DS initially decreased to 48% of the level seen in untreated MPS VI cats and then increased to 63% at day 150. From data in Table 3.7 it is obvious that although % DS fluctuates there was nevertheless an overall increase with age in both those cats receiving therapy and in untreated MPS VI cats. In addition there was a reduction in % DS in cats on all treatment regimes except at 170 days with the 1 mg rh4S dose as mentioned above. Although total GAG concentration as measured by the Alcian Blue test (section 3.2.5.1) decreased to within 1.7 times normal levels in cats on rf4S therapy, this was not reflected in HRE results which indicated that the proportion of DS remained elevated throughout. In normal cats % DS is very low, ranging from 1.6% at age 23 days to 4.4% at 170 days (HRE data not shown).

Figure 3.14: HRE of urinary GAG from MPS VI treated and untreated cats.

Urinary GAG was precipitated with CPC prior to HRE on cellulose acetate plates. Plates were stained with Alcian Blue to visualise GAG. (A) Lanes 1-5, urine from cat 249 treated with 1 mg rf4S/kg at 26, 46, 89, 150 and 175 days, respectively; lanes 6 and 7, urine from cats treated with 1 and 5 mg rh4S/kg at 173 and 149 days of age, respectively; lane 8, urine from an untreated MPS VI cat at 175 days of age. (B) Lanes 1-4, urine from cat 250 treated with 1 mg rf4S/kg at days 24, 91, 150 and 168 days; lanes 5 and 6, urine from cats treated with 1 and 5 mg rh4S/kg at 173 and 149 days of age, respectively; lane 7, urine from an untreated MPS VI cat at 175 days of age. DS (DS1 and DS2) and CS bands are indicated by arrows. The migration position of HS is also indicated although no bands in this region were observed in accordance with HS not being a storage product in MPS VI.

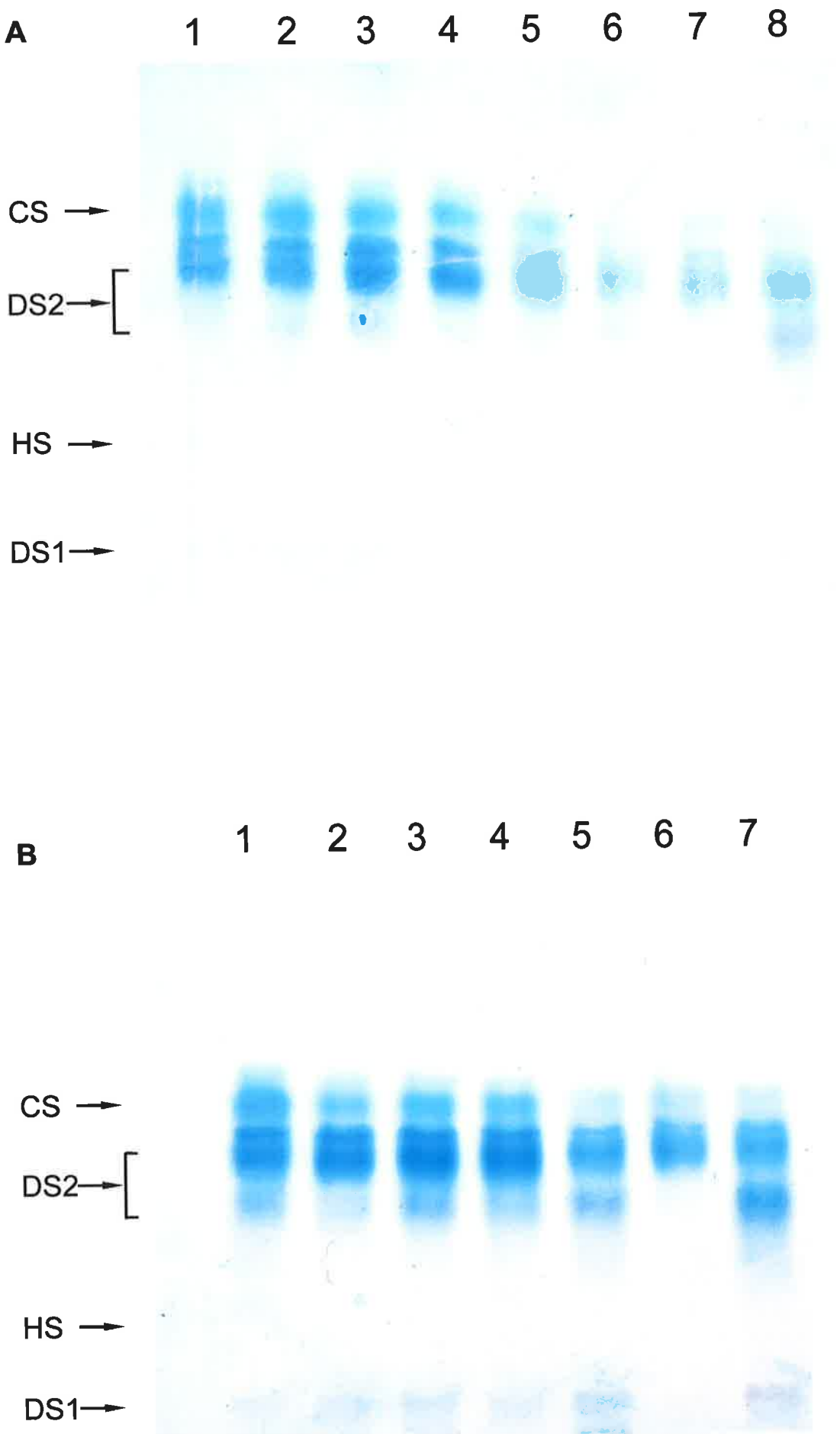
A
1
2
3
4
5
6
7
8
CS
DS2
HS
DS1
B
1
2
3
4
5
6
7
CS
DS2
HS
DS1

Table 3.7: Comparison of the percentage DS in total urinary GAG of cats on ERT with normal and untreated MPS VI cats at different ages.

Age (days)	MPS VI (no ERT)	MPS VI (1 mg rf4S/kg)	MPS VI (1 mg rh4S/kg)	MPS VI (5 mg rh4S/kg)	Normal
23	40.8 ± 4.8	36.6 (37.2, 35.9)	37.8 ± 14.1	19.4 (19.1, 19.6)	1.6 ± 1.0
49	52.4 ± 5.0	34.0*	nd	nd	3.9
90	61.9 ± 8.2	41.6 (39.2, 44.0)	37.8 ± 5.3	25.8 ± 7.1	4.4 ± 3.5
150	58.9 ± 3.7	38.2 (40.2, 36.1)	41.9 (41.7, 42.0)	37.2 ± 12.9	3.6 ± 1.2
170	62.8 ± 3.8	36.9 (35.4, 38.3)	59.3 (61.7, 56.9)	nd	4.4 ± 1.5

The percentage DS (DS1 + DS2) was estimated from densitometric analysis of urine GAG following HRE (Figure 3.14). Results are expressed as the mean ± 1 SD where the number of cats (n) is >3. Where n = 2 the mean value is given with the individual values shown in parentheses. *n = 1; nd, not determined. Except for rf4S results all data were obtained from A Crawley.

3.2.5.3 Gradient-PAGE

Sulphated GAG were isolated from cat urine using anion exchange chromatography followed by desalting on Sephadex G10 and then analysed by gradient-PAGE according to the method described in section 2.2.14.4. Gradient-PAGE, as opposed to isocratic-PAGE, has greater resolving power and can separate GAG species on the basis of charge as well as size thus permitting a more comprehensive characterisation of GAG structures. The ladder of sulphated GAG that is visualised after staining is a reflection of the different sized products excreted in urine, ranging from a tetrasaccharide to large molecular sizes. The broad range of GAG species that are observed, varying in both size and charge, implies the presence of partially degraded chains. In all urine samples analysed, a similar pattern of multiple GAG bands was observed (Figure 3.15). Major bands represent separation by size, with multiple bands surrounding each size grouping being indicative of differing sulphation (i.e., charge) patterns.

Urine from normal cats is predominantly comprised of high Mr oligosaccharides. Both the type and amount of sulphated GAG are vastly increased in untreated MPS VI cats compared with that observed in normal cats. Analysis of cats treated with 1 mg rh4S/kg showed only a minor change in this profile compared with untreated MPS VI cat urine. Samples from cats treated with 1 mg rf4S/kg showed a pattern and intensity of GAG similar to that seen in cats treated with 5 mg rh4S/kg. This differs from normal control urine mainly in the amount of low Mr oligosaccharides present. Quantification of these results by densitometric analysis of specific bands clearly demonstrated that the ratio of these bands (A:B and C:D as indicated in Figure 3.15) was almost completely normalised in those cats treated with rf4S (Table 3.8). This effect was definitely much more pronounced than 1 mg rh4S/kg and only slightly different from the 5 mg rh4S/kg dose. Compared with normal cat urine, the size and species ratios are markedly altered in MPS VI cat urine. However, overall the concentration of charged saccharides in urine was still higher in each treatment group compared with that in normal cats. Treatment of the same samples with rf4S, followed by analysis on gradient gels, demonstrated a shift in banding pattern for all samples except normal urinary GAG (Figure 3.16). The change is indicative of the removal of a 4-sulphate moiety from the non-reducing terminal residue of the GAG species present in urine from both treated and untreated MPS VI cats.

Figure 3.15: Gradient-PAGE of GAG isolated from urine of normal, untreated and treated MPS VI cats.

Lanes 1 and 2, cat 249 and 250 urine, respectively; lane 3, untreated MPS VI cat urine; lanes 4 and 5, urine from MPS VI cats treated with 1 and 5 mg rh4S/kg; respectively; lane 6, normal cat urine and lane 7, heparin oligosaccharide standards. A and B, and C and D, indicate pairs of bands for which densitometric ratios were obtained (see Table 3.8). Bands A, B, C and D in normal cat urine are very faint and not seen to full potential in this photograph.

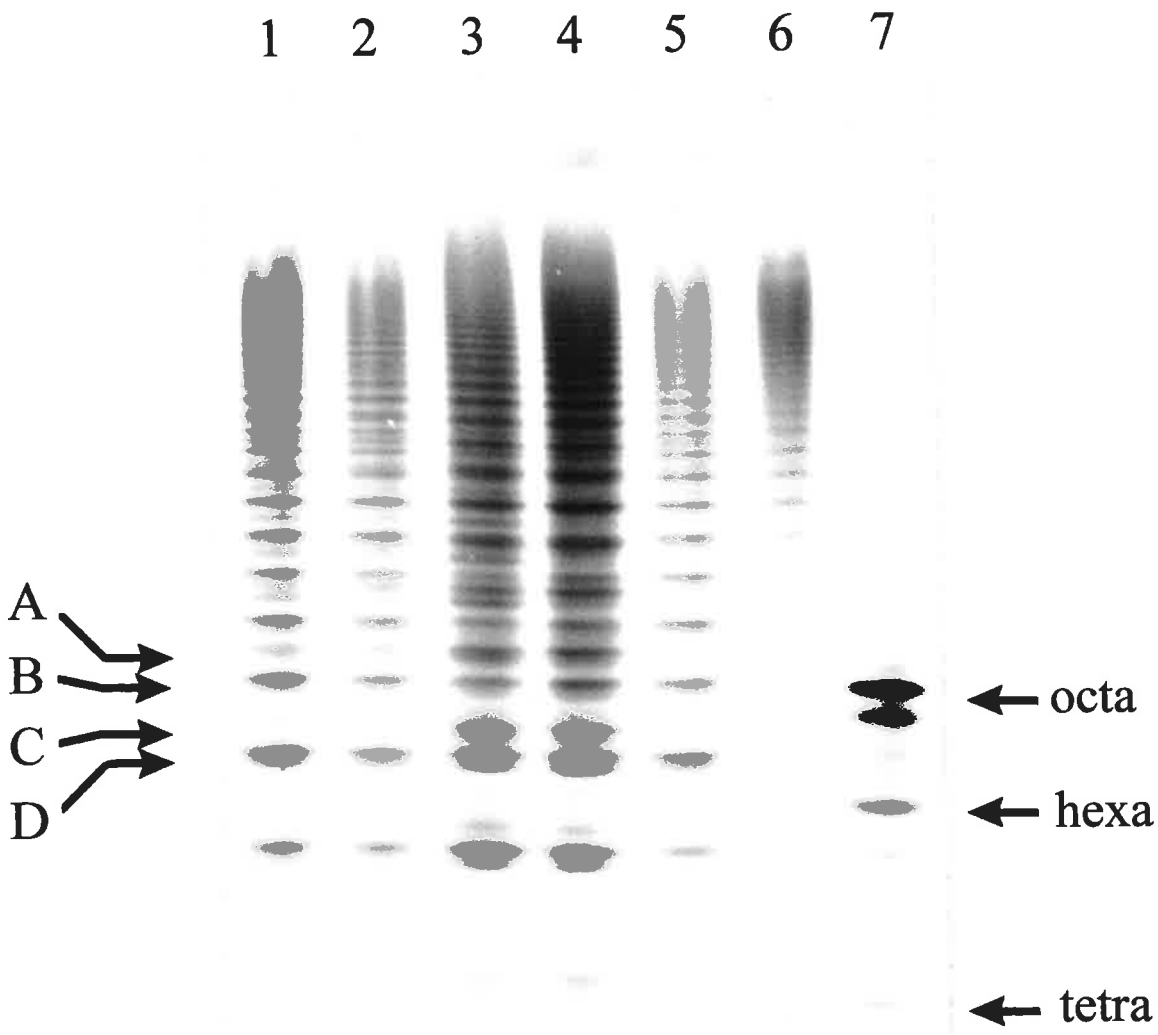
1
2
3
4
5
6
7
A
B
C
D
octa
hexa
tetra

Table 3.8: Comparison of the ratios of sulphated uronic acid-containing GAG fragments isolated from urine of normal, MPS VI untreated and MPS VI treated cats after gradient-PAGE.

	Lane, Figure 3.15	A:B	C:D
Cat 249 (1 mg rf4S/kg)	1	64:36	68:32
Cat 250 (1 mg rf4S/kg)	2	60:40	70:30
MPS VI (no treatment)	3	44:56	49:51
MPS VI (1 mg rh4S/kg)	4	46:54	52:48
MPS VI (5 mg rh4S/kg)	5	64:36	77:23
Normal cat	6	63:37	73:27

A:B and C:D are ratios of pairs of bands (Figure 3.15) analysed by densitometry.

Figure 3.16: Gradient-PAGE of GAG isolated from urine of normal, untreated and treated MPS VI cats following digestion with rf4S.

Lanes 1, 3, 6, 8, 10 and 12 are cat 249, cat 250, untreated MPS VI, MPS VI treated with 5 mg rh4S/kg, MPS VI treated with 1 mg rh4S/kg and normal cat urinary GAG, respectively, which have not been digested with rf4S. Lanes 2, 4, 7, 9, 11 and 13 are the same urinary GAG as above but these have been digested with rf4S. Lane 5, heparin oligosaccharide standards.

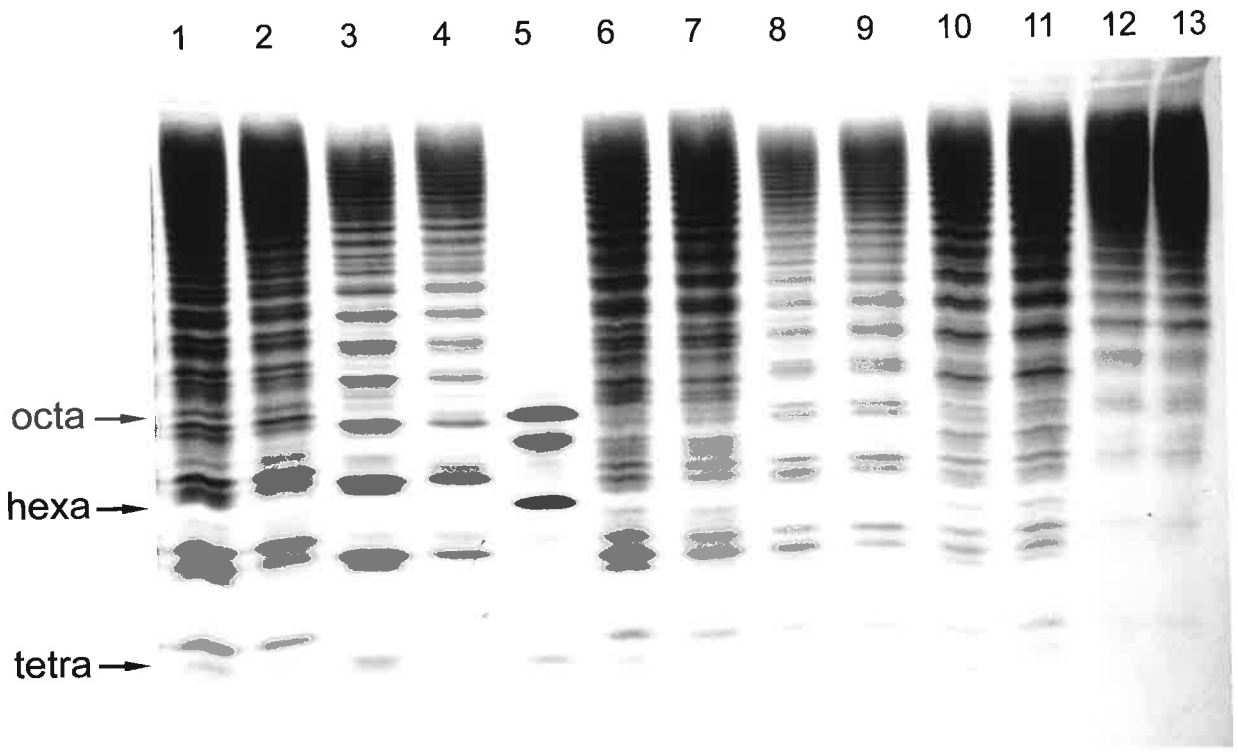
1
2
3
4
5
6
7
8
9
10
11
12
13
octa
hexa
tetra

Figure 3.17: Western blot of plasma from cats on ERT.

Blood samples were collected from cats 249 and 250 at specified times throughout therapy and the plasma isolated to test for antibody reactivity to rf4S as described in section 2.2.11. Lane 1, rf4S probed with a polyclonal to rf4S followed by detection with SAR-HRP (positive control); lanes 2-5, plasma from cat 250 at 45, 90, 150 and 168 days; lanes 6-9, plasma from cat 249 at 45, 90, 150 and 175 days; lane 10, plasma from cat 251 (a heterozygote littermate of cat 250) at day 175; lane 11, plasma from cat 140 (shown to have a positive antibody response to rh4S, titre 1 in 250,000), lane 12, negative control with 1% milk. Lanes 2-12 were probed with goat anti-cat Ig-HRP.

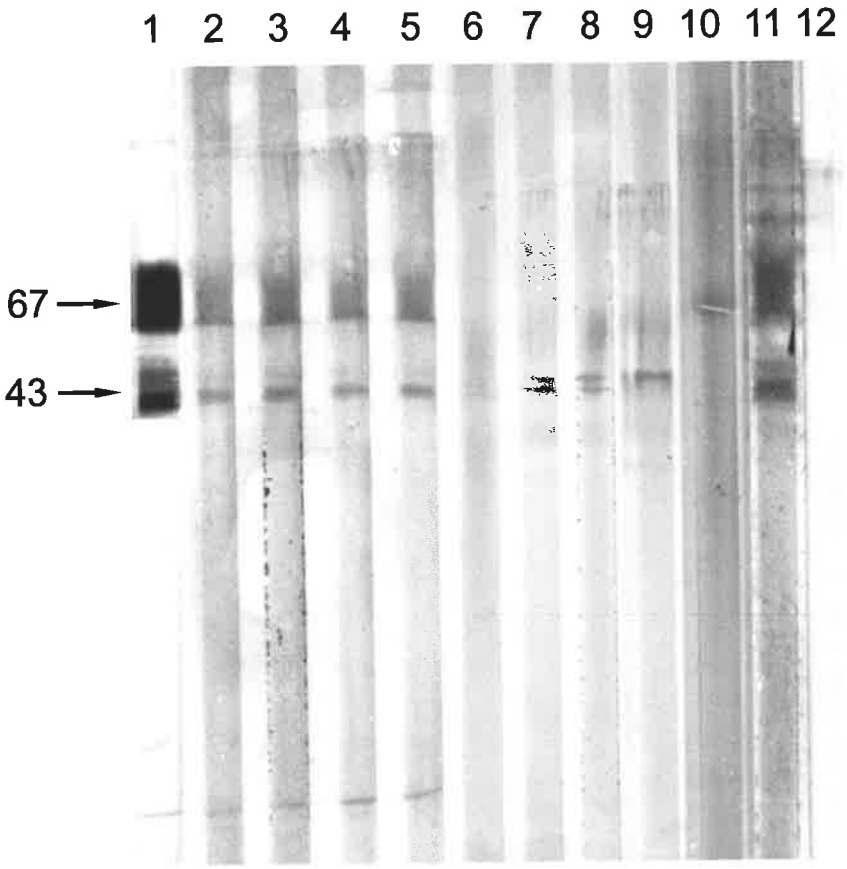
1 2 3 4 5 6 7 8 9 10 11 12
67
43

3.2.6 Antibody response

No significant antibody response to rf4S was detected in plasma from cat 249 either by Elisa or western blot, and a very low titre (1 in 5,100) was observed for cat 250 (results not shown). The protocol used for determining antibody titre was validated using plasma from cat A, which had a titre of 1 in 512,000 (cat A was treated with rh4S from 7 months of age (Crawley *et al.*, 1996). This titre was identical to that obtained by a previous analysis (Brooks *et al.*, 1997). Western blot analysis of plasma from cat 250 showed a weak response that did not change from day 90 to euthanasia (Figure 3.17). Pre-immune serum was not available to test for background reactivity. However, cat 251, a heterozygote littermate of cat 250 also showed a weak antibody response to rf4S by western blot analysis (Figure 3.17, lane 10). Cat 104, which had a high titre to rh4S also demonstrated a positive response on a western blot.

3.2.7 Residual enzyme activity in feline liver

From various tissue distribution studies of rf4S (section 2.2.19) and rh4S in cats (Crawley *et al.*, 1996; Crawley *et al.*, 1997) it was observed that the majority of intravenously administered enzyme is localised to liver (Table 3.11). Liver was therefore considered a suitable organ to compare the levels of residual 4S activity in cats treated with either f4S, or h4S. Two doses, 1 mg and 5 mg/kg body weight were used. Liver homogenates were prepared as described in section 2.2.17 and assayed using a specific radiolabelled substrate (section 2.2.5.2). The livers of cats analysed had been stored at -20 °C for various periods of time as noted. Unfortunately the only normal cat liver available at the time of analysis was from a 1 day old kitten whereas livers obtained from all other cats were either 5 or 6 months of age. All treated cats had been euthanased 48 h after receiving their last injection of enzyme.

The mean level of 4S activity in cats treated with rf4S, although higher than that seen in a normal cat, was nevertheless approximately half that in the liver of cats treated with an equivalent dose of rh4S. This in turn was about four times lower than in the 5 mg rh4S/kg dose regimen. Untreated MPS VI cats have less than 1% residual 4S enzyme activity.

Table 3.9: Residual 4S activity in liver homogenates of normal, untreated and treated MPS VI age-matched male cats.

	4S activity (pmol/min/mg total protein)
Normal	7.37
MPS VI (1 mg rf4S/kg)	12.81 (7.43, 18.81)
MPS VI (1 mg rh4S/kg)	24.08 (29.84, 18.32)
MPS VI (5 mg rh4S/kg)	92.10 (120.92, 63.28)
MPS VI (no ERT)	0.057 (0.06, 0.053)

Cat status, age at euthanasia and the time in storage of the liver sample at –20 °C (shown in parentheses) were as follows: normal cat, 1 day old (8 months), cats 249 and 250, 6 months (6 months), two MPS VI cats treated with 1 mg rh4S/kg, 6 months (32 and 38 months), two MPS VI cats treated with 5 mg rh4S/kg, 5 months (33 and 55 months) and two untreated MPS VI cats, 6 months (23 and 28 months). Results are normalised to total cell protein; the mean of two measurements is shown with individual results for each liver homogenate given in parentheses.

3.2.8 Assessment of hepatomegaly in MPS VI cats

In contrast to human MPS VI, hepatomegaly does not present as an obvious clinical symptom in the MPS VI cat (Haskins *et al.*, 1979b; Haskins *et al.*, 1983a; Di Natale *et al.*, 1992) despite the high degree of storage in liver Kupffer cells. The abdominal distension noted in affected cats has been attributed to shortened body length and the requirement to accommodate

relatively normal sized organs. To determine if MPS VI cats did display some degree of hepatomegaly, wet weights of liver from autopsy data were expressed as a percentage of total body weight. These were compared with liver weights of normal and rf4S and rh4S-treated cats.

Analysis of liver wet weight data (Table 3.10) indicated that male MPS VI cats have livers that are 24% heavier than normal age and sex-matched controls and that this difference is statistically significant. Furthermore, all treatments (1 and 5 mg rh4S/kg and 1 mg rf4S/kg) in male cats resulted in a decrease in liver size to a value not statistically different from normal male cats, but significantly different from untreated MPS VI cats. The results clearly show that male MPS VI cats do have enlarged livers and that ERT results in both the complete elimination of storage and normalisation of liver weight. There was no significant difference in liver size between age-matched normal male and female cats, or between age-matched MPS VI male and female cats. Nor was there a statistically significant difference in liver size between age-matched normal and MPS VI female cats or between age-matched MPS VI female cats and those that had received treatment. However, there was a trend towards that end and taken as a group there was a statistically significant difference between age-matched MPS VI male and female cats and those on therapy.

Table 3.10: Comparison of liver size of normal and MPS VI treated and untreated cats.

	Liver size as % total body weight
Normal male (n = 5)	3.010 ± 0.597*
MPS VI no ERT male (n = 9)	3.850 ± 0.767
Treated MPS VI male (n = 8)	2.998 ± 0.496#
Normal female (n = 4)	3.293 ± 0.251
MPS VI no ERT female (n = 8)	3.568 ± 0.932
Treated MPS VI female (n = 9)	3.033 ± 0.387
Treated MPS VI male and female (n = 22)	2.939 ± 0.459‡
MPS VI no ERT male and female (n = 22)	3.524 ± 0.755

Results are expressed as mean ± 1 SD.

n = number of cats in each group.

* Significant difference at $p<0.05$, normal vs. MPS VI untreated.

Significant difference at $p<0.05$, MPS VI treated vs. MPS VI untreated.

‡ Significant difference at $p<0.005$, MPS VI treated (males and females at all ages with all treatment regimens) vs. MPS VI untreated males and females of all ages.

3.2.9 Tissue distribution of ^{3}H-rf4S in normal cats

Four 8 day old kittens were injected intravenously with 1 mg ^{3}H-rf4S/kg and sacrificed after 4 h. Analysis of major organs after NaOH solubilisation of tissues indicated that the majority of enzyme (60%) was found in the liver (Table 3.11). Other organs with a significant, although much lower, level of radiolabelled enzyme included lung, kidney and spleen. These results are similar to all distribution studies done to date in that the majority of enzyme is found in the liver. This is not unexpected as the liver is extremely well vascularised, large and efficiently endocytoses material from circulation. When the distribution of what is mainly precursor rh4S was determined there was more enzyme activity in liver (75.42%). When predominantly mature rh4S was injected there was a reduced level found in the liver (56%), the level of rf4S was of intermediate value (60%). After 4 h, there were still detectable levels of enzyme in plasma which may account for the low levels detected in the various brain fractions as these cats were not perfused before sacrifice. In addition, capillary depletion (Triguero *et al.*, 1990) to eliminate contamination of brain samples by radioactive enzyme from brain capillaries was not done.

Table 3.11: Comparison of the tissue distribution of radiolabelled rf4S and rh4S (precursor and mature forms) as %ID in normal kittens.

Tissue	rf4S	rh4S (precursor)	rh4S (mature)
Liver	60.04 ± 5.73	75.42 ± 8.79	56.64 ± 14.39
Kidney	2.12 ± 1.14	1.48 ± 0.32	1.5 ± 0.22
Spleen	1.94 ± 1.03	1.63 ± 0.50	0.34 ± 0.20
Lung	2.94 ± 1.93	1.92 ± 0.30	1.07 ± 0.28
Heart	0.35 ± 0.15	0.43 ± 0.27	0.28 ± 0.09
Cerebrum	0.25 ± 0.13	0.29 ± 0.05	0.42 ± 0.18
Cerebellum	0.04 ± 0.03	0.02 ± 0.01	0.09 ± 0.03
Base brain	0.04 ± 0.02	0.03 ± 0.01	0.05 ± 0.02
Plasma	0.50 ± 0.12	0.52 ± 0.04	0.75 ± 0.55
n	4	3	3

^{3}H-radiolabelled 4S was produced as described in section 2.2.26 and immunopurified using F58.3-linked Affi-Gel (section 2.2.3). The precursor and mature forms of ^{3}H-rh4S were purified by chromatography over M6PR-linked Affi-Gel (Jones *et al.*, 1998). Kittens were injected with a dose of 1 mg/kg and sacrificed 4 h later. Tissues were processed for determination of radioactivity as described in section 2.2.19. Results are expressed as the mean of the %ID ± 1 SD. n = number of kittens in each group. Data for precursor and mature forms of rh4S were obtained from Leanne Hein, Department of Chemical Pathology, WCH.

3.2.10 Plasma circulating half-life of rf4S in normal cats

Plasma clearance of intravenously injected rf4S was typically biphasic showing an initial steep decline in plasma enzyme concentration followed by a longer second phase (Figure 3.18). The plasma circulating half-life for the initial phase was calculated to be 5.8 min which is similar to that for rh4S (3.6 min) when administered at a dose of 1 mg/kg. (The previously published half-life of 13.7 min (Crawley *et al.*, 1996) was incorrectly calculated. Personal communication, A. Crawley). The half-life of the second phase was estimated to be approximately 102 min.

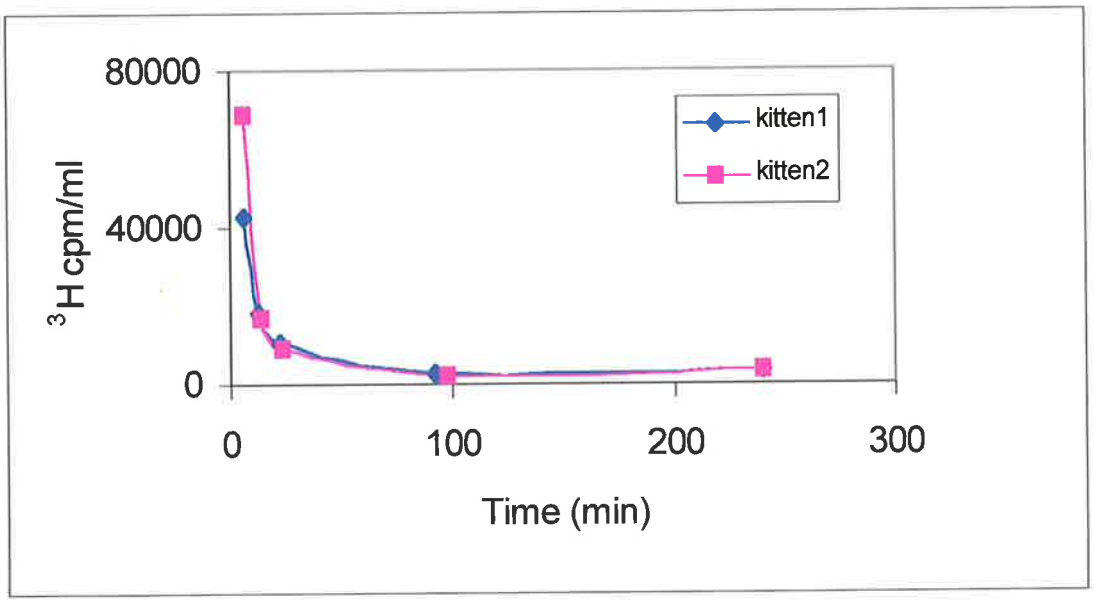

Figure 3.18: Plasma half-life of rf4S in normal kittens.

Plasma clearance of rf4S in 8 day old normal kittens after intravenous administration of ^{3}H-labelled rf4S at 1 mg/kg.

3.2 Discussion

Because rf4S had been cloned, expressed, purified and characterised and was found to be similar to rh4S in most respects, small differences in glycosylation and pI being exceptions, it was considered of clinical relevance to study the efficacy of using feline enzyme in a feline model of MPS VI. It was believed that such a study would yield valuable information with regard to what would be the analogous situation in human patient trials of species-specific (i.e., human) ERT.

MPS VI cats (L476P homozygotes) have less than 1% residual 4S activity compared to normal cats, and in a previous study in which rh4S was injected at doses of 0.2, 1 and 5 mg/kg body weight weekly from birth for up to 6 or 11 months, there was a dose-dependent reduction in pathology with the 1 mg and 5 mg rh4S doses. Urinary GAG excretion, skeletal pathology and lysosomal distension in various cell types were also decreased with the two higher doses, whereas the 0.2 mg dose was found to be too low to have any significant effect in altering any of the above parameters. A dosage rate of 1 mg rf4S/kg was chosen as firstly, differences in pathology were noticeable at this dose of h4S although they were not as marked as at the 5 mg dose, and secondly, the time and cost associated with production of enzyme were limiting. Injections were administered on a weekly basis to maintain consistency with the previous study in which the frequency of enzyme infusion was selected on the basis of tissue distribution studies of rh4S. These studies indicated that tissue half-life of enzyme was between 2-4 days. In addition, treatment was commenced at birth to maximise the effects of therapy on skeletal growth and development and to minimise the possibility of antibody response. However, the nature of the mutation in MPS VI cats suggests that some 4S protein is produced making it unlikely that rf4S would be recognised as foreign. MPS VI kittens treated from birth with rh4S, which is 90% homologous to rf4S, also did not develop an antibody response. An immune response to rh4S was only found when therapy was initiated at later stages.

The two cats in this study were unrelated and were diagnosed at birth as being MPS VI affected (L476P homozygous) on the basis of unstained eosinophils from a blood smear (Crawley *et al.*, 1997). Vacuolated lymphocytes and heavily stained basophilic granules in neutrophils and basophils substantiated this diagnosis which was later confirmed by PCR mutation analysis. Diagnosis from blood smears has proved to be reliable in all cats assigned

L476P homozygous status by this method and has proved to be superior to analysis by 4S/β-Hex ratios in white blood cell lysates. The latter method, moreover, is inappropriate for diagnosis of kittens at birth due to limitations of the volume of blood that can be safely taken.

External appearance: Treatment of the two cats in this study with 1 mg rf4S/kg resulted in significant changes to physical appearance such that, apart from the presence of mild corneal clouding, these cats were indistinguishable from age-matched littermates.

Histology: Histological analysis of tissues indicated that the 1 mg rf4S dose produced results that were as good as, or better than, a five-times higher dose of human enzyme in most of the cell types examined. Of particular interest was the total clearance of storage from smooth muscle cells across the entire width of the aorta. Treatment with human 4S demonstrated a dose-dependent gradient of correction, with storage still obvious in the inner tunica media with the 1 mg dose and in the outer tunica media with the 5 mg dose. Although storage was totally removed with feline 4S, the normal architecture of the aorta was not resolved and remained disordered. This disarray is known to occur *in utero*. Electron microscopic sections of aorta from a mid-term feline MPS VI foetus show not only an already mild degree of lysosomal storage in smooth muscle cells but also reveal some disruption of aortic structures (Figure 3.10). Whether prolonged therapy can reverse this structural abnormality, or whether it affects aortic function in the long term, is not known. As many MPS VI patients die from cardiac failure, the heart is a crucial site to be targeted in any therapy regime.

Both corneal keratocytes and cartilage chondrocytes did not respond to therapy with either rf4S or rh4S. This is reflected in the cloudy corneas and thickened cartilage over joint surfaces in all animals on all forms of therapy. Both these tissues are not only avascular but are also comprised of a dense network of extracellular matrix in which the cells are embedded. Attempts to increase enzyme penetration to these tissues by cationization of enzyme with poly-L-lysine or ethylenediamine have been unsuccessful (Byers *et al.*, 2000). However, direct injection into articular joint space may result in correction of cellular pathology. If this were the case, both systemic and targeted ERT may be required to effect a complete treatment. Although not attempted in MPS VI cats because of practical and ethical considerations, direct application of enzyme (or an active fragment of enzyme) onto the cornea may be worthy of consideration in treating corneal opacity.

Bone disease: MPS VI is a disease of predominantly skeletal and joint pathology. As discussed above, joints were refractory to all forms of ERT including species-specific enzyme (i.e., rf4S). Bone on the other hand responded reasonably well, particularly with 1 mg rf4S and 5 mg rh4S. Analysis of the L5 vertebra radiographically showed that bone shape and growth were nearly normalised. Histomorphometric analysis of the L5 vertebra indicated that the rate of bone formation and bone architecture were dramatically improved with rf4S compared with either of the two doses of human enzyme.

A study of the tibial growth plate in MPS VI cats by histomorphometric analysis has been reported (Nuttall *et al.*, 1999). Results from this study indicate that from birth to 20 days of age normal and MPS VI cats show a similar pattern of development. This is characterised by a rapid reduction in bone mineral volume due to expansion of the marrow cavity while the specific bone mineral surface remains constant. During this time, trabecular number is halved in both normal and MPS VI feline tibia. However, after 20 days bone mass in normal cats increases such that by 6 months and onwards bone volume is similar to that observed at birth. This increase in bone mass during the active growing phase is achieved predominantly by an increase in trabecular thickness while trabecular number and surface volume remain relatively unchanged. The situation in the MPS VI cat however, diverges from normal at 20 days of age. Bone mineral volume remains low and although trabecular thickness increases this is to a lesser degree than that observed in normal bone and is compounded by a continual loss of trabecular number. In effect bone formation rate is markedly depressed and MPS VI cats demonstrate severe osteopaenia.

Deformed and shortened bones are also observed radiographically. Short stature results from impaired endochondral ossification which is the process whereby cartilage is transformed into bone. This is a complex process and is described in section 1.13. The mechanisms responsible for abnormal endochondral ossification have not been elucidated. However, DS accumulation in chondrocytes appears to impair their function. Furthermore, a recent study (Gerber *et al.*, 1999) has shown that a vital step in the transition of cartilage to bone is the invasion of cartilage by blood vessels which thus provide a conduit for the recruitment of the cell types involved in cartilage resorption and bone deposition. In addition, several signals required for normal bone morphology are provided by this vasculature. These include members of the fibroblast growth factor family and the TGF-β family, as well as the angiogenic protein,

vascular endothelial growth factor (VEGF). VEGF is expressed in hypertrophic chondrocytes in the epiphyseal growth plate and was found to be an essential coordinator of chondrocyte death, chondroclast function, extracellular matrix remodelling, angiogenesis and bone formation in the growth plate. The action of VEGF has not been examined in MPS VI cats but perturbation of the normal role of this factor may be one of the causes of poor bone elongation and development.

Because MAR is not different in either normal or MPS VI bone, it implies that MPS VI osteoblasts have the ability to support mineralisation if bone matrix is present. However, the rate of bone formation is impaired in MPS VI suggesting that the problem may be due to the number of osteoblasts recruited and/or their activity. Morphometric analysis of MPS VI trabecular bone indicated that the number of osteoblasts located on the mineral surface of the L5 vertebra was identical to that in normal controls (Byers *et al.*, 1997). However, this finding is questionable as morphological identification of osteoblasts in tissue sections is problematic as the staining procedure used obscures cell boundaries. Osteoclast function has not been studied in the MPS VI cat. However, abnormal osteoclast function and morphology as well as a slower rate of bone matrix deposition have been observed in the MPS VII mouse model (Monroy *et al.*, 2002).

Hind limb paresis: The main cause of hind limb paresis in MPS VI cats is spinal cord compression which results from bony abnormalities of vertebrae. By normalising bone through ERT, cats retain mobility and show little or no evidence of spinal kyphosis.

GAG excretion: Excessive urinary GAG excretion is a feature of MPS VI that can be readily quantified to produce a non-invasive method to monitor disease progression or response to therapy as has been shown in studies of MPS VI cats treated with rf4S (this study) and rh4S (Crawley *et al.*, 1997) and in the MPS I dog (Shull *et al.*, 1994). It can also be used to diagnose MPS VI in kittens at birth although the procedure is more complicated and time consuming compared with blood film analysis.

Electrophoresis of urinary GAG on gradient polyacrylamide gels provides a means of visualising GAG chains of different sizes and sulphation patterns. The heterogeneous pattern displayed is a reflection of storage from various tissues and cell types within those tissues. This

has been clearly demonstrated by electrophoresis of GAG from MPS VI cat urine, serum and other tissues including liver, lung, kidney, spleen and bone (Byers *et al.*, 1998). The banding patterns of both urine and serum GAG show greatest similarity and yet are distinctive from GAG isolated from kidney. The implication here is that urine contains GAG that are filtered from all parts of the body while kidney GAG are peculiar to that organ.

Antibody response: The generation of an antibody response to infused enzyme in replacement therapy is of major concern as it can have severe negative consequences. These include possible life-threatening hypersensitivity/anaphylactic reactions and reduced efficacy of treatment if neutralising antibodies, which may either inactivate enzyme or incorrectly target it for degradation, are generated Brooks *et al.*, 1998). In the two cats treated with rf4S, no antibody response was detected in cat 249 and cat 250 had a titre of 1 in 5,000, which is in the normal range of normal control and untreated MPS VI cats (Brooks *et al.*, 1997). Those cats treated with rh4S from birth also showed no significant antibody titres to rh4S compared to normal control cats although hypersensitivity reactions during or soon after infusion of enzyme were noted particularly at the higher dose of 5 mg rh4S. There was no correlation between antibody titre and hypersensitivity responses. Treatment from birth may be advantageous because of the potential for inducing tolerance to foreign antigens. Cats treated with rh4S at an older age developed high antibody titres to injected enzyme although the presence of antibodies did not appear to be detrimental to therapy. Whether rf4S can generate an antibody response in older MPS VI cats is unknown, as it has not been tested. Furthermore, because the mutation in MPS VI cats is such that a very small amount of 4S protein is produced, this is probably sufficient for the infused enzyme not to be regarded as foreign.

3.2 Conclusions

In the study presented in this thesis, it has been shown that rf4S was more efficacious than an equivalent dose of rh4S and in some instances as good as, if not better, than a 5-fold higher dose of rh4S. The reasons for f4S eliciting an overall more effective therapeutic response are not clear. However, the following factors may be involved. Firstly, it was observed that treatment with rh4S resulted in all cats showing some adverse responses to the administration of enzyme at some stage during therapy, despite antihistamine premedication. In some cases, cessation of enzyme infusion followed by re-administration 30 minutes later coupled with a

slower rate of infusion was necessary to abrogate this effect. In contrast, those cats treated with rf4S demonstrated no untoward signs to enzyme infusion whatsoever. The reasons for the observed reactions in the cohort of cats treated with rh4S from birth are not obvious. These cats had low antibody titres to rh4S but these were not significantly different from those measured in untreated MPS VI and normal control cats (Brooks *et al.*, 1997). It is conceivable that the antibody titre detected in these cats, although low, may nevertheless be sufficient to elicit a transient immunogenic response such as anaphylaxis, but not one that is sufficiently severe to necessitate termination of therapy. Analysis of IgE antibodies in these cats was precluded by unavailability of suitable reagents. However, it is not clear that even when such a response is present that it would have a significant effect on the efficacy of therapy. Indeed, as discussed above, results from other animal studies (Shull *et al.*, 1994) and clinical trials of Gaucher disease (Richards *et al.*, 1993; Ponce *et al.*, 1997) suggest that the presence of even a large immune response is not necessarily detrimental to the therapeutic response. Therefore, it must be considered likely that an immune response to the human enzyme was, at the most, only a minor contributing factor to the observed differences between the efficacy of the human and feline enzymes.

Secondly, although rf4S and rh4S share similar physical and kinetic properties, the two enzymes have different pI values and glycosylation. rf4S is significantly more basic and is composed of fewer isomeric forms than its human equivalent. Based on amino acid sequence alone, the estimated pI values of both enzymes are not greatly different (6.98 for f4S and 7.58 for h4S) (Genetics Computer Group 1994 Program Manual for the Wisconsin Package, Version 8, August 1994 Genetics Computer Group, Madison, WI). The observed differences on IEF must therefore be due to variation in secondary modifications such as glycosylation and/or phosphorylation and sulphation. Results obtained from PNGase F treatment show that rh4S is more highly glycosylated than rf4S. Results from neuraminidase digestion suggest that a significant proportion of the rf4S has complex carbohydrate structures that terminate in sialic acid, whereas sialylation was not apparent in rh4S. The similarity in plasma-circulating half-life of both enzymes, namely 5.8 min for rf4S and 3.6 min for rh4S when administered at a dose of 1 mg/kg, however, implies that any difference in sialylation is not obviously altering the overall clearance rate of the enzyme. The degree of sialylation of oligosaccharide chains of proteins has been shown to influence bioactivity such as increasing plasma-circulating half-life (Morrell *et al.*, 1971; Joshi *et al.*, 1995). Furthermore the tissue half-life of f4S may be

increased in comparison with rh4S, however, this has not been determined. While it cannot be concluded at this stage that the differences in the pI and/or glycosylation of the two enzymes are contributing to the observed differences in the efficacy of therapy, it remains a possibility.

Thirdly, it is clear that an enzyme could be more effective in its native cellular environment through conserved interactions with other proteins. Although there is no evidence that 4S participates in interactions with other proteins that affect its biological activity, this remains a possibility. For example, there is some suggestion of a physical association between some lysosomal enzymes to enable substrate tunnelling (Yanagishita and Hascall, 1984; Freeman and Hopwood, 1992). Trafficking of both rf4S and rh4S enzymes *via* the M6PR appears similar, although binding constants for both enzymes to the feline receptor have not been determined. The analysis of urinary GAG from cats treated with the two enzymes by gradient-PAGE reveals quantitative differences in the species of GAG secreted. This could reflect subtle differences in substrate specificity for the two enzymes, or differences in tissue uptake of enzyme that result in the release of different GAG species.

The results in this study suggested that since as good as an effect was observed with rf4S at one-fifth of the dose of human enzyme in a cat population with a relatively severe form of MPS VI, the same may be true in human patients. Preliminary data from a Phase I/II trial in human MPS VI patients using 0.2 mg rh4S/kg body weight have indicated almost as beneficial a response in those patients in terms of reducing urinary GAG excretion as a 1 mg/kg dose (Harmatz *et al.*, 2001). These patients demonstrated increased respiratory function, better ambulation, including walking up stairs, improvement in joint flexibility, and an increase in height (which was due to realignment of hips rather than actual growth). No antibody response to injected enzyme was detected except for one patient on low dose therapy in whom the antibodies were not neutralising but actually kept the enzyme in circulation for longer. This suggests that it is the intrinsic environment (i.e., same species versus other species) rather than differences in the physical characteristics of the enzyme (i.e., glycosylation, pI, etc.) that are responsible for the differences in efficacy seen for rf4S and rh4S in MPS VI cats exemplifying the need to carefully model all aspects of animal trials.

Chapter 4: FUCOSIDOSIS

4.1 FUC: expression, purification and characterisation

4.1 Introduction

Of the over 40 different LSD that have been documented, approximately two-thirds can affect brain function resulting in a progressive mental and motor retardation from an early age. Fucosidosis is one such disease where CNS pathology is dominant. The fucosidosis English springer spaniel is a naturally occurring large animal model of the human condition. The fucosidosis dog has been well studied and documented with regard to development and behaviour as well as biochemistry and pathology (Taylor *et al.*, 1987; Taylor *et al.*, 1989b; Taylor *et al.*, 1989d). In addition, the gene for canine fucosidosis has been cloned and the causative mutation described (Occhiodoro and Anson, 1996; Skelly *et al.*, 1996). The result of this mutation, a 14-bp deletion at the 3' end of exon 1 results in a frame shift from amino acid 127 leading to a premature stop codon at amino acid 152. It is postulated that this results in the almost complete deficiency of FUC activity in all tissues. The symptoms ensuing from this profound loss of FUC activity in the fucosidosis dog (described in section 1.20) are comparable to the neurological symptoms in human fucosidosis. Although a rare disease, the availability of the fucosidosis dog has made it an important paradigm for the study and treatment of the CNS pathology that is associated with a large proportion of LSD. BMT is somewhat effective in treating this condition, however, its general applicability is restricted (see section 1.16.3). Conversely, ERT, although generally successful in the treatment of somatic tissue pathology, has limited efficacy because of the BBB. Importantly, the development of the BBB in dogs reflects the human condition where the barrier is closed at birth. This is in contrast to mouse models where the BBB is 'leaky' upto approximately 14 days after birth.

The BBB is composed of endothelial cells, held together by tight junctions formed between the plasmalemma of neighbouring cells, in cerebral capillaries and surrounded by astrocyte foot processes. The continuous membrane lining thus created separates circulating blood from the brain interstitium. Due to exclusion on the basis of size and charge, most proteins in the circulation, including lysosomal enzymes infused during ERT, do not cross the BBB. Only those proteins for which specific transport systems exist on the endothelial cell barrier can move from the peripheral circulation to the CNS. Examples of such proteins include insulin, Tf

and various growth factors. These are transported into the brain by specific receptor-mediated transcytosis. Furthermore, anti-Tf receptor antibody conjugates and anti-insulin receptor antibodies have also been shown to cross the BBB by a similar mechanism. Adsorptive-mediated transcytosis is another, albeit slower and less specific, mechanism where, by virtue of a highly positive charge, proteins can be transported across the BBB. Other means of accessing the brain, such as transient opening of the BBB following osmotic shock, or by implantation of delivery systems such as genetically modified cells or mechanical pumps, or by direct injection of enzyme into brain, while all feasible, are not without significant risk.

The aims of the experiments described in this chapter were firstly, to express, purify and characterise rcFUC; secondly, to modify rcFUC by cationization, and by conjugation to proteins which are known to be transported across the BBB; thirdly, to test the effect of these modifications on transcytosis of the enzyme across the BBB in normal rats and fourthly, if warranted, in the fucosidosis dog. The last aim was to evaluate the effects of a preliminary trial of ERT in a fucosidosis dog using rcFUC.

4.1 Results

4.1.1 Expression of rcFUC

The expression vector pEFNeocFUC was constructed and electroporated into CHO cells as described in sections 2.2.20 and 2.2.21, respectively. Forty-eight clones were isolated from a mass culture of G418-resistant cells as described in section 2.2.21.1. Medium conditioned for one day from confluent clones was assayed for FUC activity. Enzyme activity levels ranged from 0.6 to 24.2 nmoles/min/ml with an average of 1.49 nmoles/min/ml. The clone producing the highest level of FUC activity was then re-cloned twice by limiting dilution to ensure clonality. This clone, designated CHOrcFUC40-A2-4, expressed 10-13 mg of rcFUC per litre of culture medium conditioned for three days over confluent cells. Untransfected control CHO-K1 cells accumulate FUC to approximately 0.2 mg/l in medium conditioned in the same manner suggesting that rcFUC purified from CHOrcFUC40-A2-4 cells could contain in the order of 2% Chinese hamster FUC.

In order to generate pure cFUC, MDCK (canine) cells were also transfected with pEFNeocFUC (section 2.2.21). Under the conditions used for transfection only four G418-

resistant clones were obtained with DOTAP while many clones were generated using electroporation at both 330 and 800 μF capacitance. Sixty-two clones were screened for expression of FUC activity by assaying medium conditioned over confluent cultures for 3 days. Enzyme levels ranged from 0.1 to 38.8 nmoles/min/ml (average of 6.14 nmoles/min/ml). The six clones shown to secrete the highest levels of FUC activity were expanded and re-analysed. Of these six, the clone identified as producing the most FUC activity was re-cloned by limiting dilution to produce a clonal cell line designated MDCKcFUC8-6. This clone expressed approximately 2-3 mg of rcFUC/l in culture medium conditioned as described above for CHOrcFUC40-A2-4 cells. The level of FUC in untransfected MDCK cell-conditioned medium was 0.05 pg/l.

4.1.2 Large-scale production of rcFUC

CHOcFUC40-A2-4 and MDCKcFUC8-6 were seeded into two-tier cell factories and grown to confluency. Media containing 2% (v/v) FCS, and conditioned over confluent cells for 4 days, contained 6-7 mg/l and 1-2 mg/l of rcFUC, respectively. These levels were less than those obtained from CHOcFUC40-A2-4 and MDCKcFUC8-6 cells grown in 5% or 10% (v/v) FCS (13 mg/l and 3 mg/l, respectively), but were considered adequate and cost effective and allowed longterm maintenance of the cultures.

Secretion of rcFUC from MDCK cells grown in 10% (w/v) FCS and in the presence or absence of NH_4Cl was similar (2.1 mg/l and 2.4 mg/l, respectively) when the cells were conditioned over four days. A similar effect was observed with secretion from CHO cells expressing rcFUC in the presence or absence of NH_4Cl (12.1 mg/l and 11.6 mg/l, respectively). However, the percentage of what is presumably precursor FUC compared to mature enzyme was increased (10%) in the presence of NH_4Cl (see section 4.1.4.1 and Figure 4.7). In accordance with rf4S (section 3.1.1), NH_4Cl was not routinely used in culture medium of MDCKcFUC8-6 or CHOcFUC40-A2-4 cells because of its detrimental effects on cell viability.

CHO/rcFUC for ERT in the fucosidosis dog model was also produced on a larger scale in a 2 l Bioreactor (section 2.2.22) using growth conditions similar to those for CHO/rcFUC cells in cell factories. CHO/rcFUC expression levels ranged from 6-10 mg/l/day, although after 3-4 weeks levels started to decline gradually to approximately 4 mg/l/day. The Bioreactor was

generally viable for up to 6-8 weeks and during this time a total of about 150-200 mg of rcFUC could be collected.

4.1.3 Purification of rcFUC

Purification of rcFUC from conditioned medium by affinity chromatography was first attempted according to a modified method of Barker *et al.* (1988). Fucosylamine linked to agarose *via* a 1-atom spacer (Sigma F4285) was used and under the reported conditions for binding (50 mM sodium phosphate buffer, pH 6.8) no enzyme bound to the column. Changing the binding conditions to 50 mM sodium acetate buffer, pH 5 resulted in 91% of the enzyme activity loaded onto the column being found in the flowthrough and wash fractions with 9% being recovered after elution with 1% (w/v) L-fucose. Using a similar affinity matrix but with a 24-atom spacer (Sigma F3902) under identical conditions, and without exceeding the binding capacity of the column, all the FUC bound to the column and could be eluted with 1% (w/v) L-fucose. Therefore for large-scale purification of rcFUC, the following protocol was adopted. Conditioned medium was first concentrated approximately 10-15-fold by ultrafiltration and then dialysed against 50 mM sodium acetate buffer, pH 5 overnight at 4 °C. The precipitate that developed during dialysis accounted for up to 15% of the original protein concentration. However, only minor losses (5-10%) of FUC activity were observed during dialysis. The dialysed enzyme was clarified by centrifugation and applied to affinity matrix F3902. Bound enzyme was eluted with 1% (w/v) L-fucose in acetate buffer resulting in yields of enzyme generally between 40-60% of the starting material with <1% in the flowthrough and wash fractions as long as the capacity of the column was not exceeded (Figure 4.1 and Table 4.1). Bound rcFUC could also be eluted with 20 mM Tris-HCl buffer, pH 7 with similar yields although elution was delayed due to the time required to titrate the column buffer to pH 7.0. Further elution of the column with 5% (w/v) L-fucose and then 7 M urea resulted in no further recovery of FUC activity or protein (<1%). Mixing experiments in which increasing amounts of the column flowthrough were added to purified enzyme resulted in the restoration of activity to the original levels found in the material loaded (Table 4.2). This would indicate that the apparent loss of enzyme was artefactual. Isolation of the factor(s) present in the flowthrough that was responsible for the reactivation of FUC was not pursued.

Recoveries of rcFUC from the fucosylamine-agarose matrix indicated that the binding capacity of the column was approximately 0.15-0.2 mg rcFUC/ml of resin. The degree of purification

was 550-fold for MDCK/rcFUC and 12-fold for CHO/rcFUC. In both cases the enzyme was purified to apparent homogeneity as assessed by SDS-PAGE (Figure 4.2). The average specific activity of purified CHO/rcFUC and MDCK/rcFUC were 15,714 ± 1,409 and 16,423 ± 1,768 nmol/min/mg, respectively.

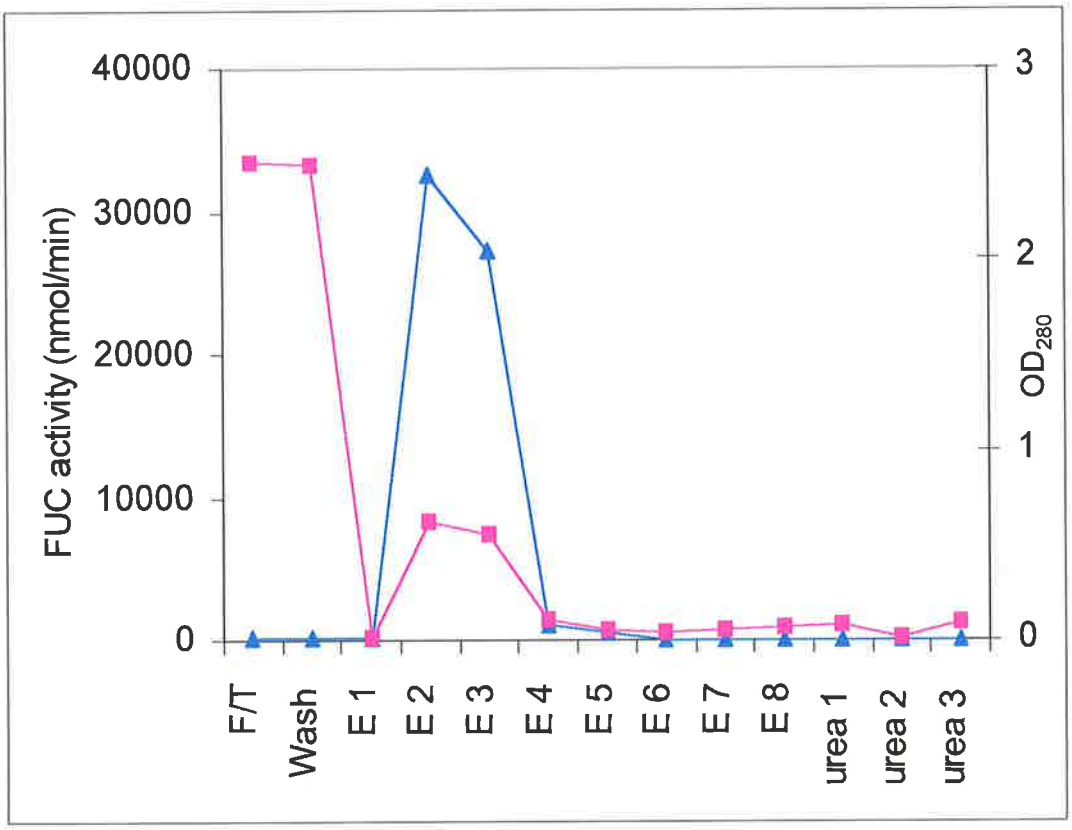

Figure 4.1: Purification of rcFUC on fucosylamine-agarose.

For experimental details see section 2.2.23. F/T, flowthrough, E1-E4 represent elution fractions from fucosylamine-agarose with 1% (w/v) L-fucose, E5-E8, with 5% (w/v) L-fucose, urea 1-3, with 7 M urea. All samples were dialysed prior to assaying with 4MUF. FUC activity (▲) and OD_{280} (■).

Table 4.1: Purification of CHO/rcFUC and MDCK/rcFUC on fucosylamine-agarose.

	FUC activity (nmol/min)	Protein (mg)	Specific Activity (nmol/min/mg)
CHO/rcFUC			
Original medium	18,680	12.34	1,514
Dialysed medium	17,160	12.14	1,414
Dialysed, centrifuged medium	16,920	10.49	1,613
Flow/through and wash	1.15	9.54	0.121
Eluate (1% (w/v) L-fucose)	7,600	0.409	18,582
MDCK/rcFUC			
Original medium	30,200	785	38.5
Dialysed medium	27,210	720	37.8
Dialysed, centrifuged medium	25,322	667.3	37.9
Flow/through and wash	240	675.5	0.36
Eluate (1% (w/v) L-fucose)	12,100	0.568	21,303

Table 4.2: Mixing experiment of rcFUC and flowthrough from fucosylamine-agarose column.

	FUC activity (nmol/min/ml)	Stimulation of FUC activity
FUC	10,010	
Flowthrough	0.45	
FUC:Flowthrough (1:1)	13,762	1.37 X
FUC:Flowthrough (1:2)	14,529	1.45 X
FUC:Flowthrough (1:5)	15,581	1.56 X
FUC:Flowthrough (1:10)	15,926	1.59 X

CHO/rcFUC was purified as described in section 2.2.23. The flowthrough from this purification procedure was added to a fixed volume of purified rcFUC in the ratios shown. Activity was determined using the fluorogenic substrate, 4MUF, taking into account the dilution factor.

4.1.4 Characterisation of rcFUC

4.1.4.1 Subunit Mr

The subunit Mr of purified rcFUC was determined by electrophoresis on a SDS 10% (w/v) polyacrylamide gel under reducing conditions (30 mM DTE). Analysis of the gel demonstrated that both MDCK/rcFUC and CHO/rcFUC were comprised of a doublet of 52 and 55 kDa (Figure 4.2). This doublet was also observed under non-reducing conditions. The larger polypeptide seen on SDS-PAGE is presumably the precursor form of the enzyme and the smaller polypeptide is the mature, lysosomal form, rather than both polypeptides being subunits of the precursor form. This interpretation is supported by the relative percentage of the two bands (larger:smaller, 70:30) in the enzyme purified from conditioned medium of cells

grown in NH_4Cl (Figure 4.7, lane 7) in comparison to enzyme expressed in the absence of NH_4Cl (larger:smaller, 50:50) (Figure 4.2, and Figure 4.7, lanes 3 and 5).

4.1.4.2 Native Mr

To determine native Mr, purified rcFUC was chromatographed over a Superose 12 column (Figure 3.2). Both CHO/rcFUC and MDCK/rcFUC had a native Mr of 156 kDa under the conditions described in section 2.2.6.1. Size exclusion chromatography of rcFUC in buffers of pH 3, 4, 5 or 7, each containing 150 mM NaCl, indicated that the Mr was similar to that obtained in 15 mM DMG, 0.5 M NaCl buffer, pH 6. Therefore, under the conditions tested there was no evidence for dissociation of the enzyme into subunits. When applied to DEAE-Sephacel under identical conditions, both CHO/rcFUC and MDCK/rcFUC bound to the matrix and required 0.2 M NaCl for elution (results not shown). Therefore, there was no evidence for the presence of two forms of rcFUC (Form I bound, Form II unbound), which could be separated by anion-exchange chromatography, as reported by Abraham *et al.* (1984) for canine liver FUC. Rat liver FUC (section 2.2.24), purified to test for cross-reactivity of monoclonal antibodies raised to CHO/rcFUC, comprised only a bound form when subjected to the same analysis (results not shown).

Figure 4.2: SDS-PAGE of CHO/rcFUC and MDCK/rcFUC.

Lane1, Mr standards, which include phosphorylase b (94 kDa), BSA (67 kDa), ovalbumin (43 kDa), carbonic anhydrase (30 kDa) and soybean trypsin inhibitor (20.1 kDa), are indicated by arrows. Lanes 2 and 3, CHO/rcFUC and MDCK/rcFUC electrophoresed under non-reducing conditions, respectively; lanes 4 and 5, CHO/rcFUC and MDCK/rcFUC electrophoresed under reducing conditions (30 mM DTE), respectively.

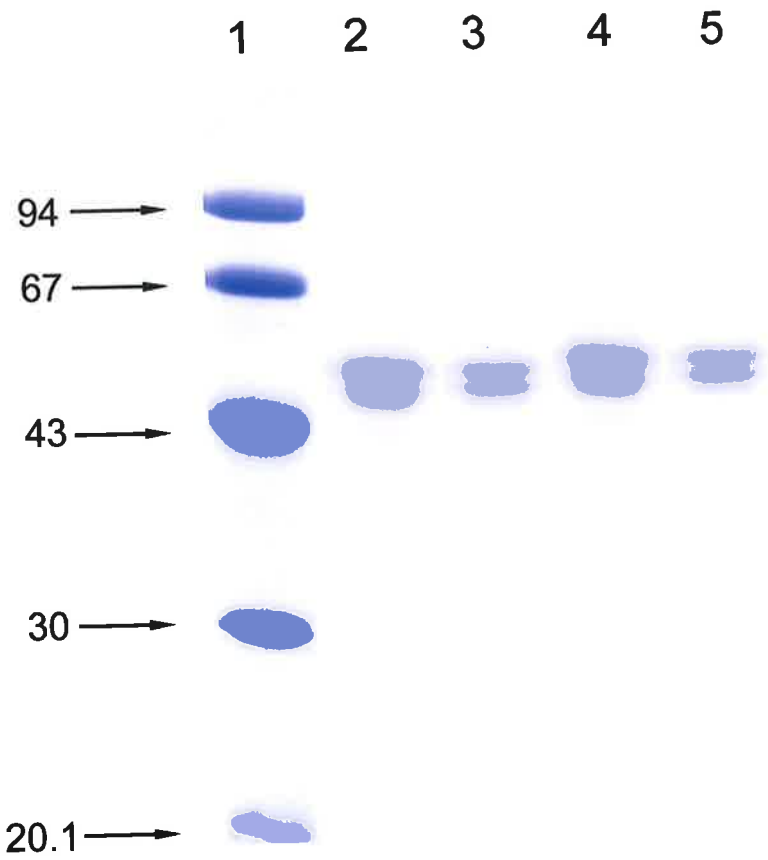
1
2
3
4
5
94
67
43
30
20.1

4.1.4.3 Kinetics

Kinetic analysis using the fluorogenic substrate 4MUF, showed that both CHO and MDCK-derived rcFUC have a broad pH range (3-9) with pH_{opt} at 7.0 and a slight shoulder at pH 4.5-5.0 (Figure 4.3). This was observed with all buffer systems tested, namely, citrate/phosphate, acetate and dimethylglutarate (DMG). To determine activity beyond pH 7.8, barbitone buffer was used and results indicated that at pH 8.2 CHO/rcFUC and MDCK/rcFUC had 65% and 75% of the maximum activity at pH 7, respectively, while at pH 9 this was reduced to 14% and 20%, respectively. When using glycine buffer to determine activity in the acidic range from pH 2.1 to 3.4, a stimulation of FUC activity compared to the other buffers used, was observed. At pH 3 this activity was identical to that seen at the pH_{opt} of 7 in DMG buffer (Figure 4.3).

Digestion of the natural substrates isolated from the brain of a fucosidosis dog clearly demonstrated a more acidic pH_{opt} of 4 (Figure 4.4). However, the turnover of natural substrate could not be quantified with a high degree of accuracy, thus limiting kinetic analysis.

When analysed using the 4MUF substrate at pH 7.0 the kinetic parameters (K_m and V_{max}), as well as the specific activity of both enzymes, were very similar (Table 4.3). Overnight storage of CHO/rcFUC at -15 °C resulted in a loss of 7% activity. However, when stored at 4 °C in PBS under sterile conditions purified rcFUC was stable for a year without significant loss of activity.

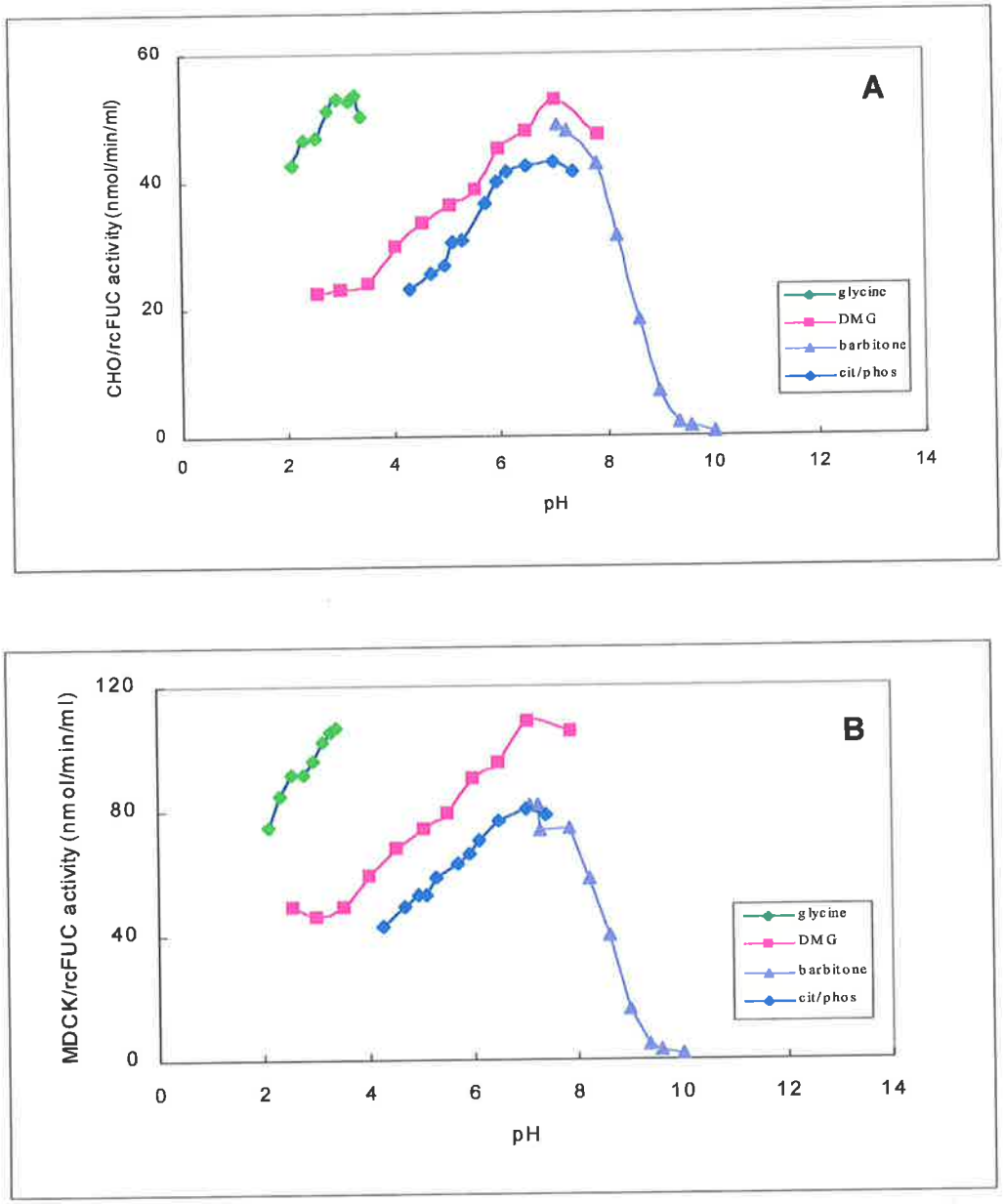

Figure 4.3: pH_{opt} of CHO/rcFUC and MDCK/rcFUC.

Purified CHO/rcFUC (A) and MDCK/rcFUC (B) were assayed in a number of buffers with various pH ranges as shown (see section 2.2.6.4c). The same enzyme batches of CHO/rcFUC and MDCK/rcFUC were used for determining pH_{opt} in DMG and glycine buffers, and a different batch of enzyme was used for citrate/phosphate and barbitone buffers.

Table 4.3: Kinetic parameters of CHO and MDCK/rcFUC in sodium dimethylglutarate and citrate/phosphate buffers.

	K_m (mM)	V_{max} (μmol/min/mg)	Specific Activity (μmol/min/mg)	pH_{opt}
CHO/rcFUC				
Dimethylglutarate buffer	0.14	19.1	16.1	7
Citrate/phosphate buffer	0.13	16.5	14.9	7
MDCK/rcFUC				
Dimethylglutarate buffer	0.10	16.8	15.1	7
Citrate/phosphate buffer	0.14	21.8	17.7	7

CHO/rcFUC and MDCK/rcFUC were affinity purified as described in section 2.2.23. Kinetic parameters were determined using the fluorogenic substrate, 4MUF (section 2.2.6.4c).

Figure 4.4: Digestion of fucosidosis dog cerebrum storage products with rcFUC at different pH values.

Lanes 1 and 8, the storage products at pH 2 and 7, respectively, in the absence of rcFUC; lanes 2-7, storage products digested with rcFUC at pH 2, 3, 4, 5, 6 and 7, respectively. Lane 9, the L-fucose standard. O, the origin; F, fucose; a-f, the storage product bands in ascending order of mobility.

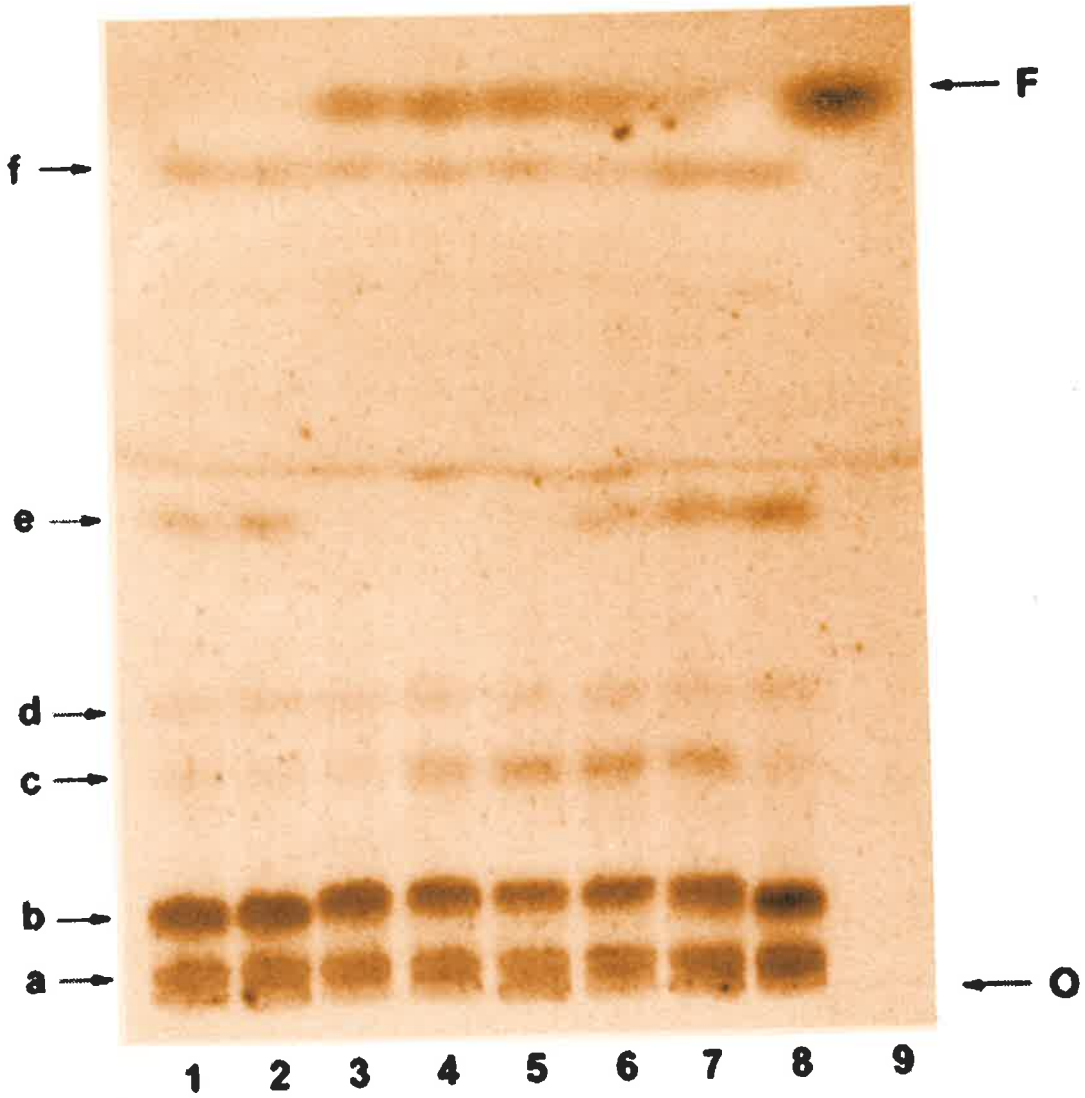
F
f
e
d
c
b
a
O
1
2
3
4
5
6
7
8
9

4.1.4.4 IEF

Chromatofocussing chromatography of CHO/rcFUC indicated a single peak of FUC activity corresponding to a pI of between 4.8 and 6 (Figure 4.5). This crude estimate was further refined by IEF to demonstrate at least seven major forms for both enzymes and show that MDCK/rcFUC was slightly more acidic (pI 4.45-6.2) than CHO/rcFUC (pI 5.5-6.5) (Figure 4.6). Treatment of CHO/rcFUC with neuraminidase resulted in no observable change in pI. However, after neuraminidase digestion the banding pattern of MDCK/rcFUC was altered such that it more closely resembled that of CHO/rcFUC (with the exception of the band at pH 4.5) (Figure 4.6).

4.1.4.5 Degree of glycosylation

To determine the degree of glycosylation of MDCK/rcFUC and CHO/rcFUC both were treated with PNGase F, an endoglycosidase that removes all N-linked oligosaccharide chains, as described in section 2.2.6.3. This treatment resulted in the doublet as observed on SDS-PAGE being converted to a single band of Mr 45 kDa (Figure 4.7).

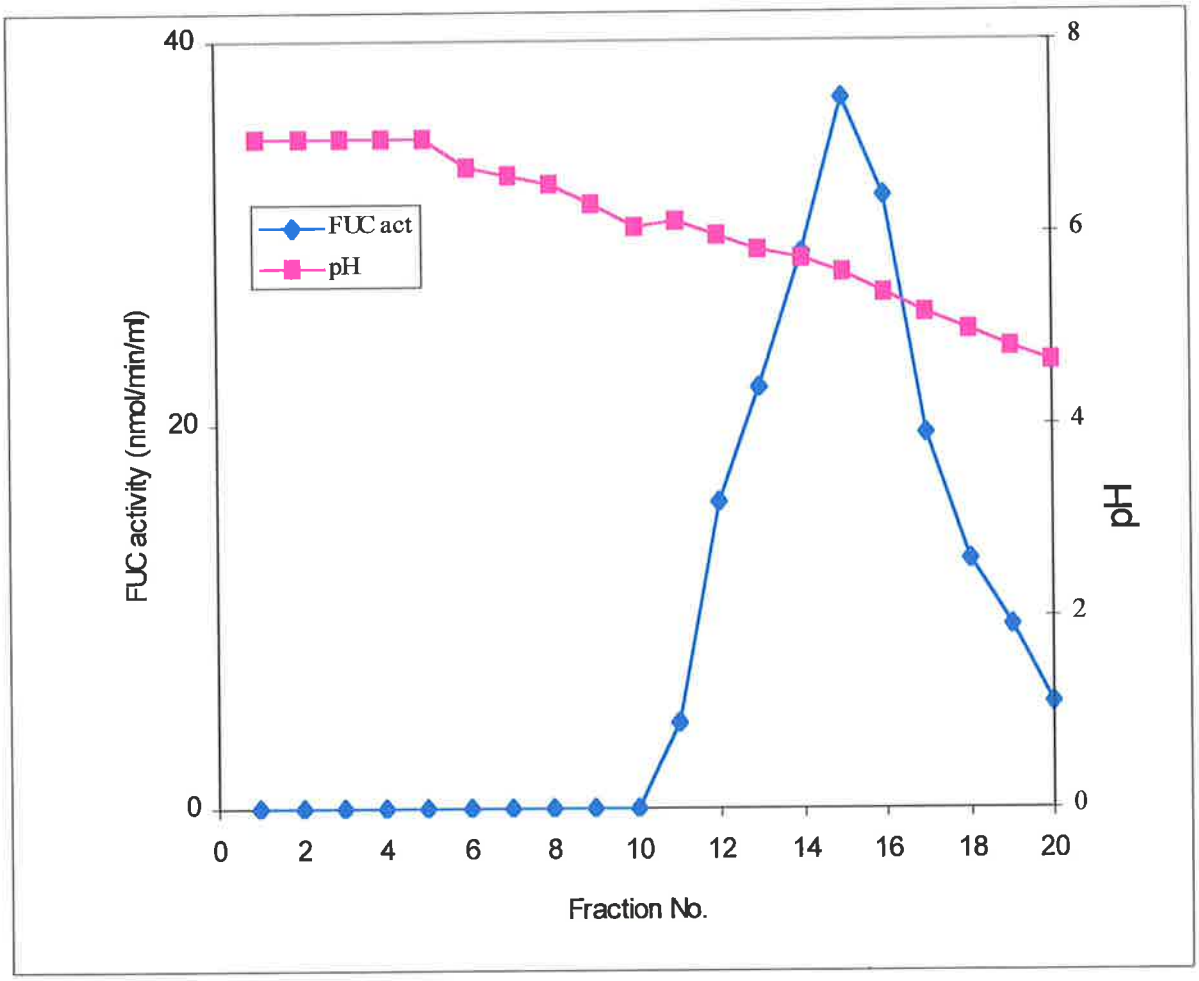

Figure 4.5: Chromatofocussing chromatography.

Purified CHO/rcFUC was applied to chromatofocussing medium PBE 94 and eluted with Polybuffer 74 (section 2.2.6.5a). Fractions were assayed for FUC activity and pH.

Figure 4.6: IEF of neuraminidase-treated CHO/rcFUC and MDCK/rcFUC.

Lane 1, IEF standards with their respective pI indicated by arrows. Lanes 2 and 4, CHO/rcFUC and MDCK/rcFUC, respectively, after neuraminidase treatment; lanes 3 and 5, untreated CHO/rcFUC and MDCK/rcFUC, respectively.

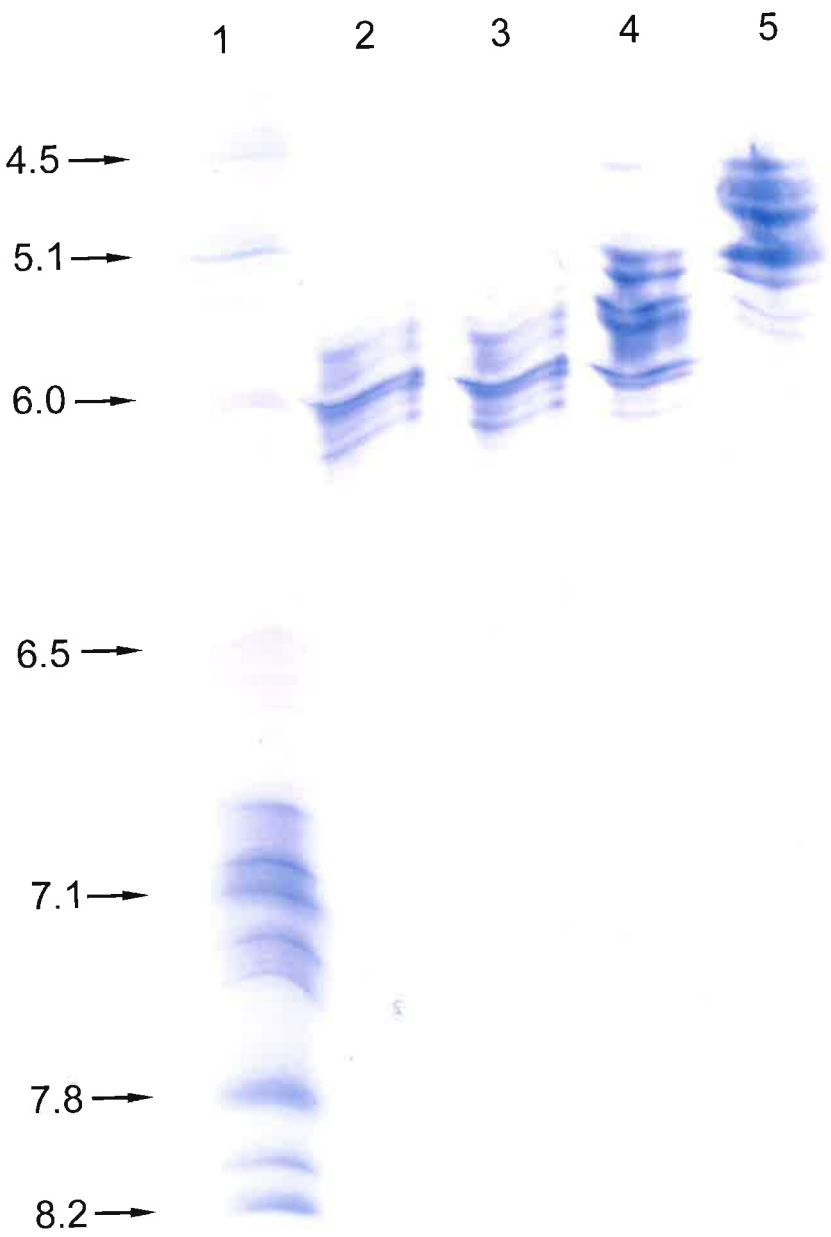
1
2
3
4
5
4.5
5.1
6.0
6.5
7.1
7.8
8.2

Figure 4.7: SDS-PAGE of PNGase F-treated MDCK/rcFUC and CHO/rcFUC.

Lane 1, Mr standards, which include phosphorylase b (94 kDa), BSA (67 kDa), ovalbumin (43 kDa), carbonic anhydrase (30 kDa) and soybean trypsin inhibitor (20.1 kDa), are indicated by arrows. Lanes 2 and 3, MDCK/rcFUC treated with PNGase F and untreated, respectively; lanes 4 and 5, CHO/rcFUC treated with PNGase F and untreated, respectively; lanes 6 and 7, CHO/rcFUC (expressed in the presence of NH_4Cl) treated with PNGase F and untreated. All samples were reduced with DTE (30 mM) prior to electrophoresis. The band at approximately 36 kDa in lanes 2, 4 and 6 is PNGase F.

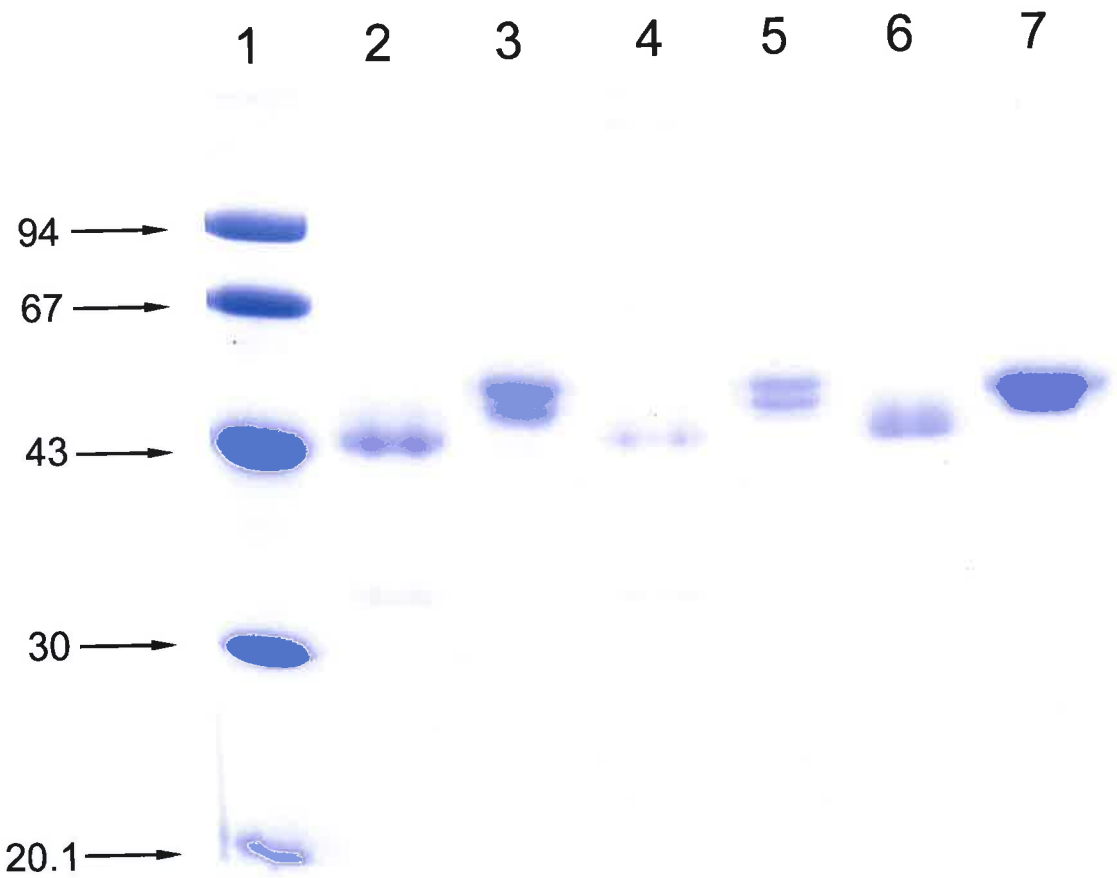
1
2
3
4
5
6
7
94
67
43
30
20.1

4.1.5 Correction of fucosidosis SF by CHO/rcFUC and MDCK/rcFUC

As canine fucosidosis SF were not available at the time of this study, human fucosidosis SF were used. Compared to normal control SF, the human fucosidosis SF in this study have no detectable levels of FUC and have a correspondingly increased (five times the normal) level of ^{3}H-L-fucose-labelled storage material (Table 4.4). Addition of exogenous enzyme resulted in a dose-dependent correction of both the enzymatic and the storage defects. The level of ^{3}H-L-fucose-labelled storage was almost normalised, and the enzyme levels completely normalised, with the higher dose of enzyme (15 nmol/min/ml in medium). The lower dose used (1.5 nmol/min/ml in medium) only partially restored intracellular enzyme levels (to approximately 14% and 7% of normal for CHO and MDCK/rcFUC, respectively) with storage reduced to approximately 60% and 80% of the levels in the uncorrected fucosidosis SF with CHO and MDCK/rcFUC, respectively. In the presence of M6P the lower dose of enzyme did not result in detectable correction of either enzymatic deficiency or storage phenotype. At the higher dose a small amount of enzyme (< 10% of normal enzyme levels) was endocytosed in the presence of M6P and this resulted in a small reduction in storage levels. Levels of β-hexosaminidase were relatively unchanged throughout. Differences in the absolute values of the experiments using CHO/rcFUC and MDCK/rcFUC were considered to be due to the experiments being performed on separate occasions.

4.1.6 Treatment of dog brain products with rcFUC

Water-soluble compounds were isolated from the brain of a fucosidosis dog as described in section 2.2.51. When analysed on TLC silica plates (section 2.2.52) they were seen to be heterogeneous in nature (Figure 4.4). They ranged in size from a fragment putatively identified as the asparagine-linked disaccharide described by Abraham *et al.* (1984) (band e) to larger oligosaccharides (bands o, a-d). The mobility of band f suggests that this product is a monosaccharide other than fucose, as fucose migrates to position F on TLC (Figure 4.4).

Table 4.4: Correction of fucosidosis SF with CHO/rcFUC and MDCK/rcFUC.

Cell line	FUC (nmol/min/mg)	^{3}H-Fucose (dpm/mg x 10^{-3})	β-Hex (nmol/min/mg)
SF4686 (normal)	1.44 ± 0.13	610 ± 38	213 ± 47
SF2184 (fucosidosis)	nd	3,169 ± 540	222 ± 8
SF2184 + CHO/rcFUC*	0.02 ± 0.05	1,925 ± 89	206 ± 17
SF2184 + CHO/rcFUC$^{\#}$	2.26 ± 0.63	736 ± 67	209 ± 36
SF2184 + CHO/rcFUC* + M6P	nd	2,662 ± 119	193 ± 13
SF2184 + CHO/rcFUC$^{\#}$ + M6P	0.13 ± 0.01	1,881 ± 165	201 ± 19
SF4634 (normal)	1.05 ± 0.05	262 ± 14	102 ± 8
SF2184	nd	902 ± 311	85 ± 10
SF2184 + MDCK/rcFUC*	0.07 ± 0.06	716 ± 192	85 ± 16
SF2184 + MDCK/rcFUC$^{\#}$	0.97 ± 0.44	324 ± 24	84 ± 13
SF2184 + MDCK/rcFUC* + M6P	nd	814 ± 173	82 ± 17
SF2184 + MDCK/rcFUC$^{\#}$ + M6P	0.08 ± 0.02	943 ± 222	84 ± 2

Normal (SF4686 and SF4634) and fucosidosis skin fibroblasts (SF2184) were metabolically labelled with ^{3}H-fucose for 48 h and then incubated with purified CHO/rcFUC or MDCK/rcFUC in the presence or absence of 5 mM M6P for 48 h. Cell lysates were assayed for ^{3}H radioactivity, total protein, β-hexosaminidase activity and FUC activity using the fluorogenic substrate, 4MUF. Results are expressed as the mean (n =3) ± 1 SD. nd, none detected. *1.5 nmol/min/ml rcFUC. $^{\#}$15 nmol/min/ml rcFUC.

To ascertain which storage products were associated with a terminal fucose moiety, extracts were digested with rcFUC at various pH values. The total disappearance of band e at pH 3-5 as well as a shift in band b between pH 3 and 7 indicated that these species had fucose moieties attached and hence represented storage material. These results also showed that enzyme activity towards these species is pH dependent. Where digestion had occurred there was a concomitant appearance of a fucose band at position F which was most intense between pH 3 and 5. As the pH increased from 5 to 7 there was a corresponding decrease in the intensity of this band. No digestion was observed at pH 2. Bands d and f were unchanged in the presence and absence of rcFUC suggesting that these bands represent non-fucosylated material. No fucose band was seen on TLC when enzyme alone was chromatographed (results not shown). Unfortunately, equivalent extracts of normal control dog brain were not available for analysis.

4.1 Discussion

rcFUC was successfully expressed in CHO cells at 10-13 mg/l of culture medium. Because of the relatively high level of FUC in (untransfected) CHO cells, a canine cell line (MDCK) was also used. However, the lower levels of FUC produced in these cells (2-3 mg/l of conditioned medium) made their use impractical. The reasons for the lower levels of expression of FUC in MDCK cells may be due to the polarised nature of these cells. Despite the possibility of small amounts of contaminating hamster FUC in rcFUC from CHO cells, CHO/rcFUC was used in most of the studies described in this thesis because of the superior production of enzyme in this system.

Both CHO/rcFUC and MDCK/rcFUC were readily purified using affinity chromatography. The differences in the degree of purification (550-fold versus 12-fold for MDCK/rcFUC and CHO/rcFUC, respectively) reflects the difference in expression levels in these cell lines as well as the degree of contamination by other proteins. Although it was originally reported that FUC was purified from human liver using fucosylamine linked to agarose *via* a one-atom spacer, it was found that binding to this matrix was extremely poor compared to a similar matrix with a 24-atom spacer. This suggests that the binding site in rcFUC is somewhat recessed within the molecule and that steric hindrance is preventing binding of the fucose moiety with the one-atom spacer.

When analysed, both CHO/rcFUC and MDCK/rcFUC were shown to have similar physical and kinetic properties. The native Mr of CHO/rcFUC and MDCK/rcFUC was estimated at 156 kDa by gel filtration chromatography. However, gel filtration often gives anomalous results for Mr of glycoproteins as it partitions proteins according to their Stoke's radii (Alhadeff *et al.*, 1975; Alhadeff, 1978). Generally more accurate native Mr estimations for glycoproteins can be obtained by sedimentation equilibrium. However, this approach was not used as the equipment for sedimentation equilibrium was not available. An attempt to verify Mr of rcFUC by Micromass Q-TOF mass spectrometry (Macquarie University Centre for Analytical Biotechnology, Sydney, NSW, Australia) was unsuccessful. The mass/charge (m/z) spectrum showed a series of broad peaks at increasing distances as m/z values increased (results not shown). The broadening of the peaks is most probably due to the presence of post-translational modification such as glycosylation, and because of this heterogeneity a definitive native Mr could not be determined.

SDS-PAGE analysis of rcFUC showed two protein bands of 55 and 52 kDa. These are presumed to represent the precursor and mature forms of rcFUC, respectively. This hypothesis is supported by analysis of purified rcFUC expressed in the presence of NH_4Cl, which increases secretion of precursor forms of lysosomal enzymes, as the enzyme secreted in the presence of NH_4Cl is enriched in the 55 kDa species (Figure 4.7, lane 7). Native Mr data in conjunction with subunit data suggest that rcFUC is a homotrimer, or possibly a homotetramer, if the native Mr is an underestimate (see below). As both the precursor and mature forms of rcFUC display identical electrophoretic mobility under reducing and non-reducing conditions, the subunits of the native forms of the precursor and mature species are not S-S bonded. Attempts to isolate subunits of rcFUC by gel filtration chromatography in buffers of different pH were unsuccessful. However, subunits of FUC have previously been shown to be active by incubating non-denaturing gradient polyacrylamide gels of cFUC overlaid with filter paper saturated with 4MUF to give fluorescent bands when viewed under UV light (Barker *et al.*, 1988).

Prior to the production of rcFUC, the enzyme had been purified from various tissues of several mammalian species including human, canine, rat and mouse liver, and from human placenta, brain and serum (reviewed in Alhadeff, 1998). Native Mr estimates by sedimentation equilibrium, density gradient centrifugation or gel filtration chromatography have indicated a

range of Mr from 175-270 kDa. FUC isolated from the mammalian tissue sources mentioned above also generally showed two closely spaced protein species of Mr ranging between 45 and 63 kDa by SDS-PAGE. Together with the native Mr data this would suggest that the enzyme normally exists as a tetramer. FUC from the liver of the marine gastropod, Charonia lampas (Butters *et al.*, 1991) was also found to be a tetrameric glycoprotein. In contrast FUC isolated from non-mammalian sources such as streptomyces sp 142 (Sano *et al.*, 1992), and the slime mould Dictyosterlium discoideum (Schopohl *et al.*, 1992), were found to exist as monomers with native Mr of 40 kDa and 62 kDa, respectively.

The difference in Mr between the precursor (55 kDa) and mature (52 kDa) forms of rcFUC appears to be in the degree of glycosylation. rcFUC has four potential N-linked glycosylation sites per subunit at asparagines 242, 252, 269 and 383. Asparagine 252 is less likely to be glycosylated because of a proline residue C-terminal to the N-X-S/T glycosylation consensus sequence (Gavel and von Heijne, 1990; Mellquist *et al.*, 1998). When digested with PNGase F, the difference between the two forms is eliminated and a single protein species of Mr 45 kDa is observed. The synthesis and processing of FUC has been studied in detail only in human skin fibroblasts (Johnson *et al.*, 1991). According to published results, the enzyme is synthesised as a precursor of 53 kDa with two N-glycan chains, one of which is complex, the other being of the high-mannose type. Processing to the mature form did not involve carbohydrate processing but was the result of proteolytic cleavage of a 3 kDa peptide fragment by thiol proteases which are present in the lysosome. The authors also demonstrated that proteolytic processing was not a requisite for enzymatic activation as in the presence of thiol protease inhibitors the unprocessed precursor enzyme was still active. However, the position of the 3 kDa fragment was not identified. The synthesis and intracellular processing of rcFUC has not been studied and the loss of a substantially sized peptide fragment has not been observed. As both the precursor and mature forms of rcFUC are reduced to the same, single Mr species after deglycosylation, this would argue against such a processing event in CHO and MDCK cells.

IEF has been used to identify isoforms in most mammalian FUC (Alhadeff, 1998). In human liver estimates of between 4 and 8 different isoforms have been published, while in human placenta the number varies from 4 to 7. However, isoform analysis of cFUC from any tissue has not been reported. In this study CHO/rcFUC and MDCK/rcFUC were found to have similar numbers of isoforms (seven) although their charges were different. Treatment with

neuraminidase indicated that MDCK/rcFUC had sialic acids present on its oligosaccharide chains whereas CHO/rcFUC appeared to have none. The more acidic nature of MDCK/rcFUC isomers supports this observation. Although the α-2,6 sialyltransferase is reported to be non-functional in CHO cells (Minch *et al.*, 1995) rf4S produced in CHO cells was sensitive to neuraminidase (section 3.1.3.4), as were iduronate-2-sulphatase and α-L-iduronidase (T Rozaklis, Department of Chemical Pathology, WCH, personal communication) suggesting that this is not so. In contrast rh4S (section 3.1.3.4), sulphamidase and α-N-acetylglucosaminidase (T Rozaklis, personal communication), from CHO cells are not sialylated. In the case of rf4S and rh4S, which share approximately 90% amino acid sequence homology and hence presumably very similar conformations, this suggests that the factors that control glycosylation are subtle and represent complex interactions between the protein species and the cell's biosynthetic machinery. However, in all of these cases it should be noted that enzyme was prepared from a single clonal cell line. The differences in glycosylation may therefore reflect variation in the cell's glycosylation machinery that is exposed by the cloning process.

Mammalian FUC share similar kinetic properties (Alhadeff, 1998). Most exhibit a broad pH spectrum of activity towards the artificial substrate, 4MUF with a pH_{opt} of 5. Canine liver FUC has a pH_{opt} of 7 with a shoulder of activity at pH 5.5. This was also observed with rcFUC although the shoulder of activity was at pH 4.5 to 5.0. Activity was stimulated in glycine buffer at low acidic pH (2.1 to 3) compared to other buffer systems used in this pH range. This may reflect the chemical protonation of the substrate by the glycine buffer, which would eliminate the need for enzyme catalysed protonation.

K_m and V_{max} values for human and canine liver FUC and rcFUC against 4MUF are relatively similar (Barker *et al.*, 1988). The catalytic mechanism of FUC has not been elucidated. Preliminary data from studies with human liver FUC (Alhadeff *et al.*, 1975) showed that the total inhibition of enzyme activity observed in the presence of Hg^{+3} and Ag^{+} was prevented by the addition of DTE (0.2-1.2 mM), implying that a cysteine residue is involved in catalysis. This has been supported by work on monkey brain (Alam and Balasubramanian, 1979) and porcine thyroid (Grove and Serif, 1981) FUC, which suggests carboxyl and sulphydryl groups are necessary for enzymatic activity. More recently, as gene and amino acid sequence data of FUC from various species have become available, a high level of identity has been observed. Canine FUC, for example, shares 82.6% and 76% nucleotide identity, and 84% and 77% amino

acid sequence homology, with human and rat FUC, respectively. In addition, information obtained from comparison of FUC from different species has identified a putative active site (Prosite Database Release 12.2, Entry no. P500385). A cysteine residue at position 297 is the only cysteine found to be conserved between mammalian FUC and FUC of the slime mould Dictyostelium discoideum (Schopohl *et al.*, 1992). This cysteine would therefore be a good candidate for a critical active site residue. Crystallisation (in collaboration with Prof. M. Guss, University of Sydney, NSW) of rcFUC to elucidate 3-D structure has been attempted but to date has been unsuccessful.

FUC hydrolyse a wide array of naturally occurring fucoglycoconjugates including glycopeptides, glycoproteins, glycolipids and blood group substances. FUC do not display the same exquisite specificity towards substrates as observed with sulphatases (see section 1.7.3) in that they can hydrolyse α-(1→2), α-(1→3), α-(1→4) and α-(1→6) fucose-saccharide bonds. In general they show greater reactivity towards α-(1→2) fucose-galactose bonds than to fucose linked α-(1→3), α-(1→4) or α-(1→6) to N-acetylglucosamine (Alhadeff, 1998).

Exogenous CHO/rcFUC and MDCK/rcFUC effectively overcame the enzymatic deficiency in severely affected fucosidosis cells and in addition reversed the level of storage in the lysosomes of these cells in a dose-dependent manner. This indicated that not only was rcFUC taken up by these cells, but that it was properly targeted to lysosomes. Both enzymatic and storage correction was greatly reduced or eliminated in the presence of M6P, confirming that endocytosis of the enzyme was *via* the M6PR-mediated pathway, as is the case for most other lysosomal enzymes (see discussion section 3.1). Therefore rcFUC appears to be similar to endogenous FUC, demonstrating M6PR uptake into cells and targeting to lysosomes where it acts on natural substrates. rcFUC also shows normal activity towards natural substrates from dog brain. In conclusion, rcFUC appears to behave in a similar manner to the endogenous enzyme, is of the required high uptake form and therefore would be suitable for ERT.

4.2 Chemical modification of rcFUC

4.2.1 Preparation of insulin fragment F007

It was previously reported (Fukuta *et al.*, 1994) that a tryptic fragment of insulin (F007) had the potential as a vector for transport of covalently linked proteins into brain. The advantage of this fragment over native insulin is the elimination of a potential hypoglycaemic effect which may be induced with native insulin. In order to produce this fragment trypsin digestion of bovine pancreatic insulin was carried out as described in section 2.2.33. This was followed by hydrophobic chromatography, which resulted in the elution of three main peptide-containing fractions (A, B, C) at acetonitrile concentrations of 27%, 38% and 40%, respectively (Figure 4.8). Fractions B and C were present in almost equivalent amounts while Fraction A was half that of Fractions B and C. Analysis of an aliquot of these fractions on Tricine-SDS polyacrylamide gels (Figure 4.9) under reducing and non-reducing conditions showed that no visible protein band was associated with Fraction A. However, both Fractions B and C were associated with peptides similar in size although the Fraction C peptide was marginally larger than the Fraction B peptide, both under reducing and non-reducing conditions. As separation of the standard molecular weight protein markers was not ideal in the mini-gel system used, it was not possible to estimate the Mr of the peptides in Fractions B and C.

To confirm the identity of the peptides in all three fractions, tandem mass spectrometry together with amino acid sequence data of tryptic peptides of bovine insulin from the Swiss Prot databank were used. Analysis of tandem mass spectrometry data indicated that Fraction A represented the tryptic peptide GFFYTPK (Mr 859 Da) (Figure 4.10). Fraction C had a Mr of 5,736 Da which corresponds to undigested bovine insulin while the Fraction B peptide, which was the peptide (F007) required for these studies, had a Mr of 4,899 which was equivalent to Fraction C minus Fraction A. Although this experiment showed that the F007 fragment could be successfully made, its preparation, especially in large quantities, proved to be relatively time-consuming. Therefore conjugates between rcFUC and native bovine pancreatic insulin were used for preliminary experiments.

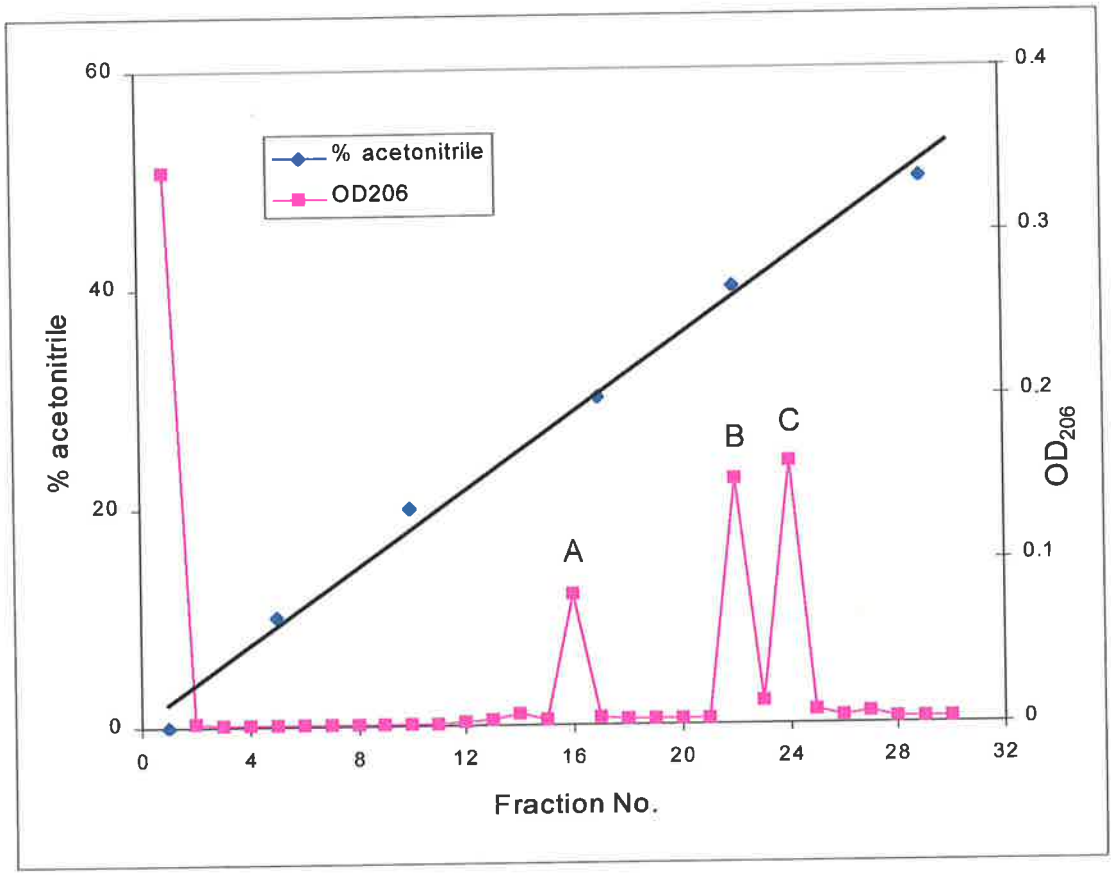

Figure 4.8: Reversed-phase HPLC of trypsin-digested bovine insulin.

A tryptic digest of bovine insulin was applied to reversed-phase HPLC (Dynamax 60AC8) column and tryptic peptides were eluted with an increasing concentration of acetonitrile in 0.1% (v/v) TFA. Fractions were monitored for protein at OD_{206}. Three main fractions (A, B and C) were eluted.

Figure 4.9: Tricine-SDS-PAGE of tryptic insulin peptides.

Lane 1, Mr standards with their respective molecular mass (in kDa) are indicated by arrows and include globin I + II (14.4 kDa), globin I + III (10.7 kDa), globin I (8.2 kDa), globin II (6.2 kDa) and globin III (2.5 kDa). Lanes 2, 3 and 4 are fractions A, B and C, eluted from reversed-phase HPLC (Figure 4.8), respectively, and electrophoresed under reducing conditions (30 mM DTE); lanes 5, 6 and 7 are Fractions A, B and C, respectively, without reduction.

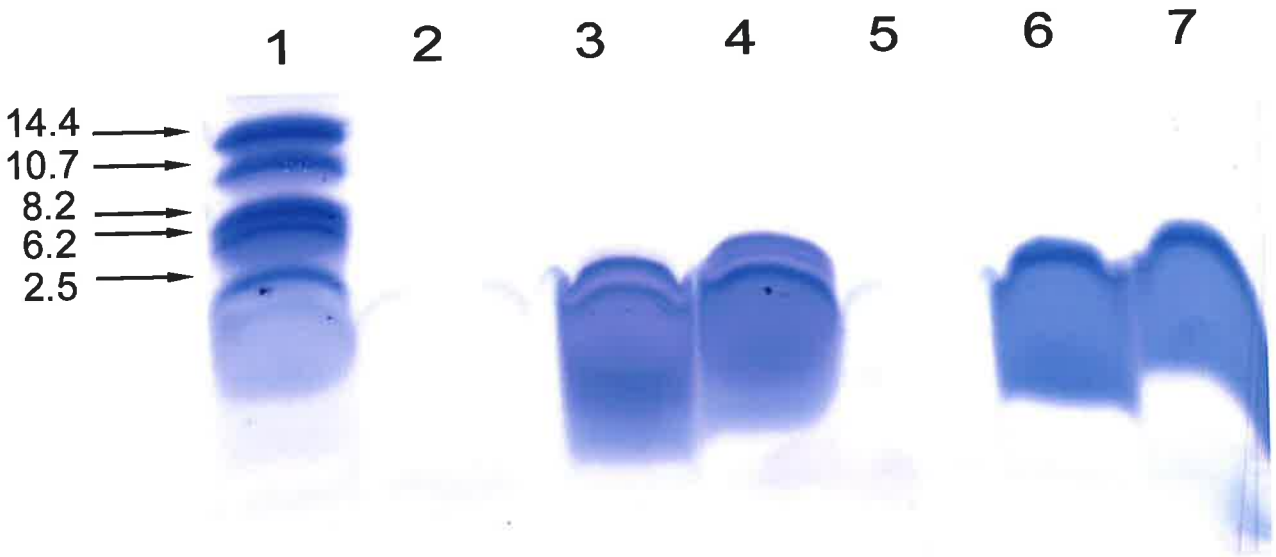
1
2
3
4
5
6
7
14.4
10.7
8.2
6.2
2.5

A chain: GIVEQCCASVCSLYQLENYCN

B chain: FVNQHLCGSHLVEALYLVCGERGFFYTPKA

Fraction A: GFFYTPK

Fraction B: GIVEQCCASVCSLYQLENYCN

FVNQHLCGSHLVEALYLVCGER

Figure 4.10: Amino acid sequence of bovine insulin and its tryptic peptides.
The amino acid sequence of the A and B chains of bovine insulin are shown. The chains are held together by S-S bonds at C_7 of the A chain and C_7 of the B chain, and C_{20} of the A chain and C_{19} of the B chain. An intrachain S-S bond is also present between C_6 and C_{11} of the A chain. Also shown are the amino acid sequences of Fraction A and Fraction B peptides. The four amino acids with free primary amino groups in intact insulin are underlined. These are the only amino acids which can be derivatized with heterobifunctional crosslinkers, such as SPDP.

4.2.2 Pyridyldithiopropionate modification of insulin and rcFUC

As a first step towards making conjugates of insulin and rcFUC, the derivatization of these proteins with the heterobifunctional crosslinker, SPDP, was investigated. Bovine pancreatic insulin was found to be poorly soluble at neutral pH in phosphate buffer. However, a 1 mg/ml solution could be prepared by warming at 37 °C for 5-10 min. Insulin was then reacted with SPDP as described in section 2.2.34. Initial attempts to remove free SPDP from the reaction mixture using a PD-10 column were unsuccessful, as there was too much overlap between the elution profiles of insulin and free SPDP. In addition, chromatography on PD-10 resulted in an unacceptable degree of dilution of the applied sample. In order to overcome these difficulties, subsequent insulin modification reaction mixtures were dialysed after quenching the reaction.

Although dialysis casing with a nominal 10,000 Da cut-off was used there was only a 10% loss of insulin protein due to dialysis (results not shown).

When an 8 to 10-fold molar excess of crosslinker was used, the degree of modification of insulin as calculated from the protein concentration and the extinction coefficient of pyridine-2-thione (released on reduction of pyridyldithiopropionate with DTE) was generally between 1.2 and 1.9 moles of pyridyldithiopropionate per mole of insulin. An 80 to 100-fold molar excess of crosslinker resulted in modification to 3.2 moles of pyridyldithiopropionate per mole of insulin. The less derivatized preparations of insulin were used for conjugating to rcFUC.

CHO/rcFUC was initially derivatized using conditions similar to those described for horseradish peroxidase (HRP) (Fukuta *et al.*, 1994) i.e., a 53-fold molar excess of SPDP to rcFUC for 30 min. Under these conditions, rcFUC was derivatized to >10 moles of pyridyldithiopropionate per mole of rcFUC with a substantial loss of FUC activity (up to 50%) which was exacerbated by the subsequent reduction reaction with DTE (a further 25% loss) (Table 4.5). Conjugation of derivatized rcFUC with derivatized insulin resulted in the formation of high Mr enzymatically inactive aggregates (Figure 4.11, A). Protection of the active site of rcFUC with L-fucose, a dialysable competitive inhibitor, and derivatization with lower concentrations of SPDP, that resulted in rcFUC with 1-3 moles of pyridyldithiopropionate per mole of rcFUC, gave better yields of activity (70%) although losses upon reduction with DTE (25%) remained the same (Table 4.5). Derivatized rcFUC was chosen in preference to derivatized insulin for reduction with DTE to produce a free sulphydryl group, as the subunits of rcFUC are not disulphide-linked (section 4.1.4.1). However, since rcFUC was shown to be inactivated (25%) with DTE, and because of further losses of activity due to derivatization and dialysis (which was necessarily extensive to remove all traces of DTE), it was decided instead to modify rcFUC with another heterobifunctional crosslinker, SATA. Therefore, no further conjugation reactions with pyridyldithiopropionate-modified rcFUC and pyridyldithiopropionate-derivatized insulin were attempted.

Table 4.5: Pyridyldithiopropionate modification of rcFUC.

	FUC activity (nmol/min/ml)	Loss of activity (%)
rcFUC	15,968	
rcFUC + SPDP*	8,143	49
rcFUC + SPDP* + DTE	6,108	62
rcFUC + SPDP* + DTE + dialysis	5,497	66
rcFUC-Insulin conjugation‡	107	99
rcFUC	16,472	
rcFUC + SPDP#	11,530	30
rcFUC + SPDP# + DTE	8,647	52
rcFUC + SPDP# + DTE + dialysis	7,350	55

* rcFUC derivatized with a 53-fold molar excess of SPDP to rcFUC. ‡ Conjugation of derivatized rcFUC with a 10-fold molar excess of SPDP-derivatized insulin. # rcFUC derivatized with a 10-fold molar excess of SPDP to rcFUC. Reduction with 25 mM DTE (to produce a free thiol group) and dialysis conditions are described in sections 2.2.34-36.

Figure 4.11: SDS-PAGE of FUC-insulin conjugates.

SDS-PAGE was carried out under non-reducing conditions. (A) Lane 1, Mr standards, which include phosphorylase b (94 kDa), BSA (67 kDa), ovalbumin (43 kDa) and carbonic anhydrase (30 kDa), are indicated by arrows; lane 2, CHO/rcFUC; lane 3, FUC-insulin aggregates formed when derivatization of FUC is >1-2 moles SPDP/mole FUC (section 4.2.2). (B) Lane 1, Mr standards as in (A); lane 2, CHO/rcFUC; lane 3, SATA-derivatized CHO/rcFUC after conjugation with SPDP-derivatized insulin (section 2.2.39).

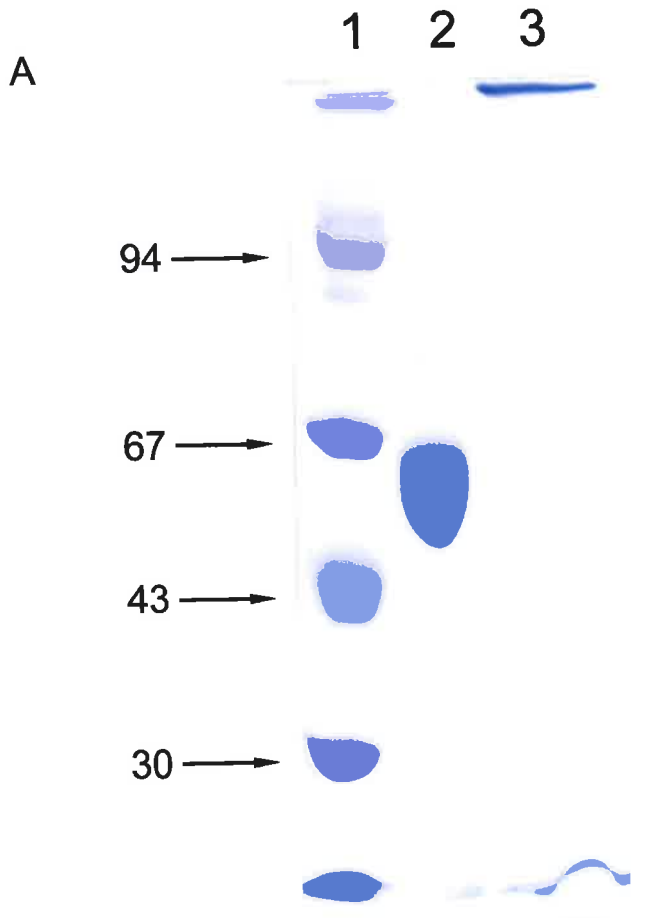
A
1
2
3
94
67
43
30

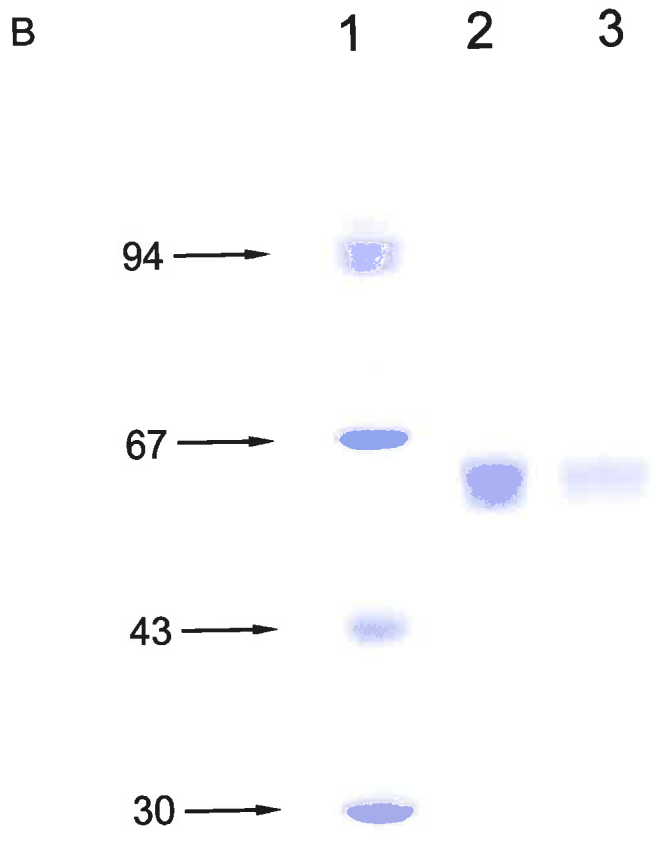
B
1
2
3
94
67
43
30

4.2.3 Thiolation of rcFUC with SATA

The conditions used for thiolation of rcFUC were a 5-fold molar excess of SATA compared to rcFUC for 30 min at room temperature (see section 2.2.37). Under these conditions 2-3 moles of SATA were added per mole of rcFUC. In addition, there was between 75-80% retention of FUC activity, 10% of which was due to loss upon post-modification dialysis (Table 4.6).

Table 4.6: Thiolation of rcFUC with SATA.

	FUC activity (nmol/min/ml)	Loss of activity (%)
rcFUC	101,423	
rcFUC-SATA	84,181	17
rcFUC-SATA after dialysis	75,763	25
rcFUC-insulin conjugation	75,839	25

rcFUC was derivatized with SATA and after dialysis was conjugated to SPDP-derivatized insulin (section 2.2.39).

4.2.4 Conjugation of SATA-derivatized rcFUC with SPDP-derivatized insulin

SATA-derivatized rcFUC was reacted with a 10-fold molar excess of SPDP-derivatized insulin in the presence of 50 mM hydroxylamine. No loss of activity was observed after an overnight incubation at room temperature (Table 4.6).

To visualise conjugates an aliquot of the reaction mixture was electrophoresed under non-reducing conditions on a SDS 10% (w/v) polyacrylamide gel. An increase in the Mr of rcFUC

by 6,000 Da, or multiples thereof, was predicted. Care was taken to ensure identical loading buffer conditions for native rcFUC and the conjugation reaction mixture. However, no difference in Mr was observed between rcFUC and the putative insulin-FUC conjugates. (Figure 4.11 B). Samples of putative conjugates of rcFUC and insulin were also reduced and electrophoresed but no insulin bands were detected (results not shown). To further ascertain the presence of insulin in conjugates, western blot analysis using a monoclonal antibody to human insulin, which crossreacts with bovine insulin, was used. However, this method failed to provide evidence for the presence of conjugates of rcFUC with insulin (results not shown). Therefore, for the reasons discussed in section 4.2.1 (Discussion), attempts to conjugate rcFUC to insulin were abandoned and attention was instead focussed on preparing conjugates between rcFUC and OX26, a mouse monoclonal antibody to the rat Tf receptor.

4.2.5 SPDP modification of OX26 through amine and carbohydrate groups

In order to make conjugates of OX26 with rcFUC derivatization of OX26 with a heterobifunctional crosslinker was necessary. Derivatization of antibodies can be achieved either *via* carbohydrate groups with PDPH or *via* primary amine groups with SPDP (Figure 4.12, A and B)

Figure 4.12: Chemical conjugation of rcFUC with OX26.

A diagrammatic representation of the reactions between rcFUC and OX26 to form conjugates. rcFUC was modified with SATA followed by deacetylation with hydroxylamine (NH_2OH) to expose a free thiol. Sulphydryl-reactive pyridyl-disulphide residues were introduced into OX26 either by mild oxidation with sodium periodate ($NaIO_4$) followed by a condensation reaction with PDPH (A) or by modification of its primary amino groups with the heterobifunctional crosslinker SPDP (B). Reaction of the thiol-containing rcFUC with either the amine- or carbohydrate-linked OX26 derivative results in the formation of covalent, disulphide-linked conjugates. (Adapted from Walus *et al.*, 1996)

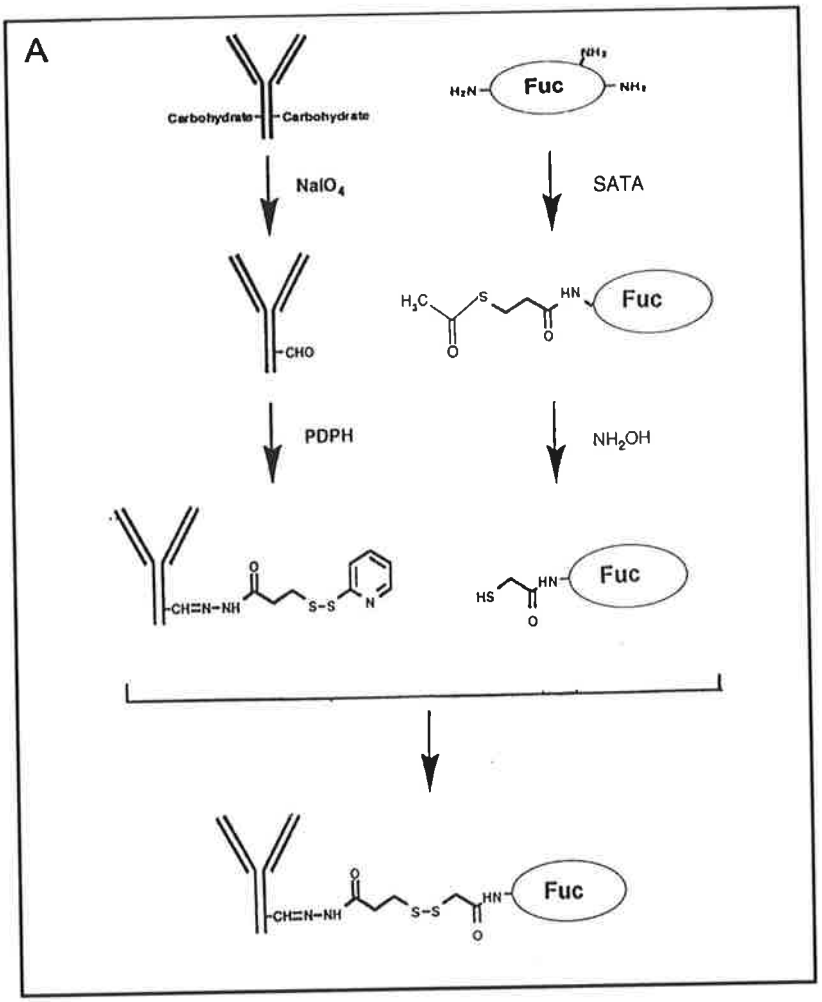
A
Carbohydrate
Carbohydrate
$NaIO_4$
CHO
PDPH
CH=N-NH
S-S
N
Fuc
NH_2
SATA
H_3C
S
HN
O
NH_2OH
HS

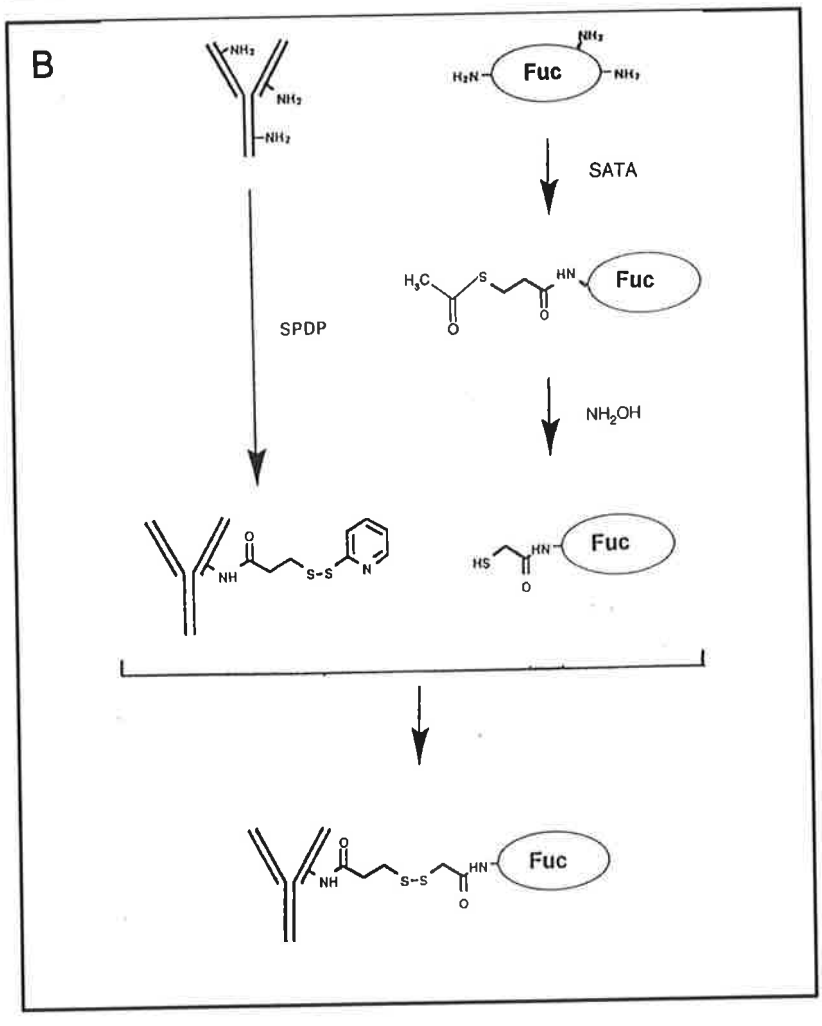
B
NH_2
SPDP
NH
S-S
N
Fuc
SATA
H_3C
S
HN
O
NH_2OH
HS

Figure 4.13: SDS-PAGE of OX26.

OX26 was purified from hybridoma medium by Protein G chromatography. Lane 1, Mr standards, which include phosphorylase b (94 kDa), BSA (67 kDa), ovalbumin (43 kDa), carbonic anhydrase (30 kDa) and α-lactalbumin (20.1 kDa), are indicated by arrows; lane 2, OX26 electrophoresed under reducing conditions.

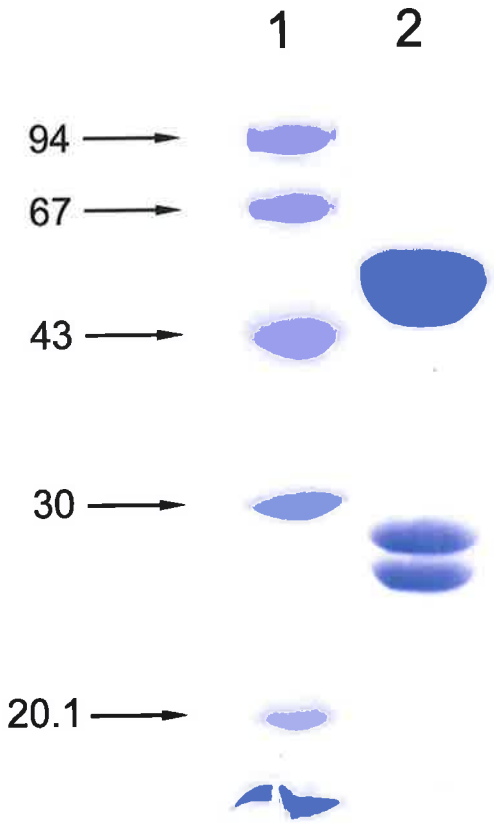
1
2
94
67
43
30
20.1

OX26 was first purified from hybridoma medium by chromatography over Protein G agarose (section 2.2.28). SDS-PAGE analysis showed a single heavy chain and double light chains suggesting the antibody was essentially pure (Figure 4.13) (Yoshikawa and Pardridge, 1992). Purified OX26 was concentrated in PBS to 5-7 mg/ml and stored at 4 °C.

After testing various concentrations of SPDP and PDPH at different incubation times, it was found that in order to introduce approximately one mole of pyridyldithiopropionate per mole of OX26, either a 15-fold molar excess of PDPH and a reaction time of 60 min, or a 5 to 20-fold molar excess of SPDP and a reaction time of between 15 and 30 min, were required. Both reactions were incubated at room temperature. A preparation of OX26 more highly derivatized with PDPH (9.4 moles of pyridyldithiopropionate per mole of OX26) was achieved using a 150-fold molar excess of PDPH and incubation for 60 min at room temperature.

4.2.6 Conjugation of SPDP-derivatized OX26 and SATA-derivatized rcFUC

When OX26 modified as above, either with PDPH through carbohydrate groups or with SPDP through amine groups, was conjugated to rcFUC derivatized with SATA (section 2.2.42) there was in general a loss of <30% FUC activity (Table 4.7). It was clear that under these conditions the reaction did not go to completion as unreacted OX26 was still visible upon analysis of conjugate material on a SDS-polyacrylamide gel (Figure 4.14, lane 1). To remove unconjugated OX26 from OX26-FUC conjugates, the reaction mixture was dialysed and applied to fucosylamine-agarose. Free rcFUC and OX26-FUC conjugates bound to the column and were eluted with L-fucose as described in section 2.2.23. After dialysis and concentration of the eluate approximately 50% of the starting FUC activity was recovered. When analysed on a SDS 5% (w/v) polyacrylamide gel under non-reducing conditions, a ladder of conjugates of Mr 200 kDa, 250 kDa and 300 kDa was observed (Figure 4.14, lane 2). These Mr species corresponded to one, two or three subunits of rcFUC (Mr ~50 kDa), respectively, linked to OX26. That the unconjugated OX26 was successfully removed by fucosylamine-agarose chromatography is demonstrated by the corresponding disappearance of the protein band at 150 kDa. Unconjugated rcFUC was also present in the conjugation preparation but the amount was difficult to estimate as rcFUC dissociates into its subunits under non-reducing conditions on SDS-PAGE. Therefore the band observed at ~55 kDa would comprise subunits of unconjugated rcFUC, as well as those subunits of conjugated rcFUC which were not covalently linked to OX26 (i.e., subunits being non-covalently linked to subunits that were themselves

covalently linked to OX26) and were dissociated under the denaturing conditions of SDS-PAGE.

In contrast to SPDP-modified OX26, PDPH-modified OX26 did not form conjugates with rcFUC derivatized with SATA (Figure 4.14, lanes 3 and 4). The same reaction with the PDPH-(over) derivatized OX26 also failed to produce conjugates or aggregates (results not shown).

Table 4.7: OX26-FUC conjugation.

Step	FUC activity (nmol/min/ml)	% Recovery
Original FUC activity	121,357	100
FUC derivatized with SATA	112,860	92.9
Conjugation of rcFUC with OX26-SPDP	101,697	83.8
Loaded onto fucosylamine-agarose column	101,045	83.3
Eluate from fucosylamine-agarose column	67,708	55.8
Conjugation of rcFUC with OX26-PDPH	121,548	
Eluate from fucosylamine-agarose column	78,840	65

rcFUC was derivatized with a 5-fold molar excess of SATA compared to rcFUC under the conditions described in section 2.2.37. It was then conjugated to SPDP-derivatized OX26 in an equimolar ratio and the resulting conjugates were purified on fucosylamine-agarose (section 2.2.42). OX26 derivatized with PDPH (15-fold molar excess) was conjugated to SATA-derivatized rcFUC and the products of the conjugation reaction were chromatographed on fucosylamine-agarose as above.

Figure 4.14: SDS-PAGE of OX26-FUC conjugates.

Conjugates of OX26-FUC were prepared and purified as described in section 2.2.42. Lane 1, the reaction mixture of conjugates prepared from SPDP-derivatized OX26 and SATA-derivatized rcFUC (Figure 4.12, B) showing conjugates of Mr 200, 250 and 300 kDa, unconjugated OX26 (150 kDa) and subunits of rcFUC (55 kDa) (indicated by arrows). Lane 2, purified conjugates after affinity chromatography on fucosylamine-agarose. Lanes 3 and 4, the reaction mixture of conjugates prepared from SATA-derivatized rcFUC and OX26 derivatized *via* carbohydrate groups with PDPH (Figure 4.12, A) before and after affinity chromatography on fucosylamine-agarose, respectively. Lanes 5 and 6, underivatized OX26 and rcFUC, respectively. SDS-PAGE was carried out on a 5% (w/v) acrylamide gel under non-reducing conditions.

4.2.7 FACS analysis of OX26-FUC conjugates

To determine the biofunctionality of OX26-FUC conjugates, binding of conjugates to rat hepatoma (H4IIE) cells was analysed by FACS (section 2.2.43). H4IIE cells were first tested with OX26 and rcFUC, with and without 5 mM M6P, to establish the presence of cell surface Tf and IGFII/M6P receptors. OX26 binding was detected with FITC-conjugated SAM antibody. To detect the binding of rcFUC, a rabbit anti-rcFUC polyclonal antibody (section 4.3.1) followed by FITC-conjugated SAR antibody was used. Fluorescence intensity measured in a non-cell-sorting flow cytometer indicated the presence of both receptors. Tf receptors appeared to be more abundant than IGFII/M6P receptors (Figure 4.15 A and B, and Table 4.8 median linear fluorescence of 184 and 16.55, respectively). The presence of M6P appeared to increase the number of surface Tf receptors detected by approximately 42% (median linear fluorescence with M6P, 316.23 and without M6P, 184). The reason for this is not clear. As expected, M6P inhibited binding of rcFUC to the M6P receptor (median linear fluorescence with M6P, 6.26 and without, 16.55, Figure 4.15, B).

Binding of OX26-FUC conjugates was then measured. Binding was analysed *via* both the OX26 and FUC moiety of the conjugates. Little difference was seen in the binding of OX26-FUC detected *via* OX26 with SAM-FITC in the presence or absence of M6P (median linear fluorescence of 21.29 and 24.55, respectively; Table 4.8 and Figure 4.15, C). Compared with OX26 alone, the mean linear fluorescence was markedly reduced (21.29 vs 316.23). However, when binding of OX26-FUC conjugates was analysed *via* the rcFUC moiety there was a 2.4-fold increase in fluorescence in the presence of M6P and this was further increased to almost 3-fold in the absence of M6P, that is, the M6P caused a small reduction in binding. In addition, detection of the conjugate *via* the FUC moiety appeared to be more efficient than detection *via* the OX26 moiety. However, analysis with the anti-rcFUC polyclonal will not distinguish between binding of free and conjugated FUC.

Table 4.8: Flow cytometry of rat hepatoma cells (H4IIE) exposed to CHO/rcFUC, OX26 and OX26-FUC conjugates.

	Median Fluorescence
H4IIE cells + FUC*	16.55
H4IIE cells + FUC* + M6P	6.26
H4IIE cells + OX26#	184.00
H4IIE cells + OX26# + M6P	316.23
H4IIE cells + **OX26**-FUC#	24.55
H4IIE cells + **OX26**-FUC# + M6P	21.29
H4IIE cells + OX26-**FUC***	72.34
H4IIE cells + OX26-**FUC*** + M6P	50.48

For experimental procedure see Materials and methods section 2.2.43. * Detection of FUC by rabbit polyclonal to CHO/rcFUC followed by SAR-FITC. # Detection of OX26 by SAM-FITC monoclonal antibody. The background median fluorescence values for SAM-FITC and rabbit anti-rcFUC polyclonal/SAR-FITC are 4.87 and 6.04, respectively.

Table 4.9: Competition binding study with OX26 and OX26-FUC conjugates in the presence and absence of M6P.

Relative concentration of OX26 to OX26-FUC	Median fluorescence	
	+ M6P	- M6P
0 X	59.35	133.35
0.1 X	77.74	107.46
1.0 X	37.86	42.17
10 X	12.86	16.55
100 X	10.37	27.38

For experimental procedure see section 2.2.44. The OX26-FUC conjugate was detected *via* the rcFUC moiety with rabbit polyclonal to CHO/rcFUC followed by SAR-FITC.

A competition study with free OX26 clearly showed that binding of OX26-FUC conjugates (detected *via* the FUC moiety) was progressively reduced by increasing amounts of OX26 Table 4.9 and Figure 4.16). The experiment was done in the presence of M6P to minimise binding *via* the M6PR. In this case the binding of OX26-FUC was reduced 5.7-fold by 100-fold molar excess of OX26. In a parallel experiment done in the absence of M6P, the binding of OX26-FUC was competed 4.9-fold. Overall, at all concentrations of OX26 the measured binding of the OX26-FUC conjugates was higher in the absence of M6P. Background fluorescence determined in the absence of OX26-FUC ranged from a median of 5-10 fluorescence units in going from 0-100 x OX26 (results not shown) and is presumably due to cross-reactivity of SAR-FITC or the rabbit anti-rcFUC antibody with OX26. No difference in background fluorescence in the presence or absence of M6P was seen.

Figure 4.15: Flow cytometry analysis of rat hepatoma cells (H4IIE).

H4IIE cells were exposed to (A), OX26 and detected with SAM-FITC; (B), CHO/rcFUC and detected with rabbit anti-rcFUC polyclonal antibody/SAR-FITC; (C), OX26-FUC conjugates which were detected *via* the OX26 component with SAM-FITC and (D), OX26-FUC conjugates detected *via* the FUC moiety with rabbit anti-rcFUC polyclonal antibody/SAR-FITC, in the presence (red line) and absence (green line) of M6P. Background fluorescence determined with H4IIE cells exposed to SAM-FITC (A and C) or rabbit anti-rcFUC polyclonal/SAR-FITC (B and D), in the absence of M6P, is shown by the blue line. Background fluorescence in the presence of M6P is identical.

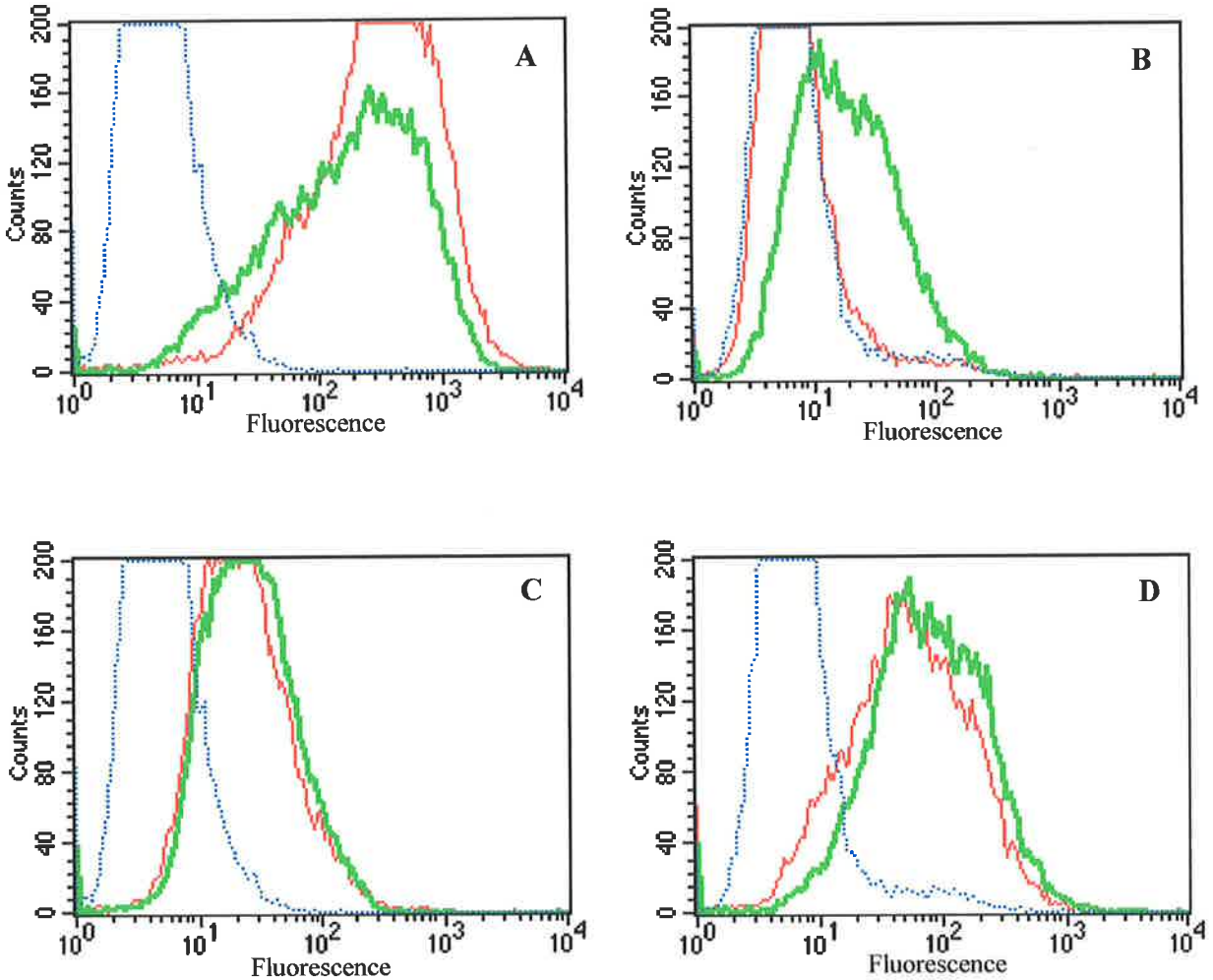
A
B
C
D
Counts
Fluorescence
0
40
80
120
160
200
10^0
10^1
10^2
10^3
10^4

Figure 4.16: Competition binding study with OX26 and OX26-FUC.

Rat hepatoma cells (H4IIE) were exposed to increasing concentrations of OX26 (0-100X) in the presence of OX26-FUC conjugates. In (A), this was done in the presence of M6P and in (B), in the absence of M6P. Bindng was detected with rabbit anti-rcFUC polyclonal antibody followed by SAR-FITC. No OX26 (red line), 0.1X OX26 (green line), 1.0X OX26 (pink line), 10X OX26 (orange line) and 100X OX26 (blue line).

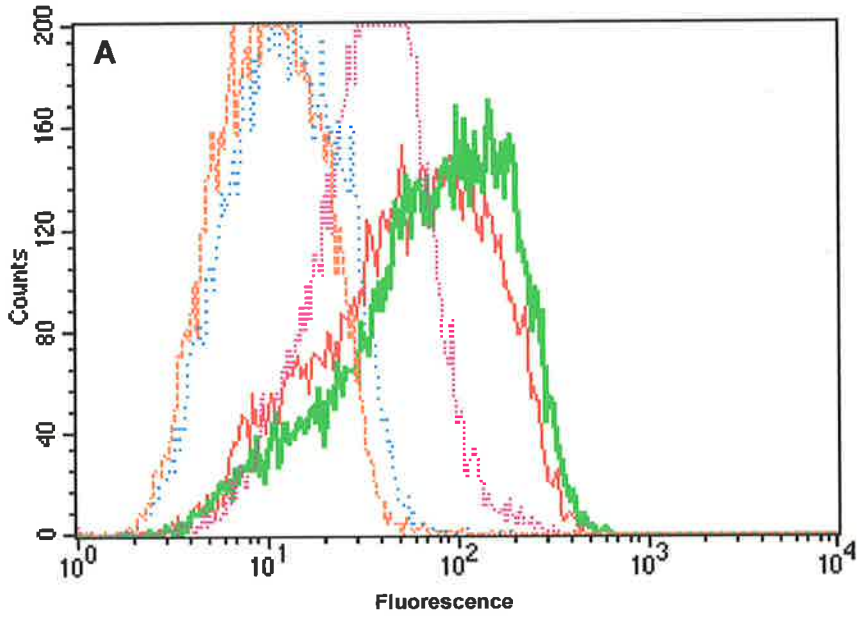
A
Counts
0
40
80
120
160
200
10^0
10^1
10^2
10^3
10^4
Fluorescence

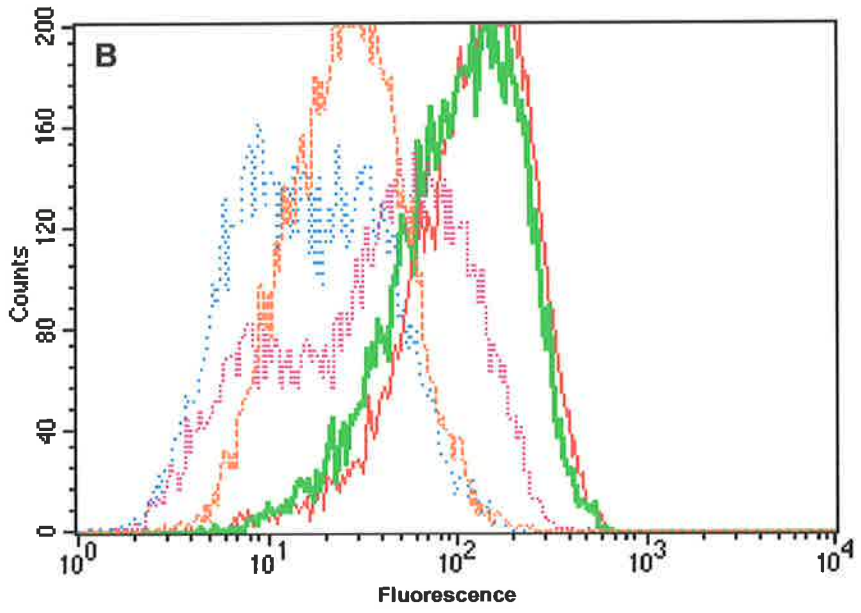
B
Counts
0
40
80
120
160
200
10^0
10^1
10^2
10^3
10^4
Fluorescence

4.2.8 Cationization of rcFUC with putrescine

Besides receptor-mediated transcytosis into brain, adsorptive-mediated transcytosis offers another possible route for delivery of lysosomal enzymes from the peripheral circulation into brain. This method relies on an electrostatic interaction between the protein to be transcytosed and the negative charge conferred by the glycocalyx on the lumenal surface. Cationization provides a means of increasing the positive charge on a protein to facilitate this process (section 1.24.1).

Cationization of rcFUC was performed by reaction with the naturally occurring polyamine, putrescine, in combination with EDC and NHS (Figure 4.17). Putrescine had little inhibitory effect on FUC activity (<5% inhibition at 400 mM putrescine) (Table 4.10). However, EDC was found to be an irreversible inhibitor of FUC activity such that a 10,000-fold molar excess (66 mM) resulted in almost complete inhibition of activity (Table 4.10). At this concentration of EDC and with 400 mM putrescine, rcFUC was almost completely cationized with its pI being increased from 4.5-6 to 8.5-9.6 (Figure 4.18). Analysis of experimental variables resulted in a protocol in which all the isomers detected by IEF were modified while approximately 70%-80% FUC activity was retained (Table 4.10). To achieve these results the conditions used were 1 mg/ml rcFUC, 400 mM putrescine, 14 mM NHS, 16 mM EDC, 100 mM $NaHPO_4$ buffer, pH 7 for 20 min at room temperature. Under these conditions the pI of rcFUC was altered from pH 4.5-6.5 to pH 6.5-8 (Figure 4.19 A). The specific activity of the cationized rcFUC was reduced to 80% of unmodified enzyme. When electrophoresed on a SDS polyacrylamide gel cationized rcFUC did not show any substantial increase in Mr per subunit. However, a small amount of aggregates was observed (Figure 4.19 B, lane 3).

Table 4.10: Cationization of rcFUC.

	FUC activity (nmol/min/ml)
rcFUC	17,380
rcFUC + 100 mM putrescine	16,311
rcFUC + 200 mM putrescine	17,188
rcFUC + 400 mM putrescine	16,676
rcFUC + 400 mM putrescine + 66 mM EDC	3.5
rcFUC + 400 mM putrescine + 16 mM EDC	16,229

rcFUC was treated with 0-400 mM putrescine and 16 or 66 mM EDC in the presence of 400 mM putrescine (section 2.2.45.)

Cationized rcFUC retained the ability to be endocytosed into human fucosidosis SF where it was effective in hydrolysing stored substrate (Table 4.11). Under the conditions tested fucosidosis SF stored approximately 10 times more fucose-containing oligosaccharides compared to normal SF. Exposure of fucosidosis SF to 15 nmol/min/ml of unmodified enzyme in culture medium resulted in intracellular levels of FUC activity of approximately 60% of normal. Concomitantly storage levels in these cells decreased by 3-fold compared with uncorrected fucosidosis SF. Exposure of fucosidosis SF to an equivalent concentration of cationized rcFUC resulted in intracellular FUC activity levels of about 88% of normal levels and a similar reduction of storage material as was observed with unmodified enzyme. In the presence of M6P endocytosis of both modified and unmodified enzyme was inhibited resulting in storage levels similar to those seen in uncorrected cells. β-Hexosaminidase levels in the fucosidosis cells were somewhat elevated compared to normal control cells and remained essentially unchanged in the experimental samples.

Figure 4.17: Cationization of rcFUC with polyamines.

(A) Naturally occurring polyamines such as putrescine, spermine and spermidine confer an increase in net positive charge of +1, +2 and +3, respectively, for each mole of polyamine covalently bound to an acidic amino acid. (B) The cationization reaction involves the activation of a surface carboxylic acid on the protein by EDC resulting in the formation of reactive esters followed by reaction with the polyamines (e.g., putrescine) as nucleophilic reagents. NHS enhances this reaction (mechanism not shown).

A

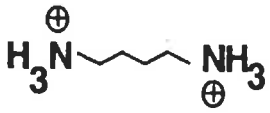

Putrescine

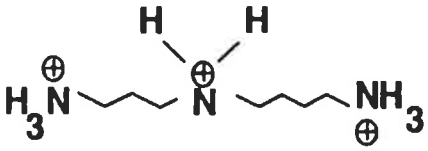

Spermidine

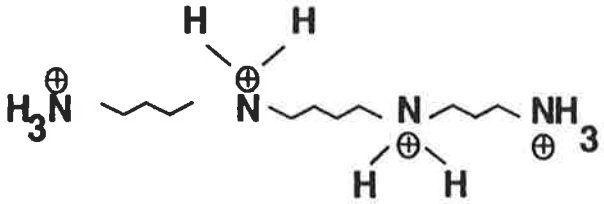

Spermine

B

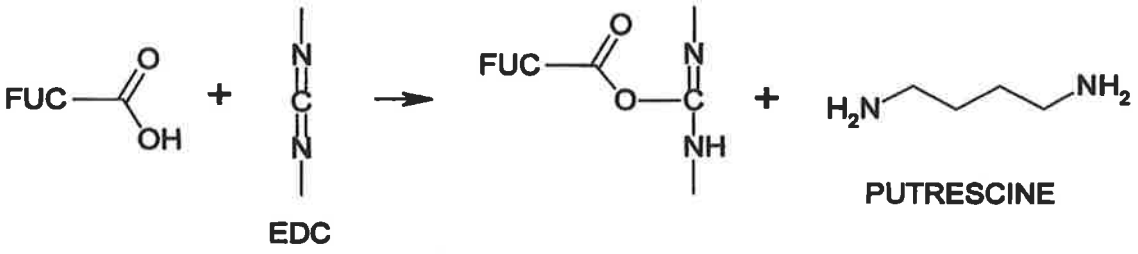

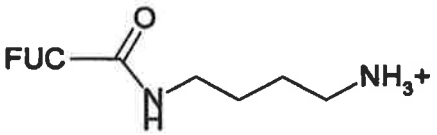

Figure 4.18: Complete cationization of CHO/rcFUC.

CHO/rcFUC was cationized with putrescine/EDC as described in section 2.2.45 and then analysed by IEF. Lane 1, IEF standards with their respective pI values indicated by arrows; lane 2, CHO/rcFUC; lanes 3 and 4, CHO/rcFUC cationized with 10,000 and 5,000-fold molar excess of EDC to CHO/rcFUC, respectively.

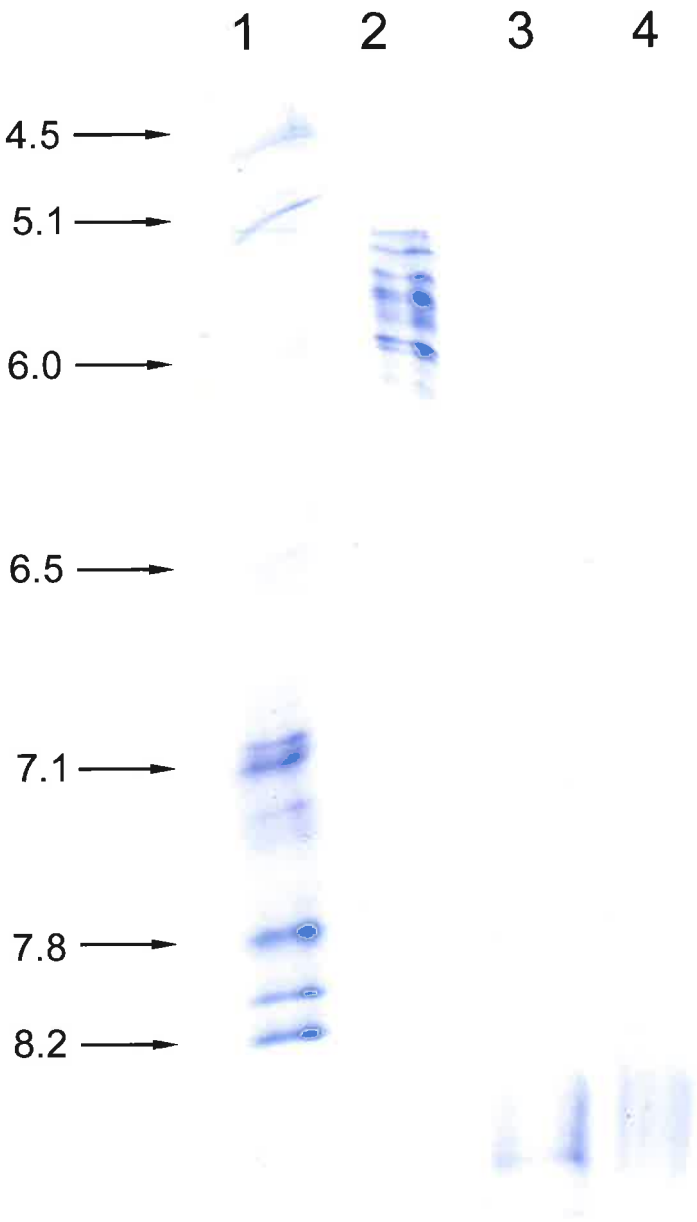
1
2
3
4
4.5
5.1
6.0
6.5
7.1
7.8
8.2

Figure 4.19: IEF and SDS-PAGE of cationized CHO/rcFUC.

CHO/rcFUC was cationized with a 1,000-fold molar excess of EDC compared to CHO/rcFUC as described in section 2.2.45. (A) IEF. Lane 1, IEF standards with their respective pI indicated by arrows; lane 2, CHO/rcFUC; lane 3, cationized CHO/rcFUC. (B) SDS-PAGE. Lane 1, Mr standards, which include phosphorylase b (94 kDa), BSA (67 kDa) and ovalbumin (43 kDa), are indicated by arrows; lane 2, CHO/rcFUC; lane 3, cationized CHO/rcFUC.

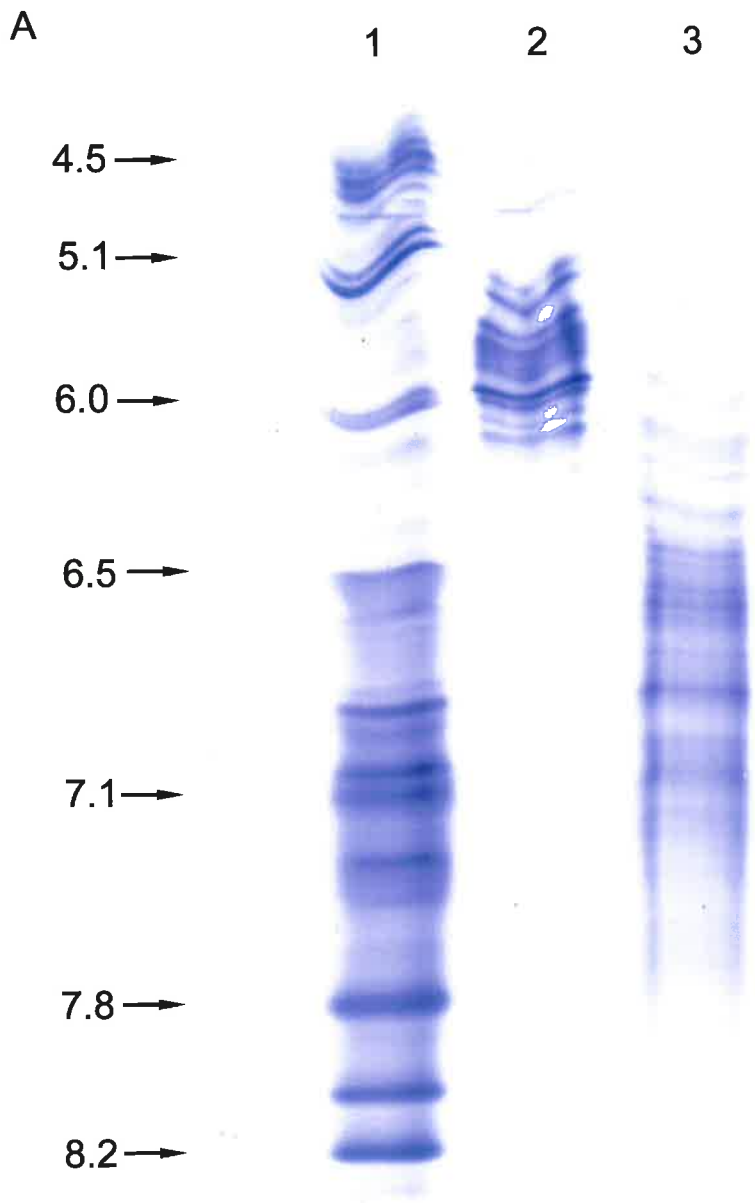
A
1
2
3
4.5
5.1
6.0
6.5
7.1
7.8
8.2

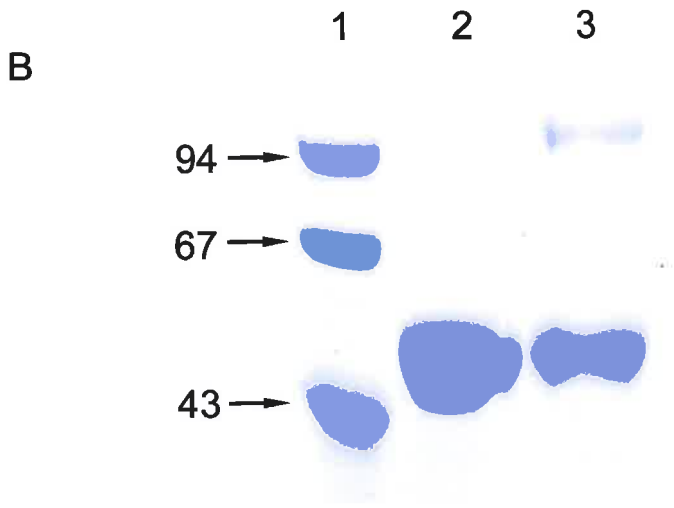
B
1
2
3
94
67
43

Table 4.11: Correction of fucosidosis skin fibroblasts with cationized CHO/rcFUC.

Cell line	FUC activity (nmol/min/mg)	^{3}H-fucose (dpm/mg)	β-hexosaminidase (nmol/min/mg)
SF5077	1.129 ± 0.467	177,907 ± 50112	66.6 ± 24.8
SF2184	0.002 ± 0	1,769,717 ± 231,949	137.7 ± 9.1
SF2184 + FUC	0.68 ± 0.284	592,818 ± 65,751	107.0 ± 27.9
SF2184 + FUC + M6P	0.101 ± 0.012	1,133,942 ± 37,124	95.7 ± 49.9
SF2184 + FUC_{cat}	0.994 ± 0.217	656,792 ± 123,867	125.7 ± 16.3
SF2184 + FUC_{cat} + M6P	0.135 ± 0.018	1,695,824 ± 340,759	130.9 ± 7.5

CHO/rcFUC was cationized with the polyamine, putrescine, as described in section 2.2.45 and Figure 4.19. Normal (SF5077) and fucosidosis skin fibroblasts (SF2184) were metabolically labelled with ^{3}H-L-fucose for 48 h and then incubated with purified CHO/rcFUC or cationized CHO/rcFUC (FUC_{cat}) (15 nmol/min/ml) in the presence or absence of 5 mM M6P for 48 h. Cells were harvested and cell lysates assayed for ^{3}H-radioactivity, total protein, β-hexosaminidase activity and FUC activity. Results are expressed as the mean (n = 3) ± 1 SD.

4.2 Discussion

4.2.1 Insulin-FUC conjugates

Previous reports suggested that insulin might be used as a vector for transporting proteins and other ligands into the brain. Due to the hypoglycaemic effect that was observed with insulin conjugates Fukuta *et al.* (1994), used a tryptic fragment (F007) of insulin. The amino acid sequence of insulin contains one lysine and one arginine (Figure 4.10). As trypsin cleaves on the carboxy side of these residues, and the lysine is the penultimate residue on the B chain, only two peptides should result from tryptic digestion of insulin. However, Fukuta *et al.* (1994) report three tryptic fragments, F001, F006 and F007. Of these F006 and F007 correspond to the two tryptic peptides predicted from cleavage specificity and F001, which has both chains terminating in tyrosine residues, would appear to be the result of digestion by chymotrypsin, presumably a contaminant in their trypsin preparation. In this study TPCK trypsin was used and two fractions, A and B, were detected. The third species detected (Fraction C) was undigested insulin. Fraction A could not be visualised on a Tricine-SDS polyacrylamide gel, presumably because either insufficient was loaded or, being of such small Mr, it was lost from the gel during fixation. Fraction B was slightly smaller than undigested insulin and was shown to be the same as F007 by mass spectrometric analysis. Although the methodology for making these peptides was successfully established, for convenience undigested insulin was used to establish methodology for derivatization and conjugation. It was considered that the hypoglycaemic effect would not preclude short-term testing of the conjugates *in vivo*.

Preliminary experiments to make insulin-FUC conjugates encountered technical obstacles. Poor solubility of bovine insulin was one issue and this restricted derivatization reactions to solutions of ≤1 mg/ml insulin. Porcine insulin is also known to be poorly soluble at neutral pH, although Fukuta *et al.* (1994) claim to use solutions of 7 mg/ml. Identifying conditions for the reproducible and controllable derivatization of insulin and FUC with SPDP, ideally where an average of 1-2 moles of pyridyldithiopropionate is added per mole of protein, were also challenging. This was particularly so for FUC given that these reactions were being done on a small-scale due to constraints on enzyme availability. Since results of the analysis to determine the number of moles of pyridyldithiopropionate bound per mole of protein will reflect a binomial distribution, values of between 1 and 2 were considered acceptable to proceed with conjugation. At excessive concentrations of SPDP, the maximum number of moles of

pyridylthiopropionate bound per mole of insulin was found to be 3.1. This is consistent with there being only four amino acids with free amine groups (the two N-terminal amino acids of the A and B chain and the lysine and arginine residues on the B chain, Figure 4.10), although the guanidinyl amino group of the arginine residue is not as reactive as the ε-amino group of lysine.

Another problem encountered in the conjugation process was the DTE needed to produce a free sulphydryl on one of the proteins derivatized with SPDP. To eliminate any potential for the disruption of S-S-linked structure of insulin, which would consequently compromise its ability to bind to its receptor, FUC was chosen for reduction with DTE as its native structure is not dependent on inter-disulphide bonds. Although each subunit of rcFUC contains intramolecular S-S bonds (there are 8 cysteine residues per subunit) at the recommended concentration of DTE (25 mM) these should not be affected (Carlsson *et al.*, 1978). However, the DTE reduction of SPDP–derivatized rcFUC resulted in at least 25% loss of FUC activity, with further losses upon the prolonged dialysis used to remove the DTE. Exhaustive dialysis for complete removal of DTE was necessary so as not to impair the efficiency of formation of subsequent S-S bonds between the two derivatized proteins. To overcome these problems, SATA-derivatization of rcFUC was chosen as an alternative. This derivatization uses mild reaction conditions, and after dialysis to remove free SATA, hydroxylamine is used in the conjugation reaction to deacetylate the protected sulphydryl group.

The next major difficulty encountered in making insulin-FUC conjugates was in developing methods for analysing the products of the conjugation reaction. Gel filtration chromatography was not suitable for separation of insulin-FUC from free FUC as the difference in Mr between the two is too small (6 kDa) to be resolved. Affinity chromatography or gel filtration chromatography would only be suitable if conjugation of FUC with insulin had gone to completion thus requiring the isolation of conjugates only, rather than conjugated and unconjugated FUC from free insulin. Analysis of rcFUC by SDS-PAGE demonstrates a relatively diffuse protein band typical of glycoproteins, making it difficult to resolve easily and unambiguously small differences in Mr. When the putative conjugates were reduced with DTE and electrophoresed on a SDS polyacrylamide gel, no band corresponding to insulin was detected. However, calculations showed that in order to visualise insulin on a polyacrylamide gel, 128 μg of conjugate would have to be loaded, assuming a stoichiometry of 1:1 and a

detection limit of approximately 10 μg. This amount of protein may interfere with the electrophoretic mobility of the proteins concerned. Western blot analysis of conjugates using a monoclonal antibody to human insulin, which is known to cross-react with bovine insulin, was also uninformative. Whether this was due to the absence of unconjugated insulin, or a lack of the required sensitivity, is unclear. In conclusion, the limitations of the possible analytical tools identified made it hard to conclusively determine whether conjugation was successful or not. In the results reported by Fukuta *et al.* (1994) the degree of derivatization of HRP or insulin are not stated. Separation of insulin-HRP from HRP was achieved by Sephadex G75 chromatography. Conjugates eluted from the chromatography matrix were detected by the presence of HRP activity but by the absence of a HRP band at a position equivalent to its native Mr of 40 kDa on SDS-PAGE. However, the size of the conjugates was not stated.

An alternative method that may provide a more sensitive analytical tool includes structuring an Elisa assay in such a way that only conjugates are detected (Walus *et al.*, 1996). This can be done with a sandwich Elisa where the first antibody recognises one half of the conjugate and the second antibody the other. For example, in the use of insulin-FUC conjugates, the Elisa plate could be coated with rabbit anti-rcFUC polyclonal to bind conjugate *via* the FUC moiety and then detected with an anti-insulin antibody. Given appropriate washing conditions to remove free FUC and free insulin, only covalently linked conjugates would result in a positive signal. The limitations to this method are firstly, the possibility of free FUC competing for binding sites which might limit the sensitivity of the assay, and secondly, the anti-insulin monoclonal antibody may not be suitable to be used in an Elisa (according to the manufacturer this particular antibody has not been tested by Elisa) or may not be able to detect the relevant epitope on insulin when insulin is conjugated to the much larger FUC molecule due to steric hindrance. When the anti-insulin monoclonal antibody used in these studies was tested against the bovine insulin it gave a relatively low titre of 1 in 640 in an Elisa. Ultimately, this approach to analysis of insulin conjugates was not pursued as for other reasons the whole idea of using insulin as a vector was rejected (see below).

Technical problems aside, the theoretical possibilities of using insulin, or more particularly the insulin fragment F007, as a vector for transcytosis across the BBB, became increasingly doubtful. As already mentioned, the 3-D structure of insulin is important for binding to the insulin receptor. This binding site is comprised of amino acids of the N-terminal of the A chain

and the C-terminal of the B-chain. All synthetic peptides, and those produced by proteolytic digestion, lacked either one or both of these binding domains or parts thereof, and were unable to bind to the insulin receptor on bovine brain microendothelial cells (Fukuta *et al.*, 1994). In the production of the F007 fragment, the C-terminal peptide of the B chain, GFFYTPK, is removed by tryptic digestion. This already compromises the affinity of binding of F007 to the insulin receptor. Fukuta *et al.* (1994) showed that binding of F007 to the insulin receptor was an order of magnitude lower compared to insulin. This may well explain why there is no hypoglycaemic effect in rats injected with F007 at the same, or even ten times the dose of insulin that induces hypoglycaemia. That is, the effect may be one of reduced binding rather than loss of signal transduction. The binding affinity of insulin-HRP was at least two orders of magnitude lower than insulin, which may indicate that the chemically-linked HRP is also masking the binding site, ostensibly by steric interference. Despite the decreased affinity of insulin for its receptor when conjugated to HRP, Fukuta *et al.* (1994) showed that transcytosis of the insulin-HRP conjugate into brain did occur at levels comparable to those seen with the OX26 vector system (0.8% of ID) (Friden *et al.*, 1991). Presumably, neither the conjugation process nor steric hindrance from HRP has adversely affected the binding of insulin to its receptor *in vivo*.

It also became increasingly obvious that, in order to maintain adequate affinity of binding for the insulin receptor, derivatization of F007 would need to be at a specific site. In F007, there are three potential sites for derivatization; the N-terminal amino acids of both chains and the arginine residue at the C-terminal of the B chain. The amino acids of the N-terminal of the A chain are involved in binding and depending on how many of the amino acids of the C-terminal of the B chain are required for binding, the arginine residue of this chain may also be involved. Therefore, it appears that the only 'safe' position for derivatization of F007 with SPDP is on the N-terminal amino acid of the B chain. The chemistry involved in protecting those amino groups not to be derivatized, and then deprotecting them after derivatization, is difficult. In conclusion, the results reported by Fukuta *et al.* (1994) would appear to be inconsistent and hard to rationalise. The use of an anti-insulin receptor antibody may provide a more realistic approach to utilising the insulin transport system for transcytosis of heterologous proteins (Coloma *et al.*, 2000; Zhang *et al.*, 2003).

4.2.2 OX26-FUC conjugates

Conjugation of SATA-derivatized CHO/rcFUC with OX26 derivatized with SPDP *via* amine groups resulted in the formation of three discrete heterologous protein species. On SDS-PAGE these were visualised as protein bands of Mr 200, 250 and 300 kDa. Assuming rcFUC is trimeric these protein bands are representative of conjugates with native Mr of 300, 450 and 600 kDa, respectively. The reason these larger Mr conjugates are not seen on SDS-PAGE is because those subunits of rcFUC which are not covalently linked to OX26 by S-S bonds migrate as subunits of approximately 55 kDa on denaturing SDS polyacrylamide gels as discussed previously (section 4.1.4.1).

When OX26 was conjugated with rcFUC, equimolar amounts of each were used. When the conjugates were analysed on SDS-PAGE, it was obvious that the reaction had not gone to completion as free OX26 and free rcFUC were still present, although the amount of the latter was masked by the dissociation of non-covalently bound subunits of rcFUC which, in the native state, would be part of the conjugate. The ability to purify conjugates would obviously simplify analysis. OX26 was readily removed from the reaction mixture, with good recovery of active conjugate, utilising fucosylamine-agarose affinity chromatography. Removal of free FUC could be most easily achieved using a Protein G column. However, the low pH conditions (100 mM $NaPO_4$ buffer, pH 3) required to elute bound proteins from this matrix would be detrimental to recovery of FUC activity. An alternative is to use size exclusion chromatography or to increase the likelihood of all rcFUC being conjugated to OX26, that is, a large (e.g., 7-10-fold) molar excess of OX26 could be used in the conjugation reaction. However, none of these methods to eliminate free FUC in the conjugate was pursued due to time constraints.

Modification of OX26 *via* carbohydrate groups is an alternate method for making conjugates. It has been reported that immunoglobulins modified *via* sialic acids on oligosaccharide chains retain antigen-binding affinity (Rodwell *et al.*, 1986). Carbohydrate modification is a two-step process. The first step involves oxidation of vicinal diols of sialic acid to produce aldehydes. The second step is reaction of the aldehydes with PDPH. Interestingly, no conjugates of OX26-FUC were observed when OX26 was derivatized through carbohydrate groups with PDPH at low stoichiometry. Moreover, no conjugates or aggregates were generated when over-derivatized OX26 (9.44 moles of pyridyldithiopropionate per mole of OX26) was used. As pyridyldithiopropionate groups were detected on OX26, the lack of conjugate formation is not

due to a failure of the derivatization process. The reason for the failure to produce conjugates is most likely due to inaccessibility of the two reactive groups because of steric hindrance. Unlike SPDP, PDPH has no spacer arm or bridge connecting its two reactive terminal moieties. It may be that steric hindrance is preventing conjugation although conjugation of OX26, derivatized *via* amine or carbohydrate, with SATA-derivatized rsCD4 using similar conditions has been documented (Walus *et al.*, 1996).

For a conjugate to achieve its purpose, the biofunctionality of both the vector (OX26) and the 'passenger' molecule (rcFUC) must be preserved. That is, OX26-FUC conjugates should still be able to bind to the Tf receptor and to the IGFII/M6P receptor and, in addition, FUC should be enzymically active. During the process of derivatization and conjugation, upto 70% of FUC activity was retained. The ability of the conjugate to bind to the Tf receptor on H4IIE rat hepatoma cells was measured by FACScan analysis. H4IIE cells express high levels of Tf receptor as shown by analysis of OX26 binding. As there is no free OX26 present in the conjugate preparation, binding of the conjugate could be analysed *via* the OX26 moiety. Binding of the conjugate to H4IIE cells appeared to be predominantly *via* the Tf receptor as it was strongly inhibited by free OX26 but not by M6P. However, the amount of binding (median fluorescence) was much lower for the conjugate than for free OX26. There are a number of reasons why this may be so. Firstly, only a small percentage of the conjugate may be able to bind to the Tf receptor due to steric hindrance by the FUC component. Secondly, conjugation may have altered the binding site of OX26 and thirdly, steric hindrance may also be reducing the detection of the OX26 component by the secondary antibody (SAM-FITC-labelled IgG) although, as this is a polyclonal reagent, this effect may be less pronounced.

The specificity of binding of rcFUC to the M6PR on H4IIE cells was demonstrated by the inhibition of binding in the presence of M6P. Analysis of the binding of conjugates *via* the FUC moiety, rather than the OX26 component, is complicated by the presence of free FUC. The difference in median fluorescence in the competition binding studies in the presence and absence of M6P is presumably indicative of this free rcFUC present in the partially purified conjugates, as conjugate binding (measured *via* OX26) is unaffected by M6P. By necessity the detection agent in this experiment is the anti-rcFUC polyclonal/SAR-FITC. Therefore, in the absence of M6P all rcFUC, either free or conjugated, will be detected whereas in the presence of M6P only conjugates bound *via* the OX26 vector will be reactive.

In summary, it was possible to demonstrate binding of the OX26-FUC conjugate to the Tf receptor only. It still remains to be shown that the M6P binding site is functional after conjugation and that these conjugates can be endocytosed into cells, targeted to the lysosome and can turnover substrate. In order to obtain an unequivocal result, all free FUC would have to be removed from the conjugate preparation. (Methods by which this could be done are discussed above.) It also remains to be demonstrated that the OX26-FUC conjugate can be transcytosed into brain across the BBB. Successful transcytosis of a number of proteins linked to OX26 such as nerve growth factor (Friden *et al.*, 1993), vasoactive intestinal protein (Bickel *et al.*, 1993; Wu and Pardridge, 1996), rsCD4 (Walus *et al.*, 1996) and avidin (Yoshikawa and Pardridge, 1992) as well as methotrexate (Friden *et al.*, 1991) have been reported. The percentage of the injected dose found in brain is relatively low (0.5-0.7%) compared to other organs such as liver. However, low amounts of enzyme were sufficient to show a physiological effect. For example, NGF conjugated to OX26 was shown to increase the survival of both cholinergic and non-cholinergic neurons of the medial septal nucleus that had been transplanted into the anterior chamber of the rat eye (Friden *et al.*, 1993). All the above proteins conjugated to OX26 are relatively small compared to rcFUC. NGF is 28 kDa, VIP is 30 kDa, rsCD4 is 45 kDa and avidin is 60 kDa. It is not known whether there is a size restriction for such a large chimeric protein as the OX26-FUC conjugate let alone larger conjugates where two or three FUC molecules are linked to OX26, to be either endocytosed into cells or transcytosed across the BBB.

In conclusion, while active conjugates were made, and were shown to bind to the Tf receptor, these studies need to be continued to demonstrate binding to M6PR, targeting to and activity in the lysosome and increased transcytosis across the BBB.

4.2.3 Cationization of rcFUC

The process of protein cationization is designed to increase positive charge and thus facilitate adsorptive-mediated transcytosis of the modified protein into brain. Cationization of CHO/rcFUC *via* carboxylic acid groups was performed by reaction with the naturally occurring polyamine, putrescine. Activation of the carboxylic acid groups to the reactive ester is dependent on the ionisation of the carboxylic acids which in turn is controlled by the pH of the cationization reaction. Cationization of rcFUC such that the pI of all the isomers was altered to

9.6 resulted in an almost total loss of FUC activity even when attempts were made to protect the active site with the competitive inhibitor, L-fucose. In order to retain reasonable FUC activity it was necessary to control the degree of cationization. This has also been found in other studies of enzyme modification such as SOD and catalase (Poduslo and Curran, 1996a; Wengenack *et al.*, 1997b) where pH of the reaction was adjusted to achieve a balance between cationization and enzyme activity without overly compromising the desired biological outcome, which in this case was uptake into brain by adsorptive-mediated transcytosis. An earlier study (Poduslo and Curran, 1996b) had shown that complete cationization of SOD, which also resulted in almost complete enzyme inactivation, was taken up by rat brain at 21-fold greater rate compared to native SOD.

Putrescine modification of CHO/rcFUC did not affect the M6P recognition signal as the enzyme was still endocytosed into lysosomes of fucosidosis cells where it was effective in removing storage products. Compared to the preparation of conjugates, putrescine modification was relatively straightforward and so the effect of cationization on plasma clearance, tissue distribution and transcytosis across the BBB was assessed *in vivo*. These experiments are described in section 4.3.

4.3 *In vivo* analysis of biodistribution of rcFUC

4.3.1 Production of antibodies to CHO/rcFUC

Polyclonal and monoclonal antibodies were produced to CHO/rcFUC in an attempt to make canine specific reagents which could be used in analyses of *in vivo* ERT experiments by immunohistochemistry, Elisa and immune capture activity assays.

Rabbit polyclonal antibody to CHO/rcFUC gave a titre of 1 in 2 x 10^6 when tested using a standard Elisa as described in section 2.2.31. This polyclonal antibody was used for detection of free FUC and FUC in OX26-FUC conjugates on cell surfaces by FACS analysis (section 4.2.7).

One hundred and twenty six hybridomas from two fusions of mouse spleen cells were screened against purified CHO/rcFUC using a standard Elisa. Results of this initial screen indicated 13 positive hybridomas of which only 5 were still positive after retesting. None of the original 13 hybridomas demonstrated a positive result in an immunobinding assay (section 2.2.30) when used for detection of purified FUC activity. However, 12 hybridomas gave a positive response on a Western blot to purified enzyme. All were of the IgM subclass (section 2.2.30). Furthermore, all showed a negative response when tested for immunohistochemical analysis of cFUC expression with CHOcFUC40-A2-4 cells (section 2.2.32) and all cross-reacted with FUC purified from rat liver (results not shown). Due to the lack of the required specificity (i.e., canine specificity and immunohistochemical reactivity) of the monoclonal antibodies for cFUC their use was not pursued.

4.3.2 Plasma clearance of ^{3}H-radiolabelled rcFUC in normal rats

Pharmacokinetic studies to determine plasma clearance of various forms of ^{3}H-rcFUC and their tissue distribution were done in normal rats. Of particular interest was analysis of uptake of enzyme by brain using capillary depletion, a technique to separate brain vasculature from brain parenchyma.

Four forms of ^{3}H-rcFUC, namely, CHO/rcFUC, MDCK/rcFUC, mature CHO/rcFUC prepared from cell lysates (section 2.2.26) and cationized CHO/rcFUC (section 2.2.45) were intravenously injected into normal rats at a dose of 1 mg/kg to determine plasma circulating

half-life and tissue distribution. CHO/rcFUC was also tested at a dose of 10 mg/kg. Regardless of dose, the clearance of all forms of rcFUC was biphasic in nature with an initial rapid phase having a half-life of approximately 1 min and a longer secondary phase ranging from 12 min to 180 min (Figure 4.20 and Table 4.12). The half-life of the second phase was dependent on the type of rcFUC infused. CHO/rcFUC at 1 or 10 mg/kg demonstrated the longest secondary phase with a half-life of 140-180 min. Cationized CHO/rcFUC was cleared more rapidly (90 min) while MDCK/rcFUC and mature CHO/rcFUC, with half-lifes of 45 min and 12 min, respectively, were cleared even more rapidly.

The amount of ^{3}H-rcFUC remaining in plasma at the end of the different distribution studies is shown in Table 4.13. In the 1 h distribution studies, CHO/rcFUC and cationized CHO/rcFUC were still present in plasma at 24.7% (result not shown) and 28.34% (Table 4.13) of the injected dose, respectively, whereas after 1 h only 4.73% of mature CHO/rcFUC was still evident. In the 4 h distribution studies with CHO/rcFUC there was approximately 10% of enzyme still in plasma irrespective of the dose (1 or 10 mg/kg body weight). Cationized CHO/rcFUC was also present in plasma at a low level after 4 h (3.96%) and MDCK/rcFUC levels were 7.78% after 4 h. Twenty four hours after administration of 1 mg CHO/rcFUC/kg, only 1.5% of the injected dose remained in circulation. The relevance of these results to the amount of FUC activity detected in brain fractions is discussed in section 4.3.1 (discussion). The residual levels of enzyme found therefore reflect the different half-lifes.

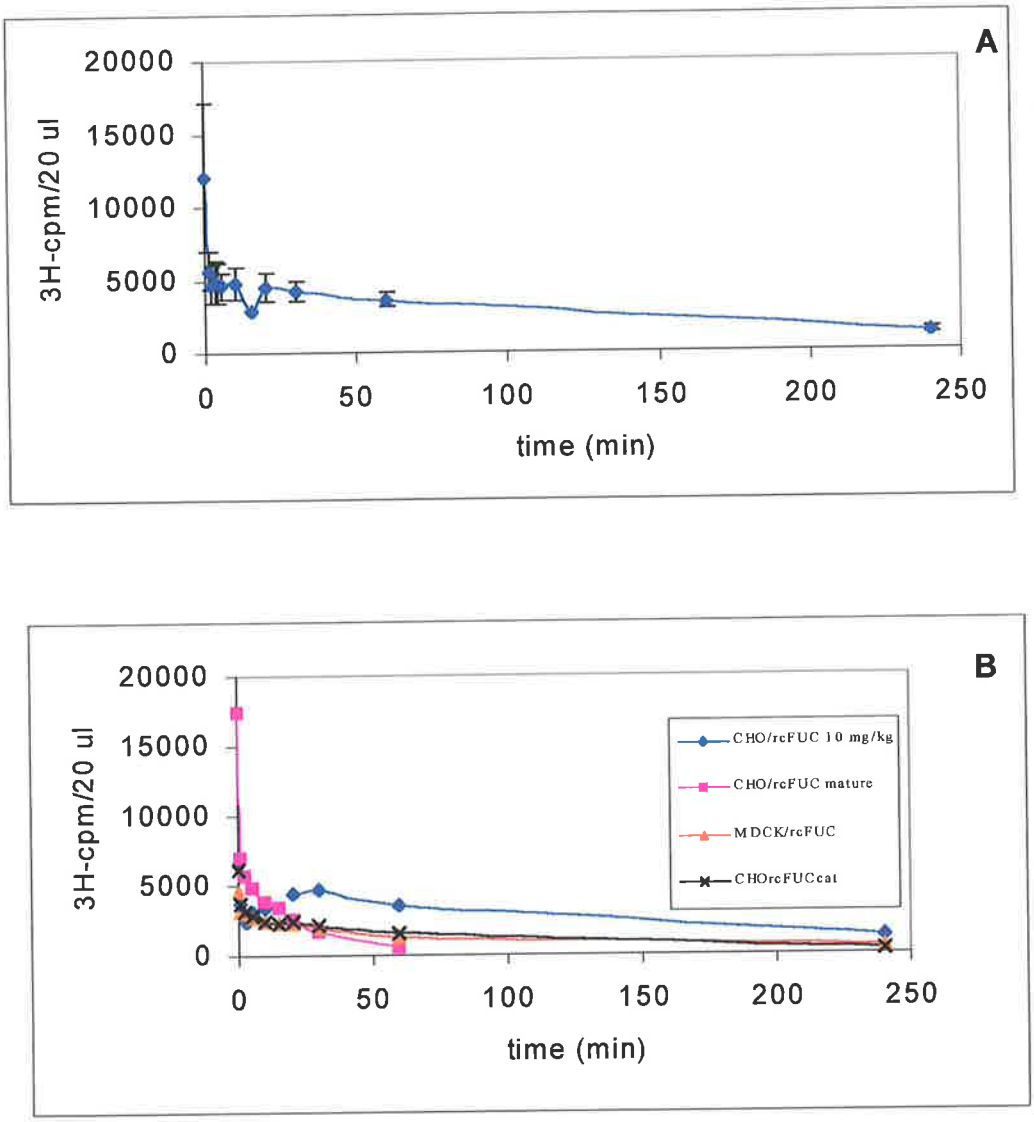

Figure 4.20: Circulating plasma half-life of rcFUC in normal rats.

(A), Normal rats were intravenously injected with ^{3}H-CHO/rcFUC at 1 mg/kg and sacrificed 4 h or 24 h later. Blood samples were removed at specified times and plasma assayed for ^{3}H cpm. (Results to 4 h shown only). (B) As above but different forms of ^{3}H-rcFUC were tested as indicated. Also shown is CHO/rcFUC at 10 mg/kg. Plasma samples were analysed for ^{3}H-cpm.

Table 4.12: Circulating plasma half-lifes in normal rats.

	Dose (mg/kg)	Time at sacrifice (h)	$T_{1/2}$ 1st Phase (min)	$T_{1/2}$ 2nd Phase (min)
CHO/rcFUC	1	4	1	180
CHO/rcFUC	1	24	1	135
CHO/rcFUC	10	4	1	140
CHO/rcFUC$_{cat}$	1	4	1	90
Mature CHO/rcFUC	1	1	1	12
MDCK/rcFUC	1	4	1	45

Normal rats were intravenously infused with ^{3}H-labelled FUC at the doses shown and sacrificed at either 1, 4 or 24 h post infusion as indicated. Blood samples were collected immediately after infusion and at specified times thereafter. $T_{1/2}$ values of the two phases of plasma clearance were determined from a plot of ^{3}H-radioactivity (cpm/20 µl) against time post-infusion (min) (Figure 4.20). The number of rats tested for each of the forms of rcFUC was 1 except for CHO/rcFUC (4 h) and (24 h) where the number was 2 and the mean values are given.

4.3.3 Tissue distribution of various forms of rcFUC in normal rats

Tissue distribution of all the forms of rcFUC mentioned in the above section was similar (Table 4.13), with the majority of the enzyme being found in the liver. Other tissues with lower but still notable levels of enzyme included kidney, lung, spleen and heart. In all the animals tested only 34-58% of injected counts was recovered. Quenching contributed to a 15-20% loss of counts. The distribution of CHO/rcFUC at 10 mg/kg was the same as for 1 mg/kg of CHO/rcFUC.

Analysis of brain samples after capillary depletion demonstrated that very little, if any enzyme was found in the brain parenchyma (0.027-0.112% of the injected dose, Table 4.14). Cationization of rcFUC appeared to have no effect on the levels of enzyme found in brain. Results of ALP and GGT assays of brain parenchyma and capillary fractions, after the capillary depletion process, indicated that the degree of contamination of brain parenchyma with capillaries was on average less than 10% (the parenchyma/vasculature ratios ranged from 4.83-17.72% with respect to ALP and 0-19.3% with respect to GGT, Table 4.15). Analysis of biodistribution of ^{14}C-inulin, a compound impervious to the BBB, to determine the degree of contamination of brain parenchyma with radioactive protein present in the blood of the brain vasculature, indicated that this was approximately 0.062% of the injected dose (results not shown).

Table 4.13: Tissue distribution of various forms of ^{3}H-labelled rcFUC in normal rats.

Normal rats were intravenously infused with 1 mg ^{3}H-labelled rcFUC/kg with the exception of * (10 mg/kg). Tissue ^{3}H-radioactivity (section 2.2.46) was determined 1, 4 or 24 h post-infusion. Results are expressed as % ID and where n = 2 the mean value is given. n = number of animals in each group; nd = no activity detected; - indicates the tissue was not collected for analysis.

	CHO	CHO	CHO*	CHO_{cat}	CHO_{cat}	CHO_{mature}	MDCK
	4 h	24 h	4 h	1 h	4 h	1 h	4 h
			%ID				
Liver	21.75	33.06	29.09	15.06	44.56	44.64	34.02
Kidney	0.82	0.47	0.56	0.79	0.33	0.14	0.23
Lung	0.51	0.28	0.30	0.27	0.16	0.09	0.14
Spleen	0.58	0.55	0.47	0.17	0.66	0.57	0.46
MLN	0.19	0.23	0.13	-	-	-	-
Pancreas	0.07	0.29	0.09	0.01	0.08	nd	0.07
Eye	0.01	0.02	nd	nd	nd	nd	nd
Aorta	0.03	0.03	0.01	nd	nd	nd	nd
Trachea	0.01	0.03	0.02	0.01	0.01	nd	nd
Heart	0.28	0.15	0.28	0.28	0.13	0.08	0.19
Plasma	11.05	1.54	9.31	28.34	3.96	4.73	7.78
Urine	nd	0.09	0.03	0.01	0.04	nd	0.07
n	2	2	1	1	1	1	1

Table 4.14: Distribution of rcFUC in the brain of normal rats.

	CHO/rcFUC	`CHO/rcFUC	CHO/rcFUC*	CHO/rcFUC$_{cat}$	CHO/rcFUC mature	MDCK/rcFUC
	4 h	24 h	4 h	4 h	1 h	4 h
			%ID			
Total brain	0.041	0.123	0.003	0.058	0.145	0.059
Parenchyma	0.052	0.083	0.027	0.055	0.024	0.112
Vasculature	0.006	0.005	0.003	0.009	0.002	0.009
n	2	2	1	1	1	1

Rats infused with various forms of ^{3}H-labelled rcFUC were sacrificed at the times indicated. The brains were removed and processed for capillary depletion (section 2.2.47). ^{3}H-radioactivity was determined in each hemisphere. Results are expressed as %ID after summation of results from the two hemispheres and where n = 2, the mean value is given. n = number of rats in each group.

Table 4.15: ALP and GGT activity in brain fractions of rats after capillary depletion.

	CHO/rcFUC 4 h	CHO/rcFUC 24 h	CHO/rcFUC* 4 h	MDCK/rcFUC 4 h	CHO/rcFUC$_{cat}$ 4 h	CHO/rcFUC mature 1 h
ALP	**Vascular enzyme activity (nmol/min/mg)**					
Parenchyma	4.96	10.13	1.01	4.66	3.58	5.18
Vasculature	83.78	123.49	5.89	94.49	69.07	29.23
P/V (%)	5.9	8.2	16.9	4.83	5.18	17.7
GGT						
Parenchyma	1.38	5.56	nd	1.01	1.87	3.45
Vasculature	38.37	60.59	05.36	35.55	20.86	17.85
P/V (%)	3.59	9.17	0	2.83	8.96	19.3

Rats were infused with various forms of rcFUC and sacrificed at the times shown. To determine the efficiency of capillary depletion (section 2.2.47) brain parenchyma (P) and vasculature (V) from these rats were assayed for alkaline phosphatase (ALP) and γ-glutamyl transpeptidase (GGT) activity (enzyme markers for brain capillaries). Results are expressed as nmol/min/mg of sonicated brain fraction lysate. P/V (%) the amount of brain vasculature contaminating the brain parenchyma expressed as a percentage. nd, no activity detected.

4.3.4 OX26-Eu^{+3} labelling

Because of the lack of sensitivity afforded by the use of ^{3}H-radiolabelled rcFUC in the rat distribution studies (see above and discussion), a more sensitive method for detecting enzyme was trialled. Eu^{+3}-labelling was chosen because it is a relatively simple procedure and results in $> 10^{10}$ counts/mg of protein compared to approximately 10^{8} cpm/mg for rcFUC metabolically labelled with ^{3}H-leucine. OX26 was chosen as a model system to evaluate both the labelling and the analysis of biodistribution of Eu^{+3}-labelled material as it provides a positive control for BBB transcytosis.

The Eu^{+3}-chelate used for labelling reacts with primary amino groups of proteins *via* its isothiocyanate group under mild reaction conditions resulting in a stable and highly soluble chelate. In DELFIA Enhancement Solution it forms a highly fluorescent chelate with ligands present in this solution and has a long fluorescent lifetime that enables it to be detected by time-resolved fluorometry. OX26 was modified with Eu^{+3}-chelate as described in section 2.2.48. Free Eu^{+3}-chelate and a small amount of aggregates that form during the reaction were separated from OX26-Eu^{+3} by gel filtration chromatography (results not shown). The concentration of Eu^{+3} bound to OX26 was calculated by reference to a Eu^{+3} standard and was found to be 165 μM which was equivalent to 62.75×10^{10} counts/mg. The number of moles of Eu^{+3} bound /mole of OX26 was estimated to be 8.13.

4.3.5 Rat tissue distribution and plasma half-life of OX26-Eu^{+3}

Infusion of OX26-Eu^{+3} into a rat at 1 mg/kg body weight (1.25×10^{10} counts) resulted in its rapid removal from circulation in a typical biphasic manner (Figure 4.21). The half-life for the initial phase was less than 2 min while that of the second phase was 50 min. After 4 h there was 3.98% of the injected dose present in plasma (Table 4.18). Analysis of the brain after capillary depletion indicated that there was approximately 0.56% of the injected dose in the brain parenchyma with 0.17% in the capillary fraction (Table 4.16). The degree of contamination of brain parenchyma by brain vasculature after capillary depletion was 8.8% and 14.5% with respect to ALP and GGT, respectively. The majority of OX26-Eu^{+3} was found in liver (48.32%) followed by kidney (7.39%), spleen (1.92%), lung (0.67%) and minor amounts in other organs (Table 4.18).

Table 4.16: Distribution of Eu^{+3}-labelled OX26 in rat brain.

	% ID
Total brain homogenate	0.98
Brain parenchyma	0.56
Brain vasculature	0.17

A normal rat was intravenously injected with 1.25 x 10^{10} counts of Eu^{+3}-labelled OX26 and 4 h later sacrificed. The brain was removed and each hemisphere was treated separately as described in section 2.2.47. Capillary depletion to separate brain parenchyma from vasculature was performed. Results are expressed as the %ID after summation of Eu^{+3} counts in both hemispheres.

Table 4.17: ALP and GGT activity in the brain fractions of a rat injected with Eu^{+3}-labelled OX26.

	ALP	GGT
	(nmol/min/mg)	
Brain parenchyma	2.56	1.98
Brain vasculature	29.08	13.67
P/V (%)	8.80	14.5

After capillary depletion the brain parenchyma and vasculature were assayed for ALP and GGT activity. Results are expressed as nmol/min/mg of sonicated brain fraction lysate. P/V (%) is the amount of brain vasculature contaminating the brain parenchyma expressed as a percentage.

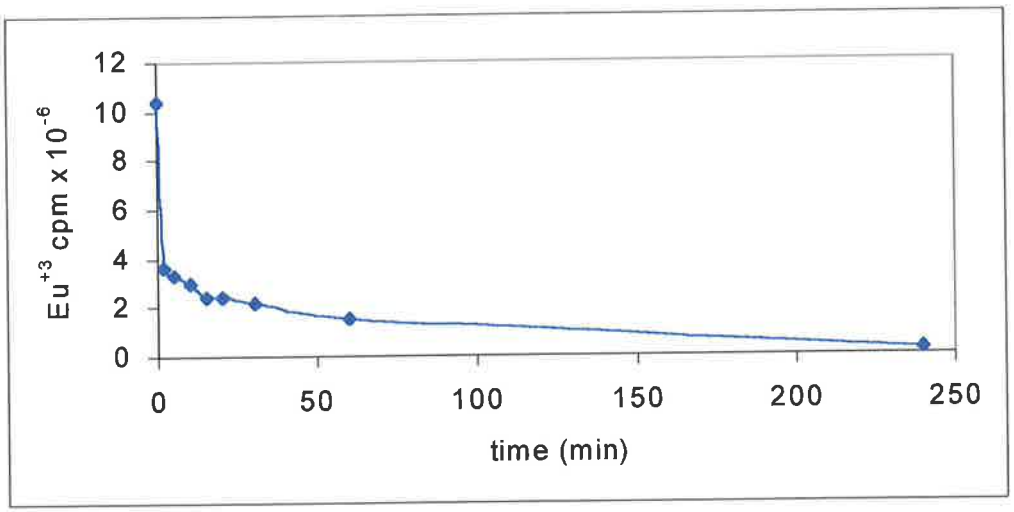

Figure 4.21: Plasma clearance of Eu^{+3}-labelled OX26.

A normal rat was injected with 1 mg/kg OX26-Eu^{+3} (1.25 x 10^{10} counts) and sacrificed 4 h later. Blood samples were removed at specified times and plasma assayed for Eu^{+3} counts as described in section 2.2.49.

Table 4.18: Distribution of Eu^{+3}-labelled OX26 in rat tissue.

Tissue	% ID
Liver	48.32
Kidney	7.39
Lung	0.67
Spleen	1.92
Pancreas	0.02
Trachea	0.02
Aorta	0.004
Eye	0.008
Heart	0.274
Plasma	3.98
Urine	0.36

A single rat was intravenously injected with 1.25 x 10^{10} cpm of Eu^{+3}-labelled OX26 and sacrificed 4 h later. Eu^{+3} counts were extracted as described in section 2.2.49 and results were calculated based on the total weight of each tissue and expressed as a % ID.

4.3.6 Tissue distribution and plasma clearance of rcFUC in fucosidosis dogs

As a prerequisite to evaluating various types of modified FUC for ERT in the fucosidosis dog model, preliminary baseline data regarding tissue distribution and plasma clearance of rcFUC in fucosidosis dogs were generated. Two male fucosidosis dogs, Bobby and Biggles, who were littermates, were used. Both animals displayed overt signs of fucosidosis at the time of experimentation (Dr. R. Taylor, University of Sydney, NSW, personal communication). Bobby was infused at age 10 months with 1 mg CHO/rcFUC/kg (13 mg total) which had a specific activity of 14,051 nmol/min/mg. Biggles was infused at age 16 months at the same dose rate (18 mg total) but with CHO/rcFUC having a slightly higher specific activity (17,000 nmol/min/mg). The difference in the specific activity of the batches of enzyme was due to the prolonged storage (2 years) of the enzyme for Bobby. CHO/rcFUC for Biggles was produced and purified immediately after expression. The purity of both batches of enzyme as assessed by SDS-PAGE was found to be similar.

Neither dog showed any adverse reaction to the infused enzyme either during infusion nor in the subsequent 48 h. Plasma clearance of CHO/rcFUC was assessed in Biggles only. The clearance was biphasic with an initial rapid phase and a longer secondary phase. Due to an insufficient number of data points the initial half-life could not be determined accurately (results not shown). However, in later studies (section 4.3.7) the half-life was estimated as 42-43 min for the first phase and 9 h for the second phase (Figure 4.22). Less than 5% FUC activity was detectable in plasma 24 h after administration.

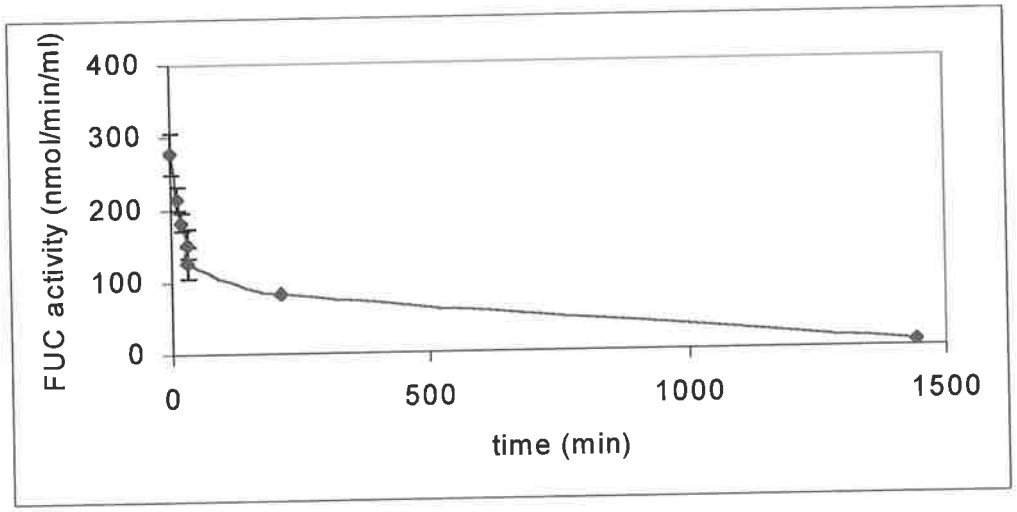

Figure 4.22: Clearance of infused rcFUC in Chelsea.

After a 10 min infusion of rcFUC blood samples were collected immediately after infusion and then at specified times thereafter. Plasma was tested for FUC activity (nmol/min/ml). Error bars = ± 1 SD.

Forty-eight hours after administration of enzyme the dogs were euthanased and tissues were analysed for residual FUC activity as described in section 2.2.53. Results indicated that in both dogs the overwhelming majority of enzyme was found in liver (94% of the injected dose in Biggles) (Table 4.19). Other organs with detectable enzyme activity in Biggles included heart (0.15%), spleen (0.13%), kidney (0.12%), lung (0.05%), lymph node (0.02%) and pancreas (0.01%) with undetectable levels in the remainder of the tissues analysed. No enzyme activity was detected in any of the brain sections. A similar trend was observed in Bobby. As weights of tissues were not available for Bobby, %ID to various organs could not be calculated.

Table 4.19: Tissue distribution of FUC in dogs.

Bobby, Biggles and Chelsea are fucosidosis affected dogs, Zanadu is a carrier. Bobby and Biggles were each infused with a single dose of CHO/rcFUC at 1 mg/kg body weight and euthanased 48 h later. Chelsea was receiving ERT for one year at doses shown in Figure 4.23 and was euthanased 48 h after a final infusion of 1 mg/kg. Tissues were processed as described in section 2.2.53 and assayed for FUC activity and total protein. Results are expressed as U (nmol/min/mg). Where tissue weights were available (Biggles and Chelsea), results are expressed as %ID). – indicates that the tissue was not available for analysis. ND, not determined (because tissue weight was not available). nd, no activity detected.

	Bobby U	Biggles U	Biggles % ID	Chelsea U	Chelsea % ID	Zanadu U
Liver	2.30	1.98	94.41	3.07	95.90	0.98
Kidney	0.31	0.02	0.12	0.02	0.07	0.79
Lung	0.05	0.01	0.05	0.01	0.06	-
Spleen	0.08	0.01	0.13	0.09	0.07	1.22
Pancreas	0.01	0.01	0.01	0.01	0.21	0.26
Eye	0.04	0.21	ND	0.02	ND	-
Muscle	nd	nd	0	0.01	ND	-
Skin	0.14	0.02	ND	0.01	ND	-
Heart	0.03	0.02	0.15	0.02	0.09	-
Bone marrow	0.24	0.23	ND	0.07	ND	-
Thyroid	0.01	nd	0	nd	0	2.65
Salivary gland	0.01	nd	0	nd	0	7.44
CSF	-	-	-	0.01	ND	-
Sciatic nerve	0.01	0.02	ND	0.01	ND	0.17
Vagus nerve	0.02	nd	0	nd	0	0.16
Cervical spinal cord	0.01	0.02	0	nd	0	0.22
Thoracic spinal cord	0.01	0.02	ND	0.01	ND	0.18
Dorsal root ganglion	-	0.02	ND	0.02	ND	0.61
Frontal cortex	nd	nd	0	nd	0	0.23
Thalamus	nd	nd	0	nd	0	0.22
Striatum	nd	nd	0	nd	0	0.24
Cerebellum	nd	nd	0	nd	0	0.19
Cerebellar nuclei	nd	0.01	ND	nd	0	0.27
Medulla	nd	0.01	0	nd	0	0.26
Lymph node	0.30	0.38	0.02	-	-	0.55
Pons	-	nd	0	-	-	-
Parathyroid	0.08	-	-	-	-	-
Corpus callosum	nd	0.01	ND	nd	0	0.20

Table 4.20: Identification of fucosidosis phenotype in dogs.

	Plasma FUC activity (nmol/min/ml)	WBC FUC activity (nmol/min/mg)	WBC β-Hex activity (nmol/min/mg)	FUC activity:β-Hex activity[#]
Biggles	0.023	0.022	29.17	0.33
Chelsea	0.023	0.002	16.52	0.39
Virgil	0.979	1.367	37.67	15.35*
Alis	0.31	1.473	23.13	17.33*
Castor	0.94	1.653	40.83	16.04*
Courtney	1.04	0.901	31.7	13.15

Biggles and Chelsea are affected dogs, the others are carriers. [#] The ratio of FUC activity:β-Hex activity is calculated from plasma FUC activity and WBC FUC and β-Hex activity according to the following equation:

5 x plasma FUC activity + 2.84[(WBC FUC activity /WBC β-Hex activity) x 100]

According to this calculation dogs are classified as follows: affected, <6; carriers, 6-<14; normal, 14-20. This calculation is valid for newborn dogs only (Healy *et al.*, 1984). *These three dogs are carriers but show ratios >14 as their plasma and WBC were assayed at an older age. Courtney, a carrier, was assayed at birth.

4.3.7 Long-term ERT in a fucosidosis dog

Chelsea, a female fucosidosis dog was initially diagnosed within 24 h of birth by a low FUC/β-hex ratio (Table 4.20). According to the Healy discriminant function (Healy *et al.*, 1984) Chelsea had a ratio of <6 which indicates affected status. This diagnosis was later confirmed by PCR/ASO analysis (Sharon Chin, Department of Chemical Pathology, WCH, personal communication). ERT at 1 mg CHO/rcFUC/kg body weight/week was commenced at 2 months of age and the dosage regimen during the course of therapy was as shown in Figure 4.23. The changes in the regimen were determined solely by the availability of enzyme. Throughout therapy Chelsea showed no adverse reactions to infused enzyme. Plasma samples were screened for antibodies to FUC as described in section 2.2.55. Only very low antibody titres in the range of 1/2,000 -<1/10,000 were detected. (Figure 4.24). No antibody titre was detected in the plasma from a carrier dog (Courtney), tested in a similar manner (Figure 4.24). In order to determine if the low titre observed in Chelsea was due to a response to Chinese hamster FUC present in the CHO/rcFUC preparation (section 4.1.1), reactivity to MDCK/rcFUC, which represents 100% canine FUC, was tested. However, no difference in the titre to CHO/rcFUC and MDCK/rcFUC was observed (Figure 4.25).

Measuring urinary excretion of storage products is one way of monitoring the efficacy of therapy in some LSD. In fucosidosis, storage products have terminal fucose moieties and are found at hypernormal levels in the urine of affected dogs. The method used (section 2.2.56) for fucose determination in fucosidosis dog urine does not discriminate between free and bound L-fucose, the latter being released during the procedure by acid hydrolysis. During ERT the level of L-fucose in Chelsea's urine fluctuated but overall there was less L-fucose than in the urine of an affected dog, Biggles (Figure 4.26). In fact the levels in the treated dog more closely resembled those found in a carrier dog, Virgil who had two to three-fold lower levels of urinary L-fucose compared to Biggles. However, these results cannot be considered conclusive as age and sex-matched normal and affected dog urine was not available for direct comparison.

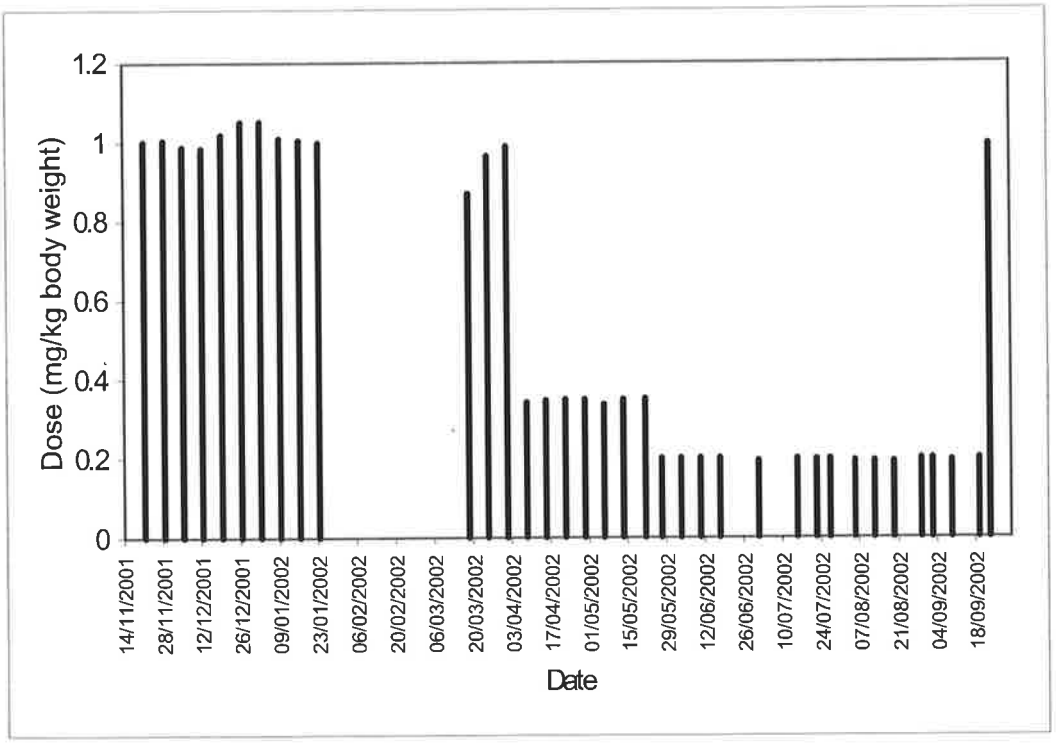

Figure 4.23: Dosage of CHO/rcFUC administered to Chelsea during the treatment period.

Chelsea was infused with a concentration of rcFUC ranging from 0.2 mg/kg to 1.0 mg/kg on a weekly basis as shown above. Enzyme was unavailable for a period of approximately 6 weeks between 28/01/01 and 14/03/02 and was infused on a fortnightly basis between 21/06/02 and 14/07/02.

At the start of therapy Chelsea weighed 4.1 kg and her progressive weight gain during the ERT trial was initially similar to that of a carrier female dog (Courtney). However, her rate of weight gain started to decline at about 100 days of age and remained between 22-27% of Courtney's rate of weight gain for the remainder of the ERT trial (Figure 4.27). In contrast, Biggles, an untreated male fucosidosis dog, showed an earlier cessation in weight gain (200 days) compared to Chelsea (260 days). Chelsea displayed no overt signs of fucosidosis up to age 11 months apart from being slower to learn (first noted at 6 months of age) compared with age-matched normal dogs. Chelsea was diagnosed with subtle but unequivocal diffuse cortical disease when assessed neurologically two weeks prior to euthanasia. She displayed excessive anxiety with minimal restraint, had occasional proprioceptive deficits with regards to positioning of the rear hindlimbs particularly when turning during walking, and was slower than normal when tested for the hopping response. Her gait and posture were normal, as were cranial nerve responses and spinal reflexes (Figure 4.28).

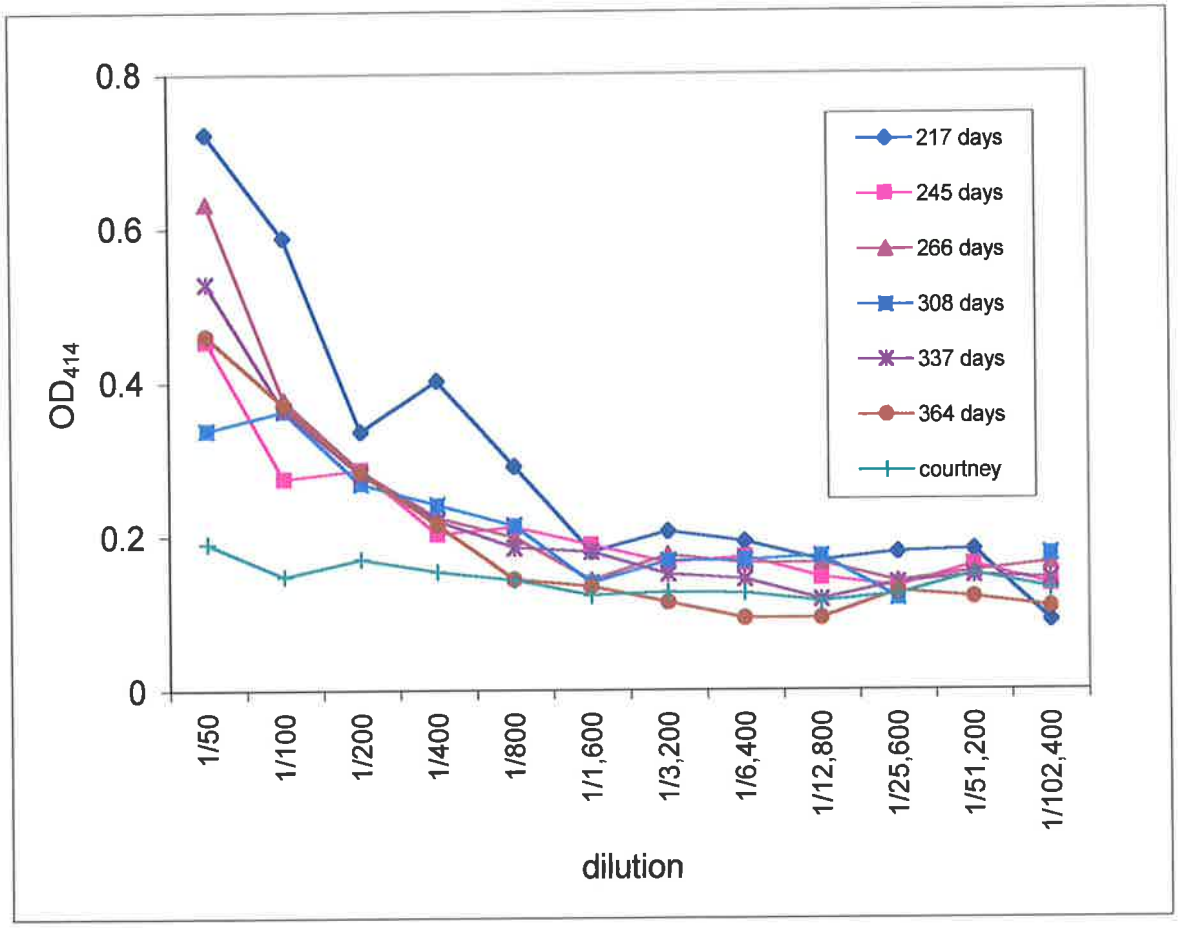

Figure 4.24: Elisa to detect antibody response to infused rcFUC.

Blood samples were collected from Chelsea prior to enzyme infusion over the treatment period and the plasma (at the ages shown) was tested in an Elisa (section 2.2.55). Plasma from Courtney, a carrier littermate that had received no ERT, was also tested.

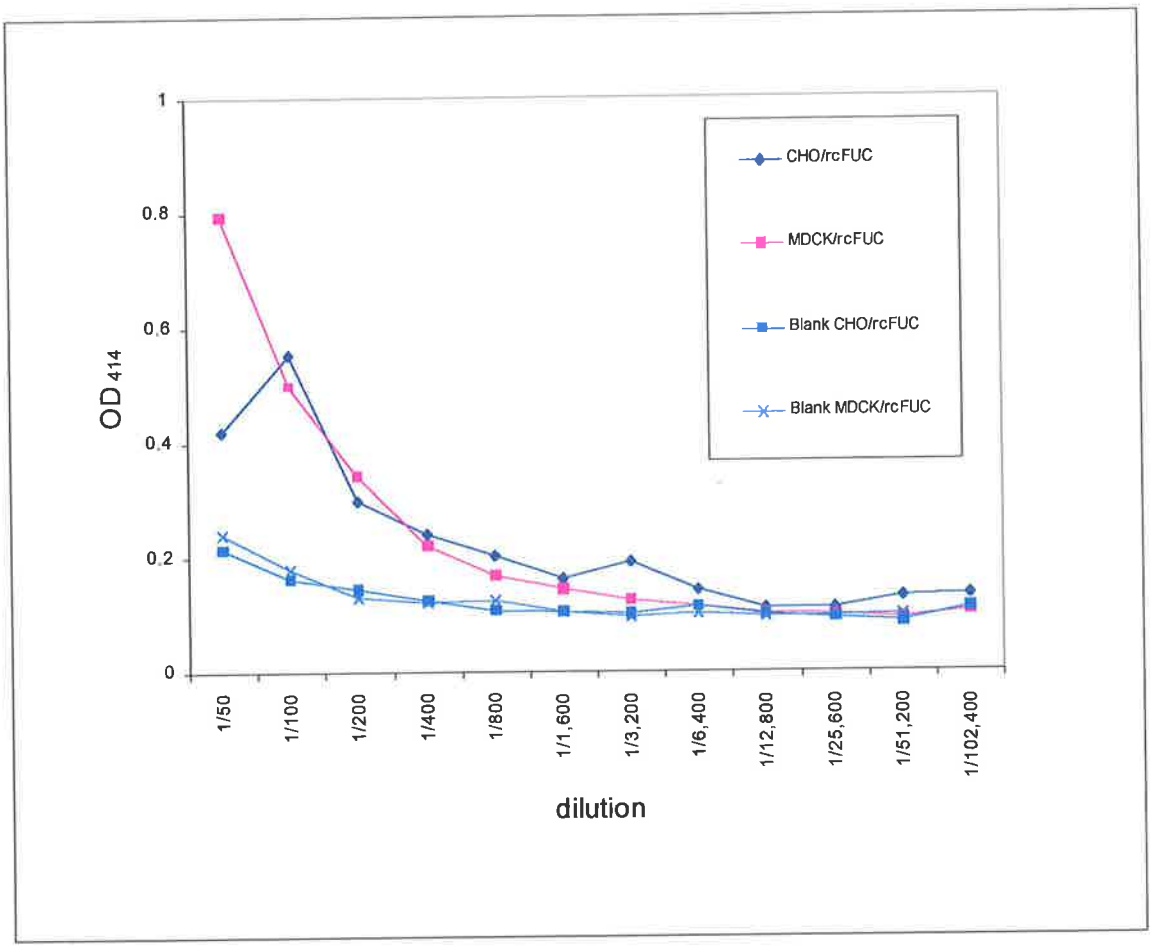

Figure 4.25: Comparison of antibody response to CHO/rcFUC and MDCK/rcFUC using an Elisa.

Plasma from Chelsea at age 217 days was tested against CHO/rcFUC and MDCK/rcFUC in an Elisa (section 2.2.55). Control wells without plasma were tested for non-specific reactivity to the two forms of enzyme.

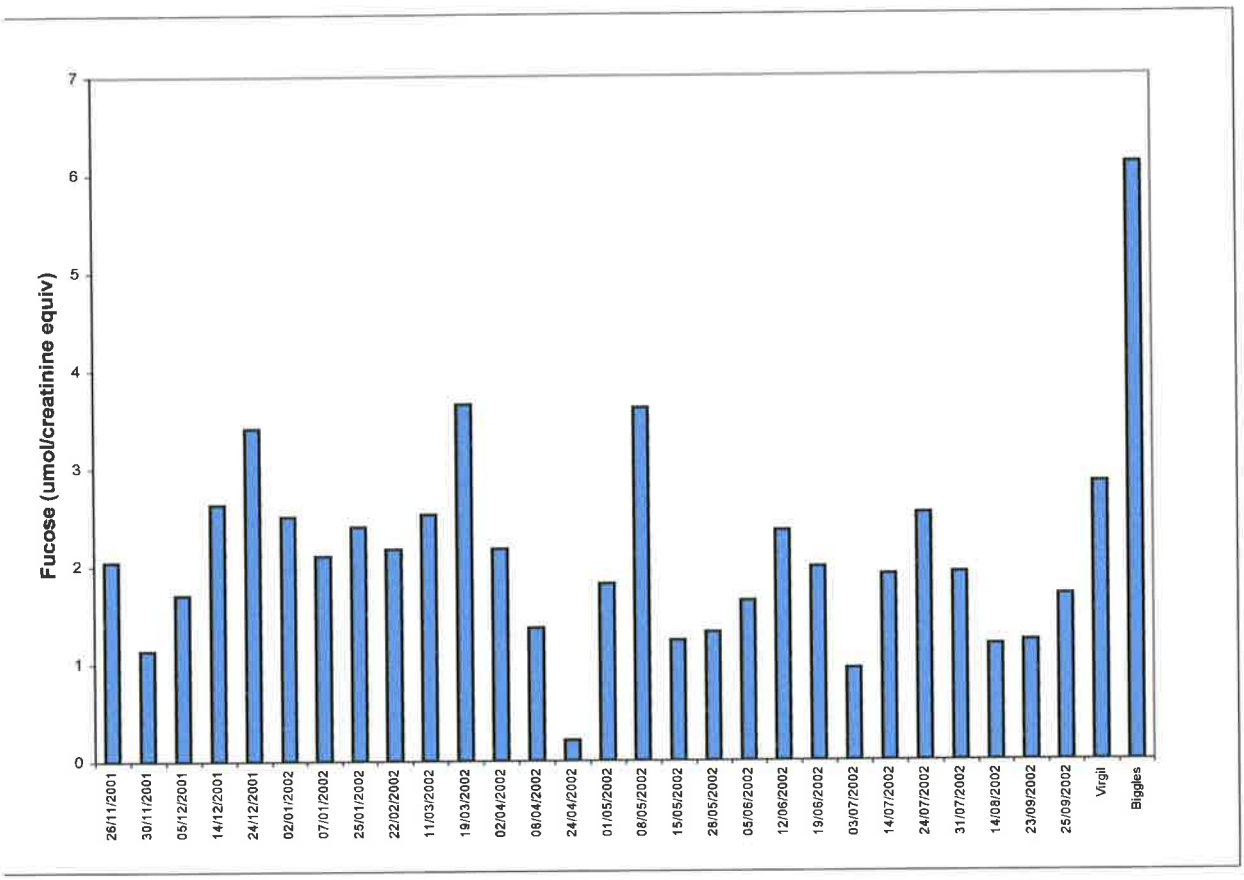

Figure 4.26: Total urinary fucose excretion in Chelsea over the treatment period.

Urine was tested for both free and bound fucose according to the method outlined in section 2.2.56. Fucose levels were compared with those from the urine of Biggles, a fucosidosis affected dog and from Virgil, a fucosidosis carrier dog. Results for Virgil and Biggles are shown far right. Urine from neither of these two dogs was matched for age. Results are expressed as μmol/creatinine equivalent.

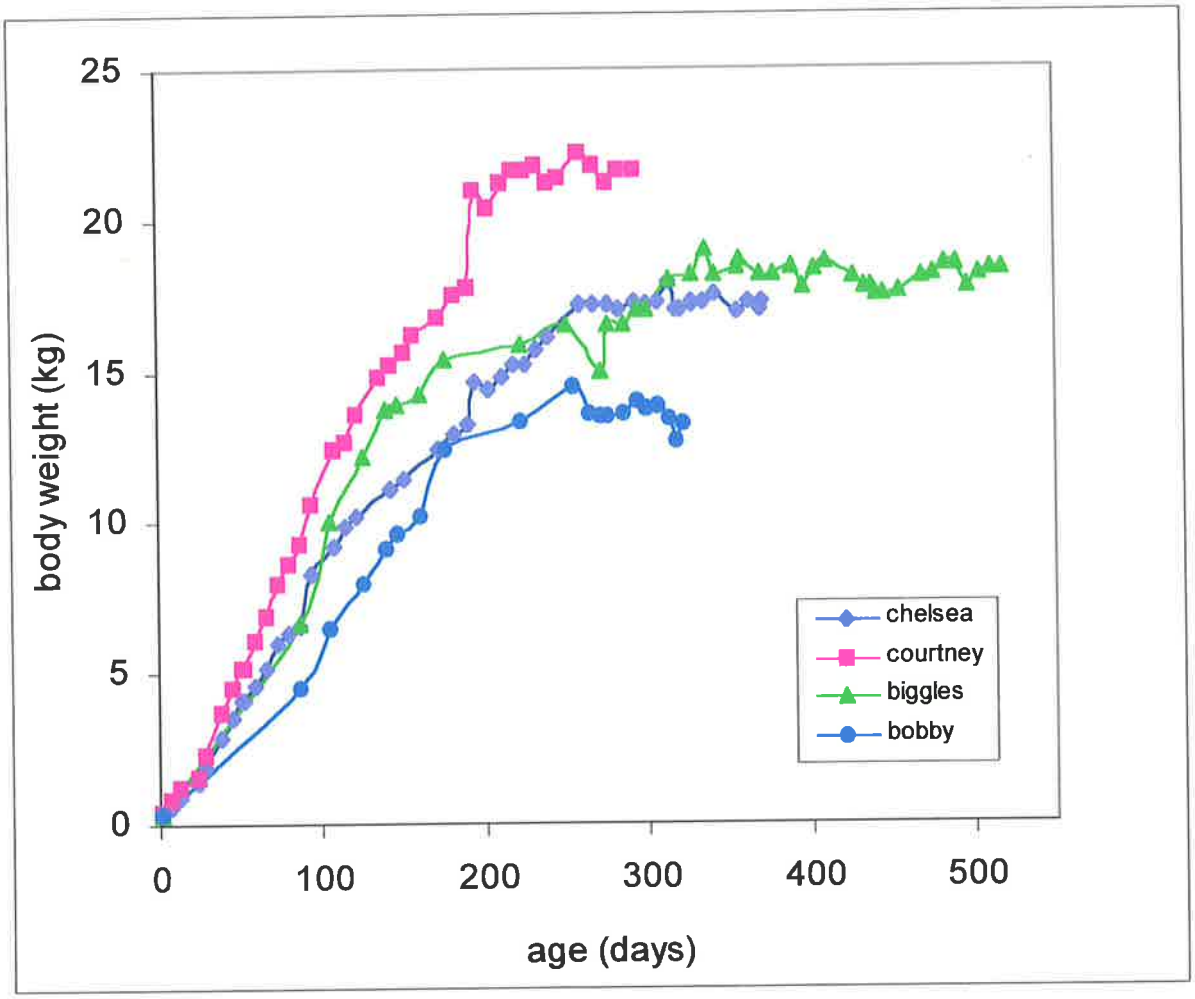

Figure 4.27: Body weight of dogs with age.

Body weight (kg) of Chelsea, a fucosidosis dog treated with ERT, and Biggles and Bobby (untreated fucosidosis dogs) is compared with that of Courtney, a fucosidosis carrier dog, as a function of age (days).

Chelsea was euthanased 48 h after receiving a final dose of enzyme at 1 mg/kg. At autopsy macroscopic examination of tissues revealed no disease pathology. Tissues and nerves collected for histological analysis have yet to be processed. Samples of tissues taken for analysis of residual FUC activity showed that the majority of the activity was found in liver (Table 4.19) with much lower levels in kidney, spleen, bone marrow and heart. The enzyme levels measured in brain and nerves are at the limits of detection of the assay. In contrast, readily detectable levels of FUC activity are seen in somatic and neurological tissues of a female carrier dog, Zanadu (Table 4.19). Again caution must be exercised in interpreting these data as they are based on limited animal numbers.

To date the histological analysis of tissue sections has not been carried out except in CSF where many of the mononuclear cells were seen to be vacuolated. The cytoplasmic vacuoles ranged from multiple small vacuoles to a few large vacuoles, which in both instances tended to push the nucleus to one side of the cell. The absolute and relative cell counts and protein concentration fell within the normal range.

Figure 4.28: Clinical appearance of Chelsea at 12 months of age.

Chelsea was infused with rcFUC at the dose rates shown (Figure 4.23) for approximately one year. These photographs were taken after the final enzyme infusion, which was 2 days prior to euthanasia. (A) Chelsea displayed a bright and alert demeanour. Occasionally she displayed a wide-based stance and was beginning to show proprioceptive deficits in the pelvic limbs. (B) The proprioceptive deficit in the right hindfoot is obvious. Also evident is distinctive thick feathering along the ventral aspect of all limbs. Feathering is a common feature in fucosidosis-affected English springer spaniels.


A


B

4.3 Discussion

4.3.1 Plasma circulating half-life and tissue distribution of various forms of rcFUC in rats

All forms of rcFUC (CHO/rcFUC, MDCK/rcFUC, mature CHO/rcFUC and cationized CHO/rcFUC) were cleared from plasma in a bi-exponential manner with a rapid initial half-life of between 1-2 min in rats. The secondary phase was variable and dependent on the form of enzyme. Cationized CHO/rcFUC ($T_{1/2}$, 90 min) was removed from circulation faster than unmodified CHO/rcFUC ($T_{1/2}$, 150 min) but more slowly than MDCK/rcFUC ($T_{1/2}$, 45 min) and mature CHO/rcFUC ($T_{1/2}$, 12 min). However, further experimentation is required to allow determination of the statistical significance of these differences in clearance rates.

To determine if the slow clearance of CHO/rcFUC was due to saturation of M6PR, a 10 x higher dose was tested. However, increasing the dose to 10 mg/kg gave a similar bi-exponential rate of clearance with similar half-lifes for each phase, thus indicating that this was not the cause for delayed clearance. The slight increase in plasma levels after the initial rapid drop is presumably due to passage of the enzyme bolus in circulation.

Alternatively, because the preparation of CHO/rcFUC comprises precursor and mature forms, it was thought that the prolonged persistence in plasma may be due to the mature form, which lacking the M6P recognition signal, may be cleared from circulation more slowly. However, the mature enzyme was actually cleared extremely rapidly corresponding to a larger percentage present in liver (Table 4.13). Although it would appear obvious that all recombinant mannose-6-phosphorylated lysosomal enzyme would be cleared in the same manner and at similar rates, this is not so. For example, r4S is cleared very rapidly (not detected in circulation after 2 h) while rcFUC is cleared more slowly. Delayed plasma clearance has also been noted with recombinant caprine N-acetylglucosamine-6-sulphatase which stays in circulation for 23.2 ± 23.3 min and α-mannosidase of which substantial levels are still detectable in plasma up to 72.5 h in guinea pigs and 79 h in rats (B King, Department of Chemical Pathology, WCH, unpublished observations). The reason for this may be that the different enzymes are being endocytosed *via* different receptors (i.e., other than the M6PR), that they have very different affinities for the M6PR or that other factors are preventing uptake. The rapid uptake of mature rcFUC suggests that uptake *via* other receptors does occur. However, this does not mean that

uptake of the precursor form is not *via* the M6PR. Sialylation has been proposed as a factor that prolongs the circulation of proteins in plasma (Morrell *et al.*, 1971; Joshi *et al.*, 1995). However, when MDCK/rcFUC, which has been shown to have sialic acid residues, was tested it too demonstrated a similar clearance pattern to CHO/rcFUC, which is not sialylated.

From the data presented in this thesis, which admittedly is based on limited animal numbers, plasma clearance of cationized rcFUC is more rapid compared to unmodified enzyme but this is not accompanied by increased levels in tissues other than liver. No increase in enzyme uptake was seen in brain. One explanation for this may be that the degree of cationization was not sufficient and the experiment should be repeated with more highly modified enzyme. However, this has the drawback of significantly reducing activity.

As mentioned previously, distribution of the various forms of enzyme were similar with the majority of enzyme found in liver. This has been observed in distribution studies of rf4S and rh4S in cats (Table 3.11). Sequestration of enzyme to liver is not surprising given that liver is a large, well-vascularized organ with an abundance of M6PR and other receptors. Therefore, regardless of the modification, enzyme will be efficiently endocytosed by liver. Limiting uptake of enzyme by liver is difficult. In one study using human placental β-glucuronidase in normal rats, removal of the abdominal viscera including spleen, and interruption of the portal circulation before infusion showed delayed plasma clearance and allowed significant uptake by bone and other organs (Achord *et al.*, 1977). As a practical consideration in patient treatment, this is obviously not feasible but it does illustrate the potential value of reducing uptake by liver.

That cationization of rcFUC did not increase transcytosis to the brain may be due to an insufficient degree of cationization. Studies with cationized IgG (pI 10.7) and rat serum albumin (pI 8-9) have indicated that cationization does not lead to enhanced uptake into all tissues. Unlike lysosomal enzymes, albumin and IgG are proteins that are normally abundant in plasma and cationization has shown to increase their uptake into brain, kidney and liver. Cationized SOD and CAT also showed increased levels in brain (Poduslo and Curran, 1996a; Poduslo and Curran, 1996b; Wengenack *et al.*, 1997b; Wengenack *et al.*, 1997a; Poduslo *et al.*, 1998; Poduslo *et al.*, 2000).

Because uptake into brain is so low compared to most other tissues it is important to be able to evaluate this level accurately. Contamination of brain tissues with blood or vasculature has to be eliminated or taken into consideration. In studies presented here exsanguination prior to dissection of brain and the subsequent rinsing of the brain in PBS, were routinely performed to minimise contamination with extraneous blood. However, contamination of brain from vasculature may still occur and needs to be accounted for. Capillary depletion is a method which allows differentiation between transcytosed enzyme and enzyme bound to brain capillaries. Success of capillary depletion was measured by ALP and GGT activity, two enzymatic markers for brain capillaries. Generally less than 10% activity of these enzymes is detected in brain parenchyma compared to brain capillaries. The level of these enzymes in the parenchyma fraction also gives a good indication how well the capillary depletion procedure was performed. Alternatively, the degree of contamination from blood in brain capillaries can be deduced from the amount of radiolabelled enzyme in plasma and the volume of blood in rat brain capillaries, which is approximately 8 µl. Contamination from this source can be significantly lowered by perfusing the animal before euthanasia or alternatively, the distribution study could be extended to such a time when no radioactivity is detected in plasma. The main difficulty with the latter method is the possibility of degradation of radiolabelled enzyme in peripheral tissues with subsequent uptake of metabolic products into brain which can compromise pharmacokinetic evaluation. Studies using unlabelled enzyme followed by its detection with monoclonal antibodies either by capture assays, quantification by Elisa or immunofluorescence, were not possible as attempts to make suitable, species-specific anti-cFUC antibodies were unsuccessful.

Considering the limited availability of enzyme for uptake into brain, as well as the relatively low specific radioactivity of enzymes using tritium labelling, a more sensitive detection method is preferable. Europium is readily covalently bound to proteins under mild conditions giving approximately 6 orders of magnitude more cpm than ^{3}H-labelled enzyme. OX26 was used as a positive control as it has been shown to be transcytosed into brain at 0.26% of the injected dose after 60 min and up to 0.5-0.7% after 24 h (Pardridge *et al.*, 1990b). When Eu^{+3}-labelled OX26 was injected into a rat it had a similar biphasic plasma-clearance curve to rcFUC and after 4 h, 3.98% of the injected dose was still present in plasma. Tissue distribution was also similar but more was found in kidney compared to spleen and other tissues which may reflect the number of Tf receptors present on the respective cells. The amount detected in brain

parenchyma was 0.56% of the injected dose (not taking into account potential contamination from brain capillaries (approximately 12%) and therefore in agreement with previous studies. This method seems worthy of further investigation particularly with a view to the analysis of OX26-FUC conjugates.

4.3.2 ERT in the fucosidosis dog

ERT in the fucosidosis dog Chelsea appeared to have an ameliorating effect on the symptoms which are normally observed in untreated fucosidosis dogs of a similar age. Apart from being slower to learn compared to age-matched normal dogs, no other overt signs of disease were obvious until approximately 11 months of age. Hypermetria and a wide-based stance at age 7 months are usually the first signs of a neurological defect before incoordination and proprioceptive deficits become evident. Chelsea displayed mild signs of CNS dysfunction at a time when most affected dogs show obvious signs (R. Taylor, personal communication). One affected animal, Biggles, for instance, had mild signs of hypermetria and ataxia and was running in circles frequently at 7 months of age. By age 9 months he was not responding to being called and by 12 months had definite proprioceptive deficits as well as increased ataxia and difficulty in maintaining balance when jumping. Neurodegeneration was more pronounced in a second affected dog, Bobby, and was obvious at an earlier age. His condition was compounded by hydrocephalous confirmed on post mortem examination.

Clinical evaluation is therefore suggestive of a positive effect on CNS pathology results from ERT. However, according to results of residual FUC activity in tissues, there was no increase in the amount of enzyme in nerves and brain segments compared with dogs given a single dose of replacement enzyme. Because the canine BBB is assumed to be fully developed at birth it was not expected that systemically infused enzyme would cross the BBB. The blood-CSF-barrier is less stringently fenestrated than the BBB but as no enzyme activity was detected in the CSF and the macrophages of the CSF were still highly vacuolated, this would suggest that significant amounts of enzyme are not being transcytosed *via* this route to the brain. Furthermore until histological examination of brain and nerve tissues is carried out it is impossible to say that ERT has had any effect on any of these tissues. Therefore the result is intriguing but without further study cannot be taken to represent a real effect.

Interestingly, only a weak antibody response to replacement enzyme was detected despite fucosidosis dogs having almost undetectable amounts of FUC. In addition, ERT was not instigated at birth, a time at which tolerization to foreign antigens can occur. The antibody response that was observed was not to the contaminating hamster FUC present in the enzyme preparations as demonstrated by similar reactivity to MDCK/rcFUC and CHO/rcFUC. The antibody response is therefore either to FUC or to a contaminant that has been carried through the purification procedure. This could be resolved by western blot analysis.

Urine fucose levels were found to be similar to those of a normal control dog. However, lack of urine samples from normal and affected age and sex-matched dogs precludes definitive conclusions to be drawn from the data in this study and instead merely illustrates a trend. However, presuming that the major proportion of urinary fucose is derived from storage material in peripheral tissues it would be expected that ERT has decreased the storage load in some tissues, particularly liver.

4.1 Conclusions

rcFUC was expressed in CHO and MDCK cells and both forms of the enzyme were similar with respect to physical and kinetic parameters. One difference observed was in pI that is most probably due to a variation in glycosylation (sialylation). Both CHO/rcFUC and MDCK/rcFUC were similar in many respects to other mammalian FUC.

In order to enhance enzyme penetration through the BBB, rcFUC was modified either by cationization or by covalent linkage to a vector molecule. Cationization was relatively easy and could be controlled such that a reasonable degree of modification could be achieved while retaining a feasible level of enzyme activity. However, compared to native enzyme cationized rcFUC conferred no advantage in transcytosis to the brain of a normal rat. This study needs to be repeated with rcFUC cationized to a greater degree to ascertain more clearly the potential for using this method for transcytosis into brain. The potential toxicity of cationized enzyme also needs to be investigated although reports in the literature suggest the safety of this approach (Pardridge *et al.*, 1990). In addition, potential immunogenicity has to be evaluated although cationization of homologous proteins results in a relatively mild immune response whereas cationized heterologous proteins have been shown to be highly immunogenic (Bickel *et al.*, 2001).

Chimeric peptide technology whereby a protein therapeutic, in this case a lysosomal enzyme, is chemically coupled to a transport vector known to cross the BBB, appears difficult, although not impossible. Difficulties were found in controlling the modification of proteins with chemical cross-linking agents such that the stoichiometry of modification of both vector and 'passenger' molecule is of the order of 1:1. Derivatization resulting in stoichiometries greater than this ratio result in subsequent conjugation reactions in which aggregates or polymers are produced. These aggregates are generally inactive and may also be too large to be transported by receptor-mediated transcytosis across the BBB. Other problems encountered included maintaining enzyme activity, and the relevant binding domains of both the vector and the passenger (enzyme) molecule, during the derivatization and conjugation reactions. The antigenicity of the chimeric molecule also needs to be evaluated as the process may result in new epitopes. Furthermore, if murine antibodies are used as vectors, as is OX26, constant exposure may result in an antibody response. However, humanisation of mouse monoclonal

antibodies, by fusing the variable region of the mouse monoclonal antibody to the constant region of human immunoglobulin (Pardridge *et al.*, 1995; Coloma *et al.*, 2000) would minimise this risk.

The results and theoretical arguments presented in this thesis indicate that the use of insulin, and more particularly the insulin tryptic fragment, F007, as a transport vector has significant limitations. The experience with OX26 shows that it is more readily coupled to the molecule of interest. OX26 conjugated to rcFUC fulfilled some of the criteria essential for suitability as an active conjugate. The binding domain for the Tf receptor of the conjugate and enzymatic activity were maintained. With Europium labelling of the OX26 moiety, uptake studies of OX26-FUC into rat brain could be more accurately determined. If these conjugates show a positive response in the rat their application in the fucosidosis dog model will be dependent on the ability of OX26 to bind to the dog Tf receptor. It is known that the OX26 antibody does not crossreact with the mouse Tf receptor (Lee *et al.*, 2000) but whether this is also the case for the dog receptor is not known. Flow cytometry using MDCK cells, which are known to have Tf receptors on their surface (Wan, 1992), may be used to ascertain the cross-reactivity of OX26 with the canine Tf receptor.

Long-term ERT in a fucosidosis affected dog, Chelsea, appeared to have some effect in delaying disease progression according to subjective clinical and neurological observations. These were supported by reasonable weight gains with age and decreased urinary fucose excretion. In addition, no substantial antibody response to infused enzyme was observed in the treated dog despite the low level of hamster FUC present in the enzyme infusion and despite the later start of therapy at 2 months of age when any advantage conferred by tolerization to foreign antigen may have been lost. However, significant levels of residual enzyme activity in tissues other than liver, and to a lesser extent in kidney, spleen and lung, were not observed. It may be that the levels of enzyme activity in some of these tissue may be below the level of detection of the enzyme assay, especially 48 h post infusion, but this very small amount of enzyme may be having an effect on clearance of some storage. Until histological assessment of tissue sections is performed it is difficult to clearly state what effect ERT is having on them. Ideally, treatment of a larger number of dogs together with age and sex-matched controls would allow for more definitive conclusions to be drawn about the effects of ERT.

Chapter 5: General conclusions and future work

5.1 Introduction

When the work described in this thesis was started the viability of using the systemic infusion of replacement enzyme for the treatment of somatic pathology in LSD had been demonstrated in a number of small and large LSD animals and clinically for Gaucher patients. Although ERT has proven remarkably effective this approach to therapy is not without limitations. These limitations are exemplified by tissues such as cartilage and cornea, which are avascular, and in which significant correction of pathology is not seen. In addition, despite the vast amount of blood directed to the brain, it too is essentially avascular by virtue of the presence of the BBB, which is discriminatory in terms of the type of molecules allowed access into the CNS. This means that patients with disease states that involve substantial CNS pathology are not regarded as suitable candidates for ERT. Considering that approximately two-thirds of all LSD patients in Australia develop CNS pathology, this means a large number of patients have no treatment options at present.

As most animal trials of ERT had been studied using the human form of the missing enzyme, the first major aim of the work described in this thesis was to evaluate the efficacy of ERT using same-species enzyme, i.e., feline 4S in MPS VI cats, the hypothesis being that native enzyme in its natural environment may be more efficacious. The second main aim was to assess the utility of chemical modification of replacement enzyme in facilitating its transport into brain after intravenous administration. The success of this approach would broaden the application of ERT to include patients with neurological disease.

5.2 Conclusions

A 6-month trial of ERT using rf4S in MPS VI cats and commenced at birth demonstrated a better outcome than a similar study using the same dose of human enzyme. In several instances rf4S was superior or equivalent in its effect as a 5-times higher dose of rh4S. Given that human MPS VI patients generally die from cardiopulmonary complications, it is of note that aorta was totally cleared of storage material and heart-valve almost totally cleared. A marked improvement in skeletal pathology with regard to bone length and bone quality was observed with rf4S, thus contributing to improvements in mobility and quality of life. As indicated in

previous studies, to maximise the benefits of therapy for patients, early onset of treatment is indicated particularly for normal bone growth and development. Commencement of ERT at birth in cats with rh4S resulted in tolerization against antibody production and therefore eliminated possible interference in these studies to compare efficacy of rf4S and rh4S to treat MPS VI. Therefore, it would appear most likely that the intrinsic interactions of native enzyme in its native cellular environment affect how well the enzyme functions. Differences in glycosylation and the presence of an extra cysteine residue in f4S (McGovern *et al.*, 1982) may be important factors in this process.

Therefore, the main implication arising from this study is that a lower dose of human enzyme than that indicated by initial trials using h4S in MPS VI cats may be appropriate in the clinical setting. This has obvious implications for the design of clinical trials. Indeed the results of this study prompted the evaluation of a Phase II trial for MPS VI patients in which 1 and 0.2 mg rh4S/kg were used (Harmatz *et al.*, 2001). Results to date indicate a comparable outcome for both doses whereas studies using rh4S in the cat suggested that a 0.2 mg/kg had little effect on pathology. The general conclusion that may be drawn from this project is that animal studies should preferably use native, rather than human, enzyme if they are most accurately to reflect clinical usage.

Strategies for enhancement of transport of enzyme into the CNS that were studied included chemical cationization and the production of enzyme-vector conjugates. Cationization of proteins has been demonstrated to be effective in the transcytosis of these compounds into brain. However, when the preservation of catalytic function is imperative, a balance between the degree of cationization and the level of enzyme activity is needed. The lower degree of cationization imposed by this constraint is reflected in less efficient transport into brain. Cationized rcFUC, which retained approximately 70-80% activity, showed no evidence of being taken up into rat brain in significant amounts.

The production of enzyme-vector conjugates proved more challenging than cationization. As with cationization, enzyme activity needs to be preserved. In addition, the binding sites of vector to its receptor on the BBB, and of the enzyme to the M6PR on brain cells, need to be preserved, although the requirement for the latter may not be as stringent given that uptake of enzyme *via* receptors other than the M6PR can be achieved in some cell types. Whether this is

also true for brain cells is not known. Ideally a stoichiometry of 1:1 (vector:enzyme) is desirable. If the stoichiometry is greater than 1:1 for either or both molecules, aggregate formation will occur and this may compromise enzyme activity or mask the binding sites of each component of the chimeric conjugate. Generally it was found to be difficult to control the modification reactions, but this may be related to the small scale of the experiments done in these studies which were limited by the quantity of material (especially recombinant enzyme) that could be produced.

The use of insulin as a vehicle was ultimately considered unviable on the basis of practical considerations regarding maintenance of its receptor binding site. OX26 as a vector molecule showed greater potential. However, during *in vivo* rat distribution studies it became increasingly obvious that the detection of ^{3}H-labelled enzyme in brain would not be sensitive enough to determine unequivocally that transcytosis had occurred. Eu^{+3} labelling of OX26 provided a better approach and levels of OX26 detected in brain (0.56% ID) were comparable to those reported in the literature.

A long-term ERT study in the fucosidosis dog model using rcFUC demonstrated enzyme activity in various tissues with the highest being in liver and undetectable levels found in brain. Urinary fucose excretion was decreased to levels seen in a heterozygote carrier dog and no antibody response was observed during treatment. Additionally, the onset of neurological symptoms appeared to be delayed. This may be due to normal variance in symptoms observed in fucosidosis dogs, the result of very low levels of enzyme reaching the CNS *via* macrophage migration across the BBB, access of enzyme to the brain *via* a BBB damaged as a result of the disease or some mechanism as yet unknown. The colonisation of brain with macrophages after BMT has been demonstrated in fucosidosis dogs. The process is slower than in other visceral organs, requiring at least 6 months to reach approximately 20% of normal enzyme activity in brain. A year-long trial of ERT may result in some cellular migration although obviously not to the same extent as in BMT studies and it would necessitate a long half-life of the enzyme within circulating macrophages. The fact that no FUC activity was detected in brain fractions may be due to the limits of detection of the enzyme assay. However, this does not preclude the presence of sufficient enzyme to have some effect on storage and pathology. Histological analysis of brain sections should shed light on whether any correction of pathology had in fact occurred in this animal.

5.3 Future work

The current confines of ERT are cost of enzyme production and the limited efficacy in treatment of avascular tissues and the CNS. To some extent these can be addressed by more efficient enzyme production i.e., better expression systems, gene amplification technology (Bielicki *et al.*, 1998) and the co-expression of factors such as the recently described MSD factor (Cosma *et al.*, 2003; Dierks *et al.*, 2003) to increase, in this instance, yields of sulphatases. The use of transgenic animals such as the chicken (Alper, 2003) offers the potential of reducing cost of recombinant enzyme production by 10-fold. Careful optimisation of dose for each patient is also important in maximising clinical efficacy and minimising cost. However, it is less obvious how effective treatment of avascular tissues can be achieved. Targeted approaches such as direct injection of replacement enzyme into joints and topical application of enzymatically active fragments of replacement enzyme for treating corneas (Thiel *et al.*, 2002) may be effective.

Treatment of CNS pathology is still problematic. The least invasive method by which this may be achieved is intravenous infusion of modified enzyme. If enzymatically active conjugates which effect BBB transcytosis can be made, this approach still remains feasible. Experimentally, the work done in this thesis shows that the systems used for investigation of this approach need to be carefully chosen. For example, the use of a mouse model of LSD CNS pathology would allow assessment of enzyme transcytosis by analysis of both enzymatic and storage levels. Given the low levels of enzyme required to prevent disease pathology, the latter may prove a more sensitive analysis, especially if analysed using a quantitative technique such as MS/MS. Rat anti-mouse Tf receptor monoclonal antibodies are available (Lee *et al.*, 2000), however, monoclonal antibodies to the insulin receptor, which are reported to be more efficient vectors than OX26 (Pardridge *et al.*, 1995; Coloma *et al.*, 2000), are not available to the mouse variant. The melanotransferrin molecule, P97, is another possible vector (Demeule *et al.*, 2002). Conjugates of P97 and α-L-iduronidase have been documented as being effective in BBB transcytosis in a mouse model of MPS I (http://biomarinpharm.com/BM ClinicalAndDevelopmentPrograms BrainResearch.html). Both cationization and the use of vectors would appear to be clinically applicable (Pardridge *et al.*, 1990b; Bickel *et al.*, 2001) although humanisation of antibodies (Morrison *et al.*, 1984; Mathieson *et al.*, 1990) would presumably be required.

Whichever strategy is eventually used in the treatment of CNS pathology, its wider application to other neurological diseases, in which the transport of the therapeutic agent is prohibited by either size or charge, is also possible. Animal models of disease are an invaluable asset in the study of disease pathogenesis and for developing and evaluating treatment strategies, provided their limitations are recognised in the extrapolation to human conditions and therapies.

Publications

The following are publications obtained by J. Bielicki during the course of this thesis. Those marked * were the result of work done in this thesis.

Yogalingam, G., Litjens, T., Bielicki, J., Crawley, A.C., Muller, V., Anson, D.S. and Hopwood, J.J. (1996) Feline mucopolysaccharidosis type VI. Characterisation of recombinant N-acetylgalactosamine 4-sulfatase and identification of a mutation causing the disease. *J Biol Chem.* **271**: 27259-27265.*

Bielicki, J., Hopwood, J.J. and Anson, D.S. (1996) Correction of Sanfilippo A skin fibroblasts by retroviral vector-mediated gene transfer. *Hum Gene Ther.* **7**: 1965-1970.

Yogalingam, G., Bielicki, J., Hopwood, J.J. and Anson, D.S. (1997) Feline mucopolysaccharidosis type VI: correction of glycosaminoglycan storage in myoblasts by retrovirus-mediated transfer of the feline N-acetylgalactosamine-4-sulfatase gene. *DNA Cell Biol.* **16** 1189-1194.

Litjens, T., Bielicki, J., Anson, D.S., Friderici, K., Jones, M.Z. and Hopwood, J.J. (1997) Expression, purification and characterization of recombinant caprine N-acetylglucosamine-6-sulphatase. *Biochem.* J. **327**: 89-94.

Nelson, K., Bielicki, J. and Anson, D.S. (1997) Immortalization and characterization of a cell line exhibiting a severe multiple sulphatase deficiency phenotype. *Biochem J.* **326**: 125-130.

Bielicki, J., Hopwood, J.J. Melville, E.L. and Anson, D.S. (1998) Recombinant human sulphamidase: expression, amplification, purification and characterization. *Biochem J.* **329**: 145-150.

Bielicki, J., Crawley, A.C., Davey, R.C.A., Varnai, J. and Hopwood, J.J. (1999) Advantages of using same species enzyme for replacement therapy in a feline model of mucopolysaccharidosis type VI. *J Biol Chem.* **274**: 36335-36343.*

Anson, D.S. and Bielicki, J. (1999) Sulphamidase. *Int J Biochem Cell Biol.* **31**: 363-367.

Bielicki, J., Muller, V., Fuller, M., Hopwood, J.J. and Anson, D.S. (2000) Recombinant canine α-L-fucosidase: expression, purification and characterization. *Mol Genet Metab.* **69**: 24-32.*

Bielicki, J. *et al.* Long-term enzyme-replacement therapy in a canine model of fucosidosis. In preparation.*

Bibliography

Abbott, N.J. and Romero, I.A. (1996) Transporting therapeutics across the blood-brain barrier. *Mol Med Today*. **2**: 106-113.

Abraham, D., Blakemore, W.F., Dell, A., Herrtage, M.E., Jones, J., Littlewood, J.T., Oates, J., Palmer, A.C., Sidebotham, R. and Winchester, B. (1984) The enzymic defect and storage products in canine fucosidosis. *Biochem J.* **222**: 25-33.

Achord, D.T., Brot, F.E., Gonzalez-Noriega, A., Sly, W.S. and Stahl, P. (1977) Human β-glucuronidase. II. Fate of infused human placental β-glucuronidase in the rat. *Pediatr Res.* **11**: 816-822.

Alam, T. and Balasubramanian, A.S. (1979) Affinity chromatography and separation of the molecular forms of monkey brain alpha-L-fucosidase on fucose-linked sepharose. *Biochim Biophys Acta.* **566**: 327-334.

Alhadeff, J.A. (1978) Gel filtration of sialoglycoproteins. *Biochem J.* **173**: 315-319.

Alhadeff, J.A. (1998) Structure and function of mammalian α-L-fucosidases. *Trends in Comparative Biochem and Physiol.* **4**: 105-118.

Alhadeff, J.A., Miller, A.L., Wenaas, H., Vedvick, T. and O'Brien, J.S. (1975) Human liver alpha-L-fucosidase. Purification, characterization, and immunochemical studies. *J Biol Chem.* **250**: 7106-7113.

Alper, J. (2003) Biotechnology. Hatching the golden egg: a new way to make drugs. *Science.* **300**: 729-730.

Altraescu, G., Hill, S., Wiggs, E., Jeffries, N., Kreps, C., Parker, C.C., Brady, R.O., Barton, N.W. and Schiffmann, R. (2001) The efficacy of enzyme replacement therapy in patients with chronic neuronopathic Gaucher's disease. *J Pediatr*, **138**, 539-547.

Anson, D.S., Bielicki, J. and Hopwood, J.J. (1992a) Correction of mucopolysaccharidosis type I fibroblasts by retroviral-mediated transfer of the human alpha-L-iduronidase gene. *Hum Gene Ther.* **3**: 371-379.

Anson, D.S., Taylor, J.A., Bielicki, J., Harper, G.S., Peters, C., Gibson, G.J. and Hopwood, J.J. (1992b) Correction of human mucopolysaccharidosis type-VI fibroblasts with recombinant N-acetylgalactosamine-4-sulphatase. *Biochem J.* **284**: 789-794.

Aronson, N.N., Jr. and Kuranda, M.J. (1989) Lysosomal degradation of Asn-linked glycoproteins. *Faseb J.* **3**: 2615-2622.

Arthur, F.E., Shivers, R.R. and Bowman, P.D. (1987) Astrocyte-mediated induction of tight junctions in brain capillary endothelium: an efficient in vitro model. *Brain Res.* **433**: 155-159.

Barker, C., Dell, A., Rogers, M., Alhadeff, J.A. and Winchester, B. (1988) Canine alpha-L-fucosidase in relation to the enzymic defect and storage products in canine fucosidosis. *Biochem J.* **254**: 861-868.

Barton, R.W. and Neufeld, E.F. (1972) A distinct biochemical deficit in the Maroteaux-Lamy syndrome (mucoploysaccharidosis VI). *J. Pediat.* **80**: 114-116.

Barton, N.W., Brady, R.O., Dambrosia, J.M., Di Bisceglie, A.M., Doppelt, S.H., Hill, S.C., Mankin, H.J., Murray, G.J., Parker, R.I., Argoff, C.E. and et al. (1991) Replacement therapy for inherited enzyme deficiency--macrophage-targeted glucocerebrosidase for Gaucher's disease. *N Engl J Med.* **324**: 1464-1470.

Baskin, D.G., Porte, D., Jr., Guest, K. and Dorsa, D.M. (1983) Regional concentrations of insulin in the rat brain. *Endocrinology.* **112**: 898-903.

Berkin, A., Szarek, W.A. and Kisilevsky, R. (2000) Synthesis of 4-deoxy-4-fluoro analogues of 2-acetamido-2-deoxy-D-glucose and 2-acetamido-2-deoxy-D-galactose and their effects on cellular glycosaminoglycan biosynthesis. *Carb Res.* **326**: 250-263.

Beutler, E. and Grabowski, G.A. (2001) Gaucher disease. In *The Metabolic and Molecular Bases of Inherited Disease.* Scriver, C.R., Beaudet, A.L., Sly, W.S., and Valle, D. (eds.) New York: McGraw-Hill, pp. 3635-3668.

Bhaumik, M., Muller, V.J., Rozaklis, T., Johnson, L., Dobrenis, K., Bhattacharyya, R., Wurzelmann, S., Finamore, P., Hopwood, J.J., Walkley, S.U. and Stanley, P. (1999) A mouse model for mucopolysaccharidosis type III A (Sanfilippo syndrome). *Glycobiology.* **9**: 1389-1396.

Bianco, P., Fisher, L.W., Young, M.F., Termine, J.D. and Robey, P.G. (1990) Expression and localization of the two small proteoglycans biglycan and decorin in developing human skeletal and non-skeletal tissues. *J Histochem Cytochem.* **38**: 1549-1563.

Bickel, U., Yoshikawa, T., Landaw, E.M., Faull, K.F. and Pardridge, W.M. (1993) Pharmacologic effects in vivo in brain by vector-mediated peptide drug delivery. *Proc Natl Acad Sci U S A.* **90**: 2618-2622.

Bickel, U. (1995) Antibody delivery through the blood-brain barrier. *Advanced drug delivery reviews.* **15**: 53-72.

Bickel, U., Kang, Y.S. and Pardridge, W.M. (1995) In vivo cleavability of a disulfide-based chimeric opioid peptide in rat brain. *Bioconjug Chem.* **6**: 211-218.

Bickel, U., Yoshikawa, T. and Pardridge, W.M. (2001) Delivery of peptides and proteins through the blood-brain barrier. *Adv Drug Deliv Rev.* **46**: 247-279.

Bielicki, J., Hopwood, J.J., Wilson, P.J. and Anson, D.S. (1993) Recombinant human iduronate-2-sulphatase: correction of mucopolysaccharidosis-type II fibroblasts and characterization of the purified enzyme. *Biochem J.* **289**: 241-246.

Bielicki, J., Fuller, M., Guo, X.H., Morris, C.P., Hopwood, J.J. and Anson, D.S. (1995) Expression, purification and characterization of recombinant human N-acetylgalactosamine-6-sulphatase. *Biochem J.* **311**: 333-339.

Bielicki, J., Hopwood, J.J., Melville, E.L. and Anson, D.S. (1998) Recombinant human sulphamidase: expression, amplification, purification and characterization. *Biochem J.* **329**: 145-150.

Birkenmeier, E.H., Davisson, M.T., Beamer, W.G., Ganschow, R.E., Vogler, C.A., Gwynn, B., Lyford, K.A., Maltais, L.M. and Wawrzyniak, C.J. (1989) Murine mucopolysaccharidosis type VII. Characterization of a mouse with beta-glucuronidase deficiency. *J Clin Invest.* **83**: 1258-1266.

Birkenmeier, E.H., Barker, J.E., Vogler, C.A., Kyle, J.W., Sly, W.S., Gwynn, B., Levy, B. and Pegors, C. (1991) Increased life span and correction of metabolic defects in murine

mucopolysaccharidosis type VII after syngeneic bone marrow transplantation. *Blood.* **78**: 3081-3092.

Bispinck, F., Fischer, J., Lullmann-Rauch, R. and Ziegenhagen, M.W. (1998) Time course of the tilorone-induced lysosomal accumulation of sulphated glycosaminoglycans in cultured fibroblasts. *Exp Toxicol Pathol.* **50**: 411-415.

Blumenkrantz, N. and Asboe-Hansen, G. (1973) New method for quantitative determination of uronic acids. *Anal Biochem.* **54**: 484-489.

Bolton, S.J., Anthony, D.C. and Perry, V.H. (1998) Loss of the tight junction proteins occludin and zonula occludens-1 from cerebral vascular endothelium during neutrophil-induced blood-brain barrier breakdown in vivo. *Neuroscience.* **86**: 1245-1257.

Bond, C.S., Clements, P.R., Ashby, S.J., Collyer, C.A., Harrop, S.J., Hopwood, J.J. and Guss, J.M. (1997) Structure of a human lysosomal sulfatase. *Structure.* **5**: 277-289.

Bosch, A., Perret, E., Desmaris, N. and Heard, J.M. (2000a) Long-term and significant correction of brain lesions in adult mucopolysaccharidosis type VII mice using recombinant AAV vectors. *Mol Ther.* **1**: 63-70.

Bosch, A., Perret, E., Desmaris, N., Trono, D. and Heard, J.M. (2000b) Reversal of pathology in the entire brain of mucopolysaccharidosis type VII mice after lentivirus-mediated gene transfer. *Hum Gene Ther.* **11**: 1139-1150.

Bove, K.E., Daugherty, C. and Grabowski, G.A. (1995) Pathological findings in Gaucher disease type 2 patients following enzyme therapy. *Hum Pathol*, **26**, 1040-1045.

Bresciani, R. and Von Figura, K. (1996) Dephosphorylation of the mannose-6-phosphate recognition marker is localized in later compartments of the endocytic route. Identification of purple acid phosphatase (uteroferrin) as the candidate phosphatase. *Eur J Biochem.* **238**: 669-674.

Bright, N.A., Reaves, B.J., Mullock, B.M. and Luzio, J.P. (1997) Dense core lysosomes can fuse with late endosomes and are re-formed from the resultant hybrid organelles. *J Cell Sci.* **110**: 2027-2040.

Brightman, M.W. and Tao-Cheng, J.H. (eds.) (1993) *Tight junctions of brain endothelium and epithelium*. New York: Raven Press.

Broadwell, R.D. (1989) Transcytosis of macromolecules through the blood-brain barrier: a cell biological perspective and critical appraisal. *Acta Neuropathol (Berl).* **79**: 117-128.

Brooks, A.I., Stein, C.S., Hughes, S.M., Heth, J., McCray, P.M., Jr., Sauter, S.L., Johnston, J.C., Cory-Slechta, D.A., Federoff, H.J. and Davidson, B.L. (2002) Functional correction of established central nervous system deficits in an animal model of lysosomal storage disease with feline immunodeficiency virus-based vectors. *Proc Natl Acad Sci U S A.* **99**: 6216-6221.

Brooks, D.A., McCourt, P.A., Gibson, G.J., Ashton, L.J., Shutter, M. and Hopwood, J.J. (1991) Analysis of N-acetylgalactosamine-4-sulfatase protein and kinetics in mucopolysaccharidosis type VI patients. *Am J Hum Genet.* **48**: 710-719.

Brooks, D.A., Gibson, G.J. and Hopwood, J.J. (1994) Immunochemical characterization of feline and human N-acetylgalactosamine 4-sulfatase. *Biochem Med Metab Biol.* **53**: 58-66.

Brooks, D.A., King, B.M., Crawley, A.C., Byers, S. and Hopwood, J.J. (1997) Enzyme replacement therapy in Mucopolysaccharidosis VI: evidence for immune responses and altered efficacy of treatment in animal models. *Biochim Biophys Acta.* **1361**: 203-216.

Brooks, D.A., Hopwood, J.J. and King, B.M. (1998) Immune response to enzyme replacement therapy: clinical signs of hypersensitivity reactions and altered enzyme distribution in a high titre rat model. *Biochim Biophys Acta.* **1407**: 163-172.

Butters, T.D., Scudder, P., Rotsaert, J., Petursson, S., Fleet, G.W., Willenbrock, F.W. and Jacob, G.S. (1991) Purification to homogeneity of Charonia lampas alpha-fucosidase by using sequential ligand-affinity chromatography. *Biochem J.* **279**: 189-195.

Byers, S., Nuttall, J.D., Crawley, A.C., Hopwood, J.J., Smith, K. and Fazzalari, N.L. (1997) Effect of enzyme replacement therapy on bone formation in a feline model of mucopolysaccharidosis type VI. *Bone.* **21**: 425-431.

Byers, S., Rozaklis, T., Brumfield, L.K., Ranieri, E. and Hopwood, J.J. (1998) Glycosaminoglycan accumulation and excretion in the mucopolysaccharidoses: characterization and basis of a diagnostic test for MPS. *Mol Genet Metab.* **65**: 282-290.

Byers, S., Crawley, A.C., Brumfield, L.K., Nuttall, J.D. and Hopwood, J.J. (2000) Enzyme replacement therapy in a feline model of MPS VI: modification of enzyme structure and dose frequency. *Pediatr Res.* **47**: 743-749.

Carlsson, J., Drevin, H. and Axen, R. (1978) Protein thiolation and reversible protein-protein conjugation. N-Succinimidyl 3-(2-pyridyldithio)propionate, a new heterobifunctional reagent. *Biochem J.* **173**: 723-737.

Chang, P.L., Ameen, M., Yu, C.Z. and Kelly, B.M. (1988) Effect of ammonium chloride on subcellular distribution of lysosomal enzymes in human fibroblasts. *Exp Cell Res.* **176**: 258-267.

Chao, H.H., Waheed, A., Pohlmann, R., Hille, A. and von Figura, K. (1990) Mannose 6-phosphate receptor dependent secretion of lysosomal enzymes. *Embo J.* **9**: 3507-3513.

Chen, H.C., Shimohigashi, Y., Dufau, M.L. and Catt, K.J. (1982) Characterization and biological properties of chemically deglycosylated human chorionic gonadotropin. Role of carbohydrate moieties in adenylate cyclase activation. *J Biol Chem.* **257**: 14446-14452.

Clarke, L.A., Russell, C.S., Pownall, S., Warrington, C.L., Borowski, A., Dimmick, J.E., Toone, J. and Jirik, F.R. (1997) Murine mucopolysaccharidosis type I: targeted disruption of the murine alpha-L-iduronidase gene. *Hum Mol Genet.* **6**: 503-511.

Cohenford, M.A., Abraham, A., Abraham, J. and Dain, J.A. (1989) Colorimetric assay for free and bound L-fucose. *Anal Biochem.* **177**: 172-177.

Colley, K.J. (1997) Golgi localization of glycosyltransferases: more questions than answers. *Glycobiology.* **7**: 1-13.

Coloma, M.J., Lee, H.J., Kurihara, A., Landaw, E.M., Boado, R.J., Morrison, S.L. and Pardridge, W.M. (2000) Transport across the primate blood-brain barrier of a genetically engineered chimeric monoclonal antibody to the human insulin receptor. *Pharm Res.* **17**: 266-274.

Cosma, M.P., Pepe, S., Annunziata, I., Newbold, R.F., Grompe, M., Parenti, G. and Ballabio, A. (2003) The multiple sulfatase deficiency gene encodes an essential and limiting factor for the activity of sulfatases. *Cell.* **113**: 445-456.

Coster, L., Carlstedt, I., Malmstrom, A. and Sarnstrand, B. (1984) Biosynthesis and secretion of dermatan sulphate proteoglycans in cultures of human skin fibroblasts. *Biochem J.* **220**: 575-582.

Cowell, K.R., Jezyk, P.F., Haskins, M.E. and Patterson, D.F. (1976) Mucopolysaccharidosis in a cat. *J Am Vet Med Assoc.* **169**: 334-339.

Cox, T., Lachmann, R., Hollak, C., Aerts, J., van Weely, S., Hrebicek, M., Platt, F., Butters, T., Dwek, R., Moyses, C., Gow, I., Elstein, D. and Zimran, A. (2000) Novel oral treatment of Gaucher's disease with N-butyldeoxynojirimycin (OGT 918) to decrease substrate biosynthesis. *Lancet.* **355**: 1481-1485.

Crawley, A.C., Brooks, D.A., Muller, V.J., Petersen, B.A., Isaac, E.L., Bielicki, J., King, B.M., Boulter, C.D., Moore, A.J., Fazzalari, N.L., Anson, D.S., Byers, S. and Hopwood, J.J. (1996) Enzyme replacement therapy in a feline model of Maroteaux-Lamy syndrome. *J Clin Invest.* **97**: 1864-1873.

Crawley, A.C., Niedzielski, K.H., Isaac, E.L., Davey, R.C., Byers, S. and Hopwood, J.J. (1997) Enzyme replacement therapy from birth in a feline model of mucopolysaccharidosis type VI. *J Clin Invest.* **99**: 651-662.

Crawley, A.C., Yogalingam, G., Muller, V.J. and Hopwood, J.J. (1998) Two mutations within a feline mucopolysaccharidosis type VI colony cause three different clinical phenotypes. *J Clin Invest.* **101**: 109-119.

Crawley, A.C., Jones, M.Z., Bonning, L.E., Finnie, J.W. and Hopwood, J.J. (1999) Alpha-mannosidosis in the guinea pig: a new animal model for lysosomal storage disorders. *Pediatr Res.* **46**: 501-509.

Crawley, A.M., Muntz, F.H., Haskins, M.E., Jones, B.R. and Hopwood, J.J. (2003) Prevalence of mucopolysaccharidosis type VI in Siamese cats. *Journal of Vet Intern Med.* **17**.

De Duve, C., Pressman, B.C. and Gianetto, R. (1955) Tissue fractionation studies. Intracellular distribution patterns of enzymes in rat liver tissue. *Biochem J*: 604.

Dell'Angelica, E.C., Mullins, C., Caplan, S. and Bonifacino, J.S. (2000) Lysosome-related organelles. *Faseb J.* **14**: 1265-1278.

Demeule, M., Poirier, J., Jodoin, J., Bertrand, Y., Desrosiers, R.R., Dagenais, C., Nguyen, T., Lanthier, J., Gabathuler, R., Kennard, M., Jefferies, W.A., Karkan, D., Tsai, S., Fenart, L., Cecchelli, R. and Beliveau, R. (2002) High transcytosis of melanotransferrin (P97) across the blood-brain barrier. *J Neurochem.* **83**: 924-933.

Desnick, R.J., Allen, K.Y., Simmons, R.L., Woods, J.E., Anderson, C.F., Najarian, J.S. and Krivit, W. (1973a) Fabry disease: correction of the enzymatic deficiency by renal transplantation. *Birth Defects Orig Artic Ser.* **9**: 88-96.

Desnick, S.J., Desnick, R.J., Brady, R.O., Pentchev, P.G., Simmons, R.L., Najarian, J.D., Swaiman, K., Sharp, H.L. and Krivit, W. (1973b) Renal transplantation in Gaucher's disease. *Birth Defects Orig Artic Ser.* **9**: 109-119.

Di Ferrante, N., Neri, G., Neri, M.E. and Hogsett, W.E. (1972) Measurement of urinary glycosaminoglycans with quaternary ammonium salts: an extension of the method. *Connect. Tissue Res.* **1**: 93-101.

Di Natale, P., Annella, T., Daniele, A., Spagnuolo, G., Cerundolo, R., de Caprariis, D. and Gravino, A.E. (1992) Animal models for lysosomal storage diseases: a new case of feline mucopolysaccharidosis VI. *J Inherit Metab Dis*. **15**: 17-24.

Dial, S.M., Byrne, T., Haskins, M., Gasper, P.W., Rose, B., Wenger, D.A. and Thrall, M.A. (1997) Urine glycosaminoglycan concentrations in mucopolysaccharidosis VI-affected cats following bone marrow transplantation or leukocyte infusion. *Clin Chim Acta*. **263**: 1-14.

Dierks, T., Schmidt, B. and von Figura, K. (1997) Conversion of cysteine to formylglycine: a protein modification in the endoplasmic reticulum. *Proc Natl Acad Sci U S A*. **94**: 11963-11968.

Dierks, T., Lecca, M.R., Schmidt, B. and von Figura, K. (1998) Conversion of cysteine to formylglycine in eukaryotic sulfatases occurs by a common mechanism in the endoplasmic reticulum. *FEBS Lett*. **423**: 61-65.

Dierks, T., Schmidt, B., Borissenko, L.V., Peng, J., Presseur, A., Mariappan, M. and von Figura, K. (2003) Multiple sulfatase deficiency is caused by mutations in the gene encoding the human C_{α}-formylglycine generating enzyme. *Cell*. **113**: 435-444.

Donsante, A., Vogler, C., Muzyczka, N., Crawford, J.M., Barker, J., Flotte, T., Campbell-Thompson, M., Daly, T. and Sands, M.S. (2001) Observed incidence of tumorigenesis in long-term rodent studies of rAAV vectors. *Gene Ther*. **8**: 1343-1346.

Dorfman, A. and Lorincz, A.E. (1957) Occurrence of urinary acid mucopolysaccharides in the Hurler syndrome. *Proc Natl Acad Sci USA*. **43**: 443-446.

Dorfman, A. and Matalon, R. (1976) The mucopolysaccharidoses (a review). *Proc Natl Acad Sci U S A*. **73**: 630-637.

Dorling, P.R., Huxtable, C.R. and Vogel, P. (1978) Lysosomal storage in Swainsona spp. toxicosis: an induced mannosidosis. *Neuropathol Appl Neurobiol*. **4**: 285-295.

Dorner, A.J., Wasley, L.C. and Kaufman, R.J. (1989) Increased synthesis of secreted proteins induces expression of glucose-regulated proteins in butyrate-treated Chinese hamster ovary cells. *J Biol Chem*. **264**: 20602-20607.

Duffy, K.R., Pardridge, W.M. and Rosenfeld, R.G. (1988) Human blood-brain barrier insulin-like growth factor receptor. *Metabolism*. **37**: 136-140.

Durand, P., Borrone, C. and Della Cella, G. (1966) A new mucopolysaccharide lipid storage disease? *Lancet*. **2**: 1313-1314.

Durand, P., Borrone, C. and Della Cella, G. (1969) Fucosidosis. *J. Pediat*. **75**: 665-674.

Ellman, G.L. (1959) Tissue sulfhydryl groups. *Arch Biochem Biophys*. **82**, 70-77.

Esko, J.D. and Lindahl, U. (2001) Molecular diversity of heparan sulfate. *J Clin Invest*. **108**: 169-173.

Evers, M., Saftig, P., Schmidt, P., Hafner, A., McLoghlin, D.B., Schmahl, W., Hess, B., von Figura, K. and Peters, C. (1996) Targeted disruption of the arylsulfatase B gene results in mice resembling the phenotype of mucopolysaccharidosis VI. *Proc Natl Acad Sci U S A*. **93**: 8214-8219.

Ferrante, P., Messali, S., Meroni, G. and Ballabio, A. (2002) Molecular and biochemical characterisation of a novel sulphatase gene: Arylsulfatase G (ARSG). *Eur J Hum Genet.* **10**: 813-818.

Ferrara, M.L., Taylor, R.M. and Stewart, G.J. (1992) Age at marrow transplantation is critical for successful treatment of canine fucosidosis. *Transplant Proc.* **24**: 2282-2283.

Folch, J., Lees, M. and Stanley, G.H.S. (1957) A simple method for the isolation and purification of total lipides from animal tissue. *J Biol Chem.* **226**: 497-509.

Folch-Pi, J. (1972) Effect of conditions of extraction on the extractability of brain gangliosides. *Adv Exp Med Biol.* **19**: 63-76.

Fransson, L.-A. (1987) Structure and function of cell-associated proteoglycans. *Trends Bioch. Sci.* **12**: 406-411.

Fratantoni, J.C., Hall, C.W. and Neufeld, E.F. (1968) Hurler and Hunter syndromes: mutual correction of the defect in cultured fibroblasts. *Science.* **162**: 570-572.

Fratantoni, J.C., Hall, C.W. and Neufeld, E.F. (1969) The defect in Hurler and Hunter syndromes. II. Deficiency of specific factors involved in mucopolysaccharide degradation. *Proc Natl Acad Sci USA.* **64**: 360-366.

Freeman, C. and Hopwood, J.J. (1992) Human alpha-L-iduronidase. Catalytic properties and an integrated role in the lysosomal degradation of heparan sulphate. *Biochem J.* **282**: 899-908.

Friden, P.M., Walus, L.R., Musso, G.F., Taylor, M.A., Malfroy, B. and Starzyk, R.M. (1991) Anti-transferrin receptor antibody and antibody-drug conjugates cross the blood-brain barrier. *Proc Natl Acad Sci U S A.* **88**: 4771-4775.

Friden, P.M., Walus, L.R., Watson, P., Doctrow, S.R., Kozarich, J.W., Backman, C., Bergman, H., Hoffer, B., Bloom, F. and Granholm, A.C. (1993) Blood-brain barrier penetration and in vivo activity of an NGF conjugate. *Science.* **259**: 373-377.

Friden, P.M. (1994) Receptor-mediated transport of therapeutics across the blood-brain barrier. *Neurosurgery.* **35**: 294-298.

Friedman, B., Vaddi, K., Preston, C., Mahon, E., Cataldo, J.R. and McPherson, J.M. (1999) A comparison of the pharmacological properties of carbohydrate remodeled recombinant and placental-derived beta-glucocerebrosidase: implications for clinical efficacy in treatment of Gaucher disease. *Blood.* **93**: 2807-2816.

Fukuta, M., Okada, H., Iinuma, S., Yanai, S. and Toguchi, H. (1994) Insulin fragments as a carrier for peptide delivery across the blood-brain barrier. *Pharm Res.* **11**: 1681-1688.

Gahl, W.A., Renlund, M. and J.G., T. (1989) Lysosomal transport disorders: cystinosis and sialic acid storage disorders. In *The Metabolic Basis of Inherited Disease.* Scriver, C.R., Beaudet, A.L., Sly, W.S., and Valle, D. (eds.) New York: McGraw-Hill, pp. 2619-2667.

Galjart, N.J., Gillemans, N., Harris, A., van der Horst, G.T., Verheijen, F.W., Galjaard, H. and d'Azzo, A. (1988) Expression of cDNA encoding the human "protective protein" associated with lysosomal beta-galactosidase and neuraminidase: homology to yeast proteases. *Cell.* **54**: 755-764.

Gao, C., Sands, M.S., Haskins, M.E. and Ponder, K.P. (2000) Delivery of a retroviral vector expressing human beta-glucuronidase to the liver and spleen decreases lysosomal storage in mucopolysaccharidosis VII mice. *Mol Ther.* **2**: 233-244.

Gasper, P.W., Thrall, M.A., Wenger, D.A., Macy, D.W., Ham, L., Dornsife, R.E., McBiles, K., Quackenbush, S.L., Kesel, M.L., Gillette, E.L. and et al. (1984) Correction of feline arylsulphatase B deficiency (mucopolysaccharidosis VI) by bone marrow transplantation. *Nature*. **312**: 467-469.

Gavel, Y. and von Heijne, G. (1990) Sequence differences between glycosylated and non-glycosylated Asn-X-Thr/Ser acceptor sites: implications for protein engineering. *Protein Eng.* **3**: 433-442.

Gennuso, R., Spigelman, M.K., Chinol, M., Zappulla, R.A., Nieves, J., Vallabhajosula, S., Alberto Paciucci, P., Goldsmith, S.J. and Holland, J.F. (1993) Effect of blood-brain barrier and blood-tumor barrier modification on central nervous system liposomal uptake. *Cancer Invest.* **11**: 118-128.

Gerber, H.P., Vu, T.H., Ryan, A.M., Kowalski, J., Werb, Z. and Ferrara, N. (1999) VEGF couples hypertrophic cartilage remodeling, ossification and angiogenesis during endochondral bone formation. *Nat Med.* **5**: 623-628.

Gibbs, D.A., Spellacy, E., Roberts, A.E. and Watts, R.W.E. (1980) The treatment of lysosomal storage disease by fibroblast transplantation. Some preliminary observations. *Birth Defects Orig Art Ser.* **16**: 457-474.

Gibson, G.J., Saccone, G.T., Brooks, D.A., Clements, P.R. and Hopwood, J.J. (1987) Human N-acetylgalactosamine-4-sulphate sulphatase. Purification, monoclonal antibody production and native and subunit Mr values. *Biochem J.* **248**: 755-764.

Gold, E.W. (1979) A simple spectrophotometric method for estimating glycosaminoglycan concentrations. *Anal Biochem.* **99**: 183-188.

Grace, M.E. and Grabowski, G.A. (1990) Human acid beta-glucosidase: glycosylation is required for catalytic activity. *Biochem Biophys Res Commun.* **168**: 771-777.

Granholm, A.C., Backman, C., Bloom, F., Ebendal, T., Gerhardt, G.A., Hoffer, B., Mackerlova, L., Olson, L., Soderstrom, S., Walus, L.R. and et al. (1994) NGF and anti-transferrin receptor antibody conjugate: short and long-term effects on survival of cholinergic neurons in intraocular septal transplants. *J Pharmacol Exp Ther.* **268**: 448-459.

Greenwood, J., Luthert, P.J., Pratt, O.E. and Lantos, P.L. (1988) Hyperosmolar opening of the blood-brain barrier in the energy-depleted rat brain. Part 1. Permeability studies. *J Cereb Blood Flow Metab.* **8**: 9-15.

Gregoriadis, G. (1989) Liposomes as carriers of drugs. Observations on vesicle fate after injection and its control. *Subcell Biochem.* **14**: 363-378.

Groth, C.G., Blomstrand, R., Dreborg, S., Hagenfeldt, L., Lofstrom, B., Ockerman, P.-A., Samuelsson, K. and Svennerholm, L. (1973) Splenic transplantation in Gaucher disease. *Birth Defects Orig Artic Ser.* **9**: 102-108.

Grove, D.S. and Serif, G.S. (1981) Porcine thyroid fucosidase. *Biochim Biophys Acta.* **662**: 246-255.

Haddad, F.S., Jones, D.H., Vellodi, A., Kane, N. and Pitt, M.C. (1997) Carpal tunnel syndrome in mucopolysaccharidoses and mucolipidoses. *J Bone Joint Surg Br.* **79**: 576-582.

Harlow, E. and Lane, D. (1988) *Antibodies: A Laboratory Manual.* Cold Spring Harbor Laboratry.

Harmatz, P., Whitely, C.B., Belani, K., Waber, L., Pais, R., Steiner, R., Plecko, B., Simon, J., Thompson, J., Waterson, J., Lammer, E., Rowe, R., Koseoglu, S., Cohen, R., Rosenfeld, H., Gutierrez, H. and Hopwood, J.J. (2001) A phaseI/II randomized, double-blind, two dose group study of recombinant human N-acetylgalactosamine-4-sulfatase (rhASB) enzyme replacement therapy in patients with mucopolysaccharidosis (MPS) VI (Maroteaux-Lamy syndrome). *Am J Hum Genet*. **69 supplement**: 674.

Hartley, W.J., Canfield, P.J. and Donnelly, T.M. (1982) A suspected new canine storage disease. *Acta Neuropathol (Berl)*. **56**: 225-232.

Hasilik, A. and von Figura, K. (1984) Processing of lysosomal enzymes in fibroblasts. In *Lysosomes in biology and pathology*. Dingle, J.T., Dean, R.T., and Sly, W. (eds.) Amsterdam: Elsevier, pp. 3-16.

Hasilik, A. (1992) The early and late processing of lysosomal enzymes: proteolysis and compartmentation. *Experientia*. **48**: 130-151.

Haskins, M.E., Jezyk, P.F. and Patterson, D.F. (1979a) Mucopolysaccharide storage disease in three families of cats with arylsulfatase B deficiency: leukocyte studies and carrier identification. *Pediatr Res*. **13**: 1203-1210.

Haskins, M.E., Jezyk, P.F., Desnick, R.J., McDonough, S.K. and Patterson, D.F. (1979b) Mucopolysaccharidosis in a domestic short-haired cat--a disease distinct from that seen in the Siamese cat. *J Am Vet Med Assoc*. **175**: 384-387.

Haskins, M.E., Aguirre, G.D., Jezyk, P.F. and Patterson, D.F. (1983a) The pathology of the feline model of mucopolysaccharidosis VI. *Am J Pathol*. **101**: 657-674.

Haskins, M.E., Bingel, S.A., Northington, J.W., Newton, C.D., Sande, R.D., Jezyk, P.F. and Patterson, D.F. (1983b) Spinal cord compression and hindlimb paresis in cats with mucopolysaccharidosis VI. *J Am Vet Med Assoc*. **182**: 983-985.

Haskins, M.E., Baker, H.J., Birkenmeier, E., Hoogerbrugge, P.M., Poorthuis, B.J., Sakiyama, T., Shull, R.M., Taylor, R.M., Thrall, M.A. and Walkley, S.U. (1991) Transplantation in animal model systems. In *Treatment of genetic diseases*. Desnick, R.J. (ed.) New York: Churchill Livingstone, pp. 183-201.

Haskins, M.E., Otis, E.J., Hayden, J.E., Jezyk, P.F. and Stramm, L. (1992) Hepatic storage of glycosaminoglycans in feline and canine models of mucopolysaccharidoses I, VI, and VII. *Vet Pathol*. **29**: 112-119.

Healy, P.J., Farrow, B.R., Nicholas, F.W., Hedberg, K. and Ratcliffe, R. (1984) Canine fucosidosis: a biochemical and genetic investigation. *Res Vet Sci*. **36**: 354-359.

Hein, L. and Lullmann-Rauch, R. (1989) Mucopolysaccharidosis and lipidosis in rats treated with tilorone analogues. *Toxicology*. **58**: 145-154.

Hers, H.G. (1973) The concept of inborn lysosomal diseases. In *Lysosomes and storage diseases*. Hers, H.G., and van Hoof, H.G. (eds.) New York: Academic Press, pp. 148-171.

Hobbs, J.R., Hugh-Jones, K., Barrett, A.J., Byrom, N., Chambers, D., Henry, K., James, D.C., Lucas, C.F., Rogers, T.R., Benson, P.F., Tansley, L.R., Patrick, A.D., Mossman, J. and Young, E.P. (1981) Reversal of clinical features of Hurler's disease and biochemical improvement after treatment by bone-marrow transplantation. *Lancet*. **2**: 709-712.

Holst, B., Bruun, A.W., Kielland-Brandt, M.C. and Winther, J.R. (1996) Competition between folding and glycosylation in the endoplasmic reticulum. *Embo J.* **15**: 3538-3546.

Hoogerbrugge, P.M., Poorthuis, B.J., Romme, A.E., van de Kamp, J.J., Wagemaker, G. and van Bekkum, D.W. (1988) Effect of bone marrow transplantation on enzyme levels and clinical course in the neurologically affected twitcher mouse. *J Clin Invest.* **81**: 1790-1794.

Hoogerbrugge, P.M., Poorthuis, B.J., Wagemaker, G., van Bekkum, D.W. and Suzuki, K. (1989) Alleviation of neurologic symptoms after bone marrow transplantation in twitcher mice. *Transplant Proc.* **21**: 2980-2981.

Hoogerbrugge, P.M., Brouwer, O.F., Bordigoni, P., Ringden, O., Kapaun, P., Ortega, J.J., O'Meara, A., Cornu, G., Souillet, G., Frappaz, D. and et al. (1995) Allogeneic bone marrow transplantation for lysosomal storage diseases. The European Group for Bone Marrow Transplantation. *Lancet.* **345**: 1398-1402.

Hopwood, J.J. and Harrison, J.R. (1982) High-resolution electrophoresis of urinary glycosaminoglycans: an improved screening test for the mucopolysaccharidoses. *Anal Biochem.* **119**: 120-127.

Hopwood, J.J., Muller, V., Harrison, J.R., Carey, W.F., Elliott, H., Robertson, E.F. and Pollard, A.C. (1982) Enzymatic diagnosis of the mucopolysaccharidoses: experience of 96 cases diagnosed in a five-year period. *Med J Aust.* **1**: 257-260.

Hopwood, J.J. and Elliott, H. (1985) Urinary excretion of sulphated N-acetylhexosamines in patients with various mucopolysaccharidoses. *Biochem J.* **229**: 579-586.

Hopwood, J.J., Elliott, H., Muller, V.J. and Saccone, G.T. (1986) Diagnosis of Maroteaux-Lamy syndrome by the use of radiolabelled oligosaccharides as substrates for the determination of arylsulphatase B activity. *Biochem J.* **234**: 507-514.

Hopwood, J.J. (1989) Enzymes that degrade heparin and heparan sulphate. In *Heparin*. Lane, D.A., and Lindhal, U. (eds.) London: Edward Arnold, pp. 191-228.

Hopwood, J.J. and Morris, C.P. (1990) The mucopolysaccharidoses. Diagnosis, molecular genetics and treatment. *Mol Biol Med.* **7**: 381-404.

Hopwood, J.J., Vellodi, A., Scott, H.S., Morris, C.P., Litjens, T., Clements, P.R., Brooks, D.A., Cooper, A. and Wraith, J.E. (1993) Long-term clinical progress in bone marrow transplanted mucopolysaccharidosis type I patients with a defined genotype. *J Inherit Metab Dis.* **16**: 1024-1033.

Hopwood, J.J. and Brooks, D.A. (1997) An introduction to the basic science and biology of the lysosome and storage diseases. In *Organelle Diseases*. Applegarth, D.A., Dimmick, J.E. and Hall, J.G. (eds.) London: Chapman and Hall, pp. 7-35.

Howell, D.S. and Dean, D.D. (1992) The biology, chemistry and biochemistry of the mammalian growth plate. In *Disorders of bone and mineral metabolism.* Coe, F.L., and Favus, M.J. (eds.) New York: Raven Press, pp. 313-353.

Humbel, R. and Collart, M. (1975) Oligosaccharides in urine of patients with glycoprotein storage diseases. I. Rapid detection by thin-layer chromatography. *Clin Chim Acta.* **60**: 143-145.

Huxtable, C.R. and Dorling, P.R. (1985) Mannoside storage and axonal dystrophy in sensory neurones of swainsonine-treated rats: morphogenesis of lesions. *Acta Neuropathol (Berl).* **68**: 65-73.

Jackson, C.E., Yuhki, N., Desnick, R.J., Haskins, M.E., O'Brien, S.J. and Schuchman, E.H. (1992) Feline arylsulfatase B (ARSB): isolation and expression of the cDNA, comparison with human ARSB, and gene localization to feline chromosome A1. *Genomics*. **14**: 403-411.

Janzer, R.C. and Raff, M.C. (1987) Astrocytes induce blood-brain barrier properties in endothelial cells. *Nature*. **325**: 253-257.

Jefferies, W.A., Brandon, M.R., Hunt, S.V., Williams, A.F., Gatter, K.C. and Mason, D.Y. (1984) Transferrin receptor on endothelium of brain capillaries. *Nature*. **312**: 162-163.

Jeyakumar, M., Butters, T.D., Cortina-Borja, M., Hunnam, V., Proia, R.L., Perry, V.H., Dwek, R.A. and Platt, F.M. (1999) Delayed symptom onset and increased life expectancy in Sandhoff disease mice treated with N-butyldeoxynojirimycin. *Proc Natl Acad Sci U S A*. **96**: 6388-6393.

Jezyk, P.F., Haskins, M.E., Patterson, D.F., Mellman, W.J. and Greenstein, M. (1977) Mucopolysaccharidosis in a cat with arylsulfatase B deficiency: a model of Maroteaux-Lamy syndrome. *Science*. **198**: 834-836.

Johnson, K.F., Hancock, L.W. and Dawson, G. (1991) Synthesis and processing of lysosomal alpha-fucosidase in cultured human fibroblasts. *Biochim Biophys Acta*. **1073**: 120-128.

Johnson, K.F. and Kornfeld, S. (1992) The cytoplasmic tail of the mannose 6-phosphate/insulin-like growth factor-II receptor has two signals for lysosomal enzyme sorting in the Golgi. *J Cell Biol*. **119**: 249-257.

Jolly, R.D. and Walkley, S.U. (1997) Lysosomal storage diseases of animals: an essay in comparative pathology. *Vet Pathol*. **34**: 527-548.

Jones, M.Z., Alroy, J., Rutledge, J.C., Taylor, J.W., Alvord, E.C., Jr., Toone, J., Applegarth, D., Hopwood, J.J., Skutelsky, E., Ianelli, C., Thorley-Lawson, D., Mitchell-Herpolsheimer, C., Arias, A., Sharp, P., Evans, W., Sillence, D. and Cavanagh, K.T. (1997) Human mucopolysaccharidosis IIID: clinical, biochemical, morphological and immunohistochemical characteristics. *J Neuropathol Exp Neurol*. **56**: 1158-1167.

Jones, M.Z., Brumfield, L.K., King, B.M., Hopwood, J.J. and Byers, S. (1998) Recombinant caprine 3H-[N-acetylglucosamine-6-sulfatase] and human 3H-[N-acetylgalactosamine-4-sulfatase]: plasma clearance, tissue distribution, and cellular uptake in the rat. *J Mol Neurosci*. **11**: 223-232.

Joshi, L., Murata, Y., Wondisford, F.E., Szkudlinski, M.W., Desai, R. and Weintraub, B.D. (1995) Recombinant thyrotropin containing a beta-subunit chimera with the human chorionic gonadotropin-beta carboxy-terminus is biologically active, with a prolonged plasma half-life: role of carbohydrate in bioactivity and metabolic clearance. *Endocrinology*. **136**: 3839-3848.

Kaiser, J. (2003) Gene therapy. RAC hears a plea for resuming trials, despite cancer risk. *Science*. **299**: 991.

Kakavanos, R., Turner, C.T., Hopwood, J.J., Kakkis, E.D. and Brooks, D.A. (2003) Immune tolerance after long-term enzyme-replacement therapy among patients who have mucopolysaccharidosis I. *The Lancet*. **361**: 1608-1613.

Kakkis, E.D., McEntee, M.F., Schmidtchen, A., Neufeld, E.F., Ward, D.A., Gompf, R.E., Kania, S., Bedolla, C., Chien, S.L. and Shull, R.M. (1996) Long-term and high-dose trials of enzyme replacement therapy in the canine model of mucopolysaccharidosis I. *Biochem Mol Med*. **58**: 156-167.

Kakkis, E.D., Schuchman, E., He, X., Wan, Q., Kania, S., Wiemelt, S., Hasson, C.W., O'Malley, T., Weil, M.A., Aguirre, G.A., Brown, D.E. and Haskins, M.E. (2001a) Enzyme replacement therapy in feline mucopolysaccharidosis I. *Mol Genet Metab.* **72**: 199-208.

Kakkis, E.D., Muenzer, J., Tiller, G.E., Waber, L., Belmont, J., Passage, M., Izykowski, B., Phillips, J., Doroshow, R., Walot, I., Hoft, R. and Neufeld, E.F. (2001b) Enzyme-replacement therapy in mucopolysaccharidosis I. *N Engl J Med.* **344**: 182-188.

Kampine, J.P., Brady, R.O., Kanfer, J.N., Feld, M. and Shapiro, D. (1966) Diagnosis of Gaucher's disease and Nieman-Pick disease with small samples of venous blood. *Science.* **155**: 86-88.

Kasper, D., Dittmer, F., von Figura, K. and Pohlmann, R. (1996) Neither type of mannose 6-phosphate receptor is sufficient for targeting of lysosomal enzymes along intracellular routes. *J Cell Biol.* **134**: 615-623.

Kelly, W.R., Clague, A.E., Barns, R.J., Bate, M.J. and MacKay, B.M. (1983) Canine alpha-L-fucosidosis: a storage disease of Springer Spaniels. *Acta Neuropathol (Berl).* **60**: 9-13.

Kjellen, L. and Lindahl, U. (1991) Proteoglycans: structures and interactions. *Annu Rev Biochem.* **60**: 443-475.

Kobayashi, T., Honke, K., Jin, T., Gasa, S., Miyazaki, T. and Makita, A. (1992) Components and proteolytic processing sites of arylsulfatase B from human placenta. *Biochim Biophys Acta.* **1159**: 243-247.

Kornfeld, R. and Kornfeld, S. (1976) Comparative aspects of glycoprotein structure. *Annu Rev Biochem.* **45**: 217-237.

Kornfeld, R. and Kornfeld, S. (1985) Assembly of asparagine-linked oligosaccharides. *Annu Rev Biochem.* **54**: 631-664.

Kornfeld, S. (1986) Trafficking of lysosomal enzymes in normal and disease states. *J Clin Invest.* **77**: 1-6.

Kornfeld, S. (1987) Trafficking of lysosomal enzymes. *Faseb J.* **1**: 462-468.

Kornfeld, S. and Mellman, I. (1989) The biogenesis of lysosomes. *Annu Rev Cell Biol.* **5**: 483-525.

Kornfeld, S. (1992) Structure and function of the mannose 6-phosphate/insulinlike growth factor II receptors. *Annu Rev Biochem.* **61**: 307-330.

Kresse, H., Rosthoj, S., Quentin, E., Hollmann, J., Glossl, J., Okada, S. and Tonnesen, T. (1987) Glycosaminoglycan-free small proteoglycan core protein is secreted by fibroblasts from a patient with a syndrome resembling progeroid. *Am J Hum Genet.* **41**: 436-453.

Krivit, W., Pierpont, M.E., Ayaz, K., Tsai, M., Ramsay, N.K., Kersey, J.H., Weisdorf, S., Sibley, R., Snover, D., McGovern, M.M. and et al. (1984) Bone-marrow transplantation in the Maroteaux-Lamy syndrome (mucopolysaccharidosis type VI). Biochemical and clinical status 24 months after transplantation. *N Engl J Med.* **311**: 1606-1611.

Laemmli, U.K. (1970) Cleavage of structural proteins during the assembly of the head of bacteriophage T4. *Nature.* **227**: 680-685.

Laidler, P. and Litynska, A. (1997) Arylsulfatase A from human placenta possesses only high mannose-type glycans. *Int J Biochem Cell Biol.* **29**: 475-483.

Laterra, J.J., Stewart, P.A. and Goldstein, G.W. (1992) Development of the BBB. In *Fetal and Neonatal Physiology*. Polin, A., and Fox, W.W. (eds.) Philadelphia: WB Saunders Co, pp. 1525-1531.

Laurent, T.C. and Fraser, J.R.E. (1992) Hyaluronan. *Faseb J.* **6**: 2397-2404.

Leaback, D.H. and Walker, P.G. (1961) Studies on glucosaminidase. The fluorometric assay of N-acetyl-β-glucosaminidase. *Biochem J.* **78**: 151-156.

Lee, H.J., Engelhardt, B., Lesley, J., Bickel, U. and Pardridge, W.M. (2000) Targeting rat anti-mouse transferrin receptor monoclonal antibodies through blood-brain barrier in mouse. *J Pharmacol Exp Ther.* **292**: 1048-1052.

Lemansky, P., Gieselmann, V., Hasilik, A. and von Figura, K. (1985) Synthesis and transport of lysosomal acid phosphatase in normal and I-cell fibroblasts. *J Biol Chem.* **260**: 9023-9030.

Lennarz, W.J. (1987) Protein glycosylation in the endoplasmic reticulum: current topological issues. *Biochemistry.* **26**: 7205-7210.

Limberis, M., Anson, D.S., Fuller, M. and Parsons, D.W. (2002) Recovery of airway cystic fibrosis transmembrane regulator function in mice with cystic fibrosis after single-dose lentivirus-mediated gene transfer. *Hum Gene Ther* **13**: 1961-1970.

Litjens, T., Baker, E.G., Beckmann, K.R., Morris, C.P., Hopwood, J.J. and Callen, D.F. (1989) Chromosomal localization of ARSB, the gene for human N-acetylgalactosamine-4-sulphatase. *Hum Genet.* **82**: 67-68.

Litjens, T., Brooks, D.A., Peters, C., Gibson, G.J. and Hopwood, J.J. (1996) Identification, expression, and biochemical characterization of N-acetylgalactosamine-4-sulfatase mutations and relationship with clinical phenotype in MPS-VI patients. *Am J Hum Genet.* **58**: 1127-1134.

Litjens, T., Bielicki, J., Anson, D.S., Friderici, K., Jones, M.Z. and Hopwood, J.J. (1997) Expression, purification and characterization of recombinant caprine N-acetylglucosamine-6-sulphatase. *Biochem J.* **327**: 89-94.

Litjens, T. and Hopwood, J.J. (2001) Mucopolysaccharidosis type VI: Structural and clinical implications of mutations in N-acetylgalactosamine-4-sulfatase. *Hum Mutat.* **18**: 282-295.

Littlewood, J.D., Herrtage, M.E. and Palmer, A.C. (1983) Neuronal storage disease in English springer spaniels. *Vet Rec.* **112**: 86-87.

Lobel, P., Fujimoto, K., Ye, R.D., Griffiths, G. and Kornfeld, S. (1989) Mutations in the cytoplasmic domain of the 275 kd mannose 6-phosphate receptor differentially alter lysosomal enzyme sorting and endocytosis. *Cell.* **57**: 787-796.

Lowry, O.H., Rosebrough, N.J., Farr, A.L., Randall, R.J. (1951) Protein measurement with the Folin-phenol reagent. *J Biol Chem.* **193**: 265-275.

Mancini, G.M., Havelaar, A.C. and Verheijen, F.W. (2000) Lysosomal transport disorders. *J Inherit Metab Dis.* **23**: 278-292.

Mapes, C.A., Anderson, R.L. and Sweeley, C.C. (1970) Enzyme replacement in Fabry's disease, an inborn error of metabolism. *Science.* **169**: 987-989.

Margolis, R.U. and Margolis, R.K. (1989) Properties of nervous tissue proteoglycans relevant to studies on Alzheimer's disease. *Neurobiol Aging.* **10**: 500-502.

Margolis, R.K. and Margolis, R.U. (1993) Nervous tissue proteoglycans. *Experientia*. **49**: 429-446.

Maroteaux, P., Leveque, B., Marie, J. and Lamy, M. (1963) Une nouvelle dysostose avec elimination urinaire de chondroitin-sulfate B. *Press Med*. **71**: 1849-1852.

Mathieson, P.W., Cobbold, S.P., Hale, G., Clark, M.R., Oliveira, D.B., Lockwood, C.M. and Waldmann, H. (1990) Monoclonal-antibody therapy in systemic vasculitis. *N Engl J Med*. **323**: 250-254.

McGovern, M.M., Vine, D.T., Haskins, M.E. and Desnick, R.J. (1982) Purification and properties of feline and human arylsulfatase B isozymes. Evidence for feline homodimeric and human monomeric structures. *J Biol Chem*. **257**: 12605-12610.

McGovern, M.M., Ludman, M.D., Short, M.P., Steinfeld, L., Kattan, M., Raab, E.L., Krivit, W. and Desnick, R.J. (1986) Bone marrow transplantation in Maroteaux-Lamy syndrome (MPS type 6): status 40 months after BMT. *Birth Defects Orig Artic Ser*. **22**: 41-53.

Meikle, P.J., Brooks, D.A., Ravenscroft, E.M., Yan, M., Williams, R.E., Jaunzems, A.E., Chataway, T.K., Karageorgos, L.E., Davey, R.C., Boulter, C.D., Carlsson, S.R. and Hopwood, J.J. (1997) Diagnosis of lysosomal storage disorders: evaluation of lysosome-associated membrane protein LAMP-1 as a diagnostic marker. *Clin Chem*. **43**: 1325-1335.

Meikle, P.J., Hopwood, J.J., Clague, A.E. and Carey, W.F. (1999a) Prevalence of lysosomal storage disorders. *Jama*. **281**: 249-254.

Meikle, P.J., Ranieri, E., Ravenscroft, E.M., Hua, C.T., Brooks, D.A. and Hopwood, J.J. (1999b) Newborn screening for lysosomal storage disorders. *Southeast Asian J Trop Med Public Health*. **30 Suppl 2**: 104-110.

Mellquist, J.L., Kasturi, L., Spitalnik, S.L. and Shakin-Eshleman, S.H. (1998) The amino acid following an asn-X-Ser/Thr sequon is an important determinant of N-linked core glycosylation efficiency. *Biochemistry*. **37**: 6833-6837.

Merril, C.R., Dunau, M.L. and Goldman, D. (1981) A rapid sensitive silver stain for polypeptides in polyacrylamide gels. *Anal Biochem*. **110**: 201-207.

Miano, M., Lanino, E., Gatti, R., Morreale, G., Fondelli, P., Celle, M.E., Stroppiano, M., Crescenzi, F. and Dini, G. (2001) Four year follow-up of a case of fucosidosis treated with unrelated donor bone marrow transplantation. *Bone Marrow Transplant*. **27**: 747-751.

Minch, S.L., Kallio, P.T. and Bailey, J.E. (1995) Tissue plasminogen activator coexpressed in Chinese hamster ovary cells with alpha(2,6)-sialyltransferase contains NeuAc alpha(2,6)Gal beta(1,4)Glc-N-AcR linkages. *Biotechnol Prog*. **11**: 348-351.

Mollgoard, K. and Saunders, N.R. (1975) Complex tight junctions of epithelial and of endothelial cells in early foetal brain. *J Neurocytol*. **4**: 453-468.

Monroy, M.A., Ross, F.P., Teitelbaum, S.L. and Sands, M.S. (2002) Abnormal osteoclast morphology and bone remodeling in a murine model of a lysosomal storage disease. *Bone*. **30**: 352-359.

Monsigny, M., Petit, C. and Roche, A.C. (1988) Colorimetric determination of neutral sugars by a resorcinol sulfuric acid micromethod. *Anal Biochem*. **175**: 525-530.

Morrell, A.G., Gregoriadis, G., Scheinberg, I.H., Hickman, J. and Ashwell, G. (1971) The role of sialic acid in determining the survival of glycoproteins in circulation. *J Biol Chem.* **246**: 1461-1467.

Morrison, S.L., Johnson, M.J., Herzenberg, L.A. and Oi, V.T. (1984) Chimeric human antibody molecules: mouse antigen-binding domains with human constant region domains. *Proc Natl Acad Sci U S A.* **81**: 6851-6855.

Muenzer, J. (1986) Mucopolysaccharidoses. *Adv Pediatr.* **33**: 269-302.

Natowicz, M.R., Short, M.P., Wang, Y., Dickersin, G.R., Gebhardt, M.C., Rosenthal, D.I., Sims, K.B. and Rosenberg, A.E. (1996) Clinical and biochemical manifestations of hyaluronidase deficiency. *N Engl J Med.* **335**: 1029-1033.

Neer, T.M., Dial, S.M., Pechman, R., Wang, P., Oliver, J.L. and Giger, U. (1995) Clinical vignette. Mucopolysaccharidosis VI in a miniature pinscher. *J Vet Intern Med.* **9**: 429-433.

Neufeld, E.F. and Ashwell, G. (1980) Carbohydrate recognition systems for receptor-mediated pinocytosis. In *The biochemistry of glycoproteins and proteoglycans*. Lennarz, W.J. (ed.) New York: Plenum Press, pp. 241-266.

Neufeld, E.F. and Muenzer, J. (2001) The mucoploysaccharidoses. In *The Metabolic and Molecular Bases of Inherited Disease.* Scriver, C.R., Beaudet, A.L., Sly, W.S., and Valle, D. (eds.) New York: McGraw-Hill, pp. 3421-3452.

Nolan, C.M. and Sly, W.S. (1989) I-cell disease and pseudo-Hurler polydystrophy: disorders of lysosomal enzyme phosphorylation and localization. In *The Metabolic Basis of Inherited Disease.* Scriver, C.R., Beaudet, A.L., Sly, W.S., and Valle, D. (eds.) New York: McGraw-Hill, pp. 1589-1601.

Norrdin, R.W., Moffat, K.S., Thrall, M.A. and Gasper, P.W. (1993) Characterization of osteopenia in feline mucopolysaccharidosis VI and evaluation of bone marrow transplantation therapy. *Bone.* **14**: 361-367.

Nuttall, J.D., Brumfield, L.K., Fazzalari, N.L., Hopwood, J.J. and Byers, S. (1999) Histomorphometric analysis of the tibial growth plate in a feline model of mucopolysaccharidosis type VI. *Calcif Tissue Int.* **65**: 47-52.

O'Brien, J.S., Willems, P.J., Fukushima, H., de Wit, J.R., Darby, J.K., Di Cioccio, R., Fowler, M.L. and Shows, T.B. (1987) Molecular biology of the alpha-L-fucosidase gene and fucosidosis. *Enzyme.* **38**: 45-53.

Occhiodoro, T., Beckmann, K.R., Morris, C.P. and Hopwood, J.J. (1989) Human alpha-L-fucosidase: complete coding sequence from cDNA clones. *Biochem Biophys Res Commun.* **164**: 439-445.

Occhiodoro, T. and Anson, D.S. (1996) Isolation of the canine alpha-L-fucosidase cDNA and definition of the fucosidosis mutation in English Springer Spaniels. *Mamm Genome.* **7**: 271-274.

Oldendorf, W.H., Hyman, S., Braun, L. and Oldendorf, S.Z. (1972) Blood-brain barrier: penetration of morphine, codeine, heroin, and methadone after carotid injection. *Science.* **178**: 984-986.

Olsen, I., Dean, M.F., Harris, G. and Muir, H. (1981) Direct transfer of a lysosomal enzyme from lymphoid cells to deficient fibroblasts. *Nature.* **291**: 244-247.

Oohira, A., Katoh-Semba, R., Watanabe, E. and Matsui, F. (1994a) Brain development and multiple molecular species of proteoglycan. *Neurosci Res.* **20**: 195-207.

Oohira, A., Matsui, F., Watanabe, E., Kushima, Y. and Maeda, N. (1994b) Developmentally regulated expression of a brain specific species of chondroitin sulfate proteoglycan, neurocan, identified with a monoclonal antibody IG2 in the rat cerebrum. *Neuroscience.* **60**: 145-157.

Pardridge, W.M., Eisenberg, J. and Yang, J. (1985) Human blood-brain barrier insulin receptor. *J Neurochem.* **44**: 1771-1778.

Pardridge, W.M., Eisenberg, J. and Yang, J. (1987) Human blood-brain barrier transferrin receptor. *Metabolism.* **36**: 892-895.

Pardridge, W.M., Triguero, D. and Buciak, J.L. (1990a) Beta-endorphin chimeric peptides: transport through the blood-brain barrier in vivo and cleavage of disulfide linkage by brain. *Endocrinology.* **126**: 977-984.

Pardridge, W.M., Triguero, D., Buciak, J. and Yang, J. (1990b) Evaluation of cationized rat albumin as a potential blood-brain barrier drug transport vector. *J Pharmacol Exp Ther.* **255**: 893-899.

Pardridge, W.M. (1991) *Peptide drug delivery to the brain.* New York: Raven Press.

Pardridge, W.M. (1993) *The blood-brain barrier.* New York: Raven Press.

Pardridge, W.M., Kang, Y.S., Buciak, J.L. and Yang, J. (1995) Human insulin receptor monoclonal antibody undergoes high affinity binding to human brain capillaries in vitro and rapid transcytosis through the blood-brain barrier in vivo in the primate. *Pharm Res.* **12**: 807-816.

Pardridge, W.M. (1997) Drug delivery to the brain. *J Cereb Blood Flow Metab.* **17**: 713-731.

Parfitt, A.M., Drezner, M.K., Glorieux, F.H., Kanis, J.A., Malluche, H., Meunier, P.J., Ott, S.M. and Recker, R.R. (1987) Bone histomorphometry: standardization of nomenclature, symbols, and units. Report of the ASBMR Histomorphometry Nomenclature Committee. *J Bone Miner Res.* **2**: 595-610.

Pastores, G.M., Sibille, A.R. and Grabowski, G.A. (1993) Enzyme therapy in Gaucher disease type 1: dosage efficacy and adverse effects in 33 patients treated for 6 to 24 months. *Blood.* **82**: 408-416.

Peters, C., Braun, M., Weber, B., Wendland, M., Schmidt, B., Pohlmann, R., Waheed, A. and von Figura, K. (1990a) Targeting of a lysosomal membrane protein: a tyrosine-containing endocytosis signal in the cytoplasmic tail of lysosomal acid phosphatase is necessary and sufficient for targeting to lysosomes. *Embo J.* **9**: 3497-3506.

Peters, C., Schmidt, B., Rommerskirch, W., Rupp, K., Zuhlsdorf, M., Vingron, M., Meyer, H.E., Pohlmann, R. and von Figura, K. (1990b) Phylogenetic conservation of arylsulfatases:cDNA cloning and expression of human arylsulfatase B. *J Biol Chem.* **265**: 3374-3381.

Peters, C., Shapiro, E.G., Anderson, J., Henslee-Downey, P.J., Klemperer, M.R., Cowan, M.J., Saunders, E.F., deAlarcon, P.A., Twist, C., Nachman, J.B., Hale, G.A., Harris, R.E., Rozans, M.K., Kurtzberg, J., Grayson, G.H., Williams, T.E., Lenarsky, C., Wagner, J.E. and Krivit, W. (1998) Hurler syndrome: II. Outcome of HLA-genotypically identical sibling and HLA-haploidentical related donor bone marrow transplantation in fifty-four children. The Storage Disease Collaborative Study Group. *Blood.* **91**: 2601-2608.

Peters, C. and Krivit, W. (2000) Hematopoietic cell transplantation for mucopolysaccharidosis IIB (Hunter syndrome). *Bone Marrow Transplant.* **25**: 1097-1099.

Pfeffer, S.R. (1988) Mannose 6-phosphate receptors and their role in targeting proteins to lysosomes. *J Membr Biol.* **103**: 7-16.

Philippart, M. (1973) Fabry disease. *Birth Defects Orig Artic Ser.* **9**: 81-87.

Platt, F.M., Neises, G.R., Reinkensmeier, G., Townsend, M.J., Perry, V.H., Proia, R.L., Winchester, B., Dwek, R.A. and Butters, T.D. (1997) Prevention of lysosomal storage in Tay-Sachs mice treated with N-butyldeoxynojirimycin. *Science.* **276**: 428-431.

Poduslo, J.F., Curran, G.L. and Berg, C.T. (1994) Macromolecular permeability across the blood-nerve and blood-brain barriers. *Proc Natl Acad Sci U S A.* **91**: 5705-5709.

Poduslo, J.F. and Curran, G.L. (1996a) Increased permeability of superoxide dismutase at the blood-nerve and blood-brain barriers with retained enzymatic activity after covalent modification with the naturally occurring polyamine, putrescine. *J Neurochem.* **67**: 734-741.

Poduslo, J.F. and Curran, G.L. (1996b) Polyamine modification increases the permeability of proteins at the blood-nerve and blood-brain barriers. *J Neurochem.* **66**: 1599-1609.

Poduslo, J.F., Curran, G.L. and Gill, J.S. (1998) Putrescine-modified nerve growth factor: bioactivity, plasma pharmacokinetics, blood-brain/nerve barrier permeability, and nervous system biodistribution. *J Neurochem.* **71**: 1651-1660.

Poduslo, J.F., Whelan, S.L., Curran, G.L. and Wengenack, T.M. (2000) Therapeutic benefit of polyamine-modified catalase as a scavenger of hydrogen peroxide and nitric oxide in familial amyotrophic lateral sclerosis transgenics. *Ann Neurol.* **48**: 943-947.

Ponce, E., Moskovitz, J. and Grabowski, G. (1997) Enzyme therapy in Gaucher disease type 1: effect of neutralizing antibodies to acid beta-glucosidase. *Blood.* **90**: 43-48.

Ponder, K.P., Melniczek, J.R., Xu, L., Weil, M.A., O'Malley, T.M., O'Donnell, P.A., Knox, V.W., Aguirre, G.D., Mazrier, H., Ellinwood, N.M., Sleeper, M., Maguire, A.M., Volk, S.W., Mango, R.L., Zweigle, J., Wolfe, J.H. and Haskins, M.E. (2002) Therapeutic neonatal hepatic gene therapy in mucopolysaccharidosis VII dogs. *Proc Natl Acad Sci U S A.* **99**: 13102-13107.

Poole, A.R., Webber, C., Pidoux, I., Choi, H. and Rosenberg, L.C. (1986) Localization of a dermatan sulfate proteoglycan (DS-PGII) in cartilage and the presence of an immunologically related species in other tissues. *J Histochem Cytochem.* **34**: 619-625.

Przybylo, M. and Litynska, A. (1997) Characterization of the oligosaccharide component of arylsulfatase B from rat liver. *Acta Biochim Pol.* **44**: 181-190.

Quentin, E., Gladen, A., Roden, L. and Kresse, H. (1990) A genetic defect in the biosynthesis of dermatan sulfate proteoglycan: galactosyltransferase I deficiency in fibroblasts from a patient with a progeroid syndrome. *Proc Natl Acad Sci U S A.* **87**: 1342-1346.

Ramsay, S.L., Meikle, P.J. and Hopwood, J.J. (2003) Determination of monosaccharides and disaccharides in mucopolysaccharidoses patients by electrospray ionisation mass spectrometry. *Mol Genet Metab.* **78**: 193-204.

Rapoport, S.I. (1996) Modulation of blood-brain barrier permeability. *J Drug Target.* **3**: 417-425.

Rapraeger, A.C. (2000) Syndecan-regulated receptor signaling. *J Cell Biol.* **149**: 995-998.

Recker, R.R. (1983) *Bone histomorphometry: Techniques and interpretation.* Florida: CRC Press, Inc.

Recker, R.R. (1992) Embryology, anatomy and microstructure of bone. In *Disorders of bone and mineral metabolism.* Coe, F.L., and Favus, M.J. (eds.) New York: Raven Press, pp. 219-240.

Reese, T.S. and Karnovsky, M.J. (1967) Fine structural localization of a blood-brain barrier to exogenous peroxidase. *J Cell Biol.* **34**: 207-217.

Richards, S.M., Olson, T.A. and McPherson, J.M. (1993) Antibody response in patients with Gaucher disease after repeated infusion with macrophage-targeted glucocerebrosidase. *Blood.* **82**: 1402-1409.

Robertson, D.A., Freeman, C., Nelson, P.V., Morris, C.P. and Hopwood, J.J. (1988) Human glucosamine-6-sulfatase cDNA reveals homology with steroid sulfatase. *Biochem Biophys Res Commun.* **157**: 218-224.

Robey, P.G., Bianco, P. and Termine, J.D. (1992) The cellular biology and molecular biochemistry of bone formation. In *Disorders of bone and mineral metabolism.* Coe, F.L., and Favus, M.J. (eds.) New York: Raven Press, pp. 241-263.

Roden, L. (1980) Structure and metabolism of connective tissue proteoglycans. In *The biochemistry of glycoproteins and proteoglycans.* Lennarz, W.J. (ed.) New York: Plenum Press, pp. 267-371.

Rodwell, J.D., Alvarez, V.L., Lee, C., Lopes, A.D., Goers, J.W., King, H.D., Powsner, H.J. and McKearn, T.J. (1986) Site-specific covalent modification of monoclonal antibodies: in vitro and in vivo evaluations. *Proc Natl Acad Sci U S A.* **83**: 2632-2636.

Rubin, L.L. and Staddon, J.M. (1999) The cell biology of the blood-brain barrier. *Annu Rev Neurosci.* **22**: 11-28.

Salahuddin, T.S., Kalimo, H., Johansson, B.B. and Olsson, Y. (1988a) Observations on exsudation of fibronectin, fibrinogen and albumin in the brain after carotid infusion of hyperosmolar solutions. An immunohistochemical study in the rat indicating longlasting changes in the brain microenvironment and multifocal nerve cell injuries. *Acta Neuropathol (Berl).* **76**: 1-10.

Salahuddin, T.S., Johansson, B.B., Kalimo, H. and Olsson, Y. (1988b) Structural changes in the rat brain after carotid infusions of hyperosmolar solutions. An electron microscopic study. *Acta Neuropathol (Berl).* **77**: 5-13.

Sands, M.S., Barker, J.E., Vogler, C., Levy, B., Gwynn, B., Galvin, N., Sly, W.S. and Birkenmeier, E. (1993) Treatment of murine mucopolysaccharidosis type VII by syngeneic bone marrow transplantation in neonates. *Lab Invest.* **68**: 676-686.

Sands, M.S., Vogler, C., Kyle, J.W., Grubb, J.H., Levy, B., Galvin, N., Sly, W.S. and Birkenmeier, E.H. (1994) Enzyme replacement therapy for murine mucopolysaccharidosis type VII. *J Clin Invest.* **93**: 2324-2331.

Sands, M.S., Vogler, C., Torrey, A., Levy, B., Gwynn, B., Grubb, J., Sly, W.S. and Birkenmeier, E.H. (1997) Murine mucopolysaccharidosis type VII: long term therapeutic effects of enzyme replacement and enzyme replacement followed by bone marrow transplantation. *J Clin Invest.* **99**: 1596-1605.

Sango, K., Yamanaka, S., Hoffmann, A., Okuda, Y., Grinberg, A., Westphal, H., McDonald, M.P., Crawley, J.N., Sandhoff, K., Suzuki, K. and et al. (1995) Mouse models of Tay-Sachs and Sandhoff diseases differ in neurologic phenotype and ganglioside metabolism. *Nat Genet.* **11**: 170-176.

Sano, M., Hayakawa, K. and Kato, I. (1992) Purification and characterization of alpha-L-fucosidase from Streptomyces species. *J Biol Chem.* **267**: 1522-1527.

Schagger, H. and von Jagow, G. (1987) Tricine-sodium dodecyl sulfate-polyacrylamide gel electrophoresis for the separation of proteins in the range from 1 to 100 kDa. *Anal Biochem.* **166**: 368-379.

Schiffmann, R., Heyes, M.P., Aerts, J.M., Dambrosia, J.M., Patterson, M.C., DeGraba, T., Parker, C.C., Zirzow, G.C., Oliver, K., Tedeschi, G., Brady, R.O. and Barton, N.W. (1997) Prospective study of neurological responses to treatment with macrophage-targeted glucocerebrosidase in patients with type 3 Gaucher's disease. *Ann Neurol.* **42**: 613-621.

Schmidt, B., Selmer, T., Ingendoh, A. and von Figura, K. (1995) A novel amino acid modification in sulfatases that is defective in multiple sulfatase deficiency. *Cell.* **82**: 271-278.

Schopohl, D., Muller-Taubenberger, A., Orthen, B., Hess, H. and Reutter, W. (1992) Purification and properties of a secreted and developmentally regulated alpha-L-fucosidase from Dictyostelium discoideum. *J Biol Chem.* **267**: 2400-2405.

Schroeder, U., Sommerfeld, P., Ulrich, S. and Sabel, B.A. (1998) Nanoparticle technology for delivery of drugs across the blood-brain barrier. *J Pharm Sci.* **87**: 1305-1307.

Schuchman, E.H., Jackson, C.E. and Desnick, R.J. (1990) Human arylsulfatase B: MOPAC cloning, nucleotide sequence of a full-length cDNA, and regions of amino acid identity with arylsulfatases A and C. *Genomics.* **6**: 149-158.

Seaman, M.N., Ball, C.L. and Robinson, M.S. (1993) Targeting and mistargeting of plasma membrane adaptors in vitro. *J Cell Biol.* **123**: 1093-1105.

Sewell, A.C. (1979) An improved thin-layer chromatographic method for urinary oligosaccharide screening. *Clin Chim Acta* **92**:411-414.

Sferra, T.J., Qu, G., McNeely, D., Rennard, R., Clark, K.R., Lo, W.D. and Johnson, P.R. (2000) Recombinant adeno-associated virus-mediated correction of lysosomal storage within the central nervous system of the adult mucopolysaccharidosis type VII mouse. *Hum Gene Ther.* **11**: 507-519.

Shapiro, W.R., Young, D.F. and Mehta, B.M. (1975) Methotrexate: distribution in cerebrospinal fluid after intravenous, ventricular and lumbar injections. *N Engl J Med.* **293**: 161-166.

Shull, R.M., Hastings, N.E., Selcer, R.R., Jones, J.B., Smith, J.R., Cullen, W.C. and Constantopoulos, G. (1987) Bone marrow transplantation in canine mucopolysaccharidosis I. Effects within the central nervous system. *J Clin Invest.* **79**: 435-443.

Shull, R.M. and Walker, M.A. (1988) Radiographic findings in a canine model of mucopolysaccharidosis I. Changes associated with bone marrow transplantation. *Invest Radiol.* **23**: 124-130.

Shull, R.M., Breider, M.A. and Constantopoulos, G.C. (1988) Long-term neurological effects of bone marrow transplantation in a canine lysosomal storage disease. *Pediatr Res.* **24**: 347-352.

Shull, R.M., Kakkis, E.D., McEntee, M.F., Kania, S.A., Jonas, A.J. and Neufeld, E.F. (1994) Enzyme replacement in a canine model of Hurler syndrome. *Proc Natl Acad Sci U S A.* **91**: 12937-12941.

Simonaro, C.M., Haskins, M.E., Kunieda, T., Evans, S.M., Visser, J.W. and Schuchman, E.H. (1997) Bone marrow transplantation in newborn rats with mucopolysaccharidosis type VI: biochemical, pathological, and clinical findings. *Transplantation.* **63**: 1386-1393.

Simonaro, C.M., Haskins, M.E. and Schuchman, E.H. (2001) Articular chondrocytes from animals with a dermatan sulfate storage disease undergo a high rate of apoptosis and release nitric oxide and inflammatory cytokines: a possible mechanism underlying degenerative joint disease in the mucopolysaccharidoses. *Lab Invest.* **81**: 1319-1328.

Sivakumur, P. and Wraith, J.E. (1999) Bone marrow transplantation in mucopolysaccharidosis type IIIA: a comparison of an early treated patient with his untreated sibling. *J Inherit Metab Dis.* **22**: 849-850.

Skelly, B.J., Sargan, D.R., Herrtage, M.E. and Winchester, B.G. (1996) The molecular defect underlying canine fucosidosis. *J Med Genet.* **33**: 284-288.

Skorupa, A.F., Fisher, K.J., Wilson, J.M., Parente, M.K. and Wolfe, J.H. (1999) Sustained production of beta-glucuronidase from localized sites after AAV vector gene transfer results in widespread distribution of enzyme and reversal of lysosomal storage lesions in a large volume of brain in mucopolysaccharidosis VII mice. *Exp Neurol.* **160**: 17-27.

Snyder, E.Y., Taylor, R.M. and Wolfe, J.H. (1995) Neural progenitor cell engraftment corrects lysosomal storage throughout the MPS VII mouse brain. *Nature.* **374**: 367-370.

Sokrab, T.E., Johansson, B.B., Kalimo, H. and Olsson, Y. (1988) A transient hypertensive opening of the blood-brain barrier can lead to brain damage. Extravasation of serum proteins and cellular changes in rats subjected to aortic compression. *Acta Neuropathol (Berl).* **75**: 557-565.

Staddon, J.M. and Rubin, L.L. (1996) Cell adhesion, cell junctions and the blood-brain barrier. *Curr Opin Neurobiol.* **6**: 622-627.

Stein, M., Braulke, T., Krentler, C., Hasilik, A. and von Figura, K. (1987) 46-kDa mannose 6-phosphate-specific receptor: biosynthesis, processing, subcellular location and topology. *Biol Chem Hoppe Seyler.* **368**: 937-947.

Storrie, B. (1988) Assembly of lysosomes: perspectives from comparative molecular cell biology. *Int Rev Cytol.* **111**: 53-105.

Suzuki, K. and Suzuki, K. (1973) Globoid cell leukodystrophy (Krabbe's disease). In *Lysosomes and storage diseases.* Hers, H.G., and van Hoof, H.G. (eds.) New York: Academic Press, pp. 395-410.

Suzuki, K., Hoogerbrugge, P.M., Poorthuis, B.J. and Bekkum, D.W. (1988) The twitcher mouse. Central nervous system pathology after bone marrow transplantation. *Lab Invest.* **58**: 302-309.

Taylor, R.M., Farrow, B.R. and Stewart, G.J. (1986) Correction of enzyme deficiency by allogeneic bone marrow transplantation following total lymphoid irradiation in dogs with lysosomal storage disease (fucosidosis). *Transplant Proc.* **18**: 326-329.

Taylor, R.M., Farrow, B.R.H. and Healy, P.J. (1987) Canine fucosidosis: Clinical findings. *J Small Anim Pract.* **28**: 89-93.

Taylor, R.M., Stewart, G.J. and Farrow, B.R. (1989a) Improvement in the neurologic signs and storage lesions of fucosidosis in dogs given marrow transplants at an early age. *Transplant Proc.* **21**: 3818-3819.

Taylor, R.M., Martin, I.C. and Farrow, B.R. (1989b) Reproductive abnormalities in canine fucosidosis. *J Comp Pathol.* **100**: 369-380.

Taylor, R.M., Stewart, G.J., Farrow, B.R. and Healy, P.J. (1989c) The effect of bone marrow-derived cells on lysosomal enzyme activity in the brain after marrow engraftment. *Transplant Proc.* **21**: 3822-3823.

Taylor, R.M., Stewart, G.J., Farrow, B.R., Byrne, J. and Healy, P.J. (1989d) Histological improvement and enzyme replacement in the brains of fucosidosis dogs after bone marrow engraftment. *Transplant Proc.* **21**: 3074-3075.

Taylor, R.M., Farrow, B.R. and Stewart, G.J. (1992) Amelioration of clinical disease following bone marrow transplantation in fucosidase-deficient dogs. *Am J Med Genet.* **42**: 628-632.

Thiel, M.A., Coster, D.J., Standfield, S.D., Brereton, H.M., Mavrangelos, C., Zola, H., Taylor, S., Yusim, A. and Williams, K.A. (2002) Penetration of engineered antibody fragments into the eye. *Clin Exp Immunol.* **128**: 67-74.

Thomas, G.H. (2001) Disorders of glycoprotein degradation: α-mannosidosis, β-mannosidosis, fucosidosis, sialidosis, aspartylglucosaminuria and carbohydrate-deficient glycoprotein syndrome. In *The Metabolic and Molecular Bases of Inherited Disease*. Scriver, C.R., Beaudet, A.L., Sly, W.S., and Valle, D. (eds.) New York: McGraw-Hill, pp. 3507-3533.

Triggs-Raine, B., Salo, T.J., Zhang, H., Wicklow, B.A. and Natowicz, M.R. (1999) Mutations in HYAL1, a member of a tandemly distributed multigene family encoding disparate hyaluronidase activities, cause a newly described lysosomal disorder, mucopolysaccharidosis IX. *Proc Natl Acad Sci U S A.* **96**: 6296-6300.

Triguero, D., Buciak, J. and Pardridge, W.M. (1990) Capillary depletion method for quantification of blood-brain barrier transport of circulating peptides and plasma proteins. *J Neurochem.* **54**: 1882-1888.

Turnbull, J.E., Fernig, D.G., Ke, Y., Wilkinson, M.C. and Gallagher, J.T. (1992) Identification of the basic fibroblast growth factor binding sequence in fibroblast heparan sulfate. *J Biol Chem.* **267**: 10337-10341.

Turnbull, J.E., Hopwood, J.J. and Gallagher, J.T. (1997) Exosequencing of heparan sulphate/heparin saccharides using lysosomal enzymes. In *A laboratory guide to glycoconjugate analysis*. Jackson, P., and Gallagher, J.T. (eds.) Basel: Birkhauser Verlag, pp. 261-277.

Tylki-Szymanska, A., Maciejko, D., Kidawa, M., Jablonska-Budaj, U. and Czartoryska, B. (1985) Amniotic tissue transplantation as a trial of treatment in some lysosomal storage diseases. *J Inherit Metab Dis.* **8**: 101-104.

Umezawa, F. and Eto, Y. (1988) Liposome targeting to mouse brain: mannose as a recognition marker. *Biochem Biophys Res Commun.* **153**: 1038-1044.

Unger, E.G., Durrant, J., Anson, D.S. and Hopwood, J.J. (1994) Recombinant alpha-L-iduronidase: characterization of the purified enzyme and correction of mucopolysaccharidosis type I fibroblasts. *Biochem J.* **304**: 43-49.

van Hoof, F. and Hers, H.G. (1968) Mucopolysaccharides by absence of a-L-fucosidase. *Lancet.* **1**: 1198.

van Houten, M. and Posner, B.I. (1979) Insulin binds to brain blood vessels in vivo. *Nature.* **282**: 623-625.

Varki, A. (1998) Factors controlling the glycosylation potential of the Golgi apparatus. *Trends Cell Biol.* **8**: 34-40.

Vellodi, A., Cragg, H., Winchester, B., Young, E., Young, J., Downie, C.J., Hoare, R.D., Stocks, R. and Banerjee, G.K. (1995) Allogeneic bone marrow transplantation for fucosidosis. *Bone Marrow Transplant.* **15**: 153-158.

Verma, I.M. and Somia, N. (1997) Gene therapy: promises, problems and prospects. *Nature.* **389**: 239-242.

Vestermark, S., Tonnesen, T., Andersen, M.S. and Guttler, F. (1987) Mental retardation in a patient with Maroteaux-Lamy. *Clin Genet.* **31**: 114-117.

Vogler, C., Sands, M., Higgins, A., Levy, B., Grubb, J., Birkenmeier, E.H. and Sly, W.S. (1993) Enzyme replacement with recombinant beta-glucuronidase in the newborn mucopolysaccharidosis type VII mouse. *Pediatr Res.* **34**: 837-840.

Vogler, C., Sands, M.S., Levy, B., Galvin, N., Birkenmeier, E.H. and Sly, W.S. (1996) Enzyme replacement with recombinant beta-glucuronidase in murine mucopolysaccharidosis type VII: impact of therapy during the first six weeks of life on subsequent lysosomal storage, growth, and survival. *Pediatr Res.* **39**: 1050-1054.

von Figura, K. and Hasilik, A. (1986) Lysosomal enzymes and their receptors. *Annu Rev Biochem.* **55**: 167-193.

Waheed, A., Gottschalk, S., Hille, A., Krentler, C., Pohlmann, R., Braulke, T., Hauser, H., Geuze, H. and von Figura, K. (1988) Human lysosomal acid phosphatase is transported as a transmembrane protein to lysosomes in transfected baby hamster kidney cells. *Embo J.* **7**: 2351-2358.

Wald, S.L. and Schmidek, H.H. (1984) Compressive myelopathy associated with type V mucoploysaccharidosis (Maroteaux-Lamy syndrome). *Neurosurgery.* **14**: 83-88.

Walkley, S.U., Thrall, M.A., Dobrenis, K., Huang, M., March, P.A., Siegel, D.A. and Wurzelmann, S. (1994) Bone marrow transplantation corrects the enzyme defect in neurons of the central nervous system in a lysosomal storage disease. *Proc Natl Acad Sci U S A.* **91**: 2970-2974.

Walkley, S.U. (1995) Pyramidal neurons with ectopic dendrites in storage diseases exhibit increased GM2 ganglioside immunoreactivity. *Neuroscience.* **68**: 1027-1035.

Walkley, S.U., Siegel, D.A. and Dobrenis, K. (1995) GM2 ganglioside and pyramidal neuron dendritogenesis. *Neurochem Res.* **20**: 1287-1299.

Walus, L.R., Pardridge, W.M., Starzyk, R.M. and Friden, P.M. (1996) Enhanced uptake of rsCD4 across the rodent and primate blood-brain barrier after conjugation to anti-transferrin receptor antibodies. *J Pharmacol Exp Ther.* **277**: 1067-1075.

Wan, J., Taub, M.E., Shah, D. and Shen, W.C. (1992) Brefeldin A enhances receptor-mediated transcytosis of transferrin in filter-grown Madin-Darby caninie kidney cells. *J Biol Chem.* **267**: 13446-13450.

Watanabe, E., Matsui, F., Keino, H., Ono, K., Kushima, Y., Noda, M. and Oohira, A. (1996) A membrane-bound heparan sulfate proteoglycan that is transiently expressed on growing axons in the rat brain. *J Neurosci Res.* **44**: 84-96.

Watanabe, H., Grubb, J.H. and Sly, W.S. (1990) The overexpressed human 46-kDa mannose 6-phosphate receptor mediates endocytosis and sorting of beta-glucuronidase. *Proc Natl Acad Sci U S A.* **87**: 8036-8040.

Watanabe, H., Kimata, K., Line, S., Strong, D., Gao, L.Y., Kozak, C.A. and Yamada, Y. (1994) Mouse cartilage matrix deficiency (cmd) caused by a 7 bp deletion in the aggrecan gene. *Nat Genet.* **7**: 154-157.

Watkins, W.M. (1980) Biochemistry and Genetics of the ABO, Lewis, and P blood group systems. *Adv Hum Genet.* **10**: 1-136, 379-385.

Weber, B., Hopwood, J.J. and Yogalingam, G. (2001) Expression and characterization of human recombinant and alpha-N-acetylglucosaminidase. *Protein Expr Purif.* **21**: 251-259.

Wengenack, T.M., Curran, G.L. and Poduslo, J.F. (1997a) Postischemic, systemic administration of polyamine-modified superoxide dismutase reduces hippocampal CA1 neurodegeneration in rat global cerebral ischemia. *Brain Res.* **754**: 46-54.

Wengenack, T.M., Curran, G.L., Olson, E.E. and Poduslo, J.F. (1997b) Putrescine-modified catalase with preserved enzymatic activity exhibits increased permeability at the blood-nerve and blood-brain barriers. *Brain Res.* **767**: 128-135.

Wenger, D.A., Gasper, P.W., Thrall, M.A., Dial, S.M., LeCouteur, R.A. and Hoover, E.A. (1986) Bone marrow transplantation in the feline model of arylsulfatase B deficiency. *Birth Defects Orig Artic Ser.* **22**: 177-186.

Wenger, D.A., Suzuki, K., Suzuki, Y. and Suzuki, K. (2001) Galactosylceramide lipidosis: Globoid cell leukodystrtophy (Krabbe disease). In *The Metabolic and Molecular Bases of Inherited Disease.* Scriver, C.R., Beaudet, A.L., Sly, W.S., and Valle, D. (eds.) New York: McGraw-Hill, pp. 3669-3694.

Whiteman, P. (1973) The quantitative determination of glycosaminoglycans in urine with Alcian Blue 8GX. *Biochem J.* **131**: 351-357.

Whitley, C.B., Belani, K.G., Chang, P.N., Summers, C.G., Blazar, B.R., Tsai, M.Y., Latchaw, R.E., Ramsay, N.K. and Kersey, J.H. (1993) Long-term outcome of Hurler syndrome following bone marrow transplantation. *Am J Med Genet.* **46**: 209-218.

Whitley, C.B., Spielmann, R.C., Herro, G. and Teragawa, S.S. (2002) Urinary glycosaminoglycan excretion quantified by an automated semimicro method in specimens conveniently transported from around the globe. *Mol Genet Metab.* **75**: 56-64.

Willems, P.J., Gatti, R., Darby, J.K., Romeo, G., Durand, P., Dumon, J.E. and O'Brien, J.S. (1991) Fucosidosis revisited: a review of 77 patients. *Am J Med Genet.* **38**: 111-131.

Willems, P.J., Seo, H.C., Coucke, P., Tonlorenzi, R. and O'Brien, J.S. (1999) Spectrum of mutations in fucosidosis. *Eur J Hum Genet.* **7**: 60-67.

Wu, D. and Pardridge, W.M. (1996) Central nervous system pharmacologic effect in conscious rats after intravenous injection of a biotinylated vasoactive intestinal peptide analog coupled to a blood-brain barrier drug delivery system. *J Pharmacol Exp Ther.* **279**: 77-83.

Yamaguchi, Y. (2001) Isolation and characterization of nervous tissue proteoglycans. *Methods Mol Biol.* **171**: 35-39.

Yanagishita, M. and Hascall, V.C. (1984) Metabolism of proteoglycans in rat ovarian granulosa cell culture. Multiple intracellular degradative pathways and the effect of chloroquine. *J Biol Chem.* **259**: 10270-10283.

Yanagishita, M. (1993) Function of proteoglycans in the extracellular matrix. *Acta Pathol Jpn.* **43**: 283-293.

Yeager, A.M., Brennan, S., Tiffany, C., Moser, H.W. and Santos, G.W. (1984) Prolonged survival and remyelination after hematopoietic cell transplantation in the twitcher mouse. *Science.* **225**: 1052-1054.

Yogalingam, G., Litjens, T., Bielicki, J., Crawley, A.C., Muller, V., Anson, D.S. and Hopwood, J.J. (1996) Feline mucopolysaccharidosis type VI. Characterization of recombinant N-acetylgalactosamine 4-sulfatase and identification of a mutation causing the disease. *J Biol Chem.* **271**: 27259-27265.

Yogalingam, G., Hopwood, J.J., Crawley, A. and Anson, D.S. (1998) Mild feline mucopolysaccharidosis type VI. Identification of an N-acetylgalactosamine-4-sulfatase mutation causing instability and increased specific activity. *J Biol Chem.* **273**: 13421-13429.

Yoshida, M., Noguchi, J., Ikadai, H., Takahashi, M. and Nagase, S. (1993a) Arylsulfatase B-deficient mucopolysaccharidosis in rats. *J Clin Invest.* **91**: 1099-1104.

Yoshida, M., Ikadai, H., Maekawa, A., Takahashi, M. and Nagase, S. (1993b) Pathological characteristics of mucopolysaccharidosis VI in the rat. *J Comp Pathol.* **109**: 141-153.

Yoshikawa, T. and Pardridge, W.M. (1992) Biotin delivery to brain with a covalent conjugate of avidin and a monoclonal antibody to the transferrin receptor. *J Pharmacol Exp Ther.* **263**: 897-903.

Yurek, D.M. and Sladek, J.R., Jr. (1990) Dopamine cell replacement: Parkinson's disease. *Annu Rev Neurosci.* **13**: 415-440.

Zhang, Y., Boado, R.J. and Pardridge, W.M. (2003) Marked enhancement in gene expression by targeting the human insulin receptor. *J Gene Med.* **5**: 157-163.

Zhao, K.W. and Neufeld, E.F. (2000) Purification and characterization of recombinant human alpha-N-acetylglucosaminidase secreted by Chinese hamster ovary cells. *Protein Expr Purif.* **19**: 202-211.

Zlokovic, B.V. and Apuzzo, M.L. (1998) Strategies to circumvent vascular barriers of the central nervous system. *Neurosurgery.* **43**: 877-878.

THESIS ADDENDA

page xv, paragraph 2, line 1. The cardiopulmonary system and the eye should be included as major sites of pathology.

page 44, line 12. The references by Sheridan *et al.* (1994) and Abreu *et al.* (1995) should be included.

page 39, paragraph 2. The first two sentences are replaced by the following. *Intravenous infusion of viral vectors is not expected to be advantageous in treating CNS pathology in animal models (or patients) which have a fully developed BBB at birth. However, both somatic and CNS pathology were improved in MPS VII mice receiving the rAAV-β-glucuronidase vector intravenously at birth and accompanied by induction of hepatocyte replication (Gao et al., 2000).*

page 39, paragraph 2, line 8. The following sentence should be included. *Gene therapy approaches utilising direct intraocular injections of rAAV encoding β-glucuronidase to treat the brains of MPS VII mice (Hennig et al., 2003), or of 4S to treat the retinal epithelium of MPS VI cats (Ho et al., 2002), as well as retrovirally-transduced bone marrow or neonatal blood cells to treat MPS VI cats (Simonaro et al,. 1999) are also proving promising.*

page 39, paragraph 3, line 5. The sentence should read '...show the presence of *hepatocellular tumours and angiosarcomas, which were virus-negative,* in these mice.'

page 45, line 3. The sentence should read 'The P/N mutation was shown to be present in a number of MPS VI cats *on three continents*.'

page 54, line 3. The following sentence should be inserted. *A combination of ERT from birth followed by BMT at 5 weeks was as beneficial as continuous ERT from birth in its effect on reducing lysosomal storage in a number of tissues, and in addition, lysosomal storage in corneal fibroblasts was also dramatically reduced by these therapies (Sands et al., 1997).*

page 134, paragraph 2, line 3. The following sentence should be included. *With regards to body weight, flexibility and neurological signs MPS VI cats treated with the higher dose of rh4S showed similar responses to cats treated with rf4S and these were in general better than those treated with the lower dose of rh4S (Crawley et al., 1997).*

page 158, line 4. The following sentence should be included. *Although body weight may not be the best parameter to use to normalise liver weight, as MPS VI cats are growth retarded, have osteopaenia and muscle atrophy and as all these symptoms are altered with treatment, it was nevertheless used in the absence of a more suitable reference parameter.*

Fig. 3.9. Legend line 3 should read '...1 mg rf4S/kg *(cat 250)* (5A)...'

Fig. 3.11. Legend line 3 should read '...the cells of a MPS VI cat *(cat 249)* treated with 1 mg rf4S/kg (B)..'

page 170, line 20. The reference by Laterra *et al.* (1992) should be inserted.
There has been no scientific study documented regarding the development of the canine BBB, however, it is generally believed to be similar to the development of the human BBB.

Table 4.4. Legend line 6. The following sentence should be included. *The decrease in storage after treatment with high-dose CHO and MDCK/rcFUC and low-dose CHO/rcFUC was significant ($p<0.05$), the decrease observed with low-dose MDCK/rcFUC was not ($p>0.05$).*

page 232, line 5. The following sentences should be included. *The skin is a large organ and some of the radioactive counts not recovered may be attributed to uptake in this organ. However, due to difficulties in solubilisation of skin tissue, results were not included as they were not considered to be accurate.*

Table 4.13. The abbreviation MNL denotes mesenteric lymph node.

page 246, lines 6-13. Clinical and behavioural observations were performed by Dr. R. Taylor and Prof. B. Farrow who have had considerable experience with normal and fucosidosis dogs over many years.

The following references should be included in the Bibliography.

Abreu, S., Hayden, J., Berthold, P., Shapiro, I.M., Decker, S., Patterson, D. and Haskins, M. (1995) Growth plate pathology in feline mucopolysaccharidosis VI. *Calcif Tissue Int.* **57**: 185-190.

Hennig, A.K., Levy, B., Ogilvie, J.M., Vogler, C.A., Galvin, N., Bassnett, S. and Sands, M.S. (2003) Intravitreal gene therapy reduces lysosomal storage in specific areas of the CNS in mucopolysacchardosis VII mice. *J Neurosci.* **15**: 3302-3307.

Ho, T.T., Maguire, A.M., Aguirre, G.D., Surace, E.M., Anand, V., Zeng, Y., Salvetti, A., Hopwood, J.J., Haskins, M.E. and Bennett, J. (2002) Phenotypic rescue after adeno-associated virus-mediated delivery of sulfatase to the retinal pigment epithelium of feline mucopolysaccharidosis VI. *J Gene Med.* **4**: 613-621.

Sheridan, O., Wortman, J., Harvey, C., Hayden, J. and Haskins, M. (1994) Craniofacial abnormalities in animal models of mucopolysaccharidoses I, VI and VII. *J Craniofac Genet Dev Biol.* **14**: 7-15.

Simonaro, C.M., Haskins, M.E., Abkowitz, J.L., Brooks, D.A., Hopwood, J.J., Zhang, J. and Schuchman, E.H. (1999) Autologous transplantation of retrovirally transduced bone marrow or neonatal blood cells into cats can lead to long-term engraftment in the absence of myeloablation. *Gene Ther.* **6**: 107-113.